ONLINE REGULATION OF RECALIBRATED NO-VISION WALKING

THE ONLINE REGULATION OF NO-VISION WALKING IN TYPICALLY CALIBRATED AND RECALIBRATED PERCEPTUAL-MOTOR STATES EXMAINED USING A CONTINUOUS POINTING TASK

By JAMES JOHN BURKITT, B.Kin. (Hons)

A Thesis Submitted to the School of Graduate Studies in Partial Fulfilment of the

Requirements for the Degree Doctor of Philosophy

McMaster University © Copyright by James J. Burkitt, April 2017

McMaster University DOCTOR OF PHILOSOPHY (2017) Hamilton, Ontario (Kinesiology)

TITLE: The online regulation of no-vision walking in typically calibrated and recalibrated perceptual-motor states examined using a continuous pointing task

AUTHOR: James John Burkitt, B.Kin. (McMaster University)

SUPERVISOR: James L. Lyons, Ph.D.

NUMBER OF PAGES: xvi, 270

LAY ABSTRACT

It is well understood that humans can effectively walk without vision to environmental locations up to 15 metres away. However, less is known about how these walking movements are controlled during the course of forward progression. This thesis fills this knowledge gap using a task that requires participants to walk forward along a straight path while keeping their right index finger pointed toward a ground-level target beside the walking path. The patterns of arm movements performed during this task are indicative of the control strategies used by the performer to mentally update their positions in space. One of the key contributions of this work is showing that humans perform this mental updating in a repetitive manner, and that these repetitions are consistently linked to early forward movements of the right leg. This pattern is maintained when walking without vision is performed in a variety of different contexts.

ABSTRACT

No-vision walking is supported in the central nervous system (CNS) by a spatial updating process. This process involves the iterative updating of a mental representation of the environment using estimates of distance traveled gleaned from locomotive kinematic activity. An effective means of examining the online regulation of this process is a continuous pointing task, which requires performers to walk along a straight-line forward trajectory while keeping their right arm straight and index finger fixated on a stationary ground-level target beside the walking path. In the current thesis, no-vision continuous pointing was examined in typically calibrated and recalibrated perceptual-motor states. Shoulder and trunk joint angles provided the basis for perceptual measures that reflected spatial updating performance and kinematic measures that reflected its underlying CNS online regulation. In the typically calibrated conditions, no-vision walking demonstrated a slight perceptual underestimation of distance traveled (Study 1). In the recalibrated conditions, no-vision walking demonstrated: a) perceptual underestimation and overestimation following adaptation periods involving walking with low and high visual gains, respectively (Study 2); and b) partial recalibration following exposures to vision and arm gains (Study 3). The latter was suggested as being impacted by task specific changes in CNS multisensory integration resulting from the development of a robust task prior and/or the altering of sensory cue weights. Importantly, this thesis used a novel trajectory parsing procedure to quantify discrete CNS perceptual updating units in the shoulder plane of elevation trajectory. The starts and ends of these updating units were consistently timed to the late left-to-early right foot swing phase of the step-

cycle, regardless of perceptual-motor state. This was suggested to reflect perceptual units that were purposely timed, but indirectly mapped, to this kinematic event. The perceptual differences in Studies 1 and 2 were at least partially reflected in these units.

ACKNOWLEDGEMENTS

Jim Lyons – We all need somebody to take a chance and give us an opportunity. You took that chance and I am very thankful for the opportunity. I have enjoyed our friendship over the years, which is something that has always remained independent of the science. Your primary focus has always been your graduate students, and you have never steered us wrong. Thank you! You have a nice bottle of Scotch coming your way.

Digby Elliott – You created a lab that was more like a family than a workplace. Despite me not being under your direct supervision, and despite you being retired by the time I started my Masters, you vested many hours into my development. Thank you!

Jenny Campos – The ideas we put together in your grad class formed the basis of this thesis. Since then, you have willingly dedicated time and effort to all aspects of my development. Thank you very much for the mentoring!

Raoul Bongers – Although the time we worked together was brief, I still incorporate the skills you taught me into my day-to-day work. Now, if I could only figure out the problem with the readNDF file.

Dave Gonzalez – Thank you for taking me on as your undergraduate research assistant and for helping get me started in academia. You are a generous man.

AB108 – Jeff Graham, Mike Sonne, Nick LaDelfa, Aaron Kociolek, Justin Weresch, Brian Richardson, Dan Garcia and Simran Ohson. Grad school would not have been the same without you guys.

Family –Lydia Burkitt, Dave Burkitt, Laura Tatum, and Jeremy Tatum: thank you for enduring me over the last 30 plus years. You have all contributed in countless ways to my pursuit of academia and happiness, which at times are two totally different things. You guys gave me opportunity, supported my decisions, and have always been reliable.

Stacey Hawkins and James Burkitt-Hawkins – My wife and son. Stace, you are the reason I pursued graduate studies, and you have made me a better student and a better person. University has given us some very interesting times, none of which I would trade for anything. Thank you for your endless support. James, you are much too young to remember any of this so let me refresh you. I wrote this document in the first year and a bit of your life. My main motivator every day was finishing work so that I could emerge from the basement home office and spend time with you. Your presence in our lives is a blessing. Also, these characters - hm,m,,m,l,l,,.i;\??» - are the first you ever typed and it is your official contribution to this body of work. I love you both very much. My apologies to the children that follow that are not included in this section, but you simply had not been born yet. I will somehow make up for it later.

DEDICATION

This thesis is dedicated to my grandfather, John D. Burkitt. Your sacrifices during the Second World War enabled me to experience the freedoms of scientific thought. For this I will always be thankful, and you will never be forgotten. A special dedication also goes to my uncle, John F. Burkitt. You were a trailblazer for our family. None of us would be where we are today without your experience, and guidance. Thank you both.

TABLE OF CONTENTS

DESCRIPTIVE NOTE ii
LAY ABSTRACT iii
ABSTRACT iv
ACKNOWLEDGEMENTS vi
DEDICATION vii
TABLE OF CONTENTS viii
LIST OF FIGURES xi
LIST OF TABLES xiii
LIST OF ABBREVIATIONS AND SYMBOLS xv
AUTHOR CONTRIBUTIONS xvi

CHAPTER 1: GENERAL INTRODUCTION
1.1 – PREAMBLE 2
1.2 – WALKING WITHOUT VISION 2
1.3 – CONTINUOUS POINTING 10
1.4 – SENSORY RECALIBRATION 18
1.5 – SUMMARY 28
1.6 – PURPOSE OF THESIS 29
1.6.1 – *Study 1* 29
1.6.2 – *Study 2* 29
1.6.3 – *Study 3* 30

CHAPTER 2: STUDY 1 - USING A NOVEL TRAJECTORY PARSING PROCEDURE TO EXAMINE ITERATIVE SPATIAL UPDATING IN NO-VISION FORWARD WALKING
2.1 – ABSTRACT 33
2.2 – INTRODUCTION 35
2.3 – METHODS 39
2.3.1 – *Participants* 39
2.3.2 – *Apparatus* 39
2.3.3 – *Procedure* 41
2.3.4 – *Data and Statistical Analysis* 42
Perceived/actual distance traveled and velocity 44
Azimuth measures 47
Step characteristics 48
Significant arm deviations 49
2.4 – RESULTS 53
2.5 – DISCUSSION 61

CHAPTER 3: STUDY 2 - THE ONLINE REGULATION OF ITERATIVE SPATIAL UPDATING FOLLOWING SENSORY RECALIBRATION TO LOW AND HIGH VISUAL GAINS

3.1 – ABSTRACT 98
3.2 – INTRODUCTION 100
3.3 – METHODS 103
3.3.1 – *Participants* 103
3.3.2 – *Apparatus* 104
3.3.3 – *Procedure* 107
Experimental task 107
Practice session 109
Experimental session 110
3.3.4 – *Data and Statistical Analysis* 112
Perceived/actual distance traveled and velocity 114
Azimuth measures 116
Step characteristics 117
Significant arm deviations 117
3.4 – RESULTS 120
3.5 – DISCUSSION 128

CHAPTER 4: STUDY 3 - THE IMPACT OF UPPER LIMB RESPONSES TO THE PERCEIVED SELF-MOTION REALIZED DURING A LOCOMTIVE CONTINUOUS POINTING TASK

4.1 – ABSTRACT 155
4.2 – INTRODUCTION 157
4.3 – METHODS 162
4.3.1 – *Participants* 162
4.3.2 – *Apparatus* 163
4.3.3 – *Procedure* 167
Experimental task 167
Practice session 169
Experimental session 170
4.3.4 – *Data and Statistical Analysis* 174
Perceived/actual distance traveled and velocity 176
Azimuth measures 179
Step characteristics 180
Significant arm deviations 181
4.4 – RESULTS 183
4.4.1 – *Omnibus Analyses* 183
4.4.2 – *Vision Gain Manipulations* 185
4.4.3 – *Arm Gain Manipulations* 192
4.4.4 – *Significant arm deviations in the step-cycle* 197
4.5 - DISCUSSION 199

CHAPTER 5: GENERAL DISCUSSION

5.1 – SIGNIFICANT ARM DEVIATIONS AND SPATIAL UPDATING 239
5.2 – SENSORY RECALIBRATION 245
5.3 – IMPLICATIONS FOR MULITSENSORY INTEGRATION 254
5.4 – CURRENT LIMITATIONS AND FUTURE DIRECTIONS 256
5.5 – APPLICATION 259
5.6 – SUMMARY 260
5.7 – REFERENCES 262

LIST OF FIGURES

CHAPTER 1	**GENERAL INTRODUCTION**	
Figure 1.1	Schematic of perceived distance traveled calculation	31
CHAPTER 2	**STUDY 1**	
Figure 2.01	Anatomical locations of retro-reflective markers	71
Figure 2.02	Anatomical locations of retro-reflective markers rendered in Visual 3D	72
Figure 2.03	Schematic of Study 1 experimental-environment layout	73
Figure 2.04	Visual 3D rendered body segments used for defining joint angles	74
Figure 2.05	Average power spectra for shoulder plane of elevation and trunk axial rotation in Study 1	75
Figure 2.06	Original and reconstructed samples of the shoulder plane of elevation and trunk axial rotation trajectories in Study 1	76
Figure 2.07	Calculations of step characteristics	77
Figure 2.08	Shoulder plane of elevation trajectories used for calculating significant arm deviations	78
Figure 2.09	Significant arm deviations indicated on shoulder plane of elevation trajectory	79
Figure 2.10	Criteria for determining significant arm deviations on shoulder plane of elevation velocity	80
Figure 2.11	Study 1: Actual walking velocity Vision by Distance interaction	81
Figure 2.12	Study 1: Perceived distance traveled Method by Target interactions	82
Figure 2.13	Study 1: Pooled perceived distance traveled for the reconstructed method	83
Figure 2.14	Study 1: Constant error Vision by Target interaction	84
Figure 2.15	Study 1: Proportional azimuth velocity trajectories for the vision trials	85
Figure 2.16	Study 1: Proportional azimuth velocity trajectories for the no-vision trials	86
Figure 2.17	Study 1: Perceived distance traveled per significant arm deviation Vision by Target interaction	87
Figure 2.18	Study 1: Frequency counts for significant arm deviation starts and ends	88
Figure 2.19	Study 1: Frequency counts for significant arm deviation starts and ends pooled across vision conditions	89
Figure 2.20	Study 1: Power spectra of the shoulder plane of elevation trajectories for the additional control data.	90

CHAPTER 3 **STUDY 2**
Figure 3.01 Schematic of Study 2 experimental-environment layout 136
Figure 3.02 Image of virtual environment 137
Figure 3.03 Study 2: Actual velocities for the 4 m no-vision trials 138
Figure 3.04 Study 2: Actual velocities for the 6 m no-vision trials 139
Figure 3.05 Study 2: Perceived distances traveled for the 4 m no vision trials 140
Figure 3.06 Study 2: Perceived distances traveled for the 6 m no vision trials 141
Figure 3.07 Study 2: Constant error for the 4 m no-vision trials 142
Figure 3.08 Study 2: Constant error for the 6 m no-vision trials 143
Figure 3.09 Study 2: Perceived distance traveled per significant arm deviation Gain by Test by Deviation Number means 144
Figure 3.10 Study 2: Frequency counts for the significant arm deviation starts 145
Figure 3.11 Study 2: Frequency counts for the significant arm deviation ends 146
Figure 3.12 Study 2: Frequency counts for the significant arm deviation starts and ends pooled across conditions 147

CHAPTER 4 **STUDY 3**
Figure 4.01 Study 3: Actual velocities for the 4 m no-vision trials 209
Figure 4.02 Study 3: Actual velocities for the 6 m no-vision trials 210
Figure 4.03 Study 3: Perceived distances traveled for the 4 m no vision trials 211
Figure 4.04 Study 3: Perceived distances traveled for the 6 m no vision trials 212
Figure 4.05 Study 3: Constant error Gain by Test interactions for the 6 m no-vision trials in the vision gain conditions 213
Figure 4.06 Study 3: Constant error Gain by Test interactions for the 4 m no-vision trials in the arm gain conditions 214
Figure 4.07 Study 3: Frequency counts for the significant arm deviation starts in the vision gain conditions 215
Figure 4.08 Study 3: Frequency counts for the significant arm deviation starts in the arm gain conditions 216
Figure 4.09 Study 3: Frequency counts for the significant arm deviation ends in the vision gain conditions 217
Figure 4.10 Study 3: Frequency counts for the significant arm deviation ends in the arm gain conditions 218
Figure 4.11 Study 3: Frequency counts for the significant arm deviation starts and ends pooled across conditions 219

LIST OF TABLES

CHAPTER 2	**STUDY 1**	
Table 2.1	Anatomical landmarks of retro-reflective marker placements	91
Table 2.2	Landmarks used to create virtual markers in the Visual 3D model	92
Table 2.3	Landmarks used to create segments in the Visual 3D model	93
Table 2.4	Study 1: Grand means for the step characteristics	94
Table 2.5	Study 1: ANOVA results for the perceived distance traveled analysis	95
Table 2.6	Study 1: R-squared values of the second-order polynomials fit to the proportional azimuth velocity trajectories	96
CHAPTER 3	**STUDY 2**	
Table 3.1	Study 2: ANOVA results for the analysis of actual walking velocity in the no-vision pre- and post-adaptation trials	148
Table 3.2	Study 2: Grand means for the step characteristics in the no-vision pre- and post-adaptation trials	149
Table 3.3	Study 2: ANOVA results for the analysis of perceived distance traveled in the vision control trials	150
Table 3.4	Study 2: ANOVA results for the analysis of perceived distance traveled in the vision control and no-vision pre-adaptation trials trials	151
Table 3.5	Study 2: ANOVA results for the analysis of perceived distance traveled in the no-vision pre- and post-adaptation trials	152
Table 3.6	Study 2: ANOVA results for the constant error analysis in the no-vision pre- and post-adaptation trials	153
CHAPTER 4	**STUDY 3**	
Table 4.01	Study 3: Sensory gain manipulations used during the adaptation periods	220
Table 4.02	Study 3: ANOVA results for the analysis of perceived distance traveled in the vision control trials	221
Table 4.03	Study 3: ANOVA results for the analysis of perceived distance traveled in the vision control trials and no-vision pre-adaptation trials	222
Table 4.04	Study 3: ANOVA results for the analysis of actual walking velocity in the 4 m no-vision pre- and post-adaptation trials for the vision gain conditions	223

Table 4.05	Study 3: ANOVA results for the analysis of actual walking velocity in the 6 m no-vision pre- and post-adaptation trials for the vision gain conditions	224
Table 4.06	Study 3: ANOVA results for the analysis of perceived distance traveled in the 4 m no-vision pre- and post-adaptation trials for the vision gain conditions	225
Table 4.07	Study 3: ANOVA results for the analysis of perceived distance traveled in the 6 m no-vision pre- and post-adaptation trials for the vision gain conditions	226
Table 4.08	Study 3: ANOVA results for the analysis of constant error at azimuth angle in the 4 m no-vision pre- and post-adaptation trials for the vision gain conditions	227
Table 4.09	Study 3: ANOVA results for the analysis of constant error at azimuth angle in the 6 m no-vision pre- and post-adaptation trials for the vision gain conditions	228
Table 4.10	Study 3: Adaptation by Gain by Test interaction means for azimuth angle at peak azimuth velocity in the no vision pre- and post-adaptation trials for the vision gain conditions	229
Table 4.11	Study 3: ANOVA results for the analysis of actual walking velocity in the 4 m no-vision pre- and post-adaptation trials for the arm gain conditions	230
Table 4.12	Study 3: ANOVA results for the analysis of actual walking velocity in the 6 m no-vision pre- and post-adaptation trials for the arm gain conditions	231
Table 4.13	Study 3: Adaptation by Test interaction means for actual walking velocity in the 4 m no-vision pre- and post-adaptation trials for the arm gain conditions	232
Table 4.14	Study 3: Adaptation by Test interaction means for actual walking velocity in the 6 m no-vision pre- and post-adaptation trials for the arm gain conditions	233
Table 4.15	Study 3: ANOVA results for the analysis of perceived distance traveled in the 4 m no-vision pre- and post-adaptation trials for the arm gain conditions	234
Table 4.16	Study 3: ANOVA results for the analysis of perceived distance traveled in the 6 m no-vision pre- and post-adaptation trials for the arm gain conditions	235
Table 4.17	Study 3: ANOVA results for the analysis of constant error at azimuth angle in the 4 m no-vision pre- and post-adaptation trials for the arm gain conditions	236
Table 4.18	Study 3: ANOVA results for the analysis of constant error at azimuth angle in the 6 m no-vision pre- and post-adaptation trials for the arm gain conditions	237

LIST OF ABBREVIATIONS AND SYMBOLS

ANOVA	analysis of variance
APV	after peak swing velocity
BPV	before peak swing velocity
CE	constant error
CNS	central nervous system
CVG	congruent visual condition
DS	double-stance preceding swing phase
HMD	head mounted display
HAG_P	high arm gain in the A_{POINT} condition (Study 3)
HAG_{WP}	high arm gain in the $A_{WALK\text{-}POINT}$ condition (Study 3)
HVG	high visual gain
HVG_W	high visual gain in the V_{WALK} condition (Study 3)
HVG_{WP}	high visual gain in the $V_{WALK\text{-}POINT}$ condition (Study 3)
HY	hybrid azimuth method
Hz	Hertz
LAG_P	low arm gain in the A_{POINT} condition (Study 3)
LAG_{WP}	low arm gain in the $A_{WALK\text{-}POINT}$ condition (Study 3)
LVG	low visual gain
LVG_W	low visual gain in the V_{WALK} condition (Study 3)
LVG_{WP}	low visual gain in the $V_{WALK\text{-}POINT}$ condition (Study 3)
NV	no-vision
PV	at peak swing velocity
RE	reconstructed azimuth method
RMS	root mean square
sd	standard deviation
SH	shoulder azimuth method
SPSS	Statistical Package for the Social Sciences
T	side-target distance along the walking path
V	vision
VE	variable error
X_{START}	distance between performer and start location
X_{TARGET}	distance between performer and side-target location
Y	side-target distance beside the walking path
Θ	azimuth angle

AUTHOR CONTRIBUTIONS

This thesis contains 5 chapters of original research that were all written by the primary author, James Burkitt. As the primary author, James Burkitt was significantly involved in all aspects of this dissertation. This includes completion and submission of the ethics application; idea conceptualization and study design; data collection, processing and analysis; results interpretation; and manuscript preparation. As the Ph.D. Supervisor, Dr. James Lyons was strongly involved in the completion and submission of the ethics application; idea conceptualization and study design; results interpretation; and the review and editing of all chapters. The Ph.D. committee consisted of Dr. Jennifer Campos, Dr. Peter Keir and Dr. Steven Hansen. The committee was involved in annual meetings that involved research updates, monitoring of progress, and the discussion of research ideas. Thus, the Ph.D. committee was continuously involved in various phases of the experimental process. The committee also reviewed and edited the document. Additionally, Dr. Campos contributed to idea conceptualization, study design and results interpretation for Studies 1 and 2 as well as contributing to results interpretation in Study 3. Dr. Keir contributed to the kinematics analysis involved in Study 1, which was carried throughout the thesis. Dr. Hansen provided theoretical insight into the interpretations of the results for Studies 2 and 3. Rebecca Pucci (Study 1), Jessica Skultety (Studies 2 and 3) and Emma Kent (Study 3) assisted with data collection. Dr. Brian Richardson designed and programmed the virtual reality set-up used in Studies 2 and 3.

CHAPTER 1:

GENERAL INTRODUCTION

1.1 – PREAMBLE

Humans are generally effective in performing goal-directed locomotive movements to a variety of environmental locations under a variety of different sensory conditions. These include running to a distant target board when performing the long jump, wayfinding across a room in the middle of the night with the lights turned off, or grabbing a glass of milk from the countertop en route to the television. Most impressive, as indicated in the second example, is the human capability to perform locomotive actions in the absence of vision. This capability is considered to involve strong associations between movement in a set of limbs and the sensory input that is used to represent perceived action in the central nervous system (CNS). Furthermore, this relationship between motor movement and perceived self-motion can be recalibrated to match environmental circumstances where the perceptions of self-motion provided by two individual sensory cues are in conflict (i.e., vision and non-visual cues). Such an event occurs during treadmill walking, where proprioception from the legs specifies forward motion and the visual system specifies no motion. The goal of the current thesis is to further understand the CNS online regulation of no-vision walking when the sensory cues to self-motion are either strongly associated (i.e., typically calibrated) or are presented in conflict (i.e., require recalibration).

1.2 – WALKING WITHOUT VISION

Humans can effectively walk without vision to previously viewed targets up to approximately 20 m away (e.g., Rieser, Ashmead, Talor, & Youngquist, 1990). Although these no-vision walking movements are not as accurate as walking with vision, they are

sufficiently precise with respect to terminal endpoint to suggest that participants have successfully acquired the target (Elliott, 1986). This capability of updating position in space in the absence of continuous visual cues to self-motion is enabled by a spatial updating process in the CNS. Spatial updating is generally considered to involve four sub-processes (see Loomis & Philbeck, 2012; Loomis, Klatzky, & Giudice, 2013), which includes: (i) the amalgamation of available sensory information into a perceptual representation (i.e., spatial image) of the environment, (ii) the estimation of position and orientation in space by integrating cues about distance, direction and speed of movement from the available sensory modalities, (iii) updating of the spatial image with the estimated change in position, and (iv) the performance of subsequent actions using the updated spatial image.

The representation that guides no-vision human locomotion (i.e., distance estimation) in straight walking conditions is constructed in the CNS, prior to locomotion, using distance information about environmental landmarks acquired from the available sensory cues (see Loomis et al., 2013). Spatial representations that support no-vision walking are most effective when they were formulated in environments rich with visual cues to egocentric target distance (Philbeck, Loomis, & Beall, 1997). However, effective representations can be formulated in the absence of vision using distance estimates provided by other sensory cues (Rieser, Guth, & Hill, 1986). Accordingly, spatial representations exist in a form that is independent of the modalities used in its formulation (see Loomis et al., 2013; Philbeck et al., 1997) and can support a wide variety of locomotive and non-locomotive behaviours (Loomis & Philbeck, 2012;

Philbeck, Woods, Arthur, & Todd, 2008; Philbeck & Loomis, 1997)). The perceptual representations common to most no-vision walking tasks use static visual cues about perceived egocentric distance to environmental stimuli (Philbeck & Loomis, 1997; Philbeck et al., 1997).

When humans walk through the natural world, they receive information about their movement from a variety of sensory sources. These include visual (i.e., optic flow), proprioceptive (i.e., position information provided by muscle length and joint angle), somatosensory (i.e., touch) and vestibular (i.e., linear and rotational accelerations) estimates of physical translation. Optimal multisensory integration is one of the more modern and widely accepted explanations of how the CNS merges information from these sensory sources into a unitary and reliable perceptual estimate (see Ernst & Banks, 2002; Ernst & Bülthoff, 2004) during the course of locomotion. In this theoretical approach, the perceptual estimates provided by all available sensory sources are integrated into a unitary CNS representation using a maximum likelihood estimate weighted linear sum (Ernst & Bülthoff, 2004). Accordingly, the contributions made by individual cues are determined by relative cue weighting, where the weights assigned to individual cues are in proportion to the inverses of their variances (Angelaki, Gu, & DeAngelis, 2009; Fetsch, Turner, DeAngelis, & Angelaki, 2009). In this case, the variance of a sensory modality refers to the stability of its input (to the CNS) over a particular period of interest. The CNS has shown to effectively adjust weights based on cue variances measured within single performance trials (Campos, Butler, & Bülthoff, 2012; Ernst & Banks, 2002) and across a series of performance trials (Campos, Butler, & Bülthoff,

2014). Ultimately, cues with lower variances receive higher weights because they are more reliable. This cue integration process is considered optimal because the variance of the multisensory estimate is lower than the variances of the estimates provided by each of the individual sensory cues (e.g., Ernst & Bülthoff, 2004; Alais, Newell, & Mamassian, 2010).

This type of optimal cue integration guides the perception of self-motion during forward locomotion through space (Butler, Campos, & Bülthoff, 2015; Frissen, Campos, Souman, & Ernst, 2011). Furthermore, the CNS has been shown to weigh body-based cues (i.e., proprioceptive and vestibular cues) higher than visual cues (optic flow) while performing these types of movements (Campos et al., 2012, 2014; Campos, Byrne, & Sun, 2010; Harris, Jenkin, & Zikovitz, 2000; c.f., Sun, Campos, & Chan, 2004). One consideration extended from this idea is the importance of proprioceptive step-cycle information in the estimation of self-motion during vision (i.e., non-target directed) and no-vision forward walking. More specifically, the reliability of this proprioceptive cue is considered to underlie the human capability to effectively walk to distant environmental targets without vision. The following discussion outlines the importance of proprioceptive inputs to the perception of self-motion during locomotion.

The contributions of proprioception acquired from step length and step frequency are of considerable importance to the estimation of spatial position (Mittelstaedt & Mittelstaedt, 2001). For example, in a distance estimation task, Durgin, Akagi, Gallistel, and Haiken (2009) reported lower between-trial variability in measures of step length and step frequency compared to step duration and the number of steps. These lower variability

measures suggested more consistent performance and thus, more reliable information available for spatial updating on a trial-to-trial basis. In another study, where Durgin et al. (2005) required performers to match visual information in a virtual environment to walking speeds presented on a treadmill, changes in speed perception were closely linked to step frequency. That is, when participants walked at the same speed, but with step frequencies that were either higher or lower than their typical step frequency (which was achieved by making modifications to step length), relatively higher and lower visual speeds were selected to match these gaits, respectively.

Target-directed walking has also been shown to consist of two identifiable and distinct processes that are differently characterized by the control of stride length (Lee, Lishman, & Thomson, 1982). Early in walking trajectories, where performers attempt to perform consistent and stereotyped step-cycle patterns, an initial process is characterized by low between-trial stride length variability and an accumulation of target relative error. Subsequently, as the participant approaches a target, a late online corrective process is used to reduce the discrepancy between the position of the performer and the position of the target. This late corrective process takes place 1-3 paces from the target and is characterized by high between-trial stride length variability. This reduces target relative error accumulated over the initial phase and allows the performer to home in on the target. In no-vision walking movements, these two processes rely on a visual representation about target position updated online using positional information provided by stride length (Farrell & Thomson, 1999; Laurent & Thomson, 1988).

Wittlinger, Wehner, and Wolf (2006) further demonstrated the importance of step-cycle information to spatial updating by examining the effect of altered stride lengths in foraging desert ants. In this study, the ants were required to perform an outbound journey from their nest to a food supply, followed by an inbound journey back to the nest. Importantly, the inbound journey required spatial updating based on the estimated distance of the outbound journey. The ants accurately performed this task in typical sensory circumstances. However, Wittlinger et al. (2006) altered the ant's stride lengths either by increasing or decreasing the lengths of their leg segments. This was accomplished by attaching the ants with stilts or by surgically removing a distal portion of their limbs, respectively. When the manipulations were performed immediately following the outbound journey, the inbound journey was overshot in the ants provided with stilts and undershot in the ants provided with stumps. These results suggested that the ants estimated distance during the outbound journey, and used the association between stride length and distance traveled on the outbound journey to inform spatial updating on the inbound journey. This was further supported when both the outbound and inbound journeys were performed with the same leg manipulations, and inbound performance returned to being accurate. Overall, these results showed that the integration of stride length informed the internal odometer used by the ants to estimate travel distance.

Chrastil and Warren (2014) demonstrated similar findings in experiments performed with humans. In their experiments, participants were required to complete outbound and inbound blind locomotive movements from a home position using either similar (i.e., walk-walk) or different (i.e., walk-throw) action modes. Their results showed

that inbound journeys were accurate in the similar condition, but resulted in performance differences in the different condition. Further, when the inbound and outbound action modes involved different tasks performed within the same effector set (i.e., walk-gallop), inbound performance differences were attributed to the differences in gait characteristics between the two tasks [1]. Furthermore, in a study by Turvey et al. (2009), similar between-task differences in locomotive distance estimation were attributed to the dynamics of inter-limb coordination as opposed to the variables existing at the level of a single-limb (e.g., step-length, step number). Overall, the results from these studies contend that the CNS estimation of distance traveled is scaled to the body-based (i.e. idiothetic) information within action modes defined by specific patterns of inter-limb coupling. That is, the end result of spatial updating (i.e., distance estimation) is bound by the kinematics of the locomotive task, as opposed to being guided by a more extrinsic calculation of perceived distance traveled.

On the basis of there being fundamental cyclic patterns to locomotive movements, CNS spatial updating is considered to operate as an iterative process (Etienne & Jeffery, 2004; Loomis & Philbeck, 2012). However, the exact nature of iterative CNS spatial updating remains somewhat speculative, since correlates are not often made between the spatial-temporal characteristics of overt physical performance and CNS information processing. One model that attempts to explain iterative spatial updating is the leaky

[1] Turvey et al. (2009) describe this as symmetry class. Running and walking were considered one symmetry class, and galloping and hesitation walking were considered another. Galloping consisted of forward translation with the right foot, followed by a catch-up step with the left foot. Hesitation walking consisted of forward translation with one foot, followed by a catch-up step, pause and forward translation with the other foot.

integrator model (Lappe & Frenz, 2009; Lappe, Jenkin, & Harris, 2007; Lappe, Stiels, Frenz, & Loomis, 2011), which was formulated to explain two task specific performance errors in no-vision walking. These errors involve perceptual underestimation when replicating a previously walked extent (i.e., actually located further along the walking path than perceived to be) and perceptual overestimation when walking to a previously viewed target (i.e., actually located not as far down the walking path as perceived to be). The basis of leaky integration is that spatial updating is continuously guided by a task specific state variable (i.e., mental representation) that is subject to updating misperception due to: a) error in estimation across the task specific updating iterations, referred to as the gain rate, and b) error in the CNS integrator that results in a continuous decay of the state variable, referred to as the leak rate. The model focuses on this latter type of error and suggests that the state variable is continuously under-perceived during task performance. Thus, the task specific errors occur because the state variable represents an additive running total (i.e., distance traveled) in the distance replication task and a subtractive running total (i.e., distance remaining to target) in the target directed task. However, apart from establishing gain rates by fitting the model to performance data, leaky integration provides a limited examination of the perceptual errors attributed to iterative updating. That is, these previously used tasks are not able to precisely characterize the gain rate at each moment during the walking trajectory and thus, the actual function that can be fit has to be extrapolated from only a few data points at the start and end of the walked paths.

Considering that many conceptualizations of spatial updating casually imply it as an iterative process (e.g., Etienne & Jeffery, 2004), one goal of this thesis is to further understand whether and/or how the iterative structure of CNS spatial updating links with locomotive kinematics. This is made possible by using the continuous pointing task, which is discussed in the following subsection, to examine spatial updating during forward linear walking.

1.3 – CONTINUOUS POINTING

The continuous pointing task is a means of measuring the online regulation of spatial updating during the course of forward linear locomotive movements. It requires participants to walk forward along a straight-line trajectory and, with a straightened arm, continuously point at a distant target located beside the walking path. During task performance, measurement of the arm azimuth angle (i.e., arm rotation angle about the vertical axis) is used as an indicator of the performer's perceived target relative positions (e.g., Campos, Siegle, Mohler, Bülthoff, & Loomis, 2009; Fukusima, Loomis, & Da Silva, 1997; Loomis, Da Silva, Fujita, & Fukusima, 1992). Specifically, at each frame of data collection, simple trigonometry is first used to calculate the performer's perceived distance along the walking path between their current location and the side target location (X_{TARGET}; see Figure 1.1). This is accomplished in equation 1 using arm azimuth angle (Θ) and the distance of the side target beside the walking path (Y). Subsequently, this can be converted to a perceived distance traveled along the walking path, measured as the distance between the performer's current location and the start location (X_{START}). This is accomplished in equation 2 by subtracting X_{TARGET} from the distance of the side target

(from the start location) along the walking path (T). Finally, the X_{START} values are accumulated across all frames of data collection to obtain a complete perceived distance traveled trajectory. Perceived velocity can be obtained by taking the derivative of this perceived distance traveled measure.

(1) $X_{TARGET} = Y\tan\Theta$,

(2) $X_{START} = T - X_{TARGET}$.

The arm kinematics of continuous pointing can be revealing about a performer's perceived target relative position. This is because continuous pointing involves a characteristic arm azimuth profile that shows decreasing positive angular values upon target approach (i.e., arm transitioning from in front of to beside the performer), is near 0° at target passage (i.e., arm straight out to the side) and shows increasing negative angular values as the target is distanced behind (i.e., arm transitioning from beside to behind the performer; see Campos et al., 2009). Assuming a constant walking speed, this pattern of arm azimuth is associated with a velocity profile that increases upon target approach, peaks at target passage and decreases following target passage. This kinematic measure is especially important when making comparisons to updating tasks that do not involve physical forward displacement, such as imagined walking (Campos et al., 2009) and walking in place (Frissen et al., 2011).

Continuous pointing has been shown to effectively measure target relative positions in full vision locomotive tasks involving linear walking (Campos et al., 2009), curvilinear walking (Frissen et al., 2011) and passive transport (Siegle, Campos, Mohler, Loomis, & Bülthoff, 2009). In these tasks, the perceived distances and velocities

measured using continuous pointing were shown to be near veridical to their respective actual measures throughout the movement trajectories. However, unlike no-vision walking, during visually-guided walking and pointing, spatial updating is not required to perform the task. This is because the task can be accomplished by simply aiming at the target under visual guidance. In many experimental contexts, performing continuous pointing movements with vision is used as a baseline measure to ensure that participants are apt in continuously pointing at a target while walking (i.e., performing the instructed task). However, to simplify the current discussion, "perceived" distance traveled will be used in both the vision and no-vision performance contexts to refer to the self-motion trajectories measured using continuous pointing. However, only in the no-vision context will spatial updating be referenced.

In comparison to performances with vision, no-vision continuous pointing also demonstrates near veridical estimates of perceived distance traveled and velocity in forward linear walking movements (Campos et al., 2009). This replicates previous studies that estimated spatial updating using only target-relative end point errors (Loomis & Philbeck, 2012). The continuous pointing task has also been effective in uncovering perceptual differences in the online control of spatial updating in atypical sensory conditions. For example, by showing differences in the azimuth velocity profiles between imagined and actual locomotion, Campos et al. (2009) demonstrated that the mental (i.e., spatial) updating involved in imagined locomotion was not comparable to that involved in vision or no-vision physical locomotion. This finding contradicted other studies showing similarities in temporal measures between imagined and actual walking performances

(i.e., movement time; see Kunz, Creem-Regehr, & Thompson, 2009 Experiment 7). Differences in azimuth velocity trajectories were also used by Frissen et al. (2011) to show that the spatial updating involved in no-vision walking in place failed to replicate that involved in no-vision actual forward walking.

Using arm azimuth angle to measure perceived self-motion during spatial updating requires three assumptions (see Siegle et al., 2009). These include: a) the accurate perception of the target prior to no-vision walking, b) alignment of the perceived and actual walking trajectories with the forward walking path at the start of a trial, with little to no lateral veer demonstrated over the course of the movement, and c) the introduction of no systematic bias by continuous pointing during task performance.

The first assumption is met in the current study, considering that the mental representations supporting the no-vision continuous pointing movements were constructed in visual environments rich in static egocentric distance cues (Philbeck & Loomis, 1997; Philbeck et al., 1997). Additionally, the walking distances examined here were well within the distance range supported by these visually based mental representations (Loomis & Philbeck, 2012).

In regards to the second assumption, human performers demonstrate idiosyncratic veering tendencies in the performance of no-vision walking tasks that can be attributed to motor noise (Kallie, Schrater, & Legge, 2007). This tendency generally results in greater end point variable errors perpendicular to the direction of travel as walking distance is increased (Elliott, 1986; Rieser, Ashmead, Talor, & Youngquist, 1990). Therefore, while we expected some trial-to-trial lateral veer in the present studies, there was no reason to

believe that performers perceived this veer and that it interrupted their continuous pointing performance and perceptual measures (Siegle et al., 2009). This is also in consideration of the unique sensory circumstance where humans can demonstrate laterally veering pathways while perceiving straight-ahead motion (Gordon, Fletcher, Melvill Jones, & Block, 1995). While other studies protected against lateral veer by providing guide ropes (Fukusima et al., 1997) or verbal feedback (Philbeck & Loomis, 1997) during the course of walking, we opted not to because the walking paths involved in this thesis were relatively short (6 m or less) and not encumbered by environmental objects in the surrounding near space. We also wanted to avoid constraining task performance and/or obstructing motion capture with the provision of guide rope or verbal feedback. Even though lateral veer was minimal in all three studies [2], the most important detail in using continuous pointing to estimate perceived linear distance traveled is that performers intend to walk straight and point as if not perceiving any lateral veer. There is no reason to preclude this assumption.

As for the third assumption, continuous pointing was not expected to introduce systematic perceptual biases during task performance because it effectively captured visually and non-visually guided walking performance in previous studies (e.g., Campos

[2] The grand means of constant error (CE; signed end point error perpendicular to the direction of travel) and variable error (VE; within participant standard deviations of CE) in veer are as follows: Study 1: CE = -0.049 m; VE = 0.098 m. Study 2: 4 m CE = -0.025 m; 4 m VE = 0.113 m, 6 m CE = 0.088 m, 6 m VE = 0.186 m; Study 3: 4 m CE = 0.005 m; 4 m VE = 0.118 m, 6 m CE = 0.06 m, 6 m VE = 0.182 m. Negative values indicate leftward deviations and positive values indicate rightward deviations.

et al., 2009). However, some studies have cited that biomechanical and methodological constraints can be introduced in continuous pointing that creates start point dependencies in the measures of perceived self-motion (Campos et al., 2009; Frissen et al., 2011; Siegle et al., 2009). That is, perceived self-motion trajectories that should otherwise be the same are impacted by where the participant is positioned at the start of a trial with respect to the target. However, these start point dependencies do not impact the overall response patterns of the participants (Siegle et al., 2009) and can be nulled by averaging across target locations (see Study 1; see Figure 2.13). Importantly, providing multiple start and target locations serves the critical role of preventing performers from guiding their continuous pointing movements by memory-based processes (Campos et al., 2009; Siegle et al., 2009). In the current thesis, multiple target positions were used in consideration of the latter.

Although it is not considered to introduce perceptual biases to spatial updating in most sensory contexts, the continuous pointing task involves CNS control constraints that are not presented in typical over ground walking (i.e., walking without pointing). This is because continuous pointing involves simultaneous upper and lower limb movements that must be coupled during task performance. In other tasks that involve the simultaneous control of the upper and lower limbs (i.e., walking and prehension, walking and discretely pointing at targets), it has been demonstrated that the kinematic performances of the limbs are different compared to instances where the limb systems are used in isolation (Rinaldi & Moraes, 2015). This has been taken to suggest that the CNS does not independently control the upper and lower limbs, but integrates their movements as a single and flexible

control unit (Chiovetto & Giese, 2013; Marteniuk & Bertram, 2001). As such, upper and lower limb control becomes mutually dependent, where changes in the spatial-temporal kinematics of one limb system occurs in response to changes in the task constraints involved with the other limb system (Rinaldi & Moraes, 2015). For example, Rinaldi and Moraes (2015) demonstrated that step duration and walking stability were altered when participants walked and reached for a dowel compared to a walking alone condition. Marteniuk, Ivens, and Bertram (2000) showed that the net displacement of the hand during a walking and reciprocal aiming task (i.e., Fitts' task performed between two stationary targets aligned with the direction of walking; Fitts, 1954) was toward the performers body instead of toward the most distant target (as occurred when the task was performed in a stationary standing condition). This demonstrated that the CNS took into account the forward translation generated by the legs when moving the hand toward the target.

The kinematic changes that result from simultaneous upper and lower limb control become more apparent as task difficulty increases. For relatively simple reaching tasks, minor increases in task difficulty can be accommodated at the level of the arm without any alterations required in the gait step-cycle (Carnahan, McFadyen, Cockell, & Halverson, 1996; c.f., Rinaldi & Moraes, 2015). However, as upper limb movements become more complex, more prominent gait modifications are required to maintain stability and forward progression (Marteniuk & Bertram, 2001; Marteniuk et al., 2000; Rinaldi & Moraes, 2015; Van Der Wel & Rosenbaum, 2007). For example, in the aforementioned Marteniuk et al. (2000) study, performers exhibited greater trunk rotation

(i.e., turning toward the targets) as target width decreased (i.e., movements became more complex) so that arm stability could be increased and target accuracy optimized. The overall findings from Marteniuk et al. (2000) were understood in the context of motor equivalence (see Abbs & Cole, 1987), where the CNS exploited the redundant degrees of freedom (see Bernstein, 1967), amidst changes in task complexity, so that the hand trajectory remained invariant across a series of trials.

In many of the tasks that have examined simultaneous upper and lower limb control, the discrete upper limb responses (i.e., grasping, pointing) seemed to occur at specific times in the walking step-cycle. For instance, Rinaldi and Moraes (2015) showed that dowel grasps most often occurred during the single-support phase of the ipsilateral leg, a strategy that was not impacted by changes in task difficulty. In a treadmill walking and virtual pointing task, Chiovetto and Giese (2013) showed that pointing consistently occurred 2-3 step-cycle phases after target stimulus presentation, regardless of the step-cycle phase in which it was presented. In a task that did not involve upper limb control, but still required coordination with respect to an external stimulus, Mauerberg and Adrian (1995) showed that the most consistent temporal coupling between the step-cycle and a metronome beat occurred when the latter was coupled to the temporal range between the heel-strike of one leg and the toe-off of the other (e.g., Muzii, Lamm Warburg, & Gentile, 1984). While the origin of these step-cycle timing patterns remains speculative and is likely task dependent, it speaks to the inherent and functional link between upper limb and lower limb control (see Georgopoulos & Grillner, 1989).

Therefore, the simultaneous upper and lower limb activity inherent to the continuous pointing task has been successfully used to measure spatial updating during forward linear walking in many performance and sensory contexts (Campos et al., 2009). Once again, a goal of this thesis is to use the continuous pointing task to understand how the iterative structure of spatial updating links with locomotive kinematics. However, another goal of the current thesis is to purposely adjust the relationship between the upper and lower limb activity during continuous pointing and examine the resulting impact on the perceptual-motor locomotive coordination involved in spatial updating. This is an important task consideration, since spatial updating is bound to the dynamics of both lower limb (Chrastil & Warren, 2014; Turvey et al., 2009) and, in some contexts, upper limb coupling (Harrison, Kuznetsov, & Breheim, 2013). The temporal relationship between upper and lower limb activity during continuous pointing will be examined throughout this thesis and considered with respect to its impact on spatial updating.

1.4 – SENSORY RECALIBRATION

The accuracy of target-directed, no-vision locomotion suggests there is a tight linkage between the motor movements involved in generating self-motion and the associated sensory information (e.g., proprioceptive and vestibular) involved in formulating the CNS perception of self-motion. In the specific case of forward walking, this sensory information appears to be strongly linked to lower limb locomotive kinematics (Chrastil & Warren, 2014; Durgin et al., 2009; Turvey et al., 2009). These linkages define the “typical” associations between perception and action, and guide performance in situations where vision is unavailable.

However, situations sometimes arise where kinematic activity in the effectors leads to discrepant perceptions of self-motion amongst the associated sensory cues. This situation is referred to as sensory conflict, as there is a disturbance in the typical association between kinematic effector activity and the associated sources of sensory information. An example of this is walking along an airport walkway in its direction of travel. This situation presents a sensory conflict because it results in an atypical association between the visual and proprioceptive rates of self-motion through space. This is created by the additional contributions to optic flow, made by passive translation on the walkway, which creates a faster-than-usual sense of visual self-motion with respect to the proprioception involved in the step-cycle. A different experience occurs when walking on an airport walkway opposite to its direction of travel or by walking on a treadmill at home. In these situations, the rates of visual self-motion are much slower or non-existent, respectively, compared to the rates of proprioceptive self-motion. In cases of such sensory conflict, the CNS must use these atypical cue associations to reconcile a unitary CNS perception of self-motion (e.g., Durgin et al., 2005).

The CNS responds to these types of conflicting perceptual-motor circumstances in a sensory recalibration process, which adjusts the relationship between kinematic leg activity and the resulting perception of self-motion (Mohler et al., 2007). In a locomotive task such as walking, sensory recalibration induces a change in the accuracy of post-adaptation spatial updating. This was demonstrated in a classic study by Rieser, Pick, Ashmead, and Garing (1995), who examined the impact of prolonged exposure to visual-proprioceptive conflict on the spatial updating involved in target-directed no-vision

walking movements. Specifically, Rieser et al. (1995) had performers walk to targets without vision before and after an adaptation period. During the adaptation period, performers walked on a treadmill mounted on an open trailer that was simultaneously pulled through the environment by a tractor. In this arrangement, sensory conflict was achieved by having performers experience optic flow from tractor speeds that were slower (i.e., faster leg kinematics or low visual gain; LVG) or faster (i.e., slower leg kinematics or high visual gain; HVG) than the leg proprioception involved with the treadmill speed. Post-adaptation recalibration was apparent because, when walking without vision to previously viewed targets, participants overshot the intended target locations following LVG adaptation and undershot the intended target locations following HVG adaptation. Since these errors occurred without changes to leg kinematic activity (i.e., step length; e.g., Durgin et al., 2005; Lackner & DiZio, 1988; Philbeck et al., 2008), Rieser et al. reasoned that recalibration resulted in the alteration of perceived distance traveled localized in the CNS.

Central to the Rieser et al. perspective is that sensory recalibration is tied to the visual consequences of our most recent kinematic actions (e.g., Pick Jr., Rieser, Wagner, & Garing, 1999). That is, adaptation to cue conflict created by walking on the trailer-mounted treadmill resulted in proprioception being recalibrated to match the visual perception of self-motion. Considering the supposition that recalibration was localized to the CNS, Rieser et al. also suggested that recalibration should transfer between two tasks that share functional CNS goals (e.g., Withagen & Michaels, 2002). Here, functional goals referred to intended task purposes. In the case of locomotion, this predicted transfer

between any two tasks that involved linear translation through space to a previously viewed target. This was supported when the recalibration of forward walking transferred to sidestepping, but not to target-directed ball throwing or turning in place (e.g., Bruggeman & Warren, 2010).

More recently, Kunz, Creem-Regehr, and Thompson (2013) extended this account to suggest that recalibration generalizes across tasks that share CNS functional goals only if the tasks involve the same effector systems. Their study examined whether the recalibration of walking transferred to wheelchair locomotion and vice versa. Although these two actions both involve the functional goal of linear translation through space, they clearly rely on different effector systems (i.e., arms versus legs) for producing self-motion. Kunz et al. showed that when the same recalibrated locomotive actions were tested before and after adaptation, the recalibration after-effects replicated those of Rieser et al. (1995). However, when walking was examined before and after adaptation to wheeling and vice versa, recalibration after-effects were minimal. This lack of recalibration transfer between functionally similar locomotive actions implied effector specific functional recalibration.

The idea of sensory recalibration being tied to the visual consequences of kinematic leg activity fails to account for the multisensory nature of the CNS (e.g., Ernst & Bülthoff, 2004). Therefore, an alternative account to that of Rieser et al. (1995) suggests that recalibration occurs when there is conflict between the CNS perception of self-motion and any of the sensory cues used in its formulation (Durgin et al., 2005). In support of this perspective, it has been shown that vision during adaptation is sufficient,

but unnecessary to induce sensory recalibration (Durgin & Pelah, 1999; Durgin, Fox, & Kim, 2003). Specifically, Durgin and Pelah (1999) examined no-vision running in place before and after adaptation to no-vision treadmill running. Compared to the baseline forward drift demonstrated during pre-adaptation performance (e.g., Philbeck et al., 2008), their results showed substantially larger forward drifting in post-adaptation no-vision running in place. This was taken to suggest that forward proprioceptive activity was recalibrated to match a stationary CNS perception of self-motion that was fostered by the absence of vision during adaptation. This resulted in the post-adaptation attempts to run-in-place being involved with forward kinematic leg activity. Furthermore, the amount of post-adaptation forward drift was greatly reduced when the sensory conflict during adaptation was minimized by the provision of virtual visual information indicative of forward self-motion (e.g., Prokop, Schubert, & Berger, 1997).

In further support of the multisensory account, Mohler et al., (2007; Experiment 2) used virtual reality to create two adaptation conditions where the same rate of optic flow was used to generate two different rates of perceived self-motion. This was accomplished by pairing a constant rate of treadmill walking with a constant rate of optic flow presented in either a small or large virtual hallway. Given that the same rate of optic flow was used to generate hall motion in both conditions, the large virtual hallway resulted in a relatively faster rate of perceived self-motion (similar to the aforementioned HVG condition) and the small virtual hallway resulted in a relatively slower rate of perceived self-motion (similar to the aforementioned LVG condition). If optic flow alone was responsible for sensory recalibration, Mohler et al. would not have anticipated any

post-adaptation effects on no-vision walking to previously viewed targets. However, the post-adaptation no-vision walking movements overshot the intended targets following small hall exposure and undershot the intended targets following large hall exposure. This supports the perspective that recalibration is based on the CNS perception of self-motion and not on the afferent information associated with a specific sensory cue (i.e., vision).

Interestingly, the sensory recalibration involved with spatial updating can be limb specific. This makes sense, considering that limbs are independently capable of producing self-motion (e.g., forward hopping on one foot). Durgin et al. (2003) showed this in a study where no-vision single leg hopping-in-place movements were performed with both legs before and after adaptation periods. During adaptation, either vision or no-vision forward hopping was performed using only one leg. This resulted one leg being “adapted” and the other being “non-adapted”. When vision was unavailable during adaptation, the adapted leg demonstrated greater post-adaptation forward drift compared to the non-adapted leg (which performed similar to pre-adaptation). This occurred because the stationary sense of self-motion experienced during adaptation was associated with forward limb activity in the former and no limb activity in the latter. The opposite occurred when vision was available during adaptation, where the non-adapted leg demonstrated less forward drift compared to the adapted leg (which performed similar to pre-adaptation). Similar limb specific after-effects were also demonstrated when running in place (i.e., using two legs) was examined before and after adaptation to single leg hopping. That is, performers exhibited post-adaptation forward drift and changes in angular orientation consistent with the calibration difference between the two legs. Such

results are consistent with CNS perceptions of self-motion being associated with limb specific kinematic activity.

The multisensory account does not support the contention that recalibration can transfer between tasks that involve similar CNS functional goals, even if they involve the same effector systems (c.f., Kunz et al., 2013). Instead, the multisensory account suggests that the transfer of recalibration occurs when there is sufficient overlap in the action units (e.g., step length) used by the CNS to glean estimates of perceived self-motion. Durgin et al. (2005) demonstrated this by adapting performers to no-vision treadmill walking and examining pre- and post-adaptation performances in running-in-place, target-directed walking and target-directed side stepping in the absence of vision. Following adaptation, participants demonstrated greater forward drift when attempting to run in place, greater target overshoot errors when walking toward a previously viewed target and no change in sidestepping performance (e.g., Philbeck et al., 2008). Interestingly, the two former tasks demonstrated recalibration transfer despite involving very different functional goals (i.e., remaining stationary versus linear translation, respectively), yet the transfer between walking and sidestepping was minimal despite the tasks being functionally similar (c.f., Rieser et al., 1995) [3].

In a series of manual aiming studies, Redding and Wallace (1992, 1993, 1996, 2002, 2005) identify two independent CNS mechanisms responsible for generating the

[3] Durgin et al. (2005) suggest methodological reasons as to why Rieser et al. (1995) showed recalibration to sidestepping.

performance after-effects that follow prolonged exposure to sensory cue conflict [4]. These mechanisms are referred to as strategic calibration and spatial alignment. Strategic calibration involves adjustments to motor planning and online control processes that result in immediate responses to changes in task and workspace constraints. For example, the task of accurately reaching for a coffee cup on a table requires the performer to identify the spatial location of the cup, formulate and execute an appropriate motor command for the intended effector (i.e., upper limb), and guide subsequent performance using online control. Being able to perform this task in a variety of different postures (e.g., seated near or far from the desk) and amidst a variety of different environmental objects (e.g., cup located in front of or behind a large bowl of bananas) relies on a strategic calibration process that makes rapid adjustments to the motor control processes used to perform this action (e.g., motor programs, feedforward and feedback control). Spatial alignment refers to prolonged changes to the sensory-motor mappings (i.e., relationships) that exist between the component elements of a perception-action system. For example, in the aforementioned task of reaching for a coffee cup, the formation of an appropriate motor command requires a consistent mapping between the visual coordinate system used to identify the cup and the effector coordinate system used to carry out the motor command.

Redding and Wallace (2001) distinguished between these processes by presenting a sensory cue conflict during the performance of target-directed upper limb aiming

[4] Redding and Wallace (2001) also identify postural adaptations as contributors to the after-effects that follow prolonged exposures to sensory cue conflict. These involve task specific physical habituations that are not associated with changes in CNS processes.

movements. This conflict was created using prism goggles that shifted the performer's visual fields rightward by approximately 11° when performing the aiming movements. This created conflict between the visual and proprioceptive estimates of limb position, such that vision indicated a non-veridical estimate of limb position and proprioception indicated a veridical estimate. To distinguish between strategic calibration and spatial alignment, the availability of visual feedback was provided at different times during the aiming trials. In one condition, it was provided at the start and target locations, and was not available during the course of the aiming movements. In another condition, it was occluded at the start location but was available for the remainder of the movement. Strategic calibration was measured using target-respective end point error measures, and showed a dependence on the availability of visual information. That is, end point variability measures were lower and end point bias measures here higher in the group where vision was available at the start location. This suggests strategic dependence on a more precise, but non-veridical visual estimate in the portion of the movement dominated by the strategic planning processes involved with motor control. Spatial alignment was examined before and after the aiming trials using novel tests designed to directly measure the alignment of the hand-head (i.e., proprioceptive) and eye-head (i.e., visual) sensory-motor systems. Spatial alignment was demonstrated in both groups and thus, operated independent of strategic calibration. In addition, the locus of alignment depended on the type of feedback available during the aiming movements. Early visual feedback fostered visual task guidance and proprioceptive alignment (hand-head), whereas late visual

feedback fostered proprioceptive guidance and visual (eye-head) alignment (Redding & Wallace, 1987, 1996).

The distinction between strategic calibration and spatial alignment becomes apparent when considering how their respective adaptation effects transfer to tasks not performed during the exposure period. In regards to strategic calibration, the motor control adjustments made in response to cue conflict are considered to transfer in a task-specific manner. This includes, for example, aiming tasks performed to the same distance and end point accuracy constraints as those performed during exposure. In regards to spatial alignment, the associated post-adaptation changes in mapping functions between sensory-motor systems are considered to transfer in a non-task specific manner. That is, the realigned mapping between two sensory-motor systems applies to any task that involves these systems.

Reconciling the after-effects demonstrated by Rieser et al. (1995), Mohler et al., (2007), and Durgin et al. (2003) in the context of the adaptive mechanisms outlined by Redding and Wallace is a difficult endeavour. This is because Redding and Wallace measured strategic calibration as task specific changes in aiming performance that occurred during the exposure periods, and spatial alignment as the after-effects that occurred in non-exposure tasks performed after the exposure period. This level of assessment was not apparent in the aforementioned locomotive tasks, nor was parsing the respective effects of strategic calibration and spatial alignment a focus in any of these studies. However, considering that Rieser et al. (1995) and Durgin et al. (2003) showed post-adaptation changes in perceived self-motion that were not associated with changes in

leg kinematics, they can be presumed as demonstrating adaptive changes in spatial alignment. That is, for these tasks to have demonstrated strategic calibration, an expectation would be post-adaptation changes in kinematic leg activity reflective of strategic motor control adjustments. Therefore, these effects can be described as a realigning of the mapping between leg sensory-motor systems and the CNS perception of self-motion. This interpretation also makes sense when considering the results of Durgin et al. (2003), where the leg specific sensory recalibrations show that the sensory-motor coordinate system of each leg independently aligns with the CNS perception of self-motion.

1.5 – SUMMARY

Overall, no-vision locomotion is considered to be guided by the iterative updating of a unitary environmental representation using estimates of distance traveled gleaned from the locomotive actions responsible for self-motion. This spatial updating process involves a tight linkage between kinematic leg activity and the associated sources of sensory information that collectively comprise the CNS perception of self-motion. Sensory recalibration can occur when there is discrepancy between the CNS perception of self-motion and any of the sensory cues used in its formulation. Such discrepancies involve deviations from the learned, and generally stable, relationship between the sensory information associated with kinematic leg activity and the CNS estimate of self-motion that is accumulated across a lifetime of task performance. Recalibration does not depend on the presence or absence of one specific sensory cue and can result in discordant after-effects within effector systems. The remainder of this thesis will refer to

post-adaptation spatial updating changes as resulting from sensory recalibration. However, results discussed in the context of the Redding and Wallace findings will be referred to as strategic calibration and spatial alignment, where appropriate.

1.6 – PURPOSE OF THESIS

The purpose of this thesis was to examine the online regulation of no-vision walking in typically calibrated and recalibrated perceptual-motor states. This was accomplished using the continuous pointing task in the following three studies:

1.6.1 – *Study 1*

Study 1 refined a previously used version of the continuous pointing task (i.e., Campos et al., 2009) to provide more precise measures of the arm and foot kinematics during typical vision and no-vision forward walking. The version of the continuous pointing task presented in Study 1 employed joint angle measures to estimate many of the perceptual measures of self-motion introduced in Campos et al. (2009) and provided kinematic data that can more rigorously examine how the CNS iteratively regulated spatial updating during forward walking. This was accomplished by having the participants walk along a 4.5 m straight-line trajectory, with or without vision, while continuously pointing at several ground-level targets located beside the walking path. The trunk and shoulder angles measured during task performance formed the basis of the perceptual and kinematic measures used to assess spatial updating.

1.6.2 – *Study 2*

Study 2 examined how the characteristic spatial updating differences following prolonged exposure to sensory cue conflict unfolded over the course of a forward walking

trajectory. The goal of this study was to extend previous accounts of online spatial updating following sensory recalibration that assessed performance using end point measures (e.g., end point walking distance). This was enabled by the online measures provided by the continuous pointing task. In Study 2, the continuous pointing task was performed without vision before and after prolonged periods of sensory adaptation to low gain, high gain and congruent visual conditions. These gains were introduced by treadmill walking while receiving optic flow from a virtual hallway presented by an Oculus Rift head mounted display.

1.6.3 – *Study 3*

The purpose of Study 3 was to determine how the upper limb coordination involved in continuous pointing was involved in the CNS perception of self-motion. This was examined by creating cue conflict with gained pointing responses and congruent vision and walking, or by pairing gained vision with congruent walking and pointing. Study 3 followed a similar format to Study 2, but introduced these different sensory conditions during the adaptation periods by: (i) representing the fingertip position in virtual space, (ii) introducing continuous pointing with the arm into the adaptation periods, and (iii) introducing sensory conflict between the arm and body by attaching low and high gains to the represented fingertip position as it moved through virtual space.

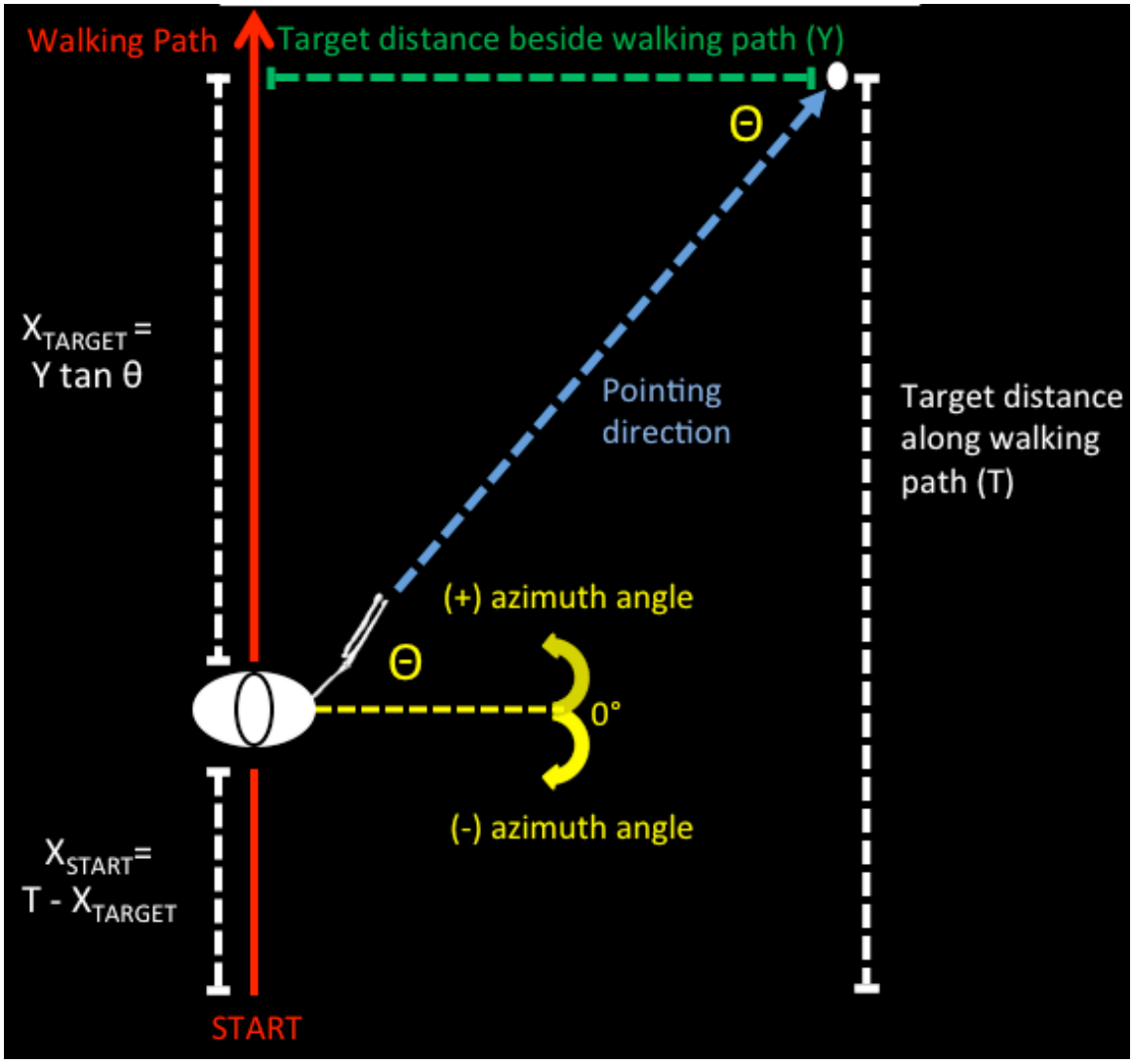

Figure 1.1. Above view schematic of the calculation of perceived distance traveled using the continuous pointing task. Participants walk forward along a linear path (solid red arrow) while keeping their right arm straight and right finger fixated (blue dashed arrow) on a stationary lateral target (white circle). Azimuth angle (Θ and yellow text) is measured as the joint rotations used to keep the finger fixated on the target. Y (green dashed line) represents lateral distance of the side target to the walking path; T (white dashed line) represents distance of the side target along walking path; X_{TARGET} represents perceived distance along the walking path between the performer and the side target; X_{START} represents perceived distance along walking path between the performer and the start location. These values are calculated at each frame of data collection and accumulated across each trial to achieve a perceived distance traveled trajectory.

CHAPTER 2:

STUDY 1

USING A NOVEL TRAJECTORY PARSING PROCEDURE TO EXAMINE ITERATIVE SPATIAL UPDATING IN NO-VISION FORWARD WALKING

2.1 – ABSTRACT

No-vision walking is supported by a spatial updating process that involves the iterative updating of a mental representation (of the environment) using estimates of distance traveled gleaned from locomotive activity. A means of examining the online regulation of this process is the continuous pointing task, which requires performers to walk along a straight-line forward trajectory while keeping their right arm straightened and finger fixated on a laterally displaced stationary target. While previous versions of this task captured estimates of perceived distance traveled throughout no-vision walking movements, they provided little information about the upper limb kinematics used to orient the fingertip in space during pointing performance. This information is important because it can provide a more refined measure of the movement strategies employed by the central nervous system (CNS) in estimating locomotive distance traveled in the absence of vision (i.e., spatial updating). Therefore, in Study 1, participants performed vision and no-vision continuous pointing movements along a 4.5 m forward linear walking path. Upper extremity joint angles and step-cycle kinematics were measured during task performance. The results showed perceptual under-estimation in the no-vision trials. Importantly, these measures of perceived self-motion were calculated using a data processing technique that combined the low-frequency reconstructed profiles of the shoulder plane of elevation and trunk axial rotation joint angle trajectories. Furthermore, measured deviations in the unprocessed shoulder plane of elevation trajectory indicated that target fixation during pointing was achieved in a discrete, as opposed to a continuous, manner. These measured arm deviations occurred most frequently during the early right

foot swing phase of the step-cycle, which suggested that iterative CNS spatial updating was consistently linked to movement in the legs. Since the differences between vision and no-vision task performance were demonstrated in these updating units, this was a strategy suggested to serve the CNS in estimating perceived distance traveled during spatial updating.

2.2 – INTRODUCTION

Early studies that examined spatial updating during forward walking employed target-directed blind-walking tasks and made inferences about its online regulation using end point error measures (i.e., constant and variable error with respect to a walking target location; e.g., Elliott, 1987; Steenhuis & Goodale, 1988). Although these early studies were useful in classifying the overall systematic behaviour of the CNS, they provided little understanding about the true online nature of spatial updating. However, Campos et al. (2009) provided a solution to this problem by introducing a novel continuous pointing task that enabled spatial updating to be measured online during the course of forward linear walking movements (e.g., Siegle et al., 2009). In this task, participants walked forward along a straight-line trajectory while keeping their right arm extended and right index finger fixated on a stationary ground-level target beside the walking path (see Figure 1.1). By establishing a measure of arm azimuth angle (i.e., rotation about the vertical axis) and by knowing the location of the side-target with respect to the walking path, perceived distance of the performer along the walking path could be calculated at each frame of data collection (see equations 1 and 2 in the General Introduction, as well as in the Methods section below). Accumulating these measures across data collection frames provided a perceived distance traveled trajectory for entire walking movements, and the derivative of this measure provided an estimate of perceived self-velocity. In both vision and no-vision walking movements, Campos et al. (2009) showed near unitary relationships between actual and perceived measures of distance traveled and velocity.

This supported other work showing that no-vision walking effectively approximated target distances up to 15-20 m away (e.g., Rieser et al., 1990).

However, despite being effective in estimating measures of perceived self-motion during forward walking, current versions of the continuous pointing task provide little information about the upper limb kinematics used to orient the fingertip in space. In upper limb aiming movements, the constituent limb kinematics can provide important information about the strategies employed by the CNS to organize movement control (Bernstein, 1967). For example, quantifying trajectory deviations has been both a common practice and valuable asset in providing insight into the CNS control of upper limb movements in goal-directed (i.e., tabletop) reaching tasks (Chua & Elliott, 1993). Specifically, trajectory parsing procedures (see Burkitt, Bongers, Elliott, Hansen, & Lyons, 2017; Burkitt, Staite, Yeung, Elliott, & Lyons, 2015; Chua & Elliott, 1993; Khan et al., 2006) have identified these movements as being composed of two distinct and identifiable processes. This includes an initial ballistic process that rapidly gets the limb to the vicinity of the target (i.e., primary movement) and a subsequent discrete control phase that reduces any discrepancy between the position of the limb and the position of the target at the end of the initial phase (i.e., secondary submovement; Elliott, Helsen, & Chua, 2001; Woodworth, 1899). By identifying these component processes in goal-directed upper limb trajectories, and in particular by measuring the relative locations of the finger and target at the end of a primary movement, the CNS has shown to strategically optimize speed, accuracy and energy expenditure in performing rapid goal-

directed movements with the upper limb to targets in near space (Lyons, Hansen, Hurding, & Elliott, 2006; see Elliott et al., 2010 for a more detailed discussion).

Considering that the continuous pointing task provides an online measure of spatial updating, the potential exists to quantify discrete trajectory adjustments in the associated upper limb responses and make inferences about their contributions to the online regulation of CNS spatial updating (Lappe & Frenz, 2009; Lappe et al., 2007, 2011). Study 1 pursued this goal by attempting to quantify trajectory deviations in the shoulder plane of elevation joint angle trajectories measured during continuous pointing performance. To the best of our knowledge, this was the first attempt at applying this approach to forward walking movements.

Current versions of the continuous pointing task (e.g., Campos et al., 2009; Siegle et al., 2009) measure arm azimuth angle as end effector rotation with respect to a central body fixation point (e.g., a head marker). Presumably, this involves measuring the angular difference between the frontal plane and the plane formed by the end effector-central fixation point. In this regard, Study 1 posed an interesting situation, as the data collection and analysis techniques used to examine joint angle kinematics (which were necessary for measuring trajectory deviations) may not be ideal for producing the aforementioned measures of perceived self-motion (e.g., perceived distance traveled). This was because these signals created fluctuations that, while ideal for kinematics analyses, could create noise when measuring the perceptual variables during continuous pointing. In light of this conundrum, Study 1 compared three azimuth angle methods, each formulated with upper body joint angle measures, in their abilities to approximate

actual self-motion through space. These included the shoulder, hybrid and reconstructed methods. The shoulder method used shoulder rotation (i.e., shoulder plane of elevation) as the azimuth angle trajectory. The hybrid method measured azimuth angle trajectory as the sum of the shoulder and trunk rotations (i.e., shoulder plane of elevation and trunk axial rotation, respectively). This method was important because it encompassed joint contributions beyond those provided by the arm. The reconstructed method, explained in greater detail in the section below, was similar in principle to the hybrid method. However, an exception was that the constituent signals were further processed, prior to their summation, to remove additional signal artefacts created by the walking movement. Of further methodological interest were the side-target locations that provided the most reliable measures of perceived self-motion and pointing kinematics.

Therefore, in Study 1, the joint angle data collected during continuous pointing performance provided measures of perceived self-motion (i.e., perceived distance traveled) and also formed the basis of a novel trajectory kinematic analysis technique. The expectations for Study 1 were that:

I. The reconstructed method would most effectively replicate perceived self-motion (e.g., Campos et al. 2009) across the variety of target locations used for continuous pointing. This was because it removed signal noise created by gait oscillations, and because it received azimuth contributions from shoulder and trunk rotations. This should enable the best measurement potential across the entire walking path. Therefore, the reconstructed method was expected to most

effectively demonstrate unitary relationships between actual and perceived distances traveled throughout entire walking trajectories.

II. Regardless of method of measurement, no-vision continuous pointing (i.e., spatial updating) performance should closely resemble vision continuous pointing performance. This was because the continuous pointing movements were performed to a walking distance close in proximity (Loomis & Philbeck, 2012) and in a lab space that enabled rich visual previews prior to no-vision performance (Philbeck & Loomis, 1997; Philbeck et al., 1997).

2.3 – METHODS

2.3.1 – *Participants*

Ten individuals (3 male, 7 female) with a mean age of 21.5 years (sd = 1.78 years) were recruited to participate in this study. Participants were self-reported right hand dominant and had normal or corrected-to-normal vision. Participants were naïve to the purposes of the study and provided written, informed consent prior to starting the experiment in accordance with the McMaster Research Ethics Board and the 1964 Declaration of Helsinki. Each experimental session took approximately 1.5 hours to complete and participants were remunerated $10 for their time.

2.3.2 – *Apparatus*

All participants wore comfortable athletic shoes and comfortable athletic shorts or pants during the experiment. Males completed the experiment shirtless and females completed the experiment wearing a sports bra, with one exception being a female participant who wore a snug fitting tank top. Participants were outfitted with 21 25 mm

retro-reflective markers (B & L Engineering, Santa Ana, California) that were captured by 10 Vicon Nexus MX-T40 (Oxford, United Kingdom) cameras at a rate of 250 Hz (see Figures 2.01 and 2.02, and Table 2.1 for the anatomical locations of marker placements). The markers were secured directly to the skin using two-sided electrode tape and medical tape that were both suitable for use on the skin. Wooden splints, consisting of two wooden chopsticks individually wrapped in medical tape, were taped to the medial and lateral aspects of the index finger and extended proximally along the forearm toward the elbow. These served to limit ulnar deviation and movements in the interphalangeal and metacarpal-interphalangeal joints during performance of the continuous pointing task. Participants were outfitted with an Ipod shuffle (Apple Inc., Cupertino, California) that played white noise through a pair of standard headphones (Sennheiser, Wedemark, Germany) at a comfortable volume. White noise was provided throughout the duration of the experimental session and served to mask the sounds of the participant's footsteps and ambient noises originating from the environment.

All walking movements were performed in the same direction along the same 4.5 m long path (see Figure 2.03). The start and end locations of the path were indicated by an inverted green "T" and a red "X", respectively. Eight possible side-target locations were indicated on the floor by small black pieces of tape, all of which were in full view of the participant when standing at the start location. Targets 1-4 were located 2 m beside the walking path and 2.1, 2.5, 2.7 and 3.2 m along the walking path, respectively. Targets 5-8 were located 3 m beside the walking path and 1.5, 1.8, 2.0 and 2.5 m along the walking path, respectively. A black circular disc 18 cm in diameter was placed on the

ground overtop of one location to indicate the side target used on each trial. Different side targets were used to prevent participants from relying on a memorized motor experience in performing the task.

2.3.3 – *Procedure*

Prior to starting the experiment, participants stood stationary in the anatomical position at the start location and a static marker calibration trial was captured from this pose. Each performance trial started with participants standing in the anatomical position at the start location. Once in this position, the experimenter started the motion capture and signaled to the participants by giving them a “thumbs-up”. This cued them to straighten their right arm (i.e., full elbow extension and full wrist pronation) and fixate their right index finger toward the side-target indicated by the black disc. This required participants to look directly at the side-target. After returning to a forward gaze, participants attempted to walk along a straight-line path with their eyes open (vision trial; V) or closed (no-vision trial; NV) while keeping their right index finger fixated on the side-target location. While walking and pointing, participants were asked to keep their arm as straight as possible and their palm facing down. Participants were also instructed to walk at a constant velocity and to stop when perceived to be in the vicinity of the end of the path (i.e., the red ‘X’). Participants were made aware that this latter instruction was only to be used as a cue to stop the walking movements and that end point accuracy with respect to the red ‘X’ was not emphasized in this task. When the participant stopped walking, the experimenter stopped the motion capture and either: a) indicated with another “thumbs-up” that the participant could walk back to the start location on their

own (following a V trial), or b) led the participant back to the start location with their eyes closed (following a NV trial). In the latter condition, the experimenter indicated participants to open their eyes by tapping them on the shoulder upon return to the start location. When back at the start location, the participants returned to the anatomical position, stood with their eyes open and awaited the start of the next trial. During the inter-trial interval, the experimenter adjusted the location of the side target disc.

Participants performed 80 continuous pointing movements, 40 in the V condition and 40 in the NV condition. Five V and 5 NV trials were performed at each side-target location. Movements were performed in alternating blocks of 10 V and 10 NV trials, with participants always starting with a block of V trials. Side-target locations were randomized on a trial-to-trial basis, with the stipulation that the same target could not be presented on 3 successive trials. One V and one NV practice trial were performed before the start of the experiment.

2.3.4 – *Data and Statistical Analysis*

The data from all trials were reconstructed using Vicon Nexus 1.8.5 software (Vicon, Oxford, UK). For each trial, the anatomical markers were labeled at every frame, missing data segments 25 frames or smaller were filled, and the data was saved in the C3D format for further processing in Visual 3D (version 4, C-motion Research Biomechanics, Kingston, Ontario).

In Visual 3D, a custom model was constructed using the static calibration trial and this model was attached to the 3D marker data for all trials. The model created virtual markers representing the wrist joint centre, elbow joint centre, shoulder anterior-posterior

joint centre, shoulder joint centre, shoulder girdle joint centre and thorax joint centre (see Figure 2.02 and Table 2.2 for the landmarks used to compute each virtual marker). The anatomical and virtual markers were then used to create body segments representing the pelvis, thorax, right upper arm and right forearm (see Figure 2.04 and Table 2.3 for the landmarks used to define each segment). Using these body segments, relative joint angles were calculated for the trunk, shoulder and elbow joints in a manner consistent with the International Society of Biomechanics standards (see Wu et al., 2005). Specifically, trunk angle represented rotation of the thorax segment with respect to the pelvis segment using an X-Y-Z Cardan sequence; shoulder angle represented rotation of the upper arm segment with respect to the thorax segment using a Z-Y-Z Cardan sequence; and elbow angle represented rotation of the forearm segment with respect to the upper arm segment using an X-Y-Z Cardan sequence.

Dependent measures were calculated for each trial using custom Matlab R2014a software (Mathworks, Natick, Massachusetts). The data from all markers and joint angles were first down-sampled to 125 Hz. The joint angle and marker data were then filtered with a second-order, dual-pass Butterworth filter with a low-pass frequency of 6 Hz. The start and end of each walking trial were determined using the velocity profiles of the foot responsible for taking the first and last steps, respectively. These velocity profiles were calculated as the derivatives of the displacement profiles for the left foot and right foot markers using a three-point finite difference algorithm. The start of walking was defined as the first instance where the velocity of the foot that took the first step reached the value of 0.02 m/s and remained above this mark for at least 25 frames (i.e., 200 ms). The end of

walking was defined as the first instance where the velocity of the foot that took the last step reached the value of 0.02 m/s and remained below this mark for at least 25 frames. In the odd circumstance where data from the left foot or right foot markers were lost at the end of a walking movement, the end of walking was calculated as the earliest missing data frame amongst the remaining anatomical markers. This had no impact on the results since the walking movements were only analyzed up to 4 m. All dependent variables were calculated between the defined start and end for each walking trial. Outlined in the remainder of this section are the calculations and statistical analyses used for determining and examining all dependent measures.

Perceived/actual distance traveled and velocity

Actual distance traveled was measured as the position of the xyphoid marker with respect to the start location. Actual walking velocity was taken as the derivative of the actual distance traveled trajectory calculated using a three-point finite difference algorithm. To determine whether participants adhered to the instruction to walk at a constant velocity, actual velocity was examined using a 2 Vision (V, NV) by 8 Target (1-8) by 8 Distance (0.5-4m) repeated measures ANOVA.

Perceived distance traveled was calculated using the azimuth angle trajectory (e.g., Campos et al. 2009). Azimuth angle refers to joint angular rotations, about the vertical axis, that are used to keep the fingertip localized on the side target. The joint angles examined in this study include the shoulder plane of elevation (see top right panel in Figure 2.04) and trunk axial rotations (see bottom right panel in Figure 2.04). The three different types of azimuth angle methods compared in this study were calculated as

follows: (i) the Shoulder Method (SH) used the shoulder plane of elevation trajectory as the azimuth angle trajectory, (ii) the Hybrid Method (HY) took the azimuth angle trajectory as the sum of the shoulder plane of elevation and trunk axial rotation trajectories, and (iii) the Reconstructed Method (RE) was produced using the following three steps; (a) the shoulder plane of elevation and trunk axial rotation trajectories were first submitted to Fast Fourier Transforms to determine the frequency contents of the two signals (see Figure 2.05), (b) both signals were reconstructed using their respective signal frequency contents that were less than 0.5 Hz, and (c) the two reconstructed signals were summed together. Therefore, the RE method is similar to the HY method, with the exception that it is removed of noise and trajectory events not associated with continuous pointing (e.g., gait oscillations). This was especially important for trunk axial rotation, which contained a global component reflective of continuous pointing performance and several local components reflective of the walking step-cycle (see Figure 2.06).

To calculate perceived distance traveled, equation 1 was used at every frame of data collection to calculate the performer's perceived instantaneous distance along the walking path with respect to the side target (X_{TARGET}; see Figure 1.1). This was done using instantaneous azimuth angle (θ) and the distance of the side target beside the walking path (Y). In equation 2, this was converted to the instantaneous perceived distance from the start location (X_{START}) by subtracting X_{TARGET} from the distance of the side target measured along the walking path (T). Accumulating the calculations of X_{START} across all data frames provided a perceived distance traveled trajectory for entire walking

trials. Taking the derivative of this measure, using a three-point finite difference algorithm, produced a measure of perceived velocity.

(1) $X_{TARGET} = Y\tan\Theta$,

(2) $X_{START} = T - X_{TARGET}$.

To examine how the measures of perceived distance and velocity approximated the actual values, when calculated with each azimuth method, root mean square (RMS) error was calculated as the perceived values with respect to the actual values. These RMS error scores were examined using 3 Method (SH, HY, RE) by 2 Vision (V, NV) by 8 Target (1-8) repeated measures ANOVAs.

To examine how perceived distance traveled unfolded throughout the course of a continuous pointing movement, in a manner that depended on the experimental conditions, perceived distance traveled was examined using what the authors term a "sliding ANOVA technique". This is where separate repeated measures ANOVAs are performed at multiple sequential iterations of a continuous independent variable. This is done to avoid congesting a single ANOVA with an independent variable whose results carry relatively little significance to the overall research question and whose levels can more or less be arbitrarily defined. The independent variable used here was actual distance traveled. This technique has been effectively used in other aiming tasks to examine the time course of pointing errors (Sarlegna et al., 2003; Scotto Di Cesare, Bringoux, Bourdin, Sarlegna, & Mestre, 2011). With this analysis, perceived distance traveled was examined using 3 Method (SH, HY, RE) by 2 Vision (V, NV) by 8 Target

(1-8) repeated measures ANOVAs run separately at distances of 0.5-4.0 m, in 0.5 m increments.

Azimuth measures

Azimuth velocity was calculated by differentiating the aforementioned azimuth trajectories using a three-point finite difference algorithm. Assuming a constant walking velocity, the azimuth velocity trajectory during continuous pointing performance should be symmetrical and parabolic, with a peak at 0° (i.e., arm straight out to the side) to coincide with target passage. To examine this behaviour in each of the azimuth calculation methods, proportional azimuth velocity trajectories were calculated for each trial by dividing azimuth velocity at each data collection frame by the maximum azimuth velocity achieved in that trial. This proportional measure enables comparisons between trials that involve even slight differences in peak azimuth velocity (Campos et al., 2009). The between-participant average profiles for each condition were fitted with second order polynomials and graphically presented.

To further examine how the azimuth pointing responses unfolded during the walking movements, constant error (i.e., signed error along the walking path) at 0° azimuth (i.e., arm pointing straight out to the side) was calculated as distance between the location of the participant and the location of the target. In effective spatial updating performance, constant error values should be near zero (i.e., passage of side-target at 0° azimuth; Campos et al., 2009). Azimuth angle at the occurrence of peak azimuth velocity was also measured. In continuous pointing performance, this should also occur at 0°

azimuth (Campos et al., 2009). These variables were each examined using 3 Method (SH, HY, RE) by 2 Vision (V, NV) by 8 Target (1-8) repeated measures ANOVAs.

Step characteristics

Characteristics of the step-cycle were examined using the left and right foot markers. For each trial, the displacement profiles of these markers (see top panel of Figure 2.07) were differentiated using a three-point finite difference algorithm to produce their respective velocity profiles (see bottom panel of Figure 2.07). To classify the start and end of each left and right foot swing event during the walking movements, the maximum peak of each constituent velocity profile was identified on the corresponding foot velocity trajectories. For each identified peak, the corresponding velocity start was identified as the first instance where the velocity trajectory dropped below 0.05 m/s on the fore side of the peak and the corresponding velocity end was identified as the first instance where the velocity dropped below 0.05 m/s on the aft side of the peak. The number of steps was calculated as the sum of the identified maximum peaks for the left and right foot velocity profiles.

Strides were considered displacements covered by the individual limbs during walking, measured as the distance along the walking path of the foot marker between the start and end of a corresponding foot event. Steps were considered distances between the two foot markers following a foot event (see top panel of Figure 2.07; e.g., Multon & Olivier, 2013), measured as the distance along the walking path between the left and right foot markers (i.e., a single stride is involved in two consecutive steps). Included for analyses were the number of steps, step length, and left and right stride lengths. The first

and last strides taken in each trial were not included in the measurement of step and stride lengths. Since multiple steps and strides occurred on each trial, step length and left and right stride lengths were reduced to average values for each trial. All step characteristics were examined using 2 Vision (V, NV) by 8 Target (1-8) repeated measures ANOVAs.

Significant arm deviations

In manual aiming tasks (for recent reviews see Elliott et al., 2010; Elliott et al., 2017), trajectory deviations provide insight into the CNS regulation of upper limb control. These deviations are inflections that indicate discrete variations in what was a previously smooth trajectory. They have been used to show that upper limb responses in accuracy-constrained tabletop reaching tasks are composed of two distinct and identifiable processes; this includes a pre-planned ballistic process and a subsequent online control process. These two processes are separated in an aiming trajectory by detecting discrete inflections in the velocity (or acceleration) traces. Examining the spatial and temporal kinematics involved with these trajectory deviations provides insight into the respective planning and online control processes used by the CNS to regulate reaching. By similarly classifying trajectory deviations in the shoulder plane of elevation trajectories of the continuous pointing movements, and examining the corresponding spatial-temporal kinematics, the goal is to provide novel insight into how the CNS regulates spatial updating during the course of a walking movement. Significant deviations will be classified below as fluctuations in the shoulder plane of elevation velocity that exceed the corresponding average shoulder plane of elevation velocity by ± 1 standard deviations. In this classification, trajectory deviations that exceed these criteria are considered to be

sufficiently different from average performance, in that they reflect purposeful and intended control. Of particular interest are how actual and perceived distances traveled unfold across the measured deviations, and how the deviations are temporally linked to the step-cycle.

Significant arm deviations were calculated using the shoulder plane of elevation velocity, which will be referred to as arm velocity in this subsection. In this continuous pointing task, a negative arm velocity is associated with keeping the finger fixated on the side target during forward walking. If the pointing task were performed in a smooth and continuous manner, a negative shoulder plane of elevation velocity would be maintained throughout each trial with little variability from a smooth linear or curvilinear profile. However, counter to what the term “continuous pointing” intuitively suggests (see Campos et al., 2009), the shoulder plane of elevation trajectories from the pointing and walking trials appear to be composed of a series of discrete discontinuities (see Figures 2.08 and 2.09). Measuring these discontinuities provides insight into the online control involved in aiming performance (e.g., Khan et al., 2006).

To quantify significant arm deviations, the shoulder plane of elevation trajectory was first differentiated using a three-point finite difference algorithm to produce an arm velocity trajectory. The arm velocity trajectory was then detrended by subtracting out the difference of a fitted second-order polynomial (see red-dashed line in Figure 2.08). A positive critical value was set as the mean arm velocity plus one standard deviation (see red horizontal line in Figure 2.10) and a negative critical value was set as the mean arm velocity minus one standard deviation (see green horizontal line in Figure 2.10).

Deviation starts were determined as the instances where the arm velocity trajectory traveled in a negative direction and reached below the positive critical value (i.e., indicative of the arm speeding up; see green circles in Figure 2.10). Deviation ends were determined as the instances where the arm velocity profile traveled in a positive direction and reached above the positive critical value (i.e., indicative of the arm slowing down; see red circles in Figure 2.10). Arm velocity trajectories were then examined between each deviation start and their associated deviation end. A deviation was deemed significant (i.e., see filled red and green circles in Figures 2.09 and 2.10) if the arm velocity trajectory between these indices achieved a magnitude equal to or less than the negative critical value (i.e., what is deemed as a significantly above average velocity). If the negative critical value was not reached between a coupled deviation start and end, one of two things happened: (a) if this occurred between the first deviation start and first deviation end for the trial (see square box in Figure 2.10), the current deviation end and the following (e.g., second) deviation start were removed and the velocity was re-examined using the next (e.g., second) deviation end. This was repeated until the negative critical value was reached between the first deviation start and a following deviation end; and (b) if this occurred mid-trajectory (i.e., not at the first deviation start; see ellipse in Figure 2.10), the current deviation start and the preceding deviation end were removed. In this case, the preceding deviation start and current deviation end formed the significant deviation.

The number of significant arm deviations per trial was examined using a 2 Vision (V, NV) by 4 Target (1-4) repeated measures ANOVA. The actual (i.e., the extent

covered on the actual distance traveled trajectory) and perceived distances traveled (i.e., the extent covered on the perceived distance traveled trajectory) were also calculated for each significant deviation. These were examined using 2 Vision (V, NV) by 4 Target (1-4) by 4 Deviation Number (1-4) repeated measures ANOVAs. The Deviation Number level was selected based on the grand mean of the aforementioned analysis of number of significant arm deviations per trial.

To examine where the significant arm deviation starts and ends occurred within the step-cycle, the starts and ends of the identified significant arm deviations were categorized to specific phases in the step-cycle. Specifically, with the exception of the first significant arm deviation start and last significant arm deviation end for each trial, all starts and ends were categorized as occurring in one of 8 step-cycle locations: double-stance preceding the swing phase (DS), before peak swing velocity (BPV), at peak swing velocity (PV) or after peak swing velocity (APV) for the left and right feet. Frequency counts for the V and NV trials were accumulated across all participants. For statistical analysis, the frequency count data were further reduced into four categories: early left foot, late left foot, early right foot and late right foot. Specifically, for each foot, the DS, BPV and PV categories were summed to make the early categories and the APV values represented the late categories. This was done in an attempt to equalize the categories into representative sizes of the step-cycle. To analyse the locations of significant arm deviation starts and ends in the step-cycle, two sets of Chi Square analyses were performed separately for the starts and ends (e.g., Rinaldi & Moraes, 2015). A first set of analyses examined the frequency count differences between the step-cycle phases

separately for the V and NV trials. The expected values for the categories in these analyses equalled ¼ of the total number of deviations for each analysis, which represented the null hypothesis of no between category differences in the total number of deviations. A second Chi Square analysis compared the V and NV trials. Here, the expected values for each category were based on the percentage of the total number of deviations in each step-phase category multiplied by the number of deviations in each vision condition (see Vincent, 2005).

All analyses were performed using SPSS software (IBM, Armonk, New York), with the exception of the Chi Square analyses that were performed manually in Microsoft Excel (Microsoft, Redmond, Washington). Alpha was set at $p < 0.05$ for all analyses. Violations of sphericity were accounted for using the Greenhouse-Geisser correction, although the reported degrees of freedom are the sphericity assumed values. All significant ANOVA effects involving more than two means were decomposed using Tukey's Honestly Significant Difference. Post-hoc tests for the Chi Square analyses were performed using SPSS software. Bonferroni adjusted binomial pairwise comparisons were used for the single category analyses, while adjusted standardized residuals that were converted to p-values and Bonferroni adjusted were used for the two category analyses.

2.4 – RESULTS

Actual velocity was used to examine whether participants adhered to the instruction to walk at a constant velocity during the continuous pointing movements. The analysis of actual walking velocity demonstrated a Vision by Distance interaction,

$F(7,63) = 4.14$, $p < 0.05$. This showed greater actual walking velocities in the V versus NV trials at all distances except 0.5 m (see Figure 2.11). A main effect of Vision, $F(1,9) = 13.65$, $p < 0.01$, showed greater actual walking velocity in the V (1.11 m/s) versus NV (1.04 m/s) trials, while a main effect of Distance, $F(7,63) = 26.14$, $p < 0.001$, showed greater actual velocities at 1.5, 2.0 and 3.0 m compared to 0.5 m (distance: 0.5 m = 0.783 m/s, 1.0 m = 1.04 m/s, 1.5 m = 1.13 m/s, 2.0 m = 1.16 m/s, 2.5 m = 1.17 m/s, 3.0 m = 1.17 m/s, 3.5 m = 1.12 m/s, 4.0 m = 1.03 m/s).

The step-cycle characteristics (i.e., number of steps, step length, and left and right stride lengths) were used to examine whether the kinematics of walking changed as a function of vision during the continuous pointing movements. Across all analyses of the step-cycle characteristics, only right stride length demonstrated a significant effect. Here, a main effect of Vision, $F(1,9) = 6.46$, $p < 0.05$, showed a longer right stride length in the V (1.26 m) versus NV (1.22 m) trials. The grand means for all step analyses are included in Table 2.4. Collectively, the results in this paragraph show that performers walked faster in the V versus NV trials, and that they adhered to the instructions by maintaining near constant velocities in the middle portions of the walking movements. Further, despite showing minimal differences in the step characteristics, the greater velocity in the V trials likely resulted from a slightly longer right stride length.

The RMS error of perceived-actual distance traveled (and velocity) was used to examine how well the calculated measure of perceived distance traveled (and velocity) approximated the actual measure of perceived distance traveled (and velocity) across the entire walking trials. The analysis of RMS error of perceived-actual distance traveled

revealed a significant Method by Vision interaction, $F(2,18) = 5.26$, $p < 0.05$. This showed higher RMS error for HY (0.48 m) than RE (0.44 m) and SH (0.45 m) in the V trials, and higher RMS error for HY (0.52 m) and SH (0.53 m) than RE (0.48 m) in the NV trials. The analysis of RMS error of perceived-actual velocity demonstrated a Method by Target interaction. This showed that across all target locations, HY (Target: 1 = 1.46 m; 2 = 1.40 m; 3 = 1.34 m; 4 = 1.45 m; 5 = 1.94 m; 6 = 1.79 m; 7 = 1.66 m; 8 = 1.51 m) demonstrated greater RMS error than RE (Target: 1 = 0.79 m; 2 = 0.71 m; 3 = 0.68 m; 4 = 0.72 m; 5 = 0.88 m; 6 = 0.80 m; 7 = 0.76 m; 8 = 0.67 m) and SH (Target: 1 = 0.90 m; 2 = 0.90 m; 3 = 0.86 m; 4 = 0.90 m; 5 = 1.02 m; 6 = 0.99 m; 7 = 0.99 m; 8 = 0.95 m). In addition, a Method by Vision interaction showed lower RMS error for HY in the NV versus V trials (HY: V = 1.63, NV = 1.50; RE: V = 0.762, NV = 0.738; SH: V = 0.942, NV = 0.935). A main effect of Method, $F(2,18) = 30.40$, $p < 0.001$, showed greater RMS error for HY (1.57) compared to RE (.750) and SH (.938), while a main effect of Target, $F(7,63) = 5.24$, $p < 0.05$, did not yield any significant differences. Overall, the RMS error scores for perceived-actual distance traveled and velocity appeared consistently lowest for the RE method.

Perceived distance traveled was used to examine the participant's perceived spatial location during the course of the continuous pointing movements, with particular interest as to whether this changed as a function of vision condition. Prior to performing the sliding AVOVAs on perceived distance traveled, an initial omnibus test was performed to determine whether perceived distance traveled increased as a function of actual distance traveled. This was necessary because the sliding ANOVA technique

examined between condition differences at specified distance intervals, without comparing differences between these intervals. For this analysis, vision and target conditions were pooled at the distance intervals ranging 0.5 – 4.0 m, in 0.5 m increments. This analysis was performed using a repeated measure ANOVA with 8 levels of Distance (0.5-4.0 m). The results showed significant differences between all distances except between 0.5 and 1.0 m, 1.0 and 1.5 m, 1.5 and 2.0 m, 2.0 and 2.5 m, 2.5 and 3.0 m, 3.0 and 3.5 m, and 3.5 and 4.0 m (0.5 m = 0.34 m; 1.0 m = 0.89 m; 1.5 m = 1.44 m; 2.0 m = 1.89 m; 2.5 m = 2.40 m; 3.0 m = 2.91 m; 3.5 m = 3.35 m; 4.0 m = 3.80 m). Therefore, perceived distance reliably increased as a function of actual distance.

F-values for the sliding ANOVA analysis of perceived distance traveled are presented in Table 2.5. In using the sliding ANOVA technique, the most relevant effects were interpreted as the ones that showed consistent patterns of results across multiple iterations of analysis. Therefore, to aid in interpretation, the perceived distance traveled results were grouped according to statistical effects. Specifically, significant Method by Target interactions were demonstrated at the analysis iterations ranging 1.0-4.0 m (see Figure 2.12). At 1.0 m, post hoc testing did not demonstrate any significant mean differences. At 1.5 m, perceived distances traveled were greater at target 5 for HY and RE compared to SH. For target 6, perceived distance traveled was greater for HY compared to SH. At 2.0 m, perceived distance traveled was greater for SH versus HY at Target 4, and for RE versus SH at target 5. At 2.5 m, perceived distance traveled was greater for HY and RE compared to SH at target 5, and was greater for HY than SH at targets 6 and 7. At 3.0 m, perceived distance traveled was greater for HY and RE compared to SH at

targets 5, 6 and 7. At 3.5 m, perceived distances traveled were greater for HY and RE compared to SH at target 5, and was greater for RE than SH at targets 6 and 7. At 4.0 m, perceived distances traveled were greater for HY and RE than SH at targets 1, 5, 6, 7 and 8, and for HY than SH at target 2. Collectively, these results showed consistently greater perceived distances traveled in HY and RE compared to SH, especially toward the end of the walking movements.

The sliding ANOVAs also showed significant Method by Vision interactions at the analysis iterations of 1.0 and 1.5 m. At 1.0 m, perceived distances traveled were greater in the NV trials for HY (V = 0.864 m; NV = 0.923 m) and RE (V = 0.864 m; NV = 0.921 m) compared to SH (V = 0.890 m; NV = 0.885 m). No differences were demonstrated in the V trials. At 1.5 m, perceived distance traveled in the V trials was greater for HY (1.48 m) compared to RE (1.41 m) and SH (1.39 m). In the NV trials, perceived distances traveled were greater for HY (1.47 m) and RE (1.45 m) compared to SH (1.40 m).

The Target main effect at 1.5 m did not show any post hoc significant mean differences. The Vision main effects at 3.0 (V = 2.99 m; NV = 2.82 m), 3.5 (V = 3.46 m; NV = 3.24 m) and 4.0 m (V = 3.94 m; NV = 3.66 m) all showed greater perceived distances traveled in the V versus NV trials (see Figure 2.13 for data in the RE condition pooled across target location). These results showed that irrespective of method or target, perceived distance traveled was greater for the V versus NV trials. Significant Method main effects were demonstrated at 2.5, 3.0, 3.5 and 4.0 m. At 2.5 (HY = 2.48 m; RE = 2.43 m; SH = 2.30 m) and 3.0 m (HY = 2.99 m; RE = 2.94 m; SH = 2.79 m), perceived

distance traveled was greater for HY compared to SH. At 3.5 m (HY = 3.40 m; RE = 3.49 m; SH = 3.16 m), perceived distance traveled was greater for RE compared to SH. At 4.0 m (HY = 3.98 m; RE = 3.94 m; SH = 3.48 m), perceived distance traveled was greater for HY and RE compared to SH.

Constant error was used to examine the participant's positions along the walking path, with respect to the side-target, at the instance of 0° azimuth. Effective spatial updating demonstrates values close to 0° in this measure. Here, more positive values indicated locations further along the walking path in relation to the target. This analysis demonstrated a Vision by Target interaction, $F(7,63) = 4.39$, $p < 0.05$. This showed greater constant error in the NV versus V trials at targets 4 and 8 (see Figure 2.14). A Method by Vision interaction, $F(2,18) = 4.63$, $p < 0.05$, showed that the greater constant error for SH (V = 0.13 m; NV = 0.29 m) compared to HY (V = 0.05 m; NV = 0.17 m) and RE (V = 0.06 m; NV = 0.17 m) was more extreme in the NV trials. A main effect of Vision, $F(1,9) = 6.78$, $p < 0.05$, showed greater constant error in the NV (.208 m) versus V (.081 m) trials. Finally, a main effect of Target, $F(7,63) = 8.30$, $p < 0.001$, showed greater constant error at target 4 compared to targets 1, 5, 6 and 7; lower constant error at target 5 compared to targets 2, 3, 4, 6 and 8; and lower constant error at target 7 versus target 2 (target: 1 = 0.103 m, 2 = 0.238 m, 3 = 0.186 m, 4 = 0.257 m, 5 = -0.007 m, 6 = 0.104 m, 7 = 0.066 m, 8 = 0.211 m).

Azimuth angle at peak azimuth velocity was used to examine the azimuth angle at which the pointing responses reached maximum velocity during the continuous pointing trials. Effective continuous pointing demonstrates values close to 0° in this measure,

which is used as an assessment of perceived target passage. The analysis of azimuth angle at peak azimuth velocity only demonstrated a main effect of Target, $F(7,63) = 3.20$, $p < 0.01$. This showed a significantly greater azimuth angle at peak azimuth velocity for target 4 compared to targets 5 and 6 (target: 1 = 0.540°, 2 = -0.591°, 3 = 0.537°, 4 = 3.54°, 5 = -4.26°, 6 = -2.84°, 7 = -1.63°, 8 = 1.51°). Overall, this showed that participants achieved peak azimuth velocity near 0° azimuths in all conditions and were thus, performing the continuous pointing responses as instructed. In performing the pointing responses, the proportional azimuth trajectory should also increase upon target approach, peak at target passage and decrease after target passage. To examine this, second order polynomials were fit to the proportional azimuth velocity trajectories for each condition. The second order polynomials are presented in Figures 2.15 (vision trials) and 2.16 (no-vision trials) and the r-squared values of these fits are presented in Table 2.6. Visual inspection of these data show that the RE method most effectively captured this characteristic response at all target locations.

The significant arm deviations were trajectory fluctuations calculated using the aforementioned trajectory parsing procedure. They were examined according to number per trial, actual and perceived distances traveled between the start and end of each deviation, and location in the step-cycle of the start and end of each deviation. Significant arm deviations were examined using only the walking trials performed to targets 1-4. This was because the shoulder plane of elevation trajectory (i.e., SH method), which was used to calculate significant arm deviations, was the most effective in estimating perceived distance traveled in movements to these targets (see above for perceived distance traveled analysis). Analysis of

the number of significant arm deviations per trial showed no significant effects (grand mean = 4.88). Analysis of actual distance traveled per significant arm deviation demonstrated a main effect of Deviation Number, $F(3,27) = 4.77$, $p < 0.05$. However, post hoc analyses did not indicate any significant mean differences (grand mean = 0.933 m). The analysis of perceived distance traveled per significant arm deviation demonstrated a Vision by Target interaction, $F(3,27) = 3.29$, $p < 0.05$. This showed greater perceived distances traveled per significant arm deviation in the V trials compared to the NV trials at Targets 2, 3 and 4 (see Figure 2.17). A main effect of Vision, $F(1,9) = 9.54$, $p < 0.05$, showed greater perceived distance traveled per significant arm deviation in the V (.979 m) versus NV (.900 m) trials. A main effect of Deviation Number, $F(3,27) = 10.03$, $p < 0.01$, showed greater perceived distance traveled per significant arm deviation in deviation 1 compared to deviation 4 (Deviation: 1 = 1.23 m, 2 = 1.01 m, 3 = 0.873 m, 4 = 0.650 m).

When examined in regards to location in the step-cycle, the analysis of significant arm deviation starts for the V, $\chi^2(3) = 616.99$, $p < 0.01$, and NV, $\chi^2(3) = 736.58$, $p < 0.01$, trials showed significant differences in the frequency counts between the phases of the step-cycle. For both trial types, the greatest frequency counts appeared in the early right category and moderately high counts appeared in the late left category (see Figure 2.18). The analysis comparing the V and NV trials was not significant, $\chi^2(3) = 2.24$, $p > 0.10$. Similar results were demonstrated for the significant arm deviation ends, where the analysis of the V, $\chi^2(3) = 856.76$, $p < 0.01$, and NV, $\chi^2(3) = 948.39$, $p < 0.01$, trials showed significant differences in the frequency counts between the phases of the step-cycle. Here, the frequency counts appeared greatest in the early right category, while the early left and late left categories both

showed greater frequencies than the late right category (see Figure 2.18). The analysis comparing the V and NV trials was not significant, $\chi^2(3) = 4.32$, $p > 0.10$.

Considering that the previous analyses failed to show differences between the V and NV trials for both the significant arm deviation starts and ends, an additional Chi Square analysis was run by pooling the V and NV trials and comparing the frequency counts of the significant arm deviation starts and ends. The expected values were based on the percentage of the total number of deviations in each step-phase category multiplied by the total number of deviations in each significant arm deviation index condition. This analysis was significant, $\chi^2(3) = 164.72$, $p < 0.01$, showing relatively greater counts in the late left and late right categories for the significant arm deviation starts, and relatively greater frequencies in the early left and early right categories for the significant arm deviation ends (see Figure 2.19). Collectively, these results showed that the vision versus no-vision differences in perceived distance traveled (i.e., accurate in vision conditions and under-perception in no-vision conditions) were reflected in the significant arm deviations. Additionally, regardless of vision condition, starts and ends of the significant arm deviations occurred with the greatest frequency in the early right foot swing portion of the step-cycle.

2.5 – DISCUSSION

Study 1 achieved the intended goal of using joint angle kinematics to measure perceived self-motion during the continuous pointing task (e.g., Campos et al., 2009). Of the three azimuth calculation methods examined in this study, the RE method was the most effective in demonstrating perceptions of perceived distance traveled and a characteristic unfolding of the azimuth angle trajectory. This could be attributed to two

important features of the RE method: a) the calculation of azimuth angle using combined shoulder and trunk rotations, and b) the removal of signal artefacts created by natural gait.

Compared to the SH method, RE demonstrated a lower RMS error of perceived-actual distance traveled and was better able to capture perceived distances traveled throughout entire walking trajectories. This was made possible by the inclusion of both shoulder and trunk rotations in the azimuth angle calculation. Considering the length of the walking path (i.e., 4.5 m) and the lateral proximity of the side targets (i.e., 2-3 m), both shoulder and trunk rotations were required to keep the finger localized on the target throughout the duration of the continuous pointing movements. The importance of this can be seen by examining the SH method, which relied only on the shoulder plane of elevation in formulating azimuth angle. Problematic for the SH method was that when shoulder rotation reached an end range of motion before the end of the walking path, this created an artificially (i.e., non-perceptual) induced under-perception of distance traveled. This could be seen as early as 2.5 m down the walking path to some of the target locations (i.e., targets 5-7). By 4.0 m, this included most target locations (i.e., targets 1 and 5-8). These results showed that using the SH method for calculating upper limb kinematics (i.e., significant arm deviations) was limited to specific target locations.

The RE method also provided the most stable measure of perceived self-velocity. Specifically, the RE method showed a lower RMS error of perceived-actual velocity compared to the HY method. Evidence of this can be seen in the lower part of Figure 2.06, where these effects could be attributed to the removal of gait oscillations from the trunk rotation trajectory. That is, even though RE and HY were both constructed by

summing together the shoulder and trunk trajectories, RE was removed of these trajectory oscillations prior to summation while HY was not. Although this process did not significantly impact the resulting calculations of perceived distances traveled, the noise created by the trajectory oscillations clearly had an impact on the derived measure of perceived self-velocity (e.g., Robertson, 2013). Although not further examined in this study, this should be an important consideration for studies more specifically interested in examining self-velocity (Siegle et al., 2009).

The methodological approach also effectively captured the performance characteristics of the azimuth angle trajectory. Typically, the azimuth velocity profile in the continuous pointing task peaks at 0° (i.e., arm straight out to the side) and decreases in a parabolic manner toward the extremes of the azimuth range (i.e., in front of and behind the performer; Campos et al., 2009; Frissen et al., 2011). This pattern is indicative of perceived target passage. Analysis of azimuth angle at peak azimuth velocity showed that peak azimuth velocities were localized near 0° regardless of method (grand mean of study = -0.398°). Although this study did not examine the proportional azimuth velocity profiles in great detail (e.g., Campos et al., 2009), a glance at Figures 2.15 and 2.16 showed that RE was most effective at capturing this profile and was well fitted with second-order polynomials. Replicating the proportional azimuth velocity profile with the current methodology sets an important example for future work that intends on examining mental (i.e., spatial) updating in tasks that involve no forward displacement, such as imagined walking (Campos et al., 2009) and walking in place (Frissen et al., 2011).

Another important methodological consideration for the continuous pointing task involved differences in outcome measures due to differences in target-relative start positions across performance trials (Campos et al., 2009; Siegle et al., 2009). Such effects are referred to as start point dependencies and occur when multiple start and/or target locations are used for a series of continuous pointing trials. Using different start/target locations served the purpose of subtlety altering motor performance on each trial so that continuous pointing was reflective of spatial updating and not a memory-based process. Start point dependencies were reported for various outcome measures (e.g., the proportional azimuth velocity profile) in Campos et al. and Siegle et al. In these studies, continuous pointing trials were performed to the same target location from one of four different starting locations. In the current study, participants always started from the same start location, but pointed to one of eight different side target locations on each trial. As a result, start point dependencies (i.e., main effects or interactions involving Target) were shown in perceived distance traveled, constant error at arm azimuth angle, azimuth angle at peak azimuth velocity, RMS error of perceived-actual velocity and perceived distance traveled per significant arm deviation. A few things must be considered when interpreting these start point dependences.

First, some start point dependences can be very informative about the effectiveness of the apparatus. For example, the analysis of perceived distance traveled showed Method by Target interactions across many of the distance iterations in the sliding ANOVA (see Table 2.5). This was very informative about a stable pattern of result across trials, as it highlighted the ineffectiveness of the SH method in measuring

perceived distance traveled to the more laterally displaced (i.e., 3 m) side-targets when performers were further down the walking path. This finding resulted in targets 1-4 being used for the significant arm deviation analysis and in targets laterally displaced 2.0 m being used for Studies 2 and 3.

Second, the start point dependencies reported in other studies have been shown to minimally impact participants overall patterns of responding (Campos et al., 2009; Siegle et al., 2009). This notion is graphically displayed in Figures 2.12, 2.15 and 2.16, where relative similarities existed amongst target locations despite there being absolute differences in performance. Furthermore, the start point dependencies in the current study only impacted the measures involved with pointing and had no impact on actual forward walking performance. That is, regardless of the target location, forward locomotive performance was consistent across trials. The general consistency in the step characteristics (i.e., number of steps, and step and stride lengths) between V and NV trials supported this claim. Therefore, with the exception of perceived distance traveled, the start point dependencies in this study appeared to minimally impact the overall patterns of responses. Even in the case of perceived distance traveled, these start point dependences appeared to factor out when averaged across targets (see Figure 2.13). Taken together, the necessity of using multiple start and/or target locations outweighed any minimal impact associated with start point dependencies.

This study also demonstrated differences between continuous pointing performance during vision and no-vision locomotion. That is, compared to the baseline measures provided in continuous pointing with vision, continuous pointing without vision

demonstrated an under-estimation of perceived distance traveled from approximately 3.0 m onwards (see Table 2.5). The fact that this was shown as a series of Vision main effects at the distance iterations ranging from 3.0-4.0 m indicated that it was a general performance trend unattributed to a specific target location or method of measurement. This finding was corroborated by greater constant error (i.e., location further along the walking path) at 0° azimuth in the NV trials, which indicated that participants were further along the walking path when perceived to be aligned with the side-target. Azimuth angles at peak azimuth velocity were also close to zero and demonstrated no difference between V and NV trials. This means that regardless of vision condition, participants were aligning peak azimuth velocity with their arm pointed nearly straight out to the side (i.e., 0° azimuth). This showed that participants were approximating perceived target passage correctly in both vision conditions, but misperceived this physical position in the NV trials.

These results were counter to our initial expectation of there being minimal difference between V and NV performance. It was also inconsistent with many other reports showing effective NV walking performance to targets up to 15-20 m away (e.g., Loomis & Philbeck, 2012; Rieser et al., 1990). However, a closer examination of the V versus NV differences in perceived distance traveled showed that they were not out of the realm of typical walking performance. This was due to the relatively small differences between vision conditions in this study (i.e., less than or equal to 28 cm). Further, these results (see Figure 2.13) appeared to visibly resemble those presented in Figure 2 of Campos et al. (2009). Importantly, the Campos et al. study found no significant

differences between vision and no-vision continuous pointing. Considering the fine-grained methodological and analysis techniques used in the current study, perhaps the V versus NV differences were detected at shorter distances in this study compared to others (e.g., Fukusima et al., 1997). That is, the errors in NV performance in other studies might have only accumulated to the point of statistical significance at distances of 15-20 m.

Irrespective of the methodological differences between studies, the under-estimation of NV continuous pointing was a trend consistent with other work that examined spatial updating (which was often indicated as target overshoot error; e.g., Philbeck et al., 2008; Rieser et al., 1990). According to a leaky integrator model (Lappe & Frenz, 2009), the updating of a task-relevant state parameter in the CNS during walking (e.g., distance traveled) was under-estimated in NV conditions. If the state parameter in the current study represented a cumulative estimation of perceived distance traveled, this model would predict under-estimation at all iterations of CNS spatial updating. Support for this finding was provided by our examination of significant arm deviations, which we considered to represent individual spatial updating iterations performed by the CNS during locomotion. Interestingly, greater perceived distances traveled per significant arm deviation were experienced in the V versus NV trials. This supported the idea that perceptual differences in NV walking were accumulated across a series of updating units.

Furthermore, in both V and NV trials, the starts and ends of the significant arm deviations had greater frequency counts early in the right foot swing phase. Related findings have been demonstrated in other tasks involving simultaneous upper and lower

limb control (e.g., walking and prehension or pointing), where discrete upper limb actions had been tied to specific phases of the step-cycle (Chiovetto & Giese, 2013; Nashner & Forssberg, 1986; Rinaldi & Moraes, 2015). In these studies, this timing had been suggested to either increase dynamic stability, assist in maintaining forward progression, reflect neural links between the discrete control involved in the upper limb and the rhythmic control involved in the lower limb, or some combination of the above. For the continuous pointing task, the strong linkage of significant arm deviations to the early portion of right leg swing was especially interesting, considering that upper limb control in continuous pointing was omnipresent and not likely to require additional stability or assistance in maintaining forward progression at a specific phase of the step-cycle. Our contention was that by linking the starts and ends of significant arm deviations to the early right foot swing phase, the CNS anchored iterative spatial updating to a consistent part of the step-cycle. Presumably, this served to aid in estimating distance traveled across iterative segments, after which it could be added to an ongoing cumulative sum. Once again, this was consistent with a leaky integrator model, which attributed updating error to CNS integration and estimation across task-specific updating iterations (Lappe & Frenz, 2009).

An alternative explanation for the significant arm deviations could be that they represented a natural by-product of the biomechanics of walking and thus, were not reflective of purposeful units of CNS spatial updating. More specifically, it was possible that the significant arm deviations represented deviations from the unidirectional and continuous pointing trajectory created by the oscillatory arm swing trajectory that

typically accompanies forward walking (i.e., anti-phase arm swing with respect to the step-cycle). In light of this possibility, additional data were collected on one participant who performed 20 walking trials (i.e., walking with typical arm swing), 20 continuous pointing trials (i.e., walking while pointing at the side target) and 20 imagined walking continuous pointing trials (i.e., imagined walking while pointing at the imagined updated location of the side target; Campos et al., 2009). The purpose of this data was to examine whether the shoulder plane of elevation trajectory of the continuous pointing movements contained component frequencies reflective of the oscillatory arm trajectory typical to forward walking. Figure 2.20 shows averages of the Fast Fourier Transforms performed on the shoulder trajectories for these conditions [5]. The top part of Figure 2.20 shows that the largest frequency component of the shoulder plane of elevation signal during typical walking was ~1 Hz, which makes sense considering that the average walking speed of Study 1 was ~1 m/s. Importantly, the continuous pointing and imagined continuous pointing shoulder trajectories did not demonstrate this noticeable 1 Hz component. This suggested that the arm swing involved in typical walking was not a predominant component in the continuous pointing trajectory.

Additionally, the significant arm deviations were determined using conservative trajectory parsing criteria (i.e., +/- 1 standard deviation from the average of the detrended arm velocity) that had been similarly implemented in another study to decipher arm reaches from the oscillatory arm trajectory typical to forward walking (Rinaldi & Moraes,

[5] Walking and continuous pointing, and continuous pointing and imagined continuous pointing were presented on separate graphs because slightly different kinematic criteria were used for defining the trajectory starts and ends in each comparison.

2015). Although the coupling of a significant arm deviation start with the early right foot swing likely took advantage of the backward arm movement that typically coincided with a forward right step, we suggest that the former was not caused by the latter (e.g., Muzii et al., 1984). Overall, we are comfortable suggesting that the significant arm deviations represented discrete online iterations of spatial updating and were not artefacts of the typical walking arm swing trajectory superimposed on the pointing movement.

Overall, the most novel contribution of this study was that the trajectory parsing criteria effectively identified iterative units of CNS spatial updating, and that the perceptual differences between V and NV walking were identified in these units. To further examine the effectiveness of this parsing procedure, Study 2 used the continuous pointing task to examine spatial updating in sensory conditions where strong CNS perceptual differences have been demonstrated. This specifically involved no-vision walking (i.e., spatial updating) before and after sensory adaptation periods characterized by prolonged exposures to visual and proprioceptive sensory cue conflicts (Rieser et al., 1995). These conflicts typically evoke sensory recalibration, where performers generally under-perceive their location in space following exposures to low visual gains (i.e., visual rate lower than proprioceptive rate) and over-perceive their location in space following exposures to high visual gains (i.e., visual rate greater than proprioceptive rate). Of interest in Study 2 was whether the continuous pointing task revealed these perceptual differences in no-vision walking and if they were reflected in the iterative spatial updating units identified by the significant arm deviations.

Figure 2.01. Anatomical locations of the retro-reflective markers. Markers are superimposed with a white circle for better clarity.

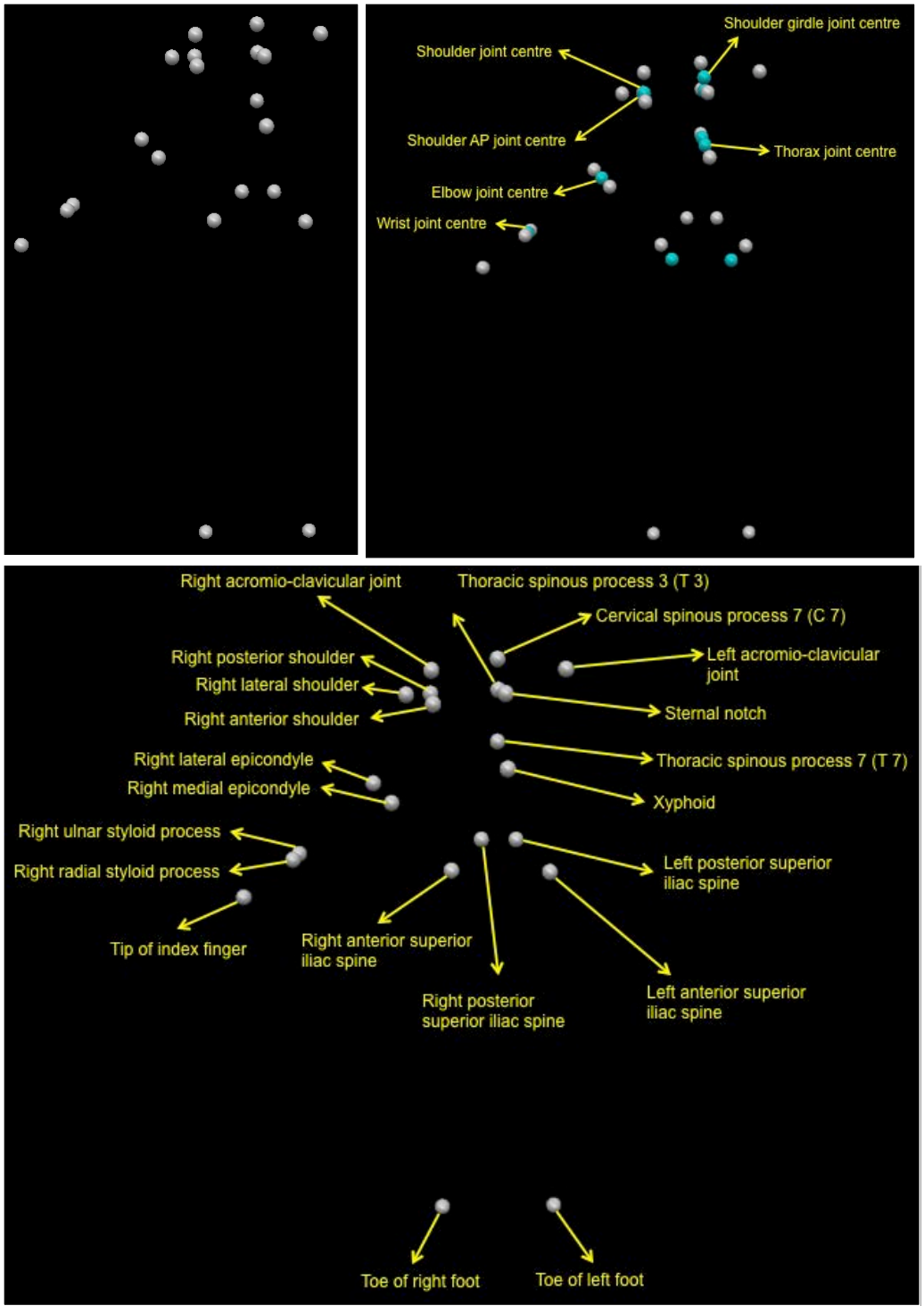

Figure 2.02. Anatomical locations of retro-reflective markers rendered in Visual 3D. This includes marker layout (Top left), marker layout with the virtual markers labeled (Top right), and marker layout with the anatomical markers labeled (Bottom).

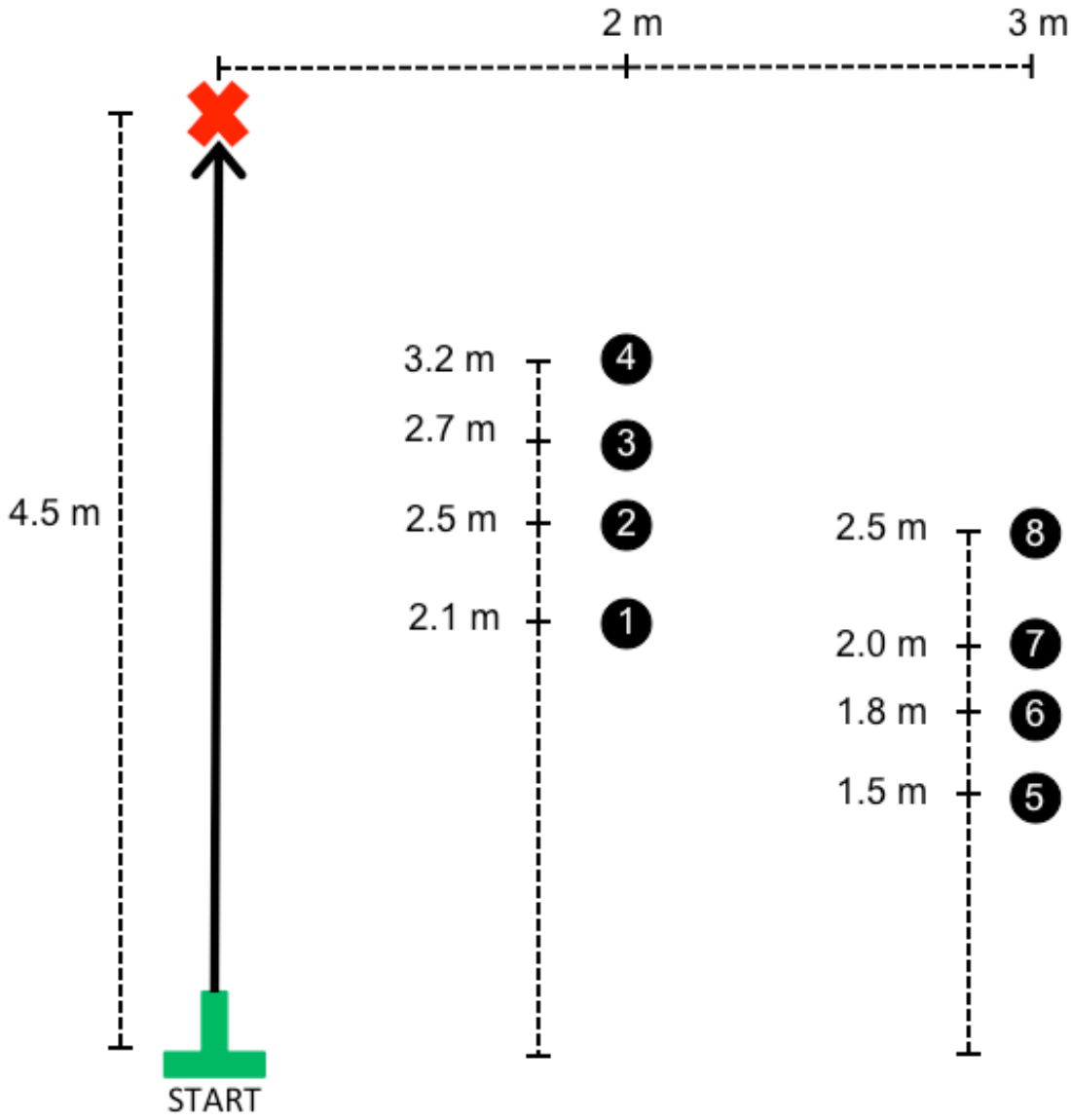

Figure 2.03. Above view schematic of the experimental layout of Study 1. Inverted green 'T' represents start location, red 'X' represents end location, solid black arrow represents intended linear walking path, and black circles represent side-target locations. Numbers inside black circles indicate target number. Dashed black lines indicate distances along and beside walking path.

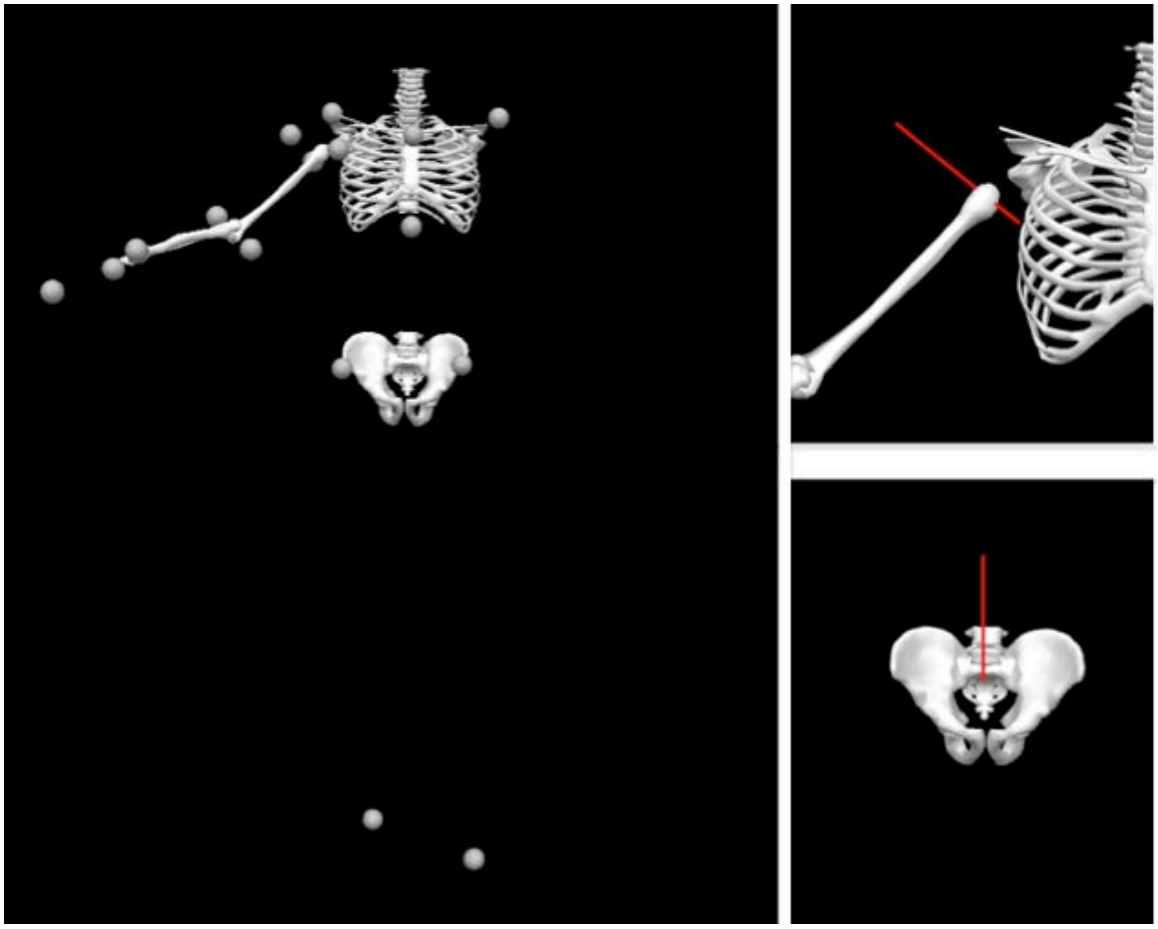

Figure 2.04. Left: Body segments created in Visual 3D using the anatomical and virtual markers. These segments represent the pelvis, thorax, right upper arm and right forearm. Upper right: Shoulder plane of elevation, with red line indicating axis of rotation. Bottom right: Trunk axial rotation, with red line indicating axis of rotation.

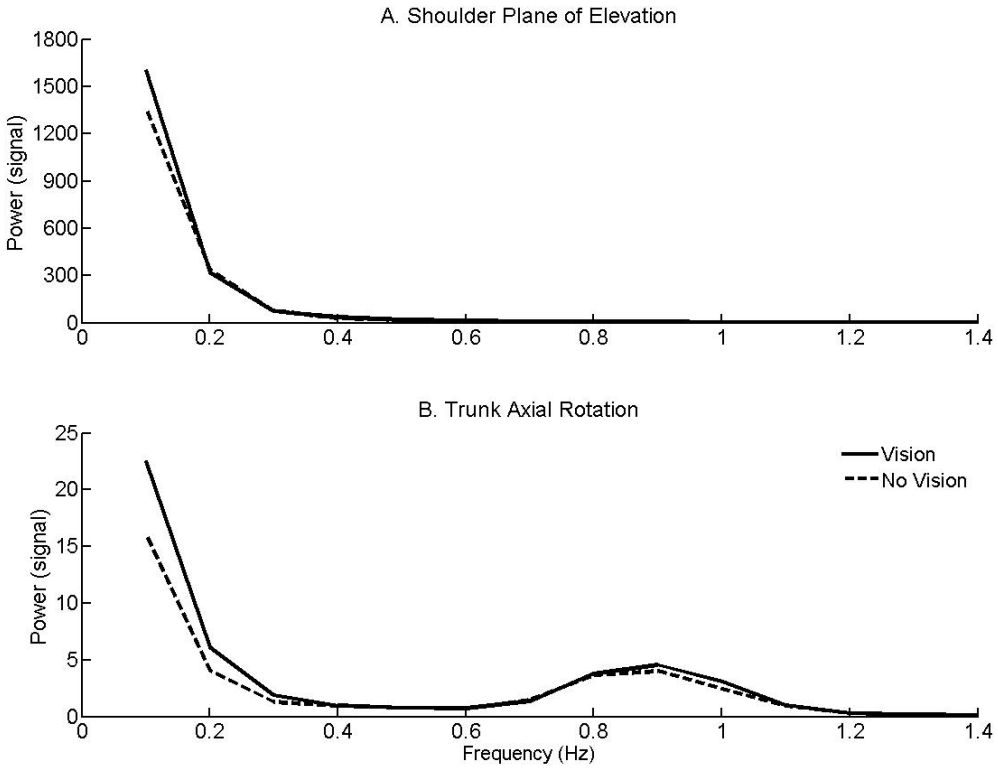

Figure 2.05. Top: Average power spectrum of the shoulder plane of elevation (top) and trunk axial rotation (bottom) trajectories. Solid lines represent vision trials; dashed lines represent no-vision trials.

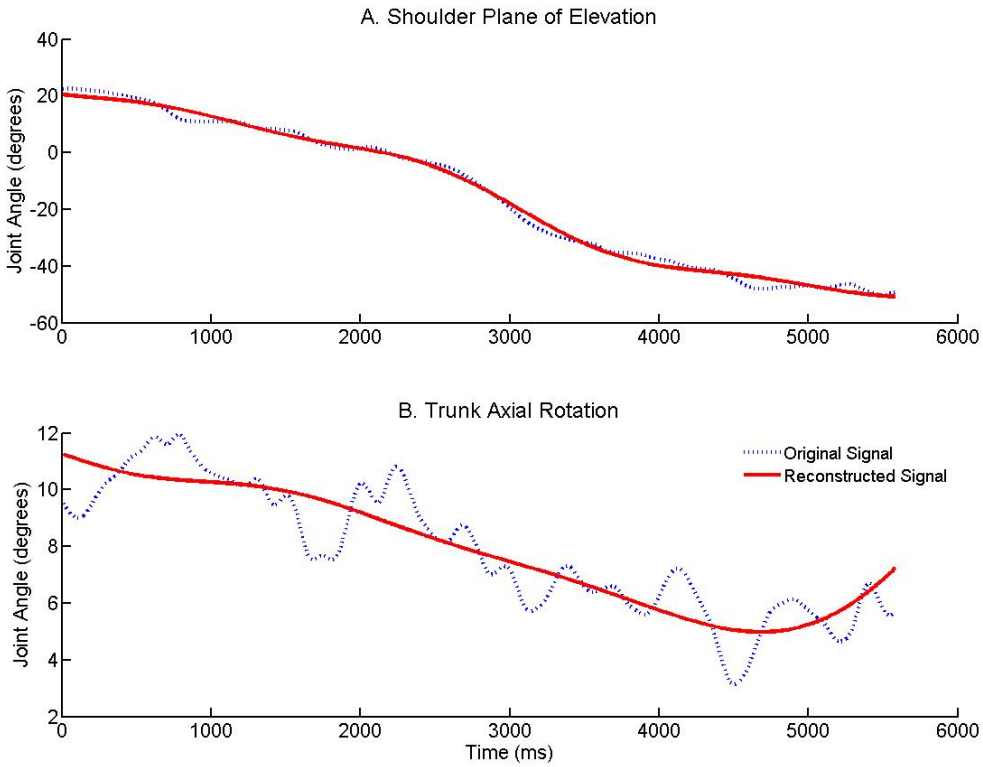

Figure 2.06. Top: Shoulder plane of elevation trajectory measured from the performance of a single representative continuous pointing trial. Positive values indicate finger pointing in a forward direction, negative values indicate finger pointing in a backward direction and zero indicates finger pointing straight out to the side. Dashed blue line represents the original joint angle trajectory filtered with a 6 Hz Butterworth filter; solid red line represents the signal reconstructed using the frequency components less than 0.5 Hz. Bottom: Trunk axial rotation trajectory. Positive y-axis values indicate leftward rotation, negative values indicate rightward rotation and zero indicates forward facing.

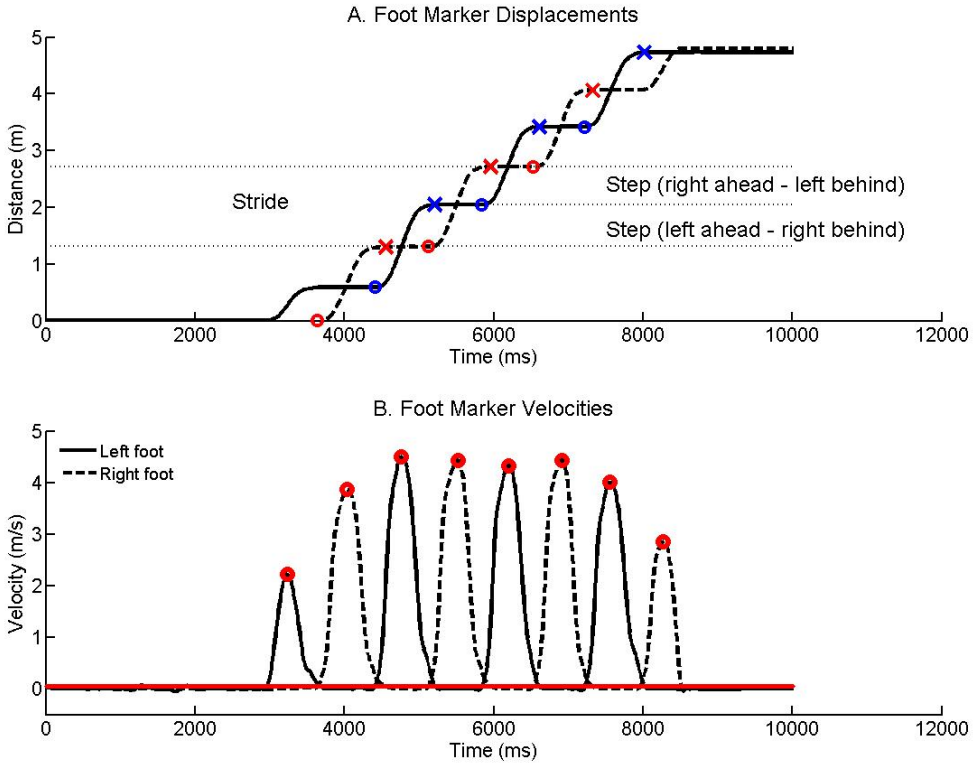

Figure 2.07. Top: Left (solid line) and right (dashed line) foot marker displacements during a typical continuous pointing trial. Circles represent starts of foot forward displacements; x's represent ends of foot forward displacements. These are indicated separately on the left (blue) and right (red) foot displacements. Horizontal dashed lines on the left side of the figure indicate a single right foot stride; horizontal dashed lines on the right side of the figure indicate a left step followed by a right step. Bottom: Left (solid line) and right (dashed line) foot marker velocities during a typical continuous pointing trial. Red circles indicate the maximum peaks of the individual velocity profiles. Red solid line indicates the criterion used to identify respective starts and ends of foot forward displacements. The criterion was set at 0.05 m/s.

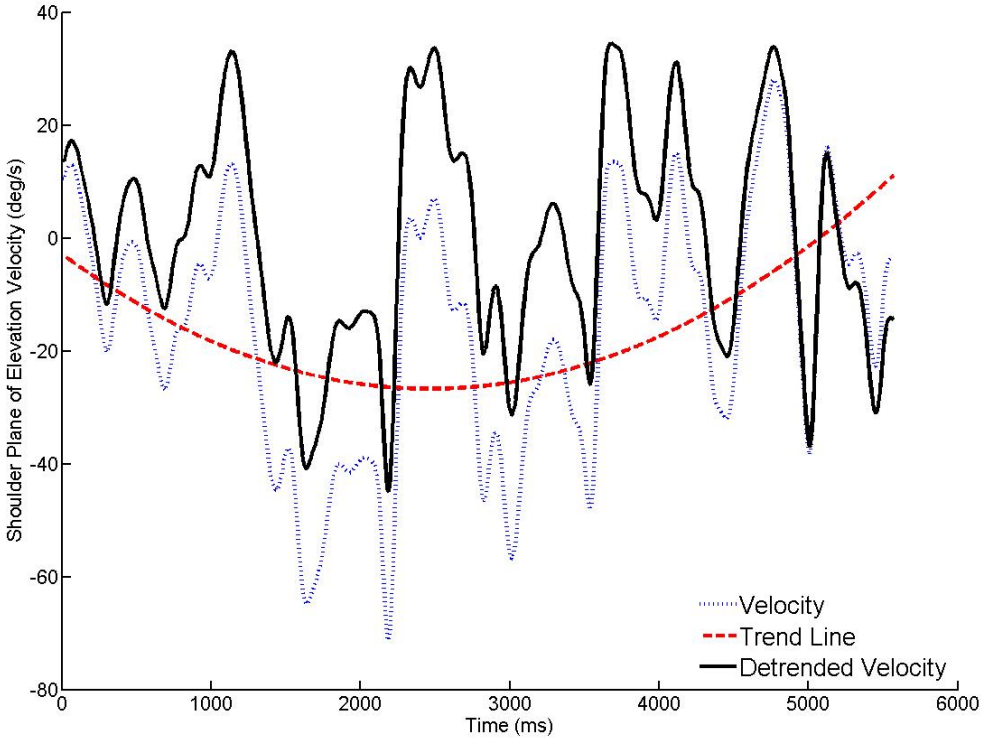

Figure 2.08. Detrending of the shoulder plane of elevation velocity in calculating significant arm deviations. Blue dashed line represents the shoulder plane of elevation velocity of a representative continuous pointing trial. Red dashed line represents the trend line (i.e., a second-order polynomial) fitted to the shoulder plane of elevation velocity. The trend reflects an overall negative velocity because the shoulder plane of elevation progresses from positive (i.e., forward pointing) to negative (i.e., backward pointing) during task performance. Black solid line represents the detrended shoulder plane of elevation velocity.

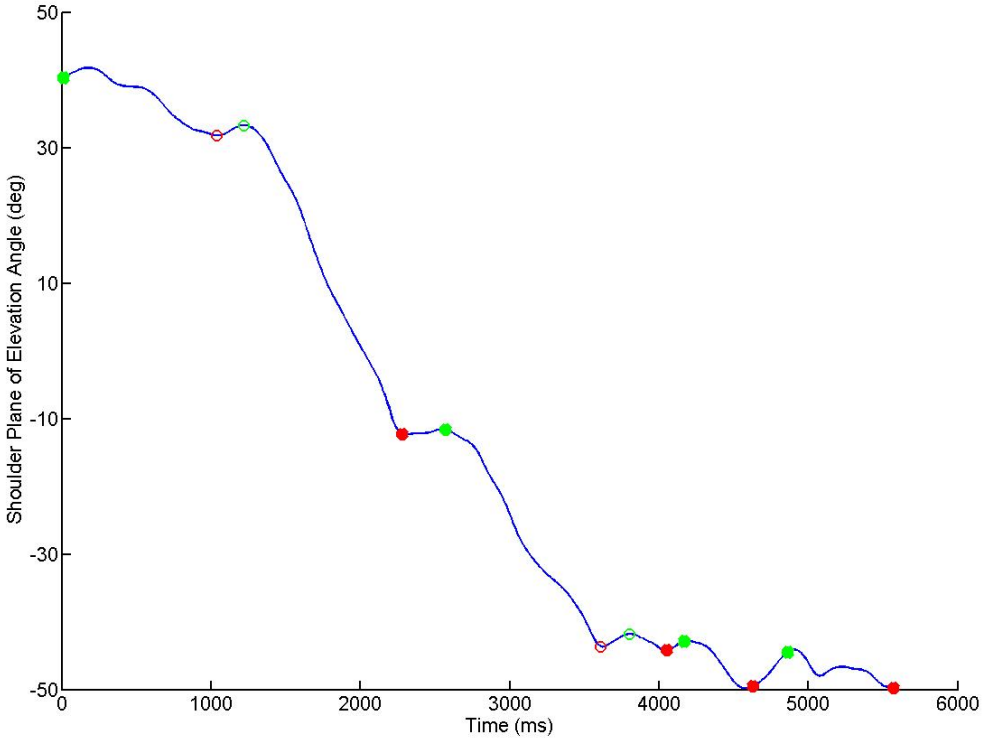

Figure 2.09. Significant arm deviations demonstrated on the shoulder plane of elevation trajectory. Blue solid line indicates the shoulder plane of elevation of a representative trial. Positive values indicate finger pointing in a forward direction, negative values indicate finger pointing in a backward direction and zero indicates finger pointing straight out to the side. Filled green circles represent significant deviations starts; filled red circles represent significant deviation ends; open green and red circles represent respective starts and ends of trajectory deviations not deemed significant.

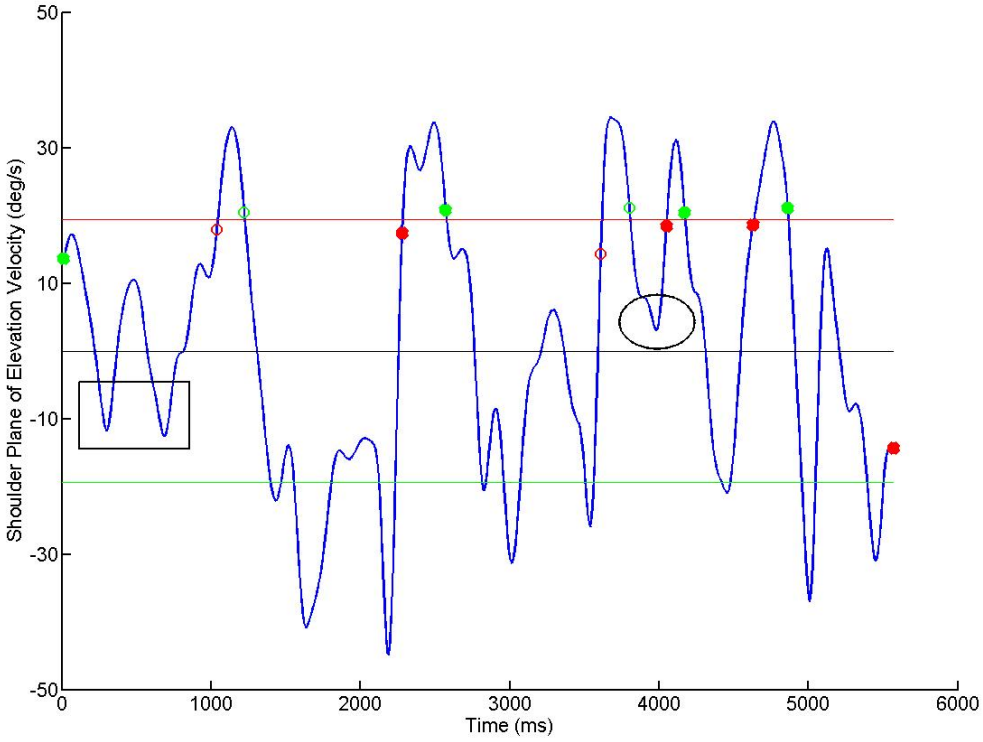

Figure 2.10. Criteria for determining a significant arm deviation on a representative continuous pointing trial. Blue solid line represents detrended shoulder plane of elevation velocity. Negative values indicate the arm speeding up in the direction reflective of forward walking; positive values indicate the arm speeding up in the direction opposite forward walking. Red solid line represents the positive critical value, indicated as one positive standard deviation from the mean detrended arm velocity. Green solid line represents the negative critical value, indicated as one negative standard deviation from the mean detrended arm velocity. Open green circles represent instances where the arm velocity trajectory traveled in a negative direction and reached below the positive critical value (an exception being at the start of a trial); open red circles represent instances where the arm velocity trajectory traveled in a positive direction and reached above the positive critical value. Significant arm deviations occurred when the velocity between a green circle and the subsequent red circle reached below the negative critical value. Filled green circles represent starts of significant arm deviations; filled red circles represent ends of significant arm deviations. Rectangular insert demonstrates a situation where the negative critical value was not reached between the first green and red open-circles. Elliptical insert demonstrates a situation where the negative critical value was not reached between the green and red circles other than those that occurred first for the trial.

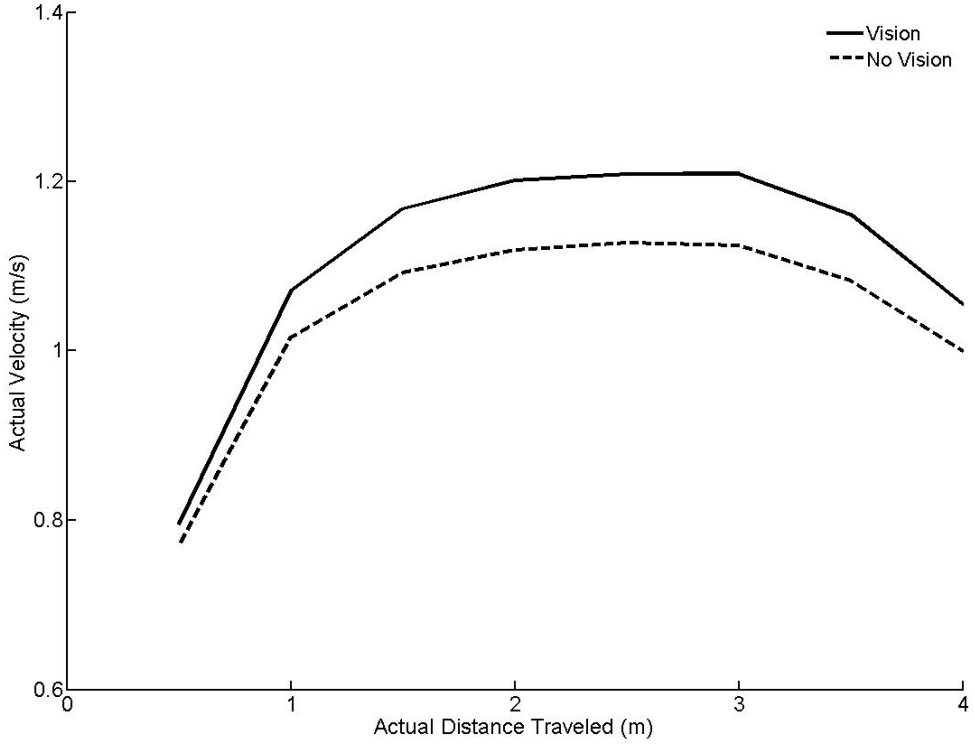

Figure 2.11. Study 1: Vision by Distance interaction for the analysis of actual walking velocity. Solid line represents vision trials; dashed line represents no-vision trials.

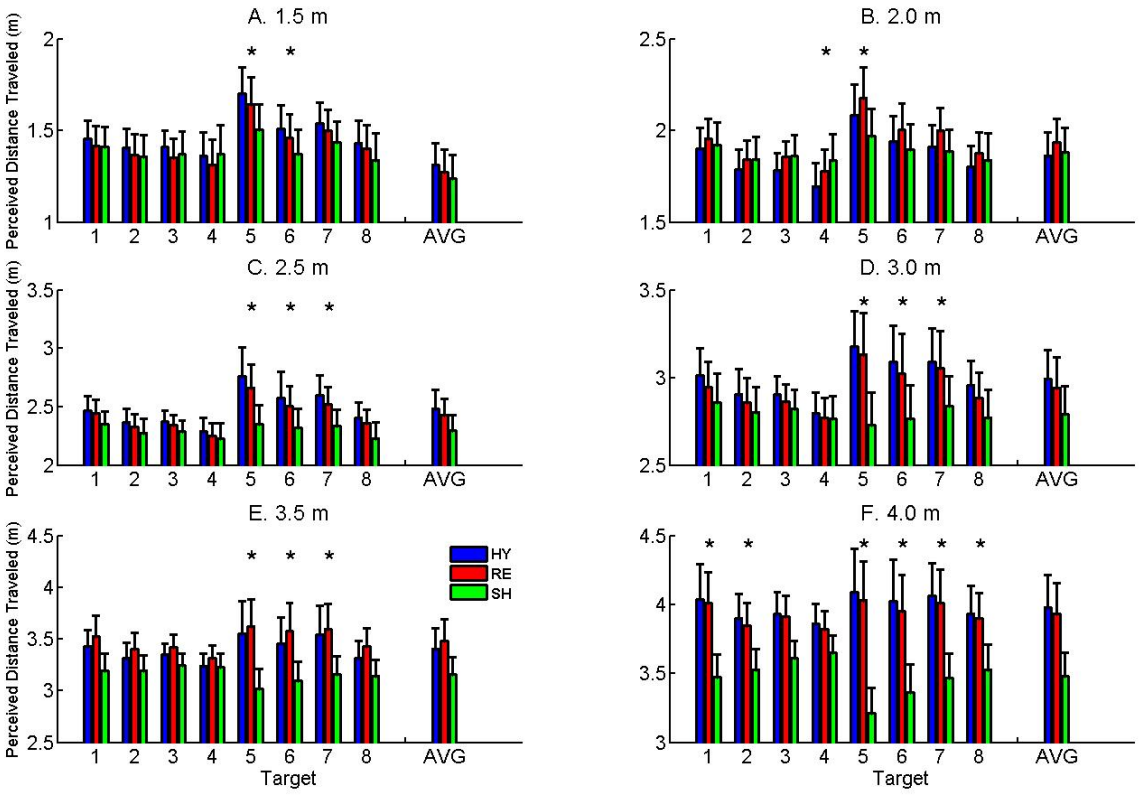

Figure 2.12. Study 1: Method by Target interactions for the analysis of perceived distance traveled at 1.5 m (top left), 2.0 m (top right), 2.5 m (middle left), 3.0 m (middle right), 3.5 m (bottom left) and 4.0 m (bottom right) of actual distance traveled. HY = hybrid method (blue); RE = reconstructed method (red); SH = shoulder method (green). Target numbers are presented along the x-axis; AVG represents the average across all target locations. Error bars represent one standard error. Asterisks indicate targets with significant mean differences between methods.

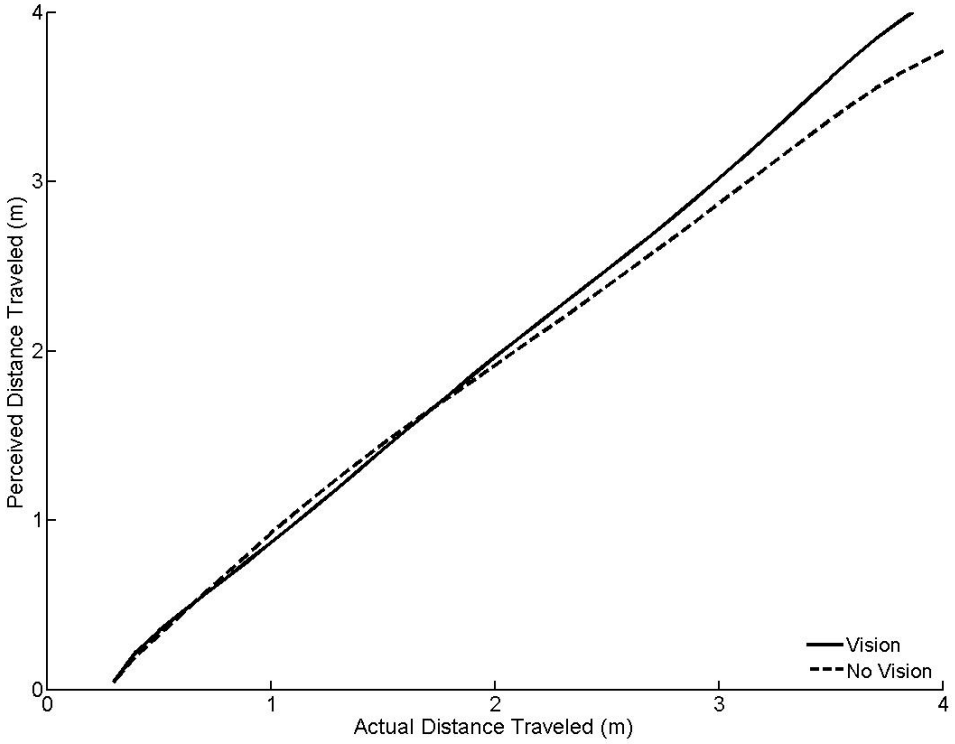

Figure 2.13. Study 1: Perceived distance traveled pooled across the eight different side-target locations included in Study 1. Data in this figure were processed using the reconstructed method of azimuth angle calculation. Solid line represents vision trials; dashed line represents no-vision trials.

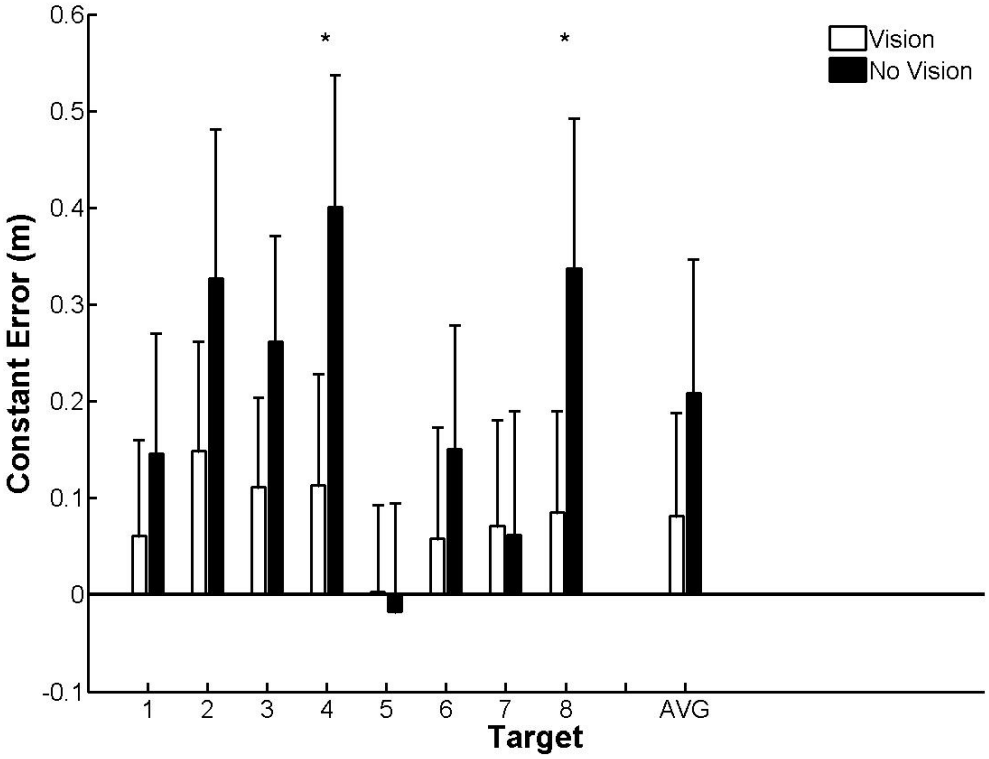

Figure 2.14. Study 1: Vision by Target interaction for the analysis of constant error with respect to the side-target at 0°azimuth. Positive values indicate distances beyond the side-target along the walking path; negative values indicate distances short of the target along the walking path. Open bars represent vision trials; filled bars represent no-vision trials. Asterisks indicate targets with significant mean differences between vision conditions. Error bars represent one standard error

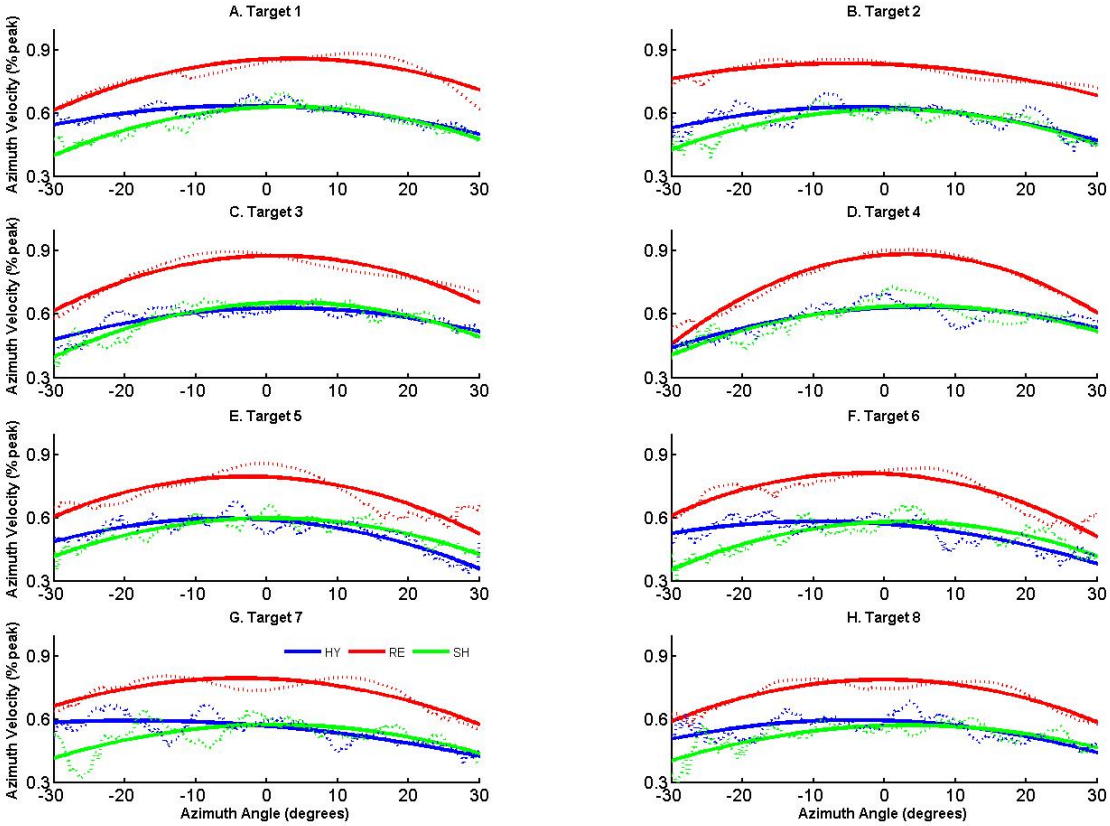

Figure 2.15. Study 1: Proportional azimuth velocity trajectories at each target location for the vision trials.Y-axis values are azimuth velocities in proportion to the peak azimuth velocity demonstrated on each trial. Dashed lines represent condition average trajectories; solid lines represent second-order polynomials fit to the condition average trajectories. HY = hybrid method (blue); RE = reconstructed method (red); SH = shoulder method (green).

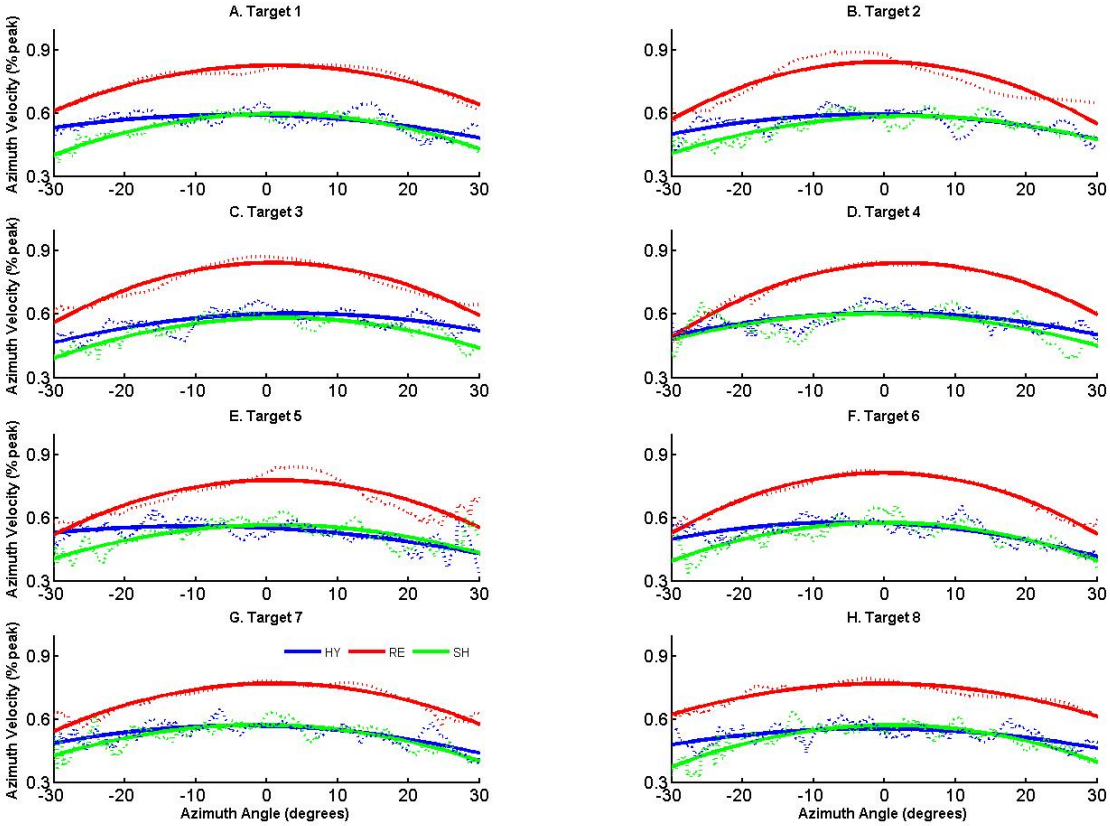

Figure 2.16. Study 1: Proportional azimuth velocity trajectories at each target location for the no-vision trials. Y-axis values are azimuth velocities in proportion to the peak azimuth velocity demonstrated on each trial. Dashed lines represent condition average trajectories; solid lines represent second-order polynomials fit to the condition average trajectories. HY = hybrid method (blue); RE = reconstructed method (red); SH = shoulder method (green).

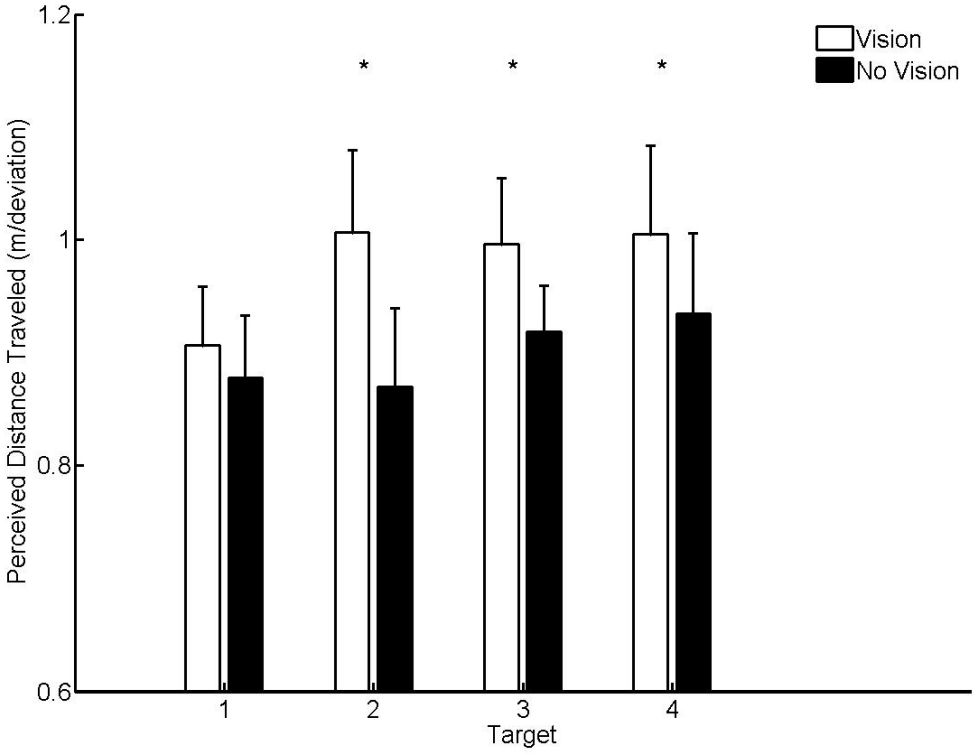

Figure 2.17. Study 1: Vision by Target interaction for the analysis of perceived distance traveled per significant arm deviation. Open bars represent vision trials; filled bars represent no-vision trials. Asterisks indicate targets with significant mean differences between vision conditions. Error bars represent one standard error.

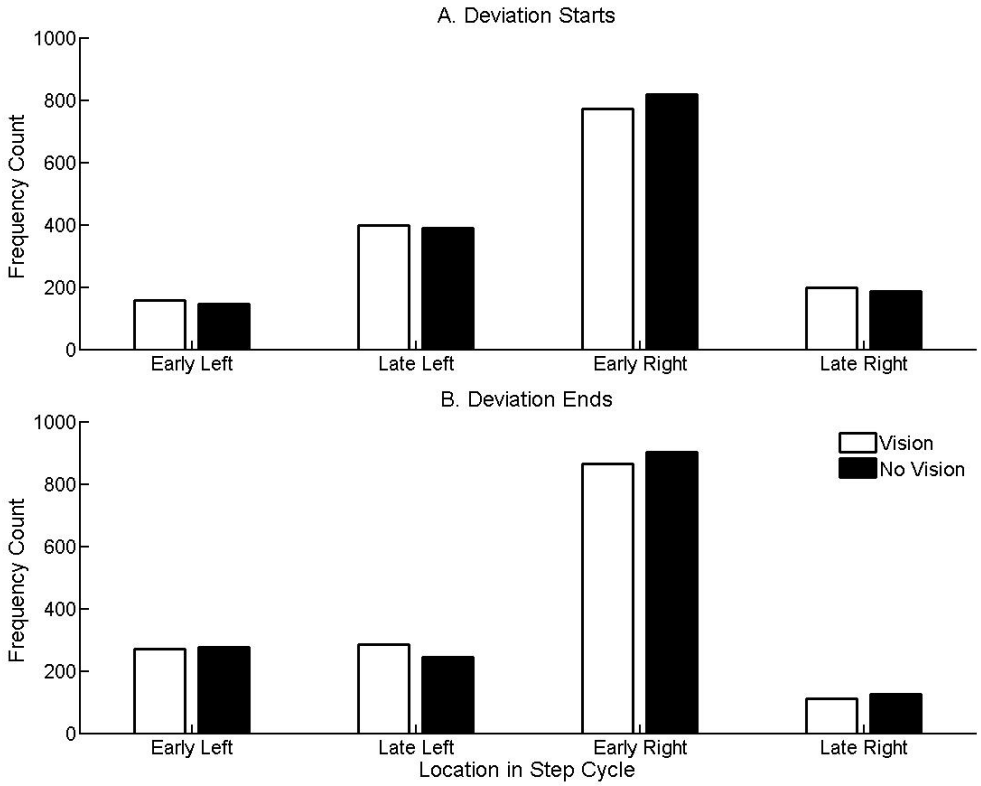

Figure 2.18. Study 1: Frequency counts for the significant arm deviation starts (top) and ends (bottom) in the four classified phases of the step-cycle. Open bars represent vision trials; filled bars represent no-vision trials.

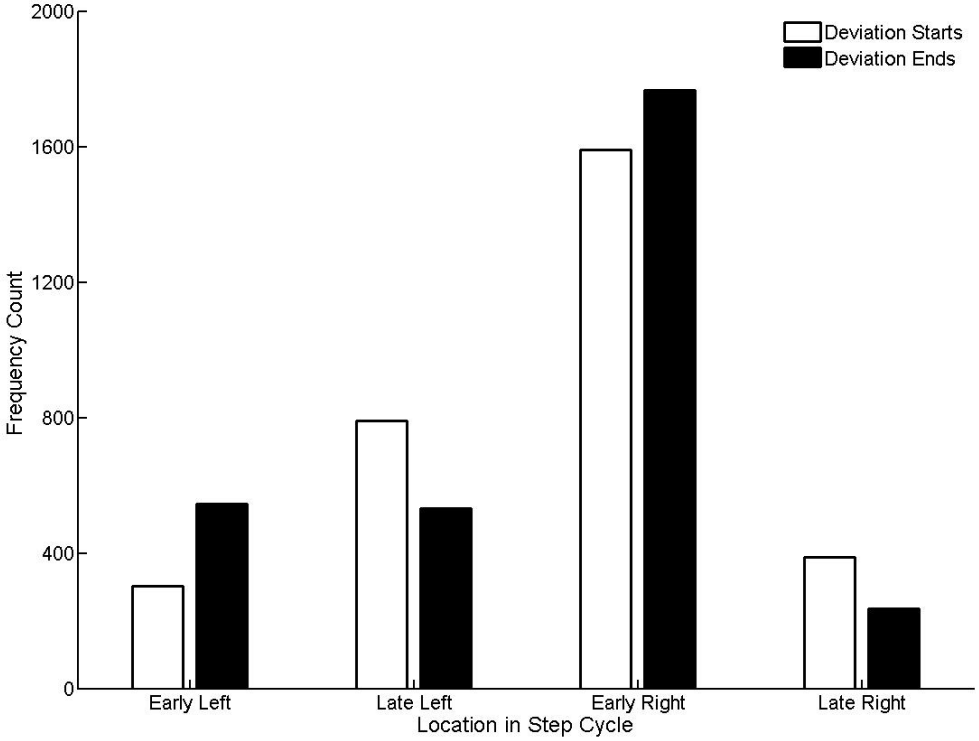

Figure 2.19. Study 1: Frequency counts for the significant arm deviation starts (open bars) and ends (filled bars) in the four classified phases of the step-cycle. Data in this figure are pooled across vision conditions.

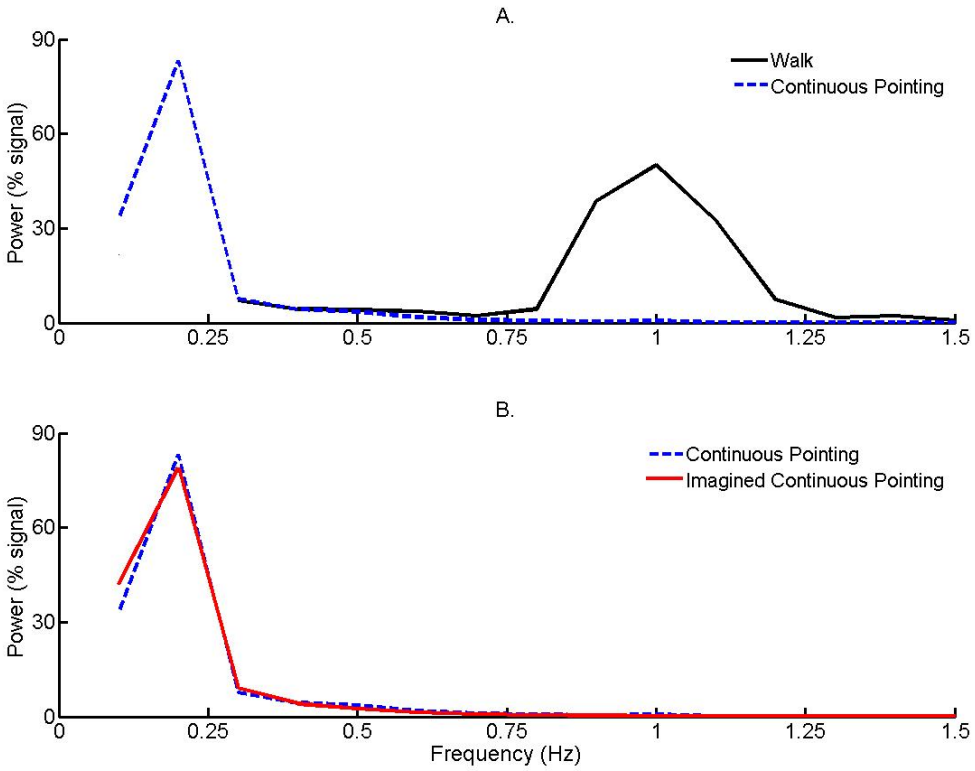

Figure 2.20. Study 1: Power spectra of the shoulder plane of elevation trajectories for the additional data collected. Top: Typical walking (solid black line) is contrasted with continuous pointing (dashed blue line). Bottom: Continuous pointing is contrasted with imagined continuous pointing (solid red line). Data in these figures are normalized to the total power of the respective signals.

Table 2.1. Anatomical landmarks of retro-reflective marker placements.

cervical spinous process 7
thoracic spinous process 3
thoracic spinous process 7
sternal notch
xyphoid process
right anterior superior iliac spine
left anterior superior iliac spine
right posterior superior iliac spine
left posterior superior iliac spine
toe of left foot
toe of right foot
right acromio-clavicular joint
left acromio-clavicular joint
right lateral shoulder
right anterior shoulder
right posterior shoulder
right medial epicondyle
right lateral epicondyle
right radial styloid process
right ulnar styloid process
central on dorsal right hand (moved to dorsal tip of index finger for Studies 2 and 3)

Note: The right lateral shoulder marker was located on the deltoid muscle approximately 5-6 cm below and in line with the right acromio-clavicular joint marker. The right anterior shoulder marker was located on the anterior aspect of the shoulder at the intersection of imaginary lines extending anteriorly from the right acromio-clavicular joint and right lateral shoulder markers. The right posterior shoulder marker was located on the posterior aspect of the shoulder at the intersection of imaginary lines extending posteriorly from the right acromio-clavicular and right lateral shoulder markers.

Table 2.2. Landmarks used to create virtual markers in the Visual 3D model.

Virtual Marker	Landmark 1	Landmark 2	Axial Offset (%)	Project From
Wrist JC	RUP	RRP	0.5	n/a
Elbow JC	RME	RLE	0.5	n/a
Shoulder APJC	RAS	RPS	0.5	n/a
Shoulder JC	RAC	Shoulder APJC	n/a	RLS
Shoulder Girdle JC	SN	C7	0.5	n/a
Thorax JC	XP	T7	0.5	n/a

Note: JC = joint centre, RUP = right ulnar styloid process, RRP = right radial styloid process, RME = right medial epicondyle, RLE = right lateral epicondyle, RAS = right anterior shoulder, RPS = right posterior shoulder, RAC = right acromio-clavicular joint, APJC = anterior-posterior joint centre, RLS = right lateral shoulder, SN = sternal notch, C7 = cervical spinous process 7, XP = xyphoid process, T7 = thoracic spinous process 7, n/a = not applicable.

Table 2.3. Landmarks used to create segments in the Visual 3D model.

Segment		Proximal Segment		Distal Segment			Markers		
Name	Type	Joint	Radius	Joint	Radius	Lateral	Orientation	Tracking	Depth (m)
Pelvis	Coda	n/a	n/a	n/a	n/a	n/a	n/a	RASIS LASIS RPSIS LPSIS	n/a
Thorax	Visual 3D	SGJC	0.5*distance(RAC, LAC)	TJC	0.5*distance(RAC, LAC)	n/a	XP (anterior)	C7 SN T7 XP	0.14
Right Upper Arm	Visual 3D	SJC	0.5*distance(RAS, RPS)	EJC	n/a	RLE	n/a	RLE RME RAS RPS RLS	n/a
Right Forearm	Visual 3D	EJC	0.5*distance(RLE, RME)	WJC	n/a	RRP	n/a	RLE RME RRP RUP	n/a

Note: n/a = not applicable, SGJC = shoulder girdle joint centre, SJC = shoulder joint centre, EJC = elbow joint centre, TJC = thorax joint centre, WJC = wrist joint centre, RAC = right acromio-clavicular joint, LAC = left acromio-clavicular joint, RAS = right anterior shoulder, RPS = right posterior shoulder, RLE = right lateral epicondyle, RME = right medial epicondyle, RUP = right ulnar styloid process, RRP = right radial styloid process, XP = xyphoid process, RASIS = right anterior superior iliac spine, LASIS = left anterior superior iliac spine, RPSIS = right posterior superior iliac spine, LPSIS = left posterior superior iliac spine, C7 = cervical spinous process 7, SN = sternal notch, T7 = thoracic spinous process 7, XP = xyphoid process, LS = lateral shoulder.

Table 2.4. Study 1: Grand means for the step characteristics.

	Step Length (m)	Left Stride Length (m)	Right Stride Length (m)	Number of Steps
Mean	0.616	1.24	1.24	8.58

Table 2.5. Study 1: Sliding ANOVA results for the analysis of perceived distance traveled.

	M	V	T	MV	MT	VT	MVT	Grand Mean (m)
0.5 m	0.310	0.009	0.526	1.22	3.57	0.690	0.788	0.343
1.0 m	0.003	2.37	1.53	**7.52****	**4.67***	1.52	0.671	0.891
1.5 m	0.670	0.203	**4.20***	**4.08***	**5.85****	1.47	0.849	1.44
2.0 m	0.601	1.84	3.82	2.90	**9.22*****	1.50	0.558	1.90
2.5 m	**5.45***	4.87	2.69	0.660	**10.06****	1.49	1.18	2.40
3.0 m	**4.49***	**9.27***	1.50	2.09	**13.31*****	1.10	1.74	2.91
3.5 m	**9.36***	**10.74****	0.568	1.85	**8.98****	1.06	1.62	3.35
4.0 m	**24.69*****	**12.01****	0.229	2.36	**13.28*****	0.629	0.838	3.80

Note. *p < 0.05. **p < 0.01. ***p < 0.001. M = Method (2,18), V = Vision (1,9), T = Target (7,63), MV = Method by Vision (2,18), MT = Method by Target (14,126), VT = Vision by Target (7,63), MVT = Method by Vision by Target (14,126). Degrees of freedom in brackets.

Table 2.6. Study 1: R-squared values of the second-order polynomials fit to the proportional azimuth velocity trajectories

	Target							
Method	1	2	3	4	5	6	7	8
				Vision				
Hybrid	0.83	0.74	0.82	0.82	0.89	0.84	0.78	0.73
Recon	0.90	0.88	0.93	0.98	0.84	0.91	0.87	0.92
Shoulder	0.91	0.89	0.92	0.82	0.90	0.86	0.67	0.77
				No-vision				
Hybrid	0.61	0.66	0.72	0.67	0.69	0.78	0.74	0.59
Recon	0.96	0.89	0.96	0.99	0.87	0.99	0.94	0.93
Shoulder	0.95	0.83	0.90	0.62	0.73	0.83	0.81	0.87

CHAPTER 3:

STUDY 2

THE ONLINE REGULATION OF ITERATIVE SPATIAL UPDATING FOLLOWING SENSORY RECALIBRATION TO LOW AND HIGH VISUAL GAINS

3.1 – ABSTRACT

Spatial updating during typical no-vision forward walking involves a learned association between leg kinematic activity and the resultant perception of self-motion interpreted by the central nervous system (CNS). Recalibration of this relationship can occur when the CNS experiences perceptions of self-motion that deviate from the typical sensory experiences associated with locomotive activity. This has been demonstrated in no-vision forward walking performance as target overestimation (i.e., perceptual underestimation) following prolonged exposure to low visual gains (LVG) and target underestimation (i.e., perceptual overestimation) following prolonged exposure to high visual gains (HVG). Following this type of sensory recalibration, spatial updating differences generally result from changes in perceived self-motion in relation to unaltered leg kinematic activity. However, previous accounts of sensory recalibration have only been able to infer about online changes in spatial updating performance from tasks that employ end point measures. The purpose of Study 2 was to address this limitation using the continuous pointing task introduced in Study 1. Therefore, participants performed no-vision forward walking movements before and after prolonged adaptation periods characterized by low gain, high gain and congruent visual conditions. During the adaptation periods, performers walked at a standard rate on a treadmill while receiving high, low and congruent rates of optic flow presented in a head-mounted display. The results showed post-adaptation perceptual differences indicative of perceptual underestimation following LVG and overestimation following HVG. Importantly, minimal changes were demonstrated in step-cycle kinematics. Furthermore, across all

experimental conditions, arm deviations during continuous pointing performances occurred most frequently during the early right foot swing phase of the step-cycle. The perceptual differences between the LVG and HVG conditions were partially reflected in these updating units.

3.2 – INTRODUCTION

For most daily locomotive movements, there is a learned association between the kinematic activity of the effector systems and the resultant perceptions of self-motion interpreted by the CNS. This relationship enables the effective performance of many locomotive tasks in the absence of vision, most notably effective no-vision walking to targets up to approximately 20 m away (Loomis & Philbeck, 2012; Rieser et al., 1990). This ability is enabled by a spatial updating process in the CNS that relies on information about distance traveled gleaned from kinematic leg activity (e.g., Chrastil & Warren, 2014; Durgin et al., 2009). However, situations sometimes arise where humans experience perceptions of self-motion during walking that deviate from the expectations associated with typical kinematic leg activity. A classic example is walking along a moving airport walkway in its direction of travel. In this example, typical kinematic activity in the legs (i.e., the step-cycle) is associated with a faster visual sense of forward self-motion through space (e.g., Mohler et al., 2007). This is because the kinematic activity involved in walking remains unchanged, while the optic flow involves contributions from walking and passive transport. The opposite situation occurs when walking on a stationary treadmill, where kinematic activity in the legs is associated with a sense of no visual self-motion through space. In these situations, incongruent sensory cues become recalibrated to match the unitary CNS perception of self-motion (Durgin et al., 2005; Ernst & Bülthoff, 2004).

For spatial updating in a locomotive task, sensory recalibration is revealed as differences in no-vision task performance before and after prolonged exposure to sensory

cue conflict. That is, performance prior to exposure reflects typical spatial updating and performance following exposure reflects changes in spatial updating due to the sensory recalibration experienced during exposure. In forward walking, this type of sensory recalibration has traditionally been created by cue conflict between the perceptual estimates of visual self-motion (i.e., optic flow) and kinematic activity in the legs (Durgin et al., 2005; Mohler et al., 2007; Rieser et al., 1995; Ziemer et al., 2013). This was achieved by exposing performers to rates of optic flow that were slower or faster than a standard rate of walking. These cue conflicts have been accomplished in several different ways, including the use of a treadmill-mounted trailer being pulled behind a tractor (Rieser et al., 1995) and the use of virtual reality to expose performers to virtual rates of optic flow that differed from treadmill (Mohler et al., 2007; Ziemer et al., 2013) or self-paced (Kunz et al., 2013) walking speeds.

Spatial updating performance following these types of recalibrations has predominantly been examined using tasks that employ end point measures. In this context, end point measures refer to performers physical locations with respect to an intended stationary target located at the end of a walking path. Specifically, following recalibration to high visual gains (i.e., extent of visual self-motion greater than the walking extent), performers generally over-perceive their forward motion through space by physically undershooting intended targets. The opposite occurs following recalibration to low visual gains (i.e., extent of walking greater than the extent of visual self-motion), where performers under-perceive their forward motion through space by physically overshooting intended targets. Considering that changes in step characteristics cannot

account for these findings (Durgin et al., 2005; Rieser et al., 1995), the sensory recalibration involved with spatial updating is considered to result from the change in perceived self-motion experienced by the CNS relative to the unaltered kinematic leg activity (e.g., Mohler et al., 2007).

As mentioned in Study 1, albeit effective at quantifying the general nature of the CNS, these types of end point measures are inadequate for making inferences about the specific online regulation involved in spatial updating. However, the continuous pointing task solves this problem by providing measures of perceived self-motion and movement kinematics throughout the course of walking movements. As indicated in Study 1, movement kinematics measured from pointing responses can be informative about the iterative structure of CNS spatial updating. Therefore, one goal of Study 2 was to examine the online regulation of recalibrated spatial updating by assessing no-vision continuous pointing performance before and after prolonged adaptation periods involving exposure to sensory cue conflict. This was achieved using a protocol where no-vision continuous pointing movements were performed before and after sensory adaptation periods. Adaptation periods in the current study involved a standard rate of treadmill walking (i.e., 1.1 m/s) paired with virtual rates of optic flow presented using a head-mounted display. The virtual rates of optic flow corresponded to congruent visual conditions (CVG), low gain visual conditions (LVG), and high gain visual conditions (HVG). These involved optic flow rates of 1.0 x, 0.5 x and 2.0 x the rate of treadmill walking, respectively.

Spatial updating differences were not expected in the no-vision continuous pointing movements performed before the adaptation periods. However, differences in perceived self-motion were expected to emerge between these conditions in the no-vision continuous pointing trials performed after the adaptation periods. Specifically, post-adaptation no-vision continuous pointing was expected to reveal:

I. Under-perception of distance traveled following LVG adaptation (i.e., less than unitary relationship between perceived and actual distance traveled),

II. Over-perception of distance traveled following HVG adaptation (i.e., greater than unitary relationship between perceived and actual distance traveled),

III. No change in perceived distance traveled following the CVG condition (i.e., unitary relationship between perceived and actual distance traveled.

The iterative CNS updating units, measured using the significant arm deviations introduced in Study 1, were expected to reflect these perceptual differences. In light of these perceptual differences however, post-adaptation changes in actual walking velocity and step kinematics (i.e., step and stride lengths) were not expected. This was because sensory recalibration was expected to involve a change in perceived self-motion gleaned from unaltered leg kinematic activity.

3.3 – METHODS

3.3.1 – *Participants*

Sixteen individuals (8 male, 8 female) with a mean age of 23.0 years (sd = 3.58 years) were recruited to participate in this study. Participants were self-reported right hand dominant and had normal or corrected-to-normal vision. Participants were naïve to

the purposes of the study and provided written, informed consent prior to starting the experiment in accordance with the McMaster Research Ethics Board and the 1964 Declaration of Helsinki. Each experimental session took approximately 2.5 hours to complete on a single day and participants were remunerated $20 for their time. The data from one participant was removed because they consistently failed to perform the experimental task as instructed.

3.3.2 – *Apparatus*

All participants completed the experiment in athletic shoes and comfortable athletic pants or shorts. Male participants performed the experiment shirtless and female participants performed the experiment in a sports bra. This attire enabled 21 25 mm retro-reflective markers to be attached directly to the skin with double-sided electrode tape and medical tape to the same anatomical locations as in Study 1 (see Figure 2.02). One exception was that the marker located on the dorsal aspect of the hand in Study 1 was moved to the dorsal tip of the index finger in the current study. These retro-reflective markers were captured by 10 Vicon Nexus MX-T40 cameras (Vicon, Oxford, UK) at a rate of 100 Hz using Vicon Nexus 2.3 software. Participants were also outfitted with custom splints (two wooden chopsticks individually wrapped in medical tape) taped to the forearm lengthwise along the ulna. These splints started at the base of the thumb, were far enough apart to straddle the ulnar styloid process, and extended along the forearm toward the elbow. The splints effectively limited ulnar deviation of the wrist during the continuous pointing movements. Participants were equipped with a remote-controlled vibrating device (I-phone; Apple Inc., Cupertino, California model) and a laser pointer

(Quartet, ACCO, Lake Zurich, Illinois) to hold in their left and right hands, respectively. The vibrating device was equipped with a custom Bluetooth application that was controlled by one of the experimenters to cue the starting and stopping of walking on every trial (see below). The laser pointer was held lengthwise along the long axis of the index finger so that the beam projected outward from underneath the fingertip when the wrist was in full pronation. This approximated an extension of the index finger and enabled participants to align the index finger directly onto the side target at the start of every trial (see below). Holding the laser pointer in this manner also limited movement of the interphalangeal and metacarpal-interphalangeal joints in the right index finger during the continuous pointing movements. White noise was provided during all of the walking trials and adaptation periods (see below) to mask the sound of footsteps and other ambient noises originating from the environment. This was delivered at a comfortable volume using an I-pod Shuffle (Apple Inc., Cupertino, California) and standard headphones (Sennheiser, Wedemark, Germany). Participants were outfitted with a baseball cap to prevent lights on the lab ceiling from providing spatial cues about distance traveled along the walking path.

All walking movements were performed in one direction along the same path (see Figure 3.01). The home position consisted of a black paper “T” taped to the floor, with the long axis indicating the direction of travel. All distances along and beside the walking path were measured with respect to the short and long axes of the home position, respectively. Six side targets were marked on the ground 2 m to the right of the walking path and 1.44 (target 1), 1.95 (target 2), 2.40 (target 3), 3.20 (target 4), 3.90 (target 5) and

4.8 m (target 6) along the walking path. These target locations were indicated with small square pieces of black tape on the lab floor that were visible to the participants at the starting location. The side target location used on each trial was indicated by a black paper circle 20 cm in diameter and placed on the ground directly overtop of one of the indicated positions. Attached to the middle of the target was a 25 mm retro-reflective marker that provided the exact position of side target used on each trial. Another 25 mm retro-reflective marker was placed beside the walking path and used to indicate the distance of the home position. Prior to starting the experiment, participants stood in the anatomical position at the start location and a static marker calibration trial was captured from this pose.

A treadmill (Horizon T.93, Johnson, Health, Tech., Taiwan) was located 2 m beside the home position and was used only during the adaptation periods (see below) to specify the kinematic speed of walking. An Oculus Rift DK (Oculus VR, Irvine, California) head mounted display (HMD) was used during treadmill walking to present a virtual hallway that specified various rates of optic flow. The Oculus Rift was controlled by an Ogre interface on a Dell Precision T5400 computer (Dell Technologies, Texas, USA) outfitted with a Linux operating system. The resolution of the Oculus rift was 1280 x 800 and was refreshed at a rate of 60 Hz. The virtual hallway was presented stereoscopically and consisted of white crosshatched lines superimposed on a black background (see Figure 3.02). Presented at random distances along both walls of the virtual hallway were maroon rectangular signs depicting the McMaster “M” logo. The dimensions of the virtual hallway were similar to those of an actual hallway located

immediately outside the laboratory. The vantage point within the virtual hallway was manually scaled to the eye height of each participant. Rotational head movements were measured by the HMD and updated in the visual display.

3.3.3 – *Procedure*

Experimental Task

This section describes the experimental task of continuous pointing. Blocks of continuous pointing trials were performed with and without vision at specific instances throughout the experimental session (see subsection below). However, the experimental task description that follows is consistent for both vision and no-vision trials, except where indicated.

All performance trials started with participants standing at the start location in the anatomical position. Once the participant was ready and in this position, one of the experimenters started the motion capture and the other experimenter subsequently activated the vibrating device. The latter was done following a “thumbs-up” signal from the first experimenter indicating that the Vicon system was active. The vibratory stimulus cued participants to straighten their right arm (i.e., full elbow extension), fully pronate their wrist and fixate the laser pointer directly on the side target. When effectively centred on the target, participants deactivated the laser, looked forward along the walking path and started walking with either their eyes open (i.e., vision trial) or closed (i.e., no-vision trial). Participants attempted to walk along a straight-line trajectory while keeping their arm straight and index finger fixated on the side-target. Participants walked at a comfortable, constant-velocity until they received a second vibratory stimulus 3-6 m

down the walking path. Upon receiving this stimulus, participants finished the step in progress and came to an abrupt stop by aligning their feet side-by-side. Once stopped, the participants immediately closed their eyes, for both vision and no-vision trials and relaxed their arm while the experimenter stopped the Vicon system from recording. In order to mask feedback about performance, participants were led back to the start location with their eyes still closed along a random and twisting pathway. Upon returning to the starting location, the experimenter indicated to the participant by tapping them on the shoulder that they could return to the anatomical position and open their eyes. Once in this position, participants were required to not move their feet while awaiting the next trial.

Vision trials were performed to endpoint distances of 3 and 5 m along the walking path and no-vision trials were performed to endpoint distances of 4 and 6 m along the walking path. Different walking distances were used for the vision and no-vision trials to prevent participants from strategically performing the no-vision trials using feedback (e.g., arm rotation, step number/length) acquired from the outcomes of the vision trials. Side targets for each walking distance were in one of three locations: targets 1-3 for 3 m, targets 2-4 for 4 m, targets 3-5 for 5 m, and targets 4-6 for 6 m (see Figure 3.01). For each walking distance, these side target locations represented near, middle and far distances that approximated 50, 65 and 80 percent of the total walking distances, respectively. Three side target locations were used for each walking distance to prevent participants from using a memorized motor experience (e.g., arm trajectory) in performing the task. Additionally, some side target locations served multiple walking distances (see Figure 3.01) to prevent participants from being informed, prior to the start of a trial, about the

distance being walked on the upcoming trial. By using several forward walking distances and several side target locations, motor performance was intended to reflect spatial updating and not anticipatory task awareness.

Practice session

This section describes the order of events and experimental conditions involved in the experimental session. Upon arrival in the lab, participants were first outfitted with the retro-reflective markers, baseball cap, vibrating device and laser pointer. The height of the participant was then measured so that the vantage point in the virtual environment could be appropriately scaled to their height. Participants took part in a practice session that was followed by the experimental session.

In the practice session, participants performed 6 practice trials of the continuous pointing task to a side target located 2 m beside and 2.8 m along the walking path. This side-target location was not included in the experimental session. Three vision trials were always practiced before three no-vision trials. After the practice trials, participants experienced a 5 min familiarization period in the HMD/treadmill set-up. This included walking on the treadmill at a rate of 1.1 m/s while experiencing congruent visual flow in the virtual environment (i.e., 1.0 x the walking speed). During this time, participants lightly grasped the two side handrails of the treadmill. White noise was not provided during the practice session so that verbal communication could be maintained with the participants.

Experimental Session

The experimental session was divided into four blocks, each consisting of 18 continuous pointing trials. Each block unfolded in the following sequential manner: 6 vision continuous pointing trials that served as controls, 6 pre-adaptation no-vision continuous pointing trials, a 10-minute adaptation period performed using the treadmill/HMD set-up, and 6 post-adaptation no-vision continuous pointing trials. Each set of 6 trials consisted of one trial performed at all combinations of 2 walking distances (vision trials: 3 and 5 m; no-vision trials: 4 and 6 m) by 3 side target locations (close, middle and far). The only stipulation with the trial orders was that no more than 2 consecutive trials could be performed to the same side target. Within each block, the same order of distance by side target was used in the no-vision pre- and post-adaptation trials. The purpose of the vision control trials was to calibrate participants to their typical association between vision and proprioception at the start of each experimental block. Due to the within-subjects design of this study, this was necessary to washout potential carry-over effects between the different experimental blocks. The purpose of the no-vision pre-adaptation trials was to provide a baseline measure of spatial updating and the purpose of the no-vision post-adaptation trials was to provide a measure of spatial updating after the sensory adaptation periods.

The 4 experimental blocks differed in the type of visual information (i.e., sensory recalibration) experienced during the adaptation periods. Specifically, participants experienced a visual speed 2.0 x the treadmill speed in the high visual gain (HVG) condition, a visual speed 0.5 x the treadmill speed in the low visual gain (LVG) condition

and a visual speed 1.0 x the treadmill speed in the congruent vision (CVG) condition. The treadmill speed was always set at 1.1 m/s, which approximated the grand mean walking speed of the participants in Study 1 (e.g., Mohler et al., 2007; Multon & Olivier, 2013). The visual speeds for the adaptation periods were selected on the basis of their effective use in previous studies (Mohler et al., 2007; Ziemer et al., 2013). Prior to starting the adaptation periods, the baseball cap, vibrating device and laser pointer were removed from the participant. The headphones/I-pod remained with the participant so that white noise could be provided during the adaptation periods. To ensure that participants remained centred on the treadmill while wearing the HMD, participants were instructed to maintain a light grasp on the treadmill handrails with both hands at all times. In viewing the virtual environment, participants were instructed to "look around" and focus on the visual information specified by the walls, ceiling and floor as they passed through the virtual environment. An auditory beep emitted by the treadmill signified the end of adaptation period after 10 minutes, at which time the treadmill was manually turned-off by an experimenter and the participant was instructed to close their eyes. At this time, the white noise was turned off, the HMD was removed and the participant was led off the treadmill and back to the start location along an unpredictable path with their eyes closed. When back at the start location, participants were verbally instructed to open their eyes and they were once again outfitted with the baseball cap, vibrating device and laser pointer. When ready, the participants assumed the anatomical position, the white noise was turned back on and the no-vision post-adaptation trials began.

In order to avoid possible contamination effects between the LVG and HVG conditions, the experimental blocks were ordered so that a CVG block always preceded a LVG and HVG block. This resulted in 4 experimental blocks that were ordered either CVG1-LVG-CVG2-HVG or CVG1-HVG-CVG2-LVG. The LVG and HVG blocks were counterbalanced between the 2nd and 4th positions across participants and across both males and females. Given the within subjects design of this study, all participants performed a total of 72 continuous pointing trials (24 V, 48 NV) and experienced a total of 40 minutes of sensory adaptation.

3.3.4 – *Data and Statistical Analysis*

Data analysis was carried out in a similar manner as Study 1. The data from all trials were reconstructed using Vicon Nexus 2.3 software (Vicon, Oxford, UK). For each trial, the anatomical markers were labeled at every frame, missing data segments 25 frames or shorter were filled, and the data was saved in the C3D format for further processing in Visual 3D (version 4, C-motion Research Biomechanics, Kingston, Ontario).

In Visual 3D, a custom model was constructed using the static calibration trial and this model was attached to the 3D marker data for all trials. The model created virtual markers representing the wrist joint centre, elbow joint centre, shoulder anterior-posterior joint centre, shoulder joint centre, shoulder girdle joint centre and throax joint centre (see Table 2.2 for the landmarks used to compute each virtual marker). The anatomical and virtual markers were then used to create body segments representing the pelvis, thorax, right upper arm and right forearm (see Table 2.3 for the landmarks used to define each

segment). Using these body segments, relative joint angles were calculated for the trunk, shoulder and elbow joints in a manner consistent with the International Society of Biomechanics standards (Wu et al., 2005). Specifically, trunk angle represented rotation of the thorax segment with respect to the pelvis segment using an X-Y-Z Cardan sequence; shoulder angle represented rotation of the upper arm segment with respect to the thorax segment using a Z-Y-Z Cardan sequence; and elbow angle represented rotation of the forearm segment with respect to the upper arm segment using an X-Y-Z Cardan sequence.

Dependent measures were calculated for each trial using custom Matlab R2014a software (Mathworks, Natick, Massachusetts). All joint angle and marker data were first filtered using a second-order, dual-pass Butterworth filter with a low-pass frequency of 6 Hz. The start and end of each walking trial were then determined using the velocity profiles of the foot responsible for taking the first and last steps, respectively. These velocity profiles were calculated as the derivatives of the displacement profiles for the left foot and right foot markers using a three-point finite difference algorithm. The start of walking was defined as the first instance where the velocity of the foot that took the first step reached the value of 0.02 m/s and remained above this mark for at least 25 frames (i.e., 250 ms). The end of walking was defined as the first instance where the velocity of the foot that took the last step reached the value of 0.02 m/s and remained below this mark for at least 25 frames. In the odd circumstance where data from the left foot or right foot markers were lost at the end of a walking movement, the end of walking was calculated as the earliest missing data frame amongst the remaining anatomical markers.

This had no impact on the results since the walking movements were only analyzed up to 2.5, 3.5, 4.5 and 5.5 m for the 3, 4, 5 and 6 m walking trials, respectively. All dependent variables were calculated between the defined start and end for each walking trial. Outlined in the remainder of this section are the calculations and statistical analyses used for determining and examining all dependent measures. Unless otherwise indicated in the descriptions that follow, data were pooled for the CVG1 and CVG2 conditions (numbers indicate the order in which the two CVG conditions were presented), and data for all analyses were collapsed across target and examined separately at each distance. Furthermore, since the purpose of this study is to examine no-vision spatial updating before and after prolonged exposures to low gain, high gain and congruent vision sensory adaptation periods, the results will focus on the no-vision pre- and post-adaptation trials unless otherwise noted.

Perceived/actual distance traveled and velocity

Actual distance traveled was measured as the position of the xyphoid marker with respect to the start location. Actual walking velocity was taken as the derivative of the actual distance traveled trajectory calculated using a three-point finite difference algorithm. Actual velocity was examined using the sliding ANOVA technique introduced in Study 1. Once again, the purpose of this technique is to avoid congesting a single ANOVA with an independent variable whose results carry relatively little significance to the overall research question and whose levels can more or less be arbitrarily defined. The independent variable used here was actual distance traveled. This analysis was performed using 3 Gain (CVG, LVG, HVG) by 2 Test (pre-adaptation, post-adaptation) repeated

measures ANOVAs run separately at 0.5 m distance iterations for the 4 m (0.5-3.5 m) and 6 m (0.5-5.5 m) no-vision trials.

Perceived distance traveled was determined using the Reconstructed method of azimuth angle trajectory calculation introduced in Study 1. Specifically, this involved: (a) submitting the shoulder plane of elevation and trunk axial rotation trajectories to Fast Fourier Transforms to determine the frequency contents of the two signals (see Figure 2.03), (b) reconstructing both signals using their respective signal frequency contents less than 0.5 Hz, and (c) summing the two reconstructed signals together. Subsequently, equations 1 and 2 were used to calculate perceived distance traveled at every frame of data collection (see Figure 1.1), and a perceived distance traveled trajectory for each trial was calculated by accumulating these values across all frames. For the vision control trials of the corresponding experimental blocks, the sliding ANOVA technique was first used to examine perceived distance traveled using 4 Gain (CVG1, CVG2, LVG, HVG) repeated measures ANOVAs run separately at 0.5 m distance iterations for the 3 m (0.5-2.5 m) and 5 m (0.5-4.5 m) walking trials. Considering the repeated measures design of this study, this was done to examine whether the vision control trials were systematically impacted by the previously experienced sensory adaptation periods. Subsequently, another sliding ANOVA was used to compare perceived distance traveled between the vision control and no-vision pre-adaptation trials. For this analysis the 4 m and 6 m pre-adaptation trials were cut down to 2.5 m and 4.5 m, respectively. This analysis was performed using 4 Gain (CVG1, CVG2, LVG, HVG) by 2 Vision (vision control, no-vision pre-adaptation) repeated measures ANOVAs run separately at 0.5 m distance

iterations for the 3 m (0.5-2.5 m) and 5 m (0.5-4.5 m) walking distances. This analysis served to examine whether the no-vision blocks of pre-adaptation continuous pointing reflected typical spatial updating (i.e., was similar to the baseline visual control trials).

To examine the no-vision pre-and post-adaptation trials, perceived distance traveled was analyzed using the sliding ANOVA technique. Specifically, 3 Gain (CVG, LVG, HVG) by 2 Test (no-vision pre-adaptation, no-vision post-adaptation) repeated measures ANOVAs were run separately at 0.5 m distance iterations for the 4 m (0.5-3.5 m) and 6 m (0.5-5.5 m) trials.

Azimuth measures

Peak azimuth velocity and azimuth angle at peak azimuth velocity were measured to examine how the azimuth pointing responses unfolded during the course of walking movements. For these analyses, azimuth velocity was calculated by differentiating the azimuth trajectory using a three-point finite difference algorithm. If performing the continuous pointing task as instructed, peak azimuth velocity would be predicted to occur at 0° azimuth (i.e., arm pointed straight out to side; (Campos et al., 2009). Since this measure is used to assess whether performers are properly coordinating their azimuth movements with perceived target passage, it should not be systematically impacted by the sensory adaptation conditions. That is, the sensory adaptations are expected to impact the actual location of perceived target passage but not the performers inherent ability to perceive it. These variables were examined separately for the 4 and 6 m walking distances using 3 Gain (CVG, LVG, HVG) by 2 Test (no-vision pre-adaptation, no-vision post-adaptation) repeated measures ANOVAs. Constant error (i.e., signed error along the

walking path) was measured as distance between the location of the participant and the location of the target when the participants achieved 20°, 15°, 10°, 5°, 0°, -5° and -10° azimuth. Negative values indicate positions before actual target passage and positive values indicate positions after actual target passage. This provides a measure of how spatial updating unfolds in what is considered the most sensitive range for measuring changes in azimuth angle. Constant error was examined using the sliding ANOVA technique separately for the 4 and 6 m walking distances. Specifically, 3 Gain (CVG, LVG, HVG) by 2 Test (no-vision pre-adaptation, no-vision post-adaptation) repeated measures ANOVAs were run separately in 5° azimuth increments (20° to -10°). A single missing ANOVA cell in this analysis was replaced using a series mean.

Step characteristics

Step characteristics were calculated using the same criteria as outlined in Study 1 (see Figure 2.07; e.g., Multon & Olivier, 2013). Included for analyses were the number of steps, step length, and left and right stride lengths. Since multiple steps and strides occurred on each trial, step length and left and right stride lengths were reduced to average values for each trial. All step characteristics were examined separately for the 4 and 6 m walking distances using 3 Gain (CVG, LVG, HVG) by 2 Test (pre-adaptation, post-adaptation) repeated measures ANOVAs.

Significant arm deviations

Significant arm deviations were calculated using the same kinematic criteria applied to the Shoulder azimuth method outlined in Study 1 (see Figures 2.08. 2.09 and 2.10). The number of significant arm deviations per trial was examined separately for the

4 and 6 m walking distances using 3 Gain (CVG, LVG, HVG) by 2 Test (pre-adaptation, post-adaptation) repeated measures ANOVAs. The actual (i.e., the extent covered on the actual distance traveled trajectory) and perceived (i.e., the extent covered on the perceived distance traveled trajectory) distances traveled were also calculated for each significant deviation. These were examined using 3 Gain (CVG, LVG, HVG) by 2 Test (pre-adaptation, post-adaptation) by 4 (or 5) Deviation Number repeated measures ANOVAs. The Deviation Number level was selected based on the grand mean of the aforementioned analysis of number of significant arm deviations per trial. This number represented 4 for the 4 m trials and 5 for the 6 m trials. Since these were average values, this resulted in situations where some performers did not meet these numbers of deviations. Thus, 5 missing ANOVA cells were replaced in each of these analyses using series means.

Locations of the significant arm deviation starts and ends in the step-cycle were also examined using the same criteria as Study 1. Specifically, frequency counts for the different test (no-vision pre-adaptation, no-vision post-adaptation) and gain (CVG1, CVG2, LVG, HVG) trials were accumulated across all participants. For statistical analysis, these frequency count data were reduced into the same four categories as Study 1: early left foot, late left foot, early right foot and late right foot. To examine the locations of significant arm deviation starts and ends in the step-cycle, three sets of Chi Square analyses were performed separately on the significant arm deviation starts and ends (e.g., Rinaldi & Moraes, 2015). First, comparisons were made between the frequency counts of the test conditions (i.e., vision control, no-vision pre-adaptation, no-

vision post-adaptation) within each of the gain conditions (i.e., CVG1, CVG2, LVG, HVG). The expected values for each category were based on the percentage of the total number of deviations in each step-phase category multiplied by the number of deviations in each test condition (see Vincent, 2005). Second, data were pooled across test conditions and frequency counts were compared between the phases of the step-cycle within each gain condition. The expected values for this analysis equalled ¼ of the total number of deviations for each analysis, which represented the null hypothesis of no between categorical differences in the total number of deviations. Lastly, frequency counts between the different gain conditions were compared. The expected values for each category were based on the percentage of the total number of deviations in each step-phase category multiplied by the number of deviations in each gain condition.

All analyses were performed using SPSS software (IBM, Armonk, New York), with the exception of the Chi Square analyses that were performed manually in Microsoft Excel (Microsoft, Redmond, Washington). Alpha was set at $p < 0.05$ for all analyses. Violations of sphericity were accounted for using the Greenhouse-Geisser correction, although the reported degrees of freedom are the sphericity assumed values. All significant ANOVA effects involving more than two means were decomposed using Tukey's Honestly Significant Difference. Post-hoc tests for the Chi Square analyses were performed using SPSS software. Bonferroni adjusted binomial pairwise comparisons were used for the single category analyses, while adjusted standardized residuals that were converted to p-values and Bonferroni adjusted were used for the two category analyses.

3.4 – RESULTS

Actual velocity was used to examine whether participants adhered to the instruction to walk at a constant velocity during the continuous pointing movements, and also whether the gain manipulations during the adaptation periods had an impact on the participant's actual motions through space. For the actual velocity analysis, F-values of the sliding ANOVA results are presented in Table 3.1 and the data are displayed in Figures 3.03 and 3.04. For the 4 m walking distance, Test main effects at 3.0 and 3.5 m showed greater actual walking velocities in no-vision post-adaptation (3.0 m = 1.15 m/s; 3.5 m = 1.09 m/s) compared to no-vision pre-adaptation (3.0 m = 1.12 m/s; 3.5 m = 1.06 m/s). For the 6 m walking distance, the Test main effects at 0.5 and 1.0 m showed greater actual walking velocities in no-vision pre-adaptation (0.5 m = 0.759 m/s; 1.0 m = 1.02 m/s) compared to no-vision post-adaptation (0.5 m = 0.708 m/s; 1.0 m = 0.989 m/s). However, at 4.5 and 5.0 m, the Test main effects showed greater actual walking velocities in no-vision post-adaptation (4.5 m = 1.12 m/s; 5.0 m = 1.06 m/s) compared to no-vision pre-adaptation (4.5 m = 1.09 m/s; 5.0 m = 1.02 m/s). Although these collective results showed that walking velocity was impacted by pre- and post-adaptation performance, most important was that gain condition did not systematically impact the actual walking velocities. Further, averages of the grand means from Table 3.1 were 1.05 m/s and 1.07 m/s for the 4 and 6 m walking distances, respectively. These values were close to the actual walking velocity grand mean demonstrated in Study 1 (1.08 m/s). Thus, the no-vision pre-adaptation, no-vision post-adaptation and Study 1 actual walking velocities

resembled the treadmill speed of 1.1 m/s used in the adaptation periods (e.g, Multon & Olivier, 2013; Philbeck et al., 2008).

The step-cycle characteristics (i.e., number of steps, step length, and left and right stride length) were used to examine whether the kinematics of walking changed as a function of the gain manipulations presented during the adaptation periods. Analyses of the step characteristics revealed no significant main effects or interactions ($p > 0.05$), with the exception of a Test main effect for right stride length in the 4 m walking trials, $F(1,14) = 7.17$, $p < 0.05$ (see Table 3.2 for the grand means). Accordingly, right stride length was greater in the no-vision post-adaptation trials (1.25 m) compared to the no-vision pre-adaptation trials (1.24 m). To determine whether the step characteristics changed as a function of walking distance, an additional analysis was performed on each step characteristic variable using a 2 Distance (4 m, 6 m) by 3 Gain (CVG, LVG, HVG) by 2 Test (no-vision pre-adaptation, no-vision post-adaptation) repeated measures ANOVA. With the exception of an expected Distance main effect on the number of steps, $F(1,14) = 801.96$, $p < 0.001$, there were no significant main effects or interactions ($p > 0.056$). All together, these data showed that the gain manipulations and distances walked did not influence the step characteristics used to perform the walking trials.

Perceived distance traveled was used to examine the participant's perceived spatial locations during the course of the continuous pointing movements, with particular interest as to whether these changed as a function of the gain manipulations presented during the adaptation periods. Prior to performing the sliding AVOVAs on perceived distance traveled, omnibus tests were performed for each walking distance to determine

whether perceived distance traveled increased as a function of actual distance traveled. This was necessary because the sliding ANOVA technique examined between condition differences at specific distance intervals, without comparing differences between intervals. Gain and test conditions were pooled at 0.5 m distance intervals for each of the following analyses. For the 3 m trials, this analysis was performed using a 5 Distance (0.5-2.5 m) repeated measures ANOVA. The results showed significant differences between all distances (0.5 m = 0.97 m; 1.0 m = 1.38 m; 1.5 m = 1.78 m; 2.0 m = 2.18 m; 2.5 m = 2.61 m). For the 4 m trials, this analysis was performed using 7 Distance (0.5-3.5 m) repeated measures ANOVA. The results showed significant differences between all distances except between 0.5 and 1.0 m, 1.0 and 1.5 m, 1.5 and 2.0 m, 2.0 and 2.5 m, 2.5 and 3.0 m, and 3.0 and 3.5 m (0.5 m = 1.21 m; 1.0 m = 1.56 m; 1.5 m = 1.90 m; 2.0 m = 2.27 m; 2.5 m = 2.69 m; 3.0 m = 3.06 m; 3.5 m = 3.43 m). For the 5 m trials, this analysis was performed using a 9 Distance (0.5-4.5 m) repeated measures ANOVA. The results showed significant differences between all distances except between 0.5 and 1.0 m, 1.0 and 1.5 m, 1.5 and 2.0 m, 2.0 and 2.5 m, 2.5 and 3.0 m, 3.0 and 3.5 m, 3.5 and 4.0 m, and 4.0 and 4.5 m (0.5 m = 1.50 m; 1.0 m = 1.81 m; 1.5 m = 2.08 m; 2.0 m = 2.39 m; 2.5 m = 2.78 m; 3.0 m = 3.17 m; 3.5 m = 3.62 m; 4.0 m = 4.01 m; 4.5 m = 4.32). For the 6 m trials, this analysis was performed using an 11 Distance (0.5-4.5 m) repeated measures ANOVA. The results showed significant differences between all distances except between 0.5 and 1.0-2.0 m, 1.0 and 1.5-2.5 m, 1.5 and 2.0-3.0 m, 2.0 and 2.5-3.5 m, 2.5 and 3.0-3.5 m, 3.0 and 3.5-4.0 m, 3.5 and 4.0-4.5 m, 4.0 and 4.5-5.0 m, 4.5 and 5.0-5.5 m, and 5.0 and 5.5 m (0.5 m = 1.93 m; 1.0 m = 2.17 m; 1.5 m = 2.38 m; 2.0 m = 2.63 m; 2.5

m = 2.91 m; 3.0 m = 3.19 m; 3.5 m = 3.57 m; 4.0 m = 3.92 m; 4.5 m = 4.28 m; 5.0 m = 4.63 m; 5.5 m = 4.93 m). These analyses showed that, for the most part, perceived distance traveled increased as a function of actual distance traveled.

For the vision control trials, no significant effects were found in the sliding ANOVA analysis of perceived distance traveled ($p > 0.083$; see Table 3.3 for F-values). This means that the blocks of vision trials demonstrated no systematic biases following performances of the gain adaptation conditions. Additionally, the perceived distance traveled analysis that compared the vision control and no-vision pre-adaptation trials showed only Vision main effects (see Table 3.4 for F-values of the sliding ANOVAs). Accordingly, for the distance iterations of 0.5-2.0 m in the 3 m walking trials and 0.5-2.5 m in the 5 m walking trials, perceived distances traveled in the no-vision pre-adaptation trials were greater than those in the vision control trials. Since there were no main effects or interactions involving Gain ($p > 0.105$), perceived distances traveled in the no-vision pre-adaptation trials were not impacted by the experimental order of gain adaptation conditions. This means that the vision control trials served their intended purpose of washing out potential carry-over effects between successive experimental blocks, and that any no-vision post-adaptation effects reported below can be assumed to result from sensory recalibration experienced in the adaptation periods.

For the analysis of perceived distance traveled in the no-vision pre- and post-adaptation trials, F-values for the sliding ANOVA results are presented in Table 3.5. For the 4 m walking distances, Gain by Test interactions at the distance iterations of 2.0-3.0 m showed greater no-vision post-adaptation perceived distances traveled in HVG compared

to LVG (see Figure 3.05). The main effect of Gain at 3.5 m showed a greater perceived distance traveled in HVG (3.73 m) compared to LVG (3.50 m). For the 6 m walking distances, the Gain by Test interaction at 5.5 m showed a greater no-vision post-adaptation perceived distance traveled in HVG compared to LVG (see Figure 3.06). The main effect of Test at 0.5 m showed a greater perceived distance traveled in no-vision pre-adaptation (1.75 m) compared to no-vision post-adaptation (1.69 m), while the Gain main effect at 5.0 m showed a greater perceived distance traveled in HVG (4.89 m) compared to LVG (4.68 m). Overall, these findings fit with the expectation that distance traveled would be under-perceived following low visual gain adaptation and over-perceived following high visual gain adaptation.

Constant error was used to examine the participant's positions along the walking path, with respect to the side-target, at the instances of 20° to -10° azimuth, in 5° increments. This is the most sensitive range for assessing pointing performance, for which changes as a function of the gain manipulations presented during the adaptation periods were of particular interest. For the constant error analysis, F-values of the sliding ANOVA results are presented in Table 3.6. In these analyses, relatively greater (i.e., more positive) constant error at the azimuth iterations indicates locations further down the walking path. In the 4 m walking trials, Gain by Test interactions at azimuth angles of 0° and -5° showed greater no-vision post-adaptation constant error in LVG compared to HVG (see Figure 3.07). At -10° azimuth, this interaction showed greater post-adaptation constant error in CVG and LVG compared to HVG. There were no significant effects in the 6 m walking trials ($p > 0.075$; see Figure 3.08).

Azimuth angle at peak azimuth was used to examine the azimuth angle at which the pointing responses reached maximum velocity during the continuous pointing trials. Effective continuous pointing demonstrates values close to 0° in this measure, which is used as an assessment of perceived target passage. The analyses of azimuth angle at peak azimuth velocity (grand means: 4 m = -0.888°; 6 m = 0.476°) and peak azimuth velocity (grand means: 4 m = 34.74 °/s; 6 m = 32.87 °/s) demonstrated no significant effects for either walking distance. In showing no gain-related effects in these measures, performers were assumed to have effectively perceived target passage. This means that the constant error patterns indicated perceptual differences created by sensory recalibrations and were not artefacts created by incorrectly performed pointing responses.

The significant arm deviations were trajectory fluctuations calculated using the aforementioned trajectory parsing procedure. They were examined according to number per trial, actual and perceived distances traveled between the start and end of each deviation, and location in the step-cycle of the start and end of each deviation. Analysis of the number of significant arm deviations per trial showed no significant effects (grand means: 4 m = 4.17, 6 m = 5.54). The analysis of actual distance traveled per significant arm deviation at the 4 m walking distance showed a significant main effect of Deviation Number, $F(3,42) = 19.22$, $p < 0.001$. Accordingly, a greater actual distance was traveled in deviation 1 compared to deviations 2-4, as well as in deviation 2 compared to deviation 4 (Deviation: 1 = 1.14 m, 2 = 0.860 m, 3 = 0.790 m, 4 = 0.620 m). For the 6 m walking distance, a main effect of Deviation Number, $F(4,56) = 40.65$, $p < 0.001$, showed a greater actual distance traveled in deviation 1 compared to deviations 2-5 (Deviation: 1 =

1.58 m, 2 = 0.920 m, 3 = 0.920 m, 4 = 0.800 m, 5 = 0.720). For perceived distance traveled per significant arm deviation, analysis at the 4 m walking distance demonstrated a significant main effect of Deviation Number, $F(3,42) = 6.35$, $p < 0.01$. This showed greater perceived distances traveled in deviations 1 and 2 compared to deviation 4 (Deviation: 1 = 0.802 m, 2 = 0.766 m, 3 = 0.689 m, 4 = 0.516 m). The Gain by Test by Deviation Number interaction narrowly missed reaching the conventional level of statistical significance ($p = 0.052$). However, as presented in Figure 3.09, there was a trend toward greater perceived distances traveled in the first three post-adaptation deviations in HVG compared to LVG. This pattern seemed to be reversed in the last deviation. At the 6 m walking distance, a Test by Deviation Number interaction, $F(4,56) = 2.63$, $p < 0.05$, demonstrated a greater perceived distance traveled in no-vision post-adaptation (Deviation: 1 = 0.83 m, 2 = 0.70 m, 3 = 0.75 m, 4 = 0.57 m, 5 = 0.54 m) compared to no-vision pre-adaptation at deviation 1 (Deviation: 1 = 0.71 m, 2 = 0.65 m, 3 = 0.67 m, 4 = 0.65 m, 5 = 0.58 m). Further, a main effect of Gain, $F(2,28) = 5.78$, $p < 0.01$, showed an overall greater perceived distance traveled per deviation in HVG (.709 m) compared to CVG (.640 m) and LVG (.647 m).

When examined in regards to location in the step-cycle, the analyses comparing test conditions for significant arm deviation starts were non-significant in all of the gain conditions (CVG1: $\chi^2(6) = 4.24$, $p > 0.10$; CVG2: $\chi^2(6) = 0.96$, $p > 0.10$; LVG: $\chi^2(6) = 10.40$, $p > 0.10$; HVG: $\chi^2(6) = 2.74$, $p > 0.10$). However, when the frequency counts were pooled across test conditions and comparisons are made between the step-cycle phases, the analyses were significant in all of the gain conditions (CVG1: $\chi^2(3) = 347.21$, $p <$

0.01; CVG2: $\chi^2(3) = 479.85$, $p < 0.01$; LVG: $\chi^2(3) = 409.62$, $p < 0.01$; HVG: $\chi^2(3) = 483.81$, $p < 0.01$). Specifically, for all gain conditions, these analyses showed greater frequency counts in the late left and early right categories compared to the early left and late right categories (see Figure 3.10). Furthermore, in LVG and HVG, the late right category showed greater frequency counts than the early left category. Analysis of the frequencies between the different gain conditions was not significant, $\chi^2(9) = 15.11$, $p > 0.05$. Similar results were demonstrated for the significant arm deviation ends. Specifically, there were no differences between the frequency counts of the test conditions in any of the gain conditions (CVG1: $\chi^2(6) = 6.11$, $p > 0.10$; CVG2: $\chi^2(6) = 6.93$, $p > 0.10$; LVG: $\chi^2(6) = 7.61$, $p > 0.10$; HVG: $\chi^2(6) = 6.74$, $p > 0.10$). When pooled across test conditions, the analyses showed significant differences in the frequency counts of the step-cycle phases in all of the gain conditions (CVG1: $\chi^2(3) = 432.90$, $p < 0.01$; CVG2: $\chi^2(3) = 437.10$, $p < 0.01$; LVG: $\chi^2(3) = 435.33$, $p < 0.01$; HVG: $\chi^2(3) = 417.52$, $p < 0.01$). This demonstrated greater frequency counts in the early left and early right phases compared to the late left and late right phases in all of the gain conditions (see Figure 3.11). Furthermore, the late left category showed greater frequencies than the late right category in all gain conditions; and the early right category showed greater frequencies than the early left category in CVG2, LVG and HVG. The analysis of the frequency counts between gain conditions was not significant, $\chi^2(9) = 9.89$, $p > 0.10$.

Considering that there were no significant differences between the gain and test conditions for both significant arm deviation starts and ends, an additional Chi Square analysis was performed by pooling frequency counts across gain and test conditions and

examining the frequency counts between significant arm deviation starts and ends. Expected values were based on the percentage of the total number of deviations in each step-phase category multiplied by the total number of deviations in each of the significant arm deviation start and end categories. This analysis was significant, $\chi^2(3) = 1288.52$, $p < 0.01$, which showed relatively greater significant arm deviation end frequencies in the early left and early right phases, and relatively greater significant arm deviation start frequencies in the late left and late right phases (see Figure 3.12). However, in both significant arm deviation starts and ends, the highest frequency counts were shown in the early right phase. Collectively, the significant arm deviation results showed no gain or test related changes in the location of the significant arm deviation starts and ends in the step-cycle. Thus, in a similar manner to Study 1, the starts of significant arm deviations were robustly linked to the late left-to-early right phase of the step-cycle. Considering the aforementioned gain related changes in perceived distance traveled and constant error, this suggested that the perceptual differences resulting from sensory recalibration unfolded across each updating unit involved in a walking movement. These differences appeared to accumulate to the point of statistical significance at the end of a walking trajectory.

3.5 – DISCUSSION

Study 2 showed that the sensory recalibration of spatial updating during no-vision walking resulted from a change in the CNS perception of self-motion derived from unaltered kinematic leg activity (Durgin et al., 2005; Rieser et al., 1995). This was demonstrated during no-vision walking as an under-perception of self-motion following

LVG adaptation and an over-perception of self-motion following HVG adaptation. Specifically, greater perceived distances traveled following HVG adaptation and shorter perceived distances traveled following LVG adaptation emerged toward the end of the 4 m and 6 m walking paths. The perceived distances traveled following the CVG conditions consistently remained neutral. Importantly, these post-adaptation differences in perceived self-motion were not accompanied with gain related changes in the step characteristics and actual walking velocities. Presumably then, the proprioceptive information involved with the kinematic activity of walking was recalibrated in the CNS to match the perception of self-motion driven by the rate of virtual optic flow (Mohler et al., 2007).

Despite these gain related differences in perceived self-motion, the pointing responses showed that participants effectively indicated their intended target passage during the walking trials. In typical continuous pointing, perceived target passage is considered to occur at 0° azimuth as the arm also reaches peak azimuth velocity. For all gain and test conditions in the current study, azimuth angles at peak azimuth velocity were close 0° (grand mean of study = -0.206°) and there were no significant effects demonstrated for peak azimuth velocity. This means that the performers abilities to approximate perceived target passage were not directly impacted by the visual gain manipulations. These results showed that the pointing responses remained unbiased indicators of perceived target passage, even after exposure to the adaptation conditions. However, despite effectively indicating perceived target passage, the performers physical locations of perceived target passage were systematically impacted by the gain conditions. Specifically, in the no-vision post-adaptation continuous pointing trials for the

4 m walking distance, participants were further down the walking path in perceiving target passage following LVG adaptation compared to HVG adaptation. Once again, CVG remained neutral to these conditions. These results persisted as constant error differences at the azimuth angles of -5° and -10°. Although these latter findings were specific to the 4 m walking distance, a similar trend was visible for the 6 m trials (see Figures 3.07 and 3.08).

Interestingly, the analysis of significant arm deviations showed no gain-related effects involving number per trial or actual distance traveled per deviation. However, in the 4 m walking movements, there was a trend toward greater no-vision post-adaptation perceived distances traveled per significant arm deviation in HVG versus LVG. In the 6 m trials, a gain main effect showed an overall greater perceived distance traveled per significant arm deviation in HVG versus the LVG and CVG conditions. This means that the aforementioned gain-related differences in no-vision post-adaptation perceived distance traveled were likely the result of perceptual differences accumulated across iterations of spatial updating. These findings contribute to the model of CNS spatial updating introduced in Study 1. Specifically, Study 1 used a leaky integrator model (Lappe & Frenz, 2009) to suggest that during continuous pointing, a task-relevant state parameter was updated in the CNS during no-vision walking. In the current version of the continuous pointing task, this state parameter can be considered to represent a cumulative (i.e., additive) estimation of perceived distance traveled. According to leaky integration, this state parameter was underestimated in no-vision performance and resulted in a misestimating of spatial position as spatial extent increased. In Study 1, this state

parameter was underestimated in the no-vision walking movements, a finding that was indicated in the CNS updating units identified by the significant arm deviations. The aforementioned perceptual differences between the LVG, CVG and HVG conditions at the CNS updating iterations suggests that a similar updating mechanism was used by participants in the current study.

Furthermore, the sensory recalibrations demonstrated in this study had no impact on significant arm deviation location in the step-cycle. That is, regardless of gain or test condition, significant arm deviation starts had greater frequencies in the late left and early right step-cycle phases and significant arm deviation ends had greater frequencies in the early left and early right step-cycle phases. This relationship suggests that the starts and ends of spatial updating iterations were fundamentally linked to early movement in the right leg, irrespective of changes in experimental condition (e.g., Rinaldi & Moraes, 2015). Presumably, the high frequency count of significant arm deviation ends in the early left phase indicated preparation for a subsequent significant arm deviation start in the early right phase. These patterns of results were similar to those demonstrated in Study 1, which showed no difference in the significant arm deviation start and end patterns between vision and no-vision movements.

Study 1 suggested that by linking the starts and ends of significant arm deviations to the late left-to-early right foot swing phases, the CNS anchored iterative spatial updating to a consistent part of the step-cycle. This was presumed to aid in the estimation of distance traveled across iterative segments, after which it was added to an ongoing cumulative sum. This modelling of spatial updating was consistent with a leaky integrator

model, which attributed updating error to CNS integration and estimation across task-specific updating iterations (Lappe & Frenz, 2009). In the current study, this mechanism of linking arm deviations to a specific step-cycle event presumably served the same purpose. The fact that the CNS maintained this stable relationship in no-vision walking following prolonged exposures to sensory adaptation supports the notion that the CNS organized iterations of spatial updating with movement in the dominant limb, and that this tactic was quite robust. This also supports the notion that recalibrated spatial updating resulted from changes in how the CNS perceived self-motion in relation to stable leg kinematic activity (Durgin et al., 2005; Rieser et al., 1995).

Redding and Wallace (see 2005 for a review) identified two CNS mechanisms as forming the basis for performance after-effects that followed prolonged exposure to sensory cue conflict. These included strategic calibration and spatial alignment. Specifically, strategic calibration referred to adaptations in motor control that adjusted for immediate changes to task and workspace conditions, while spatial alignment referred to adaptations in the mappings between component elements of a sensory-motor system. The recalibration effects described in this study can be considered as spatial alignment, since the post-adaptation changes in spatial updating were not accompanied by changes in step-cycle kinematics. This suggests that adaptations to strategic motor control did not influence post-adaptation locomotive performance. Additionally, the post-adaptation perceptual differences amongst the LVG, CVG and HVG conditions were indicated in the continuous pointing movements. Since pointing movements were not performed during the sensory adaptation periods, there was no means of strategically adjusting the control

of these movements on the basis of experiencing the gain conditions. Therefore, the sensory recalibration effects in this study can be considered as a realigning of the mapping between leg sensory-motor systems and the CNS perception of self-motion. However, since the current study was not designed to specifically assess the impacts of strategic calibration and spatial alignment on recalibrated locomotive performance, future study is warranted.

In the current study, continuous pointing trials started with participants fixating a laser on the side-target during the initial visual preview. This was done to directly align participants pointing responses with the side-target at the start of every trial. Although it was not expected to dramatically impact the perceptual measures of self-motion, pointing with the laser introduced a start point dependency that was not present in Study 1. This is clearly identified by comparing Figure 2.13 from Study 1 (see also Figures 4.03 and 4.04 in Study 3) and Figures 3.05 and 3.06 from the current study. Specifically, compared to those in Study 1, the measures of perceived distance traveled in the current study appeared non-linear with a y-intercept greater than zero. Although this start point dependency did not impact the ability to make relative comparisons between gain conditions, it impacted the absolute spatial accuracy of the perceptual measures.

This start point dependency can possibly be explained as dissociations between the intended and actual projected locations of the pointing responses toward the side-targets. Since the laser was not used in Study 1, the locations to where participants thought they were pointing was different from where they were actually pointing. To experience this dissociation, hold a laser pen directly underneath the right index fingertip

and point at an object across the room without activating the laser. Once fixated on the target object, activate the laser beam. The likely outcome will be that the laser beam projects to a location not precisely aligned with the target object. In Study 1, where the laser pointer was not used, this error was irrelevant because it likely remained consistent throughout the durations of walking trials. In the current study, pointing with the laser prior to walking (i.e., during the visual preview) initially aligned the intended and actual pointing projections. However, once no-vision walking commenced in the pre- and post-adaptation trials, the dissociated relationship immediately retuned and resulted in the aforementioned target specific aiming errors. For the vision trials, peripheral vision was likely used to maintain the initial arm-target alignment up until target passage, at which time it could no longer be maintained and the dissociated relationship returned. This might account for the Vision main effects in the 3 m and 5 m walking distances, which appeared only for the analyses up to 2.0 m and 2.5 m, respectively (see Table 3.4). These distances approximated the average side target distances used for these walking paths (average target distance: 3 m walking = 1.93 m; 5 m walking = 3.17 m) and contradicted Study 1 by showing greater perceived distances traveled in the no-vision trials (see also Study 3). Since the goal of continuous pointing was to measure perception along the forward walking path, as opposed to pointing accuracy to targets in far space, the initial pointing method used in Study 1 was readopted for Study 3.

In summary, this study showed perceptual differences in no-vision continuous pointing movements performed before and after prolonged exposures to low and high visual gain adaptations. In this context, proprioceptive leg activity was considered to

recalibrate to the perception of self-motion driven by optic flow (Mohler et al., 2007). Most interesting is that in spite of these changes in CNS self-motion perception, kinematic leg activity remained unaltered and a strong relationship persisted between the significant arm deviations and the step-cycle (see also Study 1). While this strong relationship was considered to indicate iterative spatial updating performed by the CNS (see Study 1), it also highlighted a robust coordinative behaviour between the upper and lower limb activity involved in locomotion (Chiovetto & Giese, 2013; Marteniuk & Bertram, 2001; Marteniuk et al., 2000; Rinaldi & Moraes, 2015; Van Der Wel & Rosenbaum, 2007). In certain contexts, coordinated activity between the upper and lower limbs during locomotion has been shown to impact distance perception (Harrison et al., 2013). Considering that these upper limb responses also provide direct indications of target relative spatial location (Campos et al., 2009), it is possible that in some way, this upper limb activity uniquely contributed to the CNS perception of self-motion experienced during the continuous pointing task. Study 3 examined this possibility by introducing gained upper limb pointing responses into the sensory adaptation periods. Of interest was whether prolonged adaptations to these sensory cue conflicts resulted in upper limb activities that became recalibrated to match the perceptions of self-motion established by the visually specified rates of self-motion.

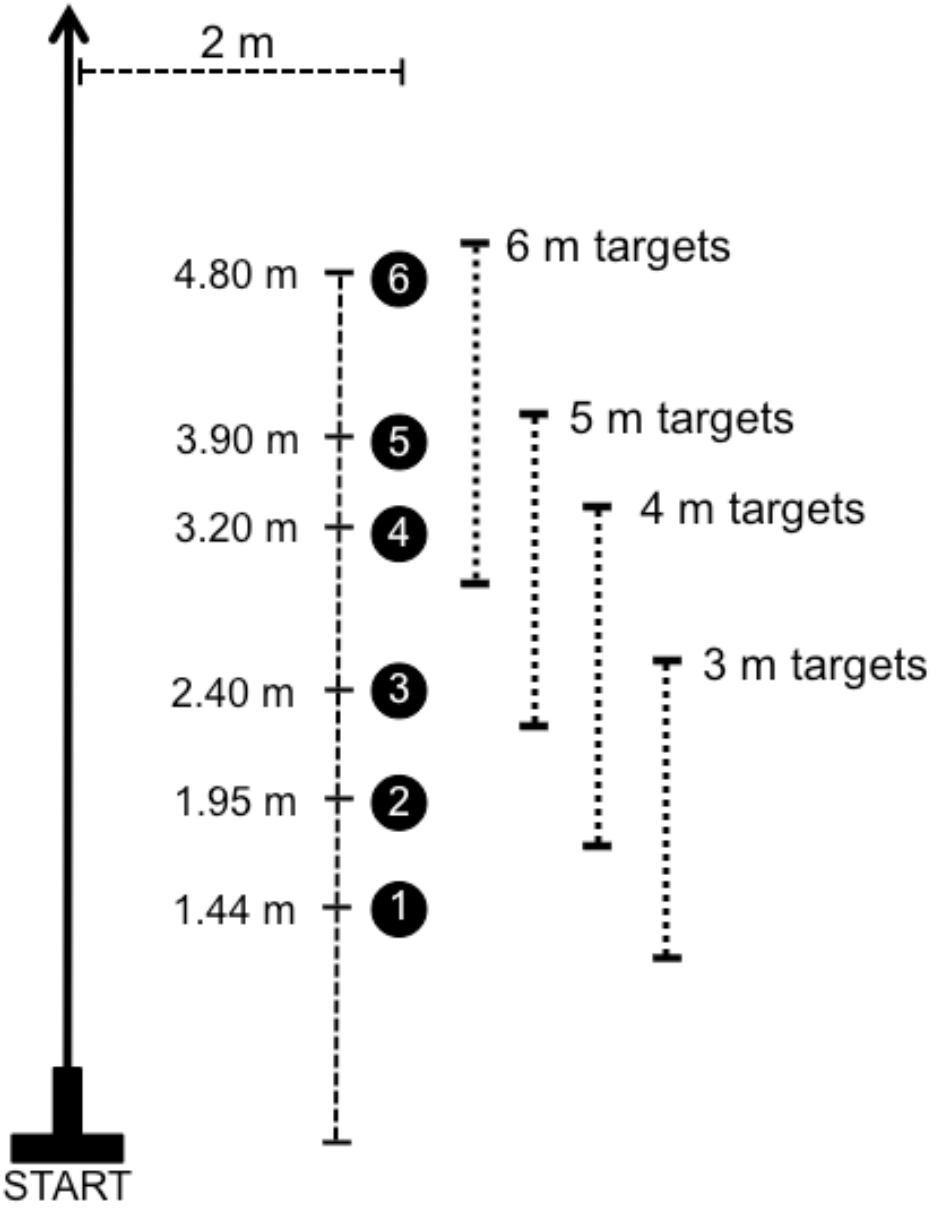

Figure 3.01. Above view schematic of the experimental layout of Studies 2 and 3. Inverted black 'T' represents start location; vertical black arrow represents linear walking path; black circles represent the side-target locations, with the numbers indicating target number. Dashed black lines to the left of the targets indicate distances along and beside walking path. Dashed black lines to the right of the targets indicate the target locations used for the respective walking distances.

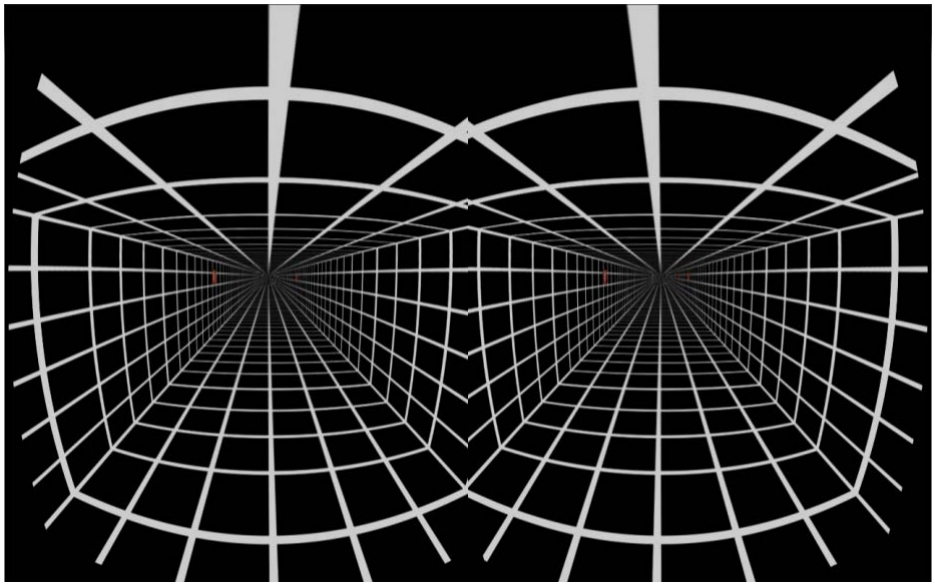

Figure 3.02. Virtual hallway presented during the sensory adaptation periods using the Oculus Rift head-mounted display.

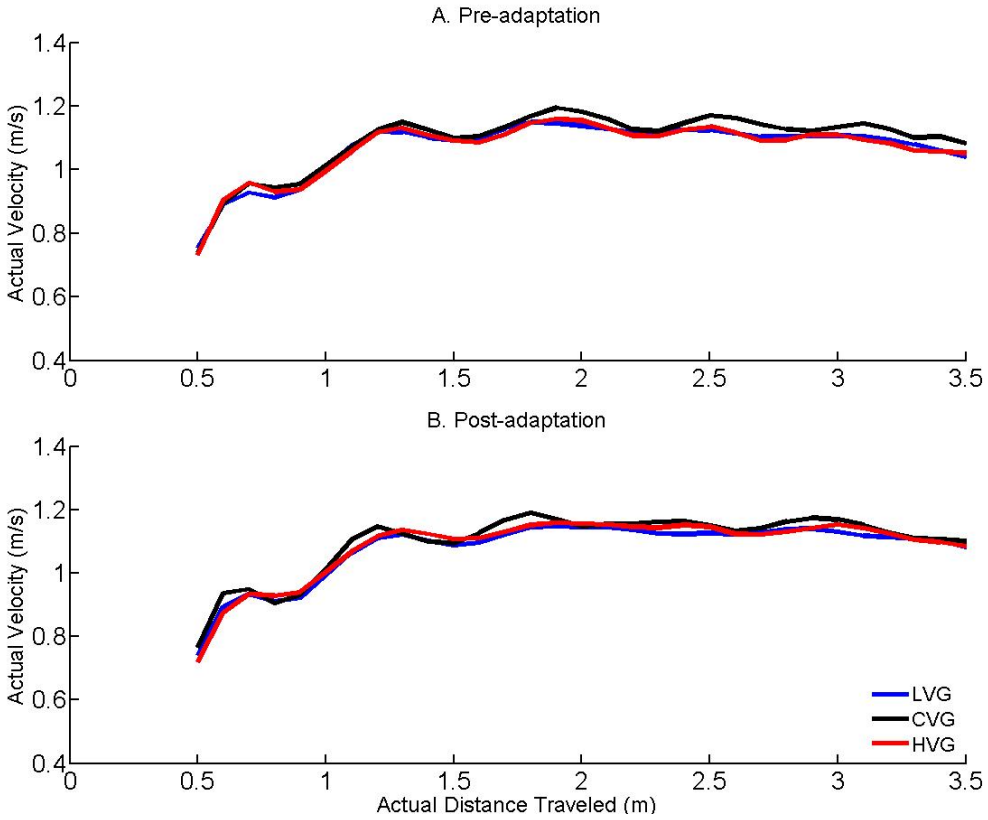

Figure 3.03. Study 2: Actual velocity trajectories for the pre-adaptation (top) and post-adaptation (bottom) 4 m no-vision continuous pointing trials. LVG = low visual gain condition (blue); CVG = congruent visual condition (black); HVG = high visual gain condition (red).

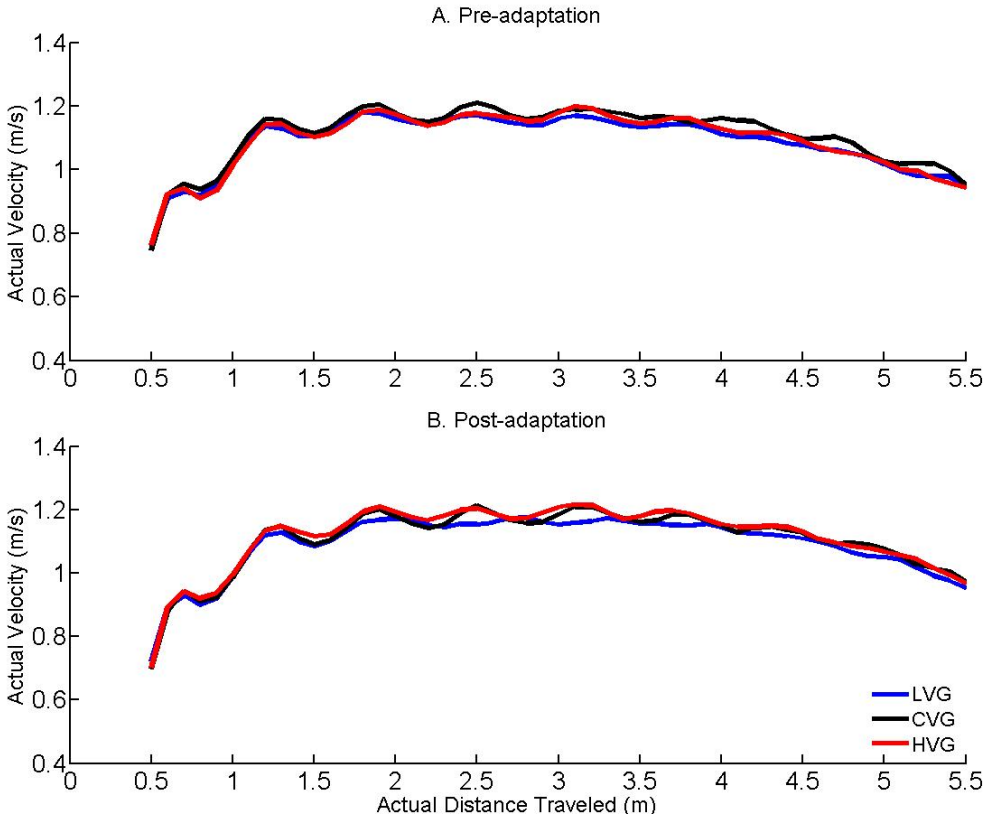

Figure 3.04. Study 2: Actual velocity trajectories for the pre-adaptation (top) and post-adaptation (bottom) 6 m no-vision continuous pointing trials. LVG = low visual gain condition (blue); CVG = congruent visual condition (black); HVG = high visual gain condition (red).

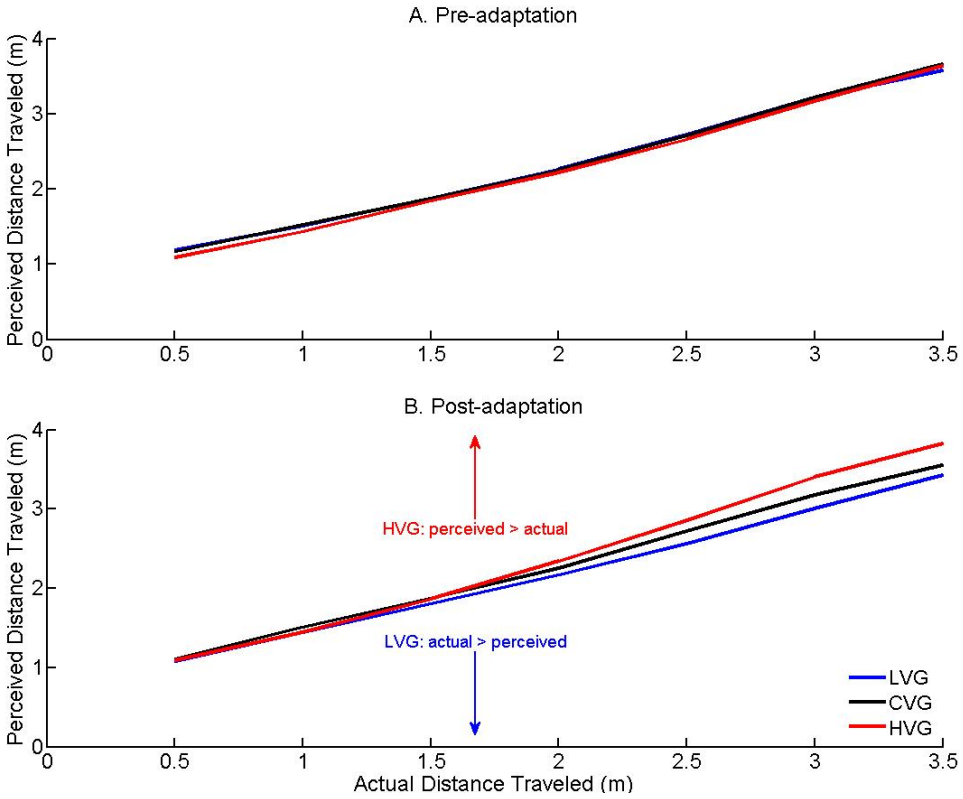

Figure 3.05. Study 2: Perceived distances traveled for the pre-adaptation (top) and post-adaptation (bottom) 4 m no-vision continuous pointing trials. LVG = low visual gain condition (blue); CVG = congruent visual condition (black); HVG = high visual gain condition (red). The words and arrows in the bottom figure show the hypothesized predictions of the post-adaptation gain related differences.

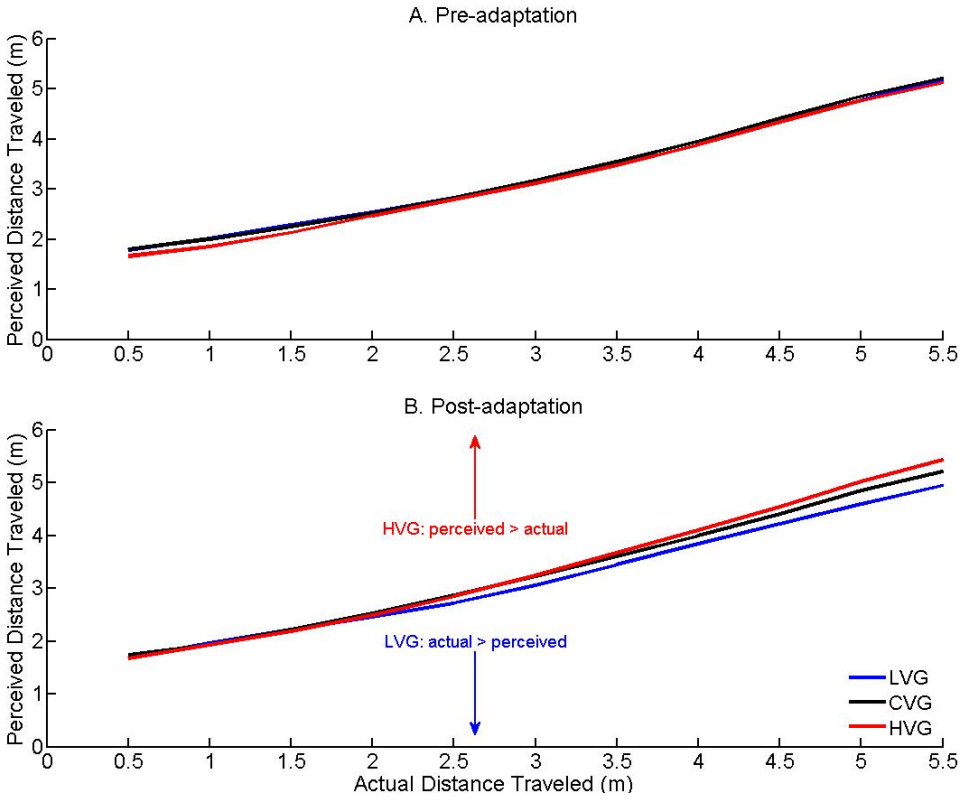

Figure 3.06. *Study 2: Perceived distance traveled for the pre-adaptation (top) and post-adaptation (bottom) 6 m no-vision continuous pointing trials. LVG = low visual gain condition (blue); CVG = congruent visual condition (black); HVG = high visual gain condition (red). The words and arrows in the bottom figure show the hypothesized predictions of the post-adaptation gain related differences.*

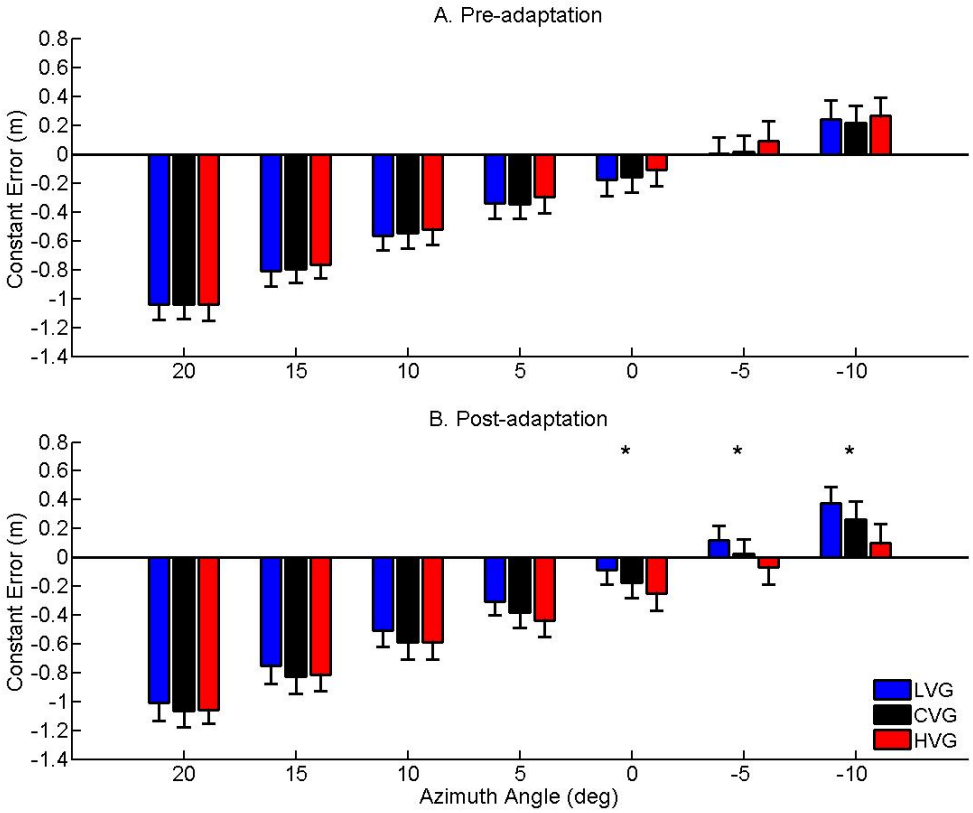

Figure 3.07. Study 2: Constant error with respect to the side-target at 20° to -10° azimuth angle for the pre-adaptation (top) and post-adaptation (bottom) 4 m no-vision continuous pointing trials. Positive values indicate distances beyond the side-target along the walking path; negative values indicate distances short of the target along the walking path. LVG = low visual gain condition (blue); CVG = congruent visual condition (black); HVG = high visual gain condition (red). Asterisks indicate azimuth angles with significant mean differences between gain conditions. Error bars represent one standard error.

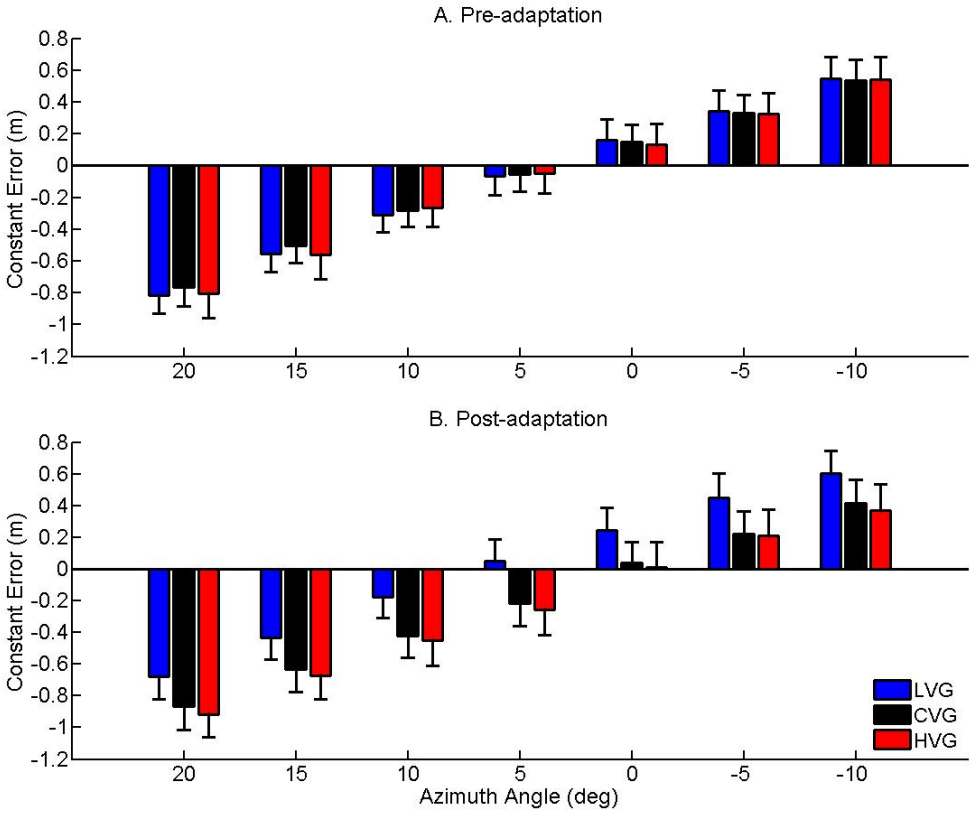

Figure 3.08. *Study 2: Constant error with respect to the side-target at 20° to -10° azimuth angle for the pre-adaptation (top) and post-adaptation (bottom) 6 m no-vision continuous pointing trials. Positive values indicate distances beyond the side-target along the walking path; negative values indicate distances short of the target along the walking path. LVG = low visual gain condition (blue); CVG = congruent visual condition (black); HVG = high visual gain condition (red). Error bars represent one standard error.*

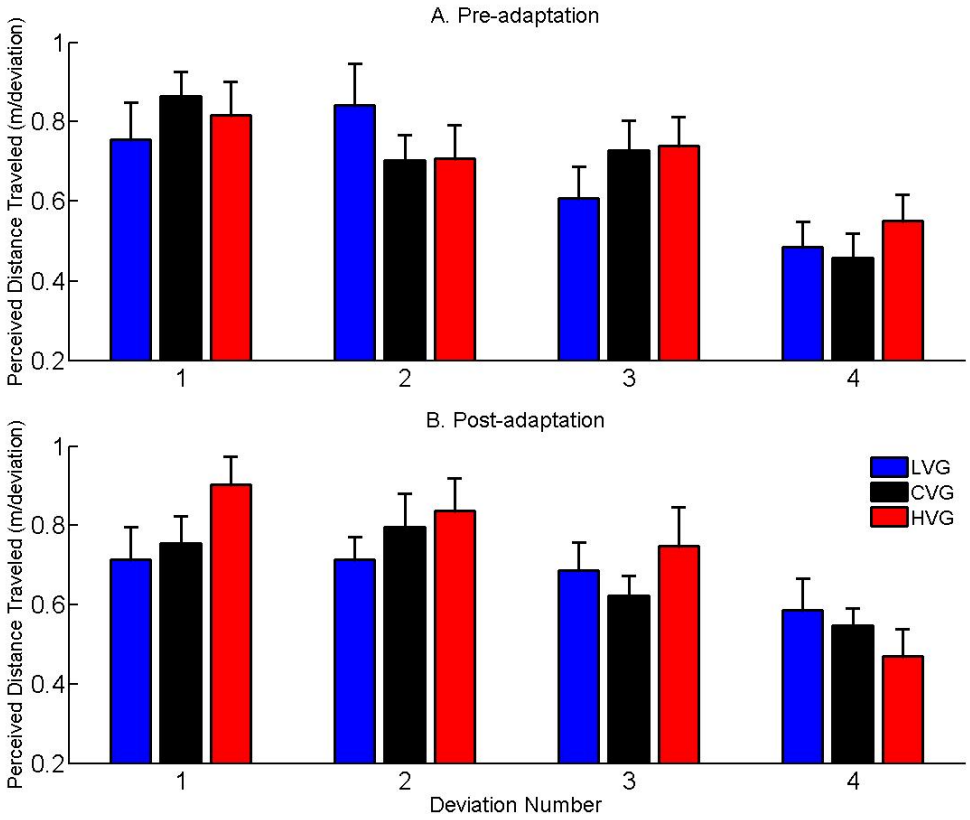

Figure 3.09. Study 2: Gain by Test by Deviation Number means for perceived distance traveled per significant arm deviation for the pre-adaptation (top) and post-adaptation (bottom) 4 m no-vision continuous pointing trials. This interaction narrow missed reaching the conventional level of statistical significance (p = 0.052). LVG = low visual gain condition (blue); CVG = congruent visual condition (black); HVG = high visual gain condition (red). Error bars represent one standard error.

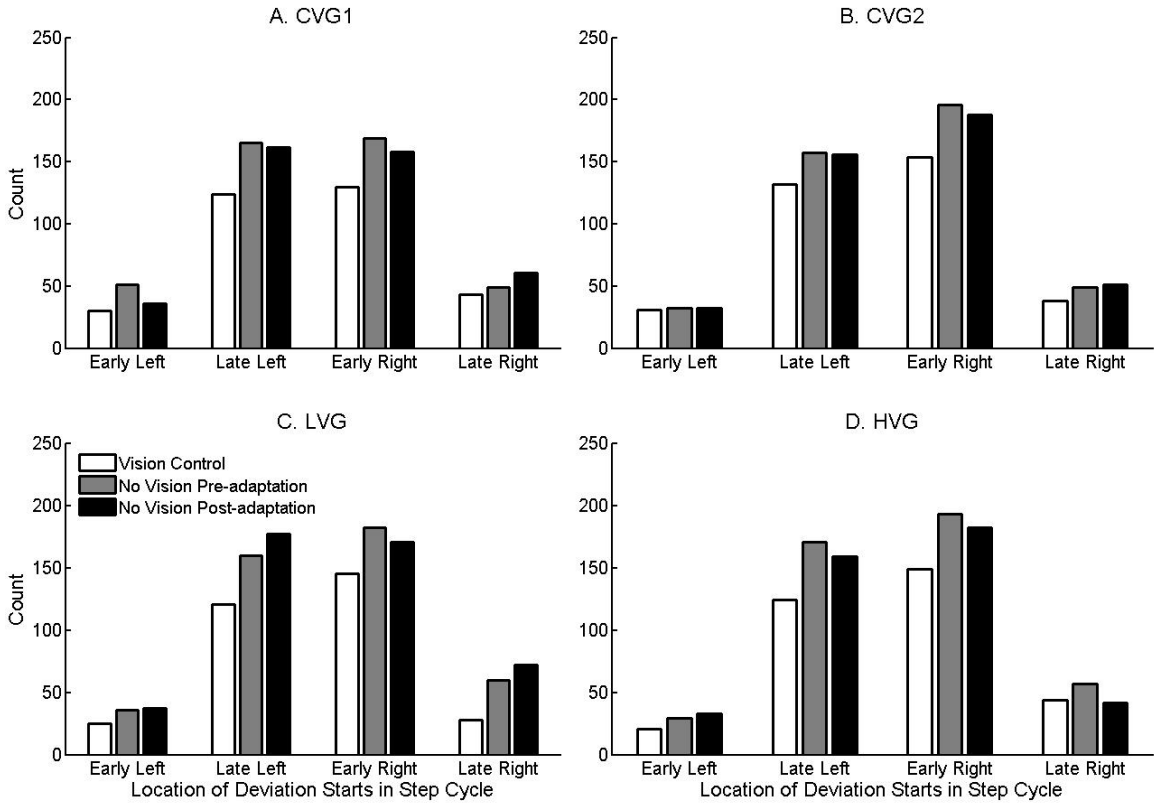

Figure 3.10. Study 2: Frequency counts for the significant arm deviation starts in the four classified phases of the step-cycle for CVG1 (top left), CVG2 (top right), LVG (bottom left), HVG (bottom right). CVG1 = first block of the congruent visual condition; CVG2 = second block of the congruent visual condition; LVG = low visual gain condition; HVG = high visual gain condition. Open bars represent vision control continuous pointing trials; filled grey bars represent no-vision pre-adaptation continuous pointing trials; filled black bars represent no-vision post-adaptation continuous pointing trials.

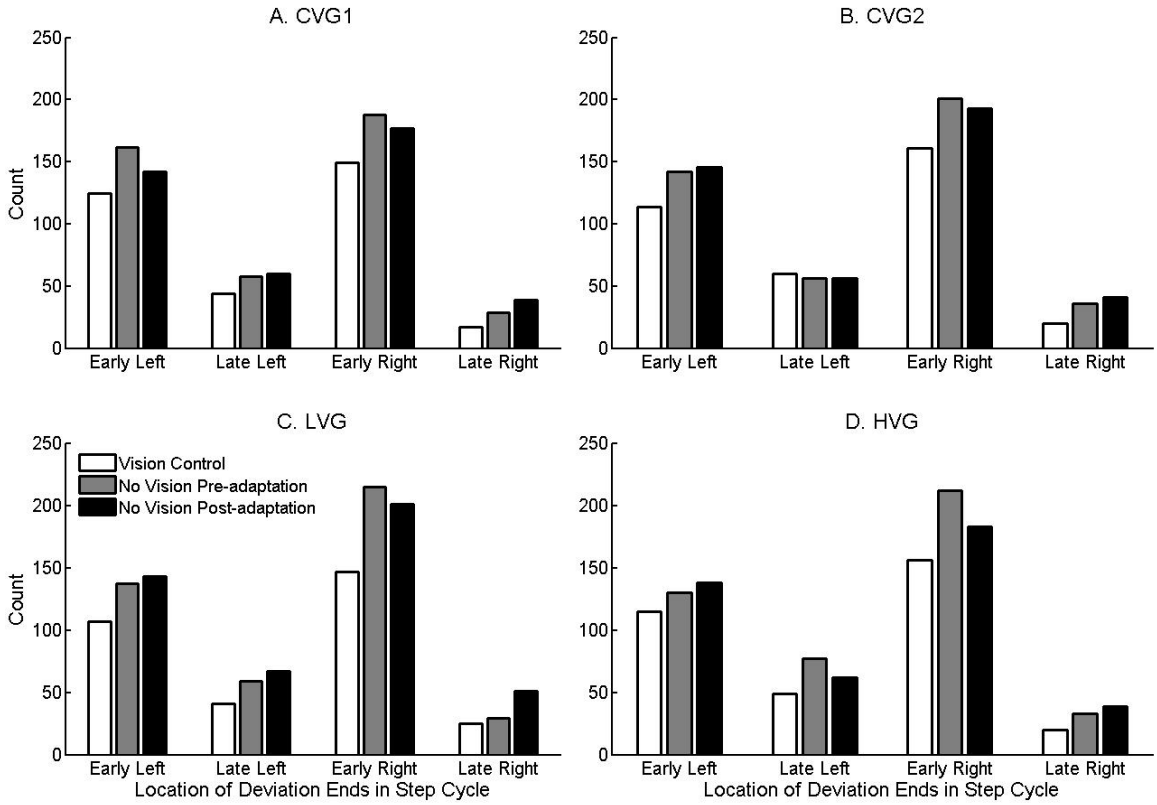

Figure 3.11. Study 2: Frequency counts for the significant arm deviation ends in the four classified phases of the step-cycle for CVG1 (top left), CVG2 (top right), LVG (bottom left), HVG (bottom right). CVG1 = first block of the congruent visual condition; CVG2 = second block of the congruent visual condition; LVG = low visual gain condition; HVG = high visual gain condition. Open bars represent vision control continuous pointing trials; filled grey bars represent no-vision pre-adaptation continuous pointing trials; filled black bars represent no-vision post-adaptation continuous pointing trials.

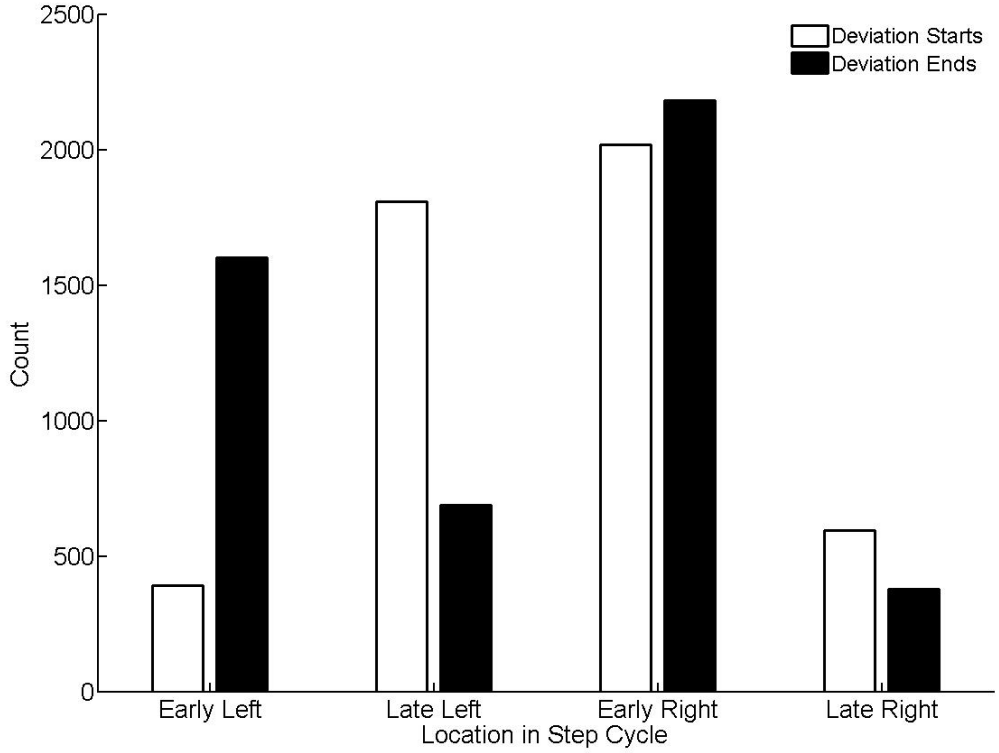

Figure 3.12. Study 2: Frequency counts for the significant arm deviation starts (open bars) and ends (filled bars) in the four classified phases of the step-cycle. Data in this figure are pooled across gain and test conditions.

Table 3.1. Study 2: Sliding ANOVA results for the actual velocity analysis in the no-vision pre- and post-adaptation trials.

	4 m				6 m			
	F-values			Grand mean (m)	F-values			Grand mean (m)
Distance (m)	G	T	GT		G	T	GT	
0.5	1.38	< 0.001	1.00	0.742	0.558	**10.62****	0.059	0.734
1.0	1.02	0.182	0.941	1.00	0.164	**11.59****	1.23	1.01
1.5	0.122	0.067	0.667	1.10	0.401	0.961	1.72	1.10
2.0	0.558	0.373	1.73	1.15	0.336	1.24	0.221	1.12
2.5	1.16	0.042	1.34	1.14	1.97	0.072	0.975	1.19
3.0	1.51	**8.31***	0.513	1.13	3.10	0.169	1.20	1.18
3.5	1.11	**8.70***	0.548	1.10	0.573	1.64	2.05	1.16
4.0	-	-	-	-	1.07	1.51	1.55	1.14
4.5	-	-	-	-	0.532	**7.19***	0.075	1.11
5.0	-	-	-	-	0.188	**10.00****	0.177	1.04
5.5	-	-	-	-	0.126	1.94	0.102	0.956

Note. *p < 0.05. **p < 0.01. ***p < 0.001. G = Gain (2, 28), T = Test (1,14), GT = Gain by Test (2,28). Degrees of freedom in brackets.

Table 3.2. Study 2: Grand means for the step characteristics of the 4 and 6 m no-vision pre- and post-adaptation trials.

Distance	Step Length (m)	Left Stride Length (m)	Right Stride Length (m)	Number of Steps
4 m	0.618	1.27	1.24	7.41
6 m	0.623	1.26	1.25	10.48

Table 3.3. Study 2: Sliding ANOVA results for the analysis of perceived distance traveled in the vision control trials.

	3 m		5 m	
Iteration (m)	F	Grand Mean (m)	F	Grand Mean (m)
0.5	1.38	0.963	0.787	1.49
1.0	1.12	1.38	0.700	1.81
1.5	1.69	1.78	1.12	2.08
2.0	1.95	2.18	0.577	2.40
2.5	2.38	2.61	0.225	2.78
3.0	-	-	0.065	3.17
3.5	-	-	0.581	3.62
4.0	-	-	0.971	4.01
4.5	-	-	1.76	4.32

Note. *p < 0.05. **p < 0.01. ***p < 0.001. Degrees of freedom: Gain (3,42).

Table 3.4. Study 2: Sliding ANOVA results for the analysis of the perceived distance traveled in the vision control and no-vision pre-adaptation trials.

	3 m					5 m				
	F-values			Means (m)		F-values			Means (m)	
Distance (m)	G	V	GV	VC	NVPRE	G	V	GV	VC	NVPRE
0.5	1.84	**106.14*** **	0.550	0.963	1.23	2.09	**138.74*** **	1.97	1.49	1.95
1.0	0.674	**47.49*** **	1.18	1.38	1.56	1.37	**46.95*** **	0.616	1.81	2.18
1.5	0.505	**25.78*** **	1.87	1.78	1.90	1.50	**34.37*** **	0.850	2.08	2.39
2.0	0.739	**6.24***	2.17	2.18	2.26	0.687	**22.78*** **	0.174	2.40	2.64
2.5	0.991	2.65	1.93	2.61	2.68	0.851	**5.66***	0.685	2.78	2.90
3.0	-	-	-	-	-	0.949	0.162	1.72	3.17	3.19
3.5	-	-	-	-	-	0.177	2.45	1.30	3.62	3.55
4.0	-	-	-	-	-	0.146	4.45	1.79	4.01	3.90
4.5	-	-	-	-	-	0.380	1.00	2.18	4.32	4.26

Note. *p < 0.05. **p < 0.01. ***p < 0.001. G = Gain (3,42), V = Vision (1,14), GV = Gain by Vision (3,42). Degrees of freedom in brackets. VC = vision control trials, NVPRE = no-vision pre-adaptation trials.

Table 3.5. Study 2: Sliding ANOVA results for the analysis of perceived distance traveled in the no-vision pre- and post-adaptation trials.

	4 m				6 m			
	F-values			Grand mean (m)	F-values			Grand mean (m)
Distance (m)	G	T	GT		G	T	GT	
0.5	0.774	3.91	1.35	1.12	1.66	**4.68***	0.847	1.72
1.0	2.06	0.641	0.733	1.48	2.99	0.501	1.44	1.95
1.5	0.308	0.397	1.14	1.86	2.09	0.191	1.07	2.22
2.0	1.08	0.159	**4.04***	2.25	0.353	0.178	0.642	2.50
2.5	2.64	0.419	**6.26****	2.70	1.33	0.016	1.32	2.81
3.0	**5.01***	0.011	**4.84***	3.19	2.01	0.329	2.61	3.17
3.5	**7.42****	0.316	3.14	3.61	1.30	1.23	2.89	3.55
4.0	-	-	-	-	1.13	1.06	2.46	3.95
4.5	-	-	-	-	2.56	0.408	2.56	4.38
5.0	-	-	-	-	**5.00***	0.403	3.51	4.81
5.5	-	-	-	-	**3.62***	0.303	**4.66***	5.18

Note. *p < 0.05. **p < 0.01. ***p < 0.001. G = Gain (2, 28), T = Test (1,14), GT = Gain by Test (2,28). Degrees of freedom in brackets.

Table 3.6. Study 2: Sliding ANOVA results for the analysis of constant error at azimuth angle in the no-vision pre- and post-adaptation trials.

	4 m				6 m			
	F-values			Grand mean (m)	F-values			Grand mean (m)
Azimuth angle (°)	G	T	GT		G	T	GT	
20	0.202	0.021	0.251	-1.04	0.908	0.226	2.00	-0.809
15	0.189	0.032	0.872	-0.795	1.06	0.465	1.80	-0.560
10	0.183	0.522	1.14	-0.553	1.46	1.44	2.73	-0.317
5	0.658	2.94	2.19	-0.351	1.90	2.21	2.84	-0.098
0	0.541	0.868	**4.22***	-0.160	1.95	0.843	1.46	0.122
-5	0.511	0.210	**4.94***	0.032	2.24	0.483	1.75	0.314
-10	2.98	0.071	**5.55****	0.244	1.94	2.54	1.10	0.503

Note. *p < 0.05. **p < 0.01. ***p < 0.001. G = Gain (2, 28), T = Test (1,14), GT = Gain by Test (2,28). Degrees of freedom in brackets.

CHAPTER 4:

STUDY 3

THE IMPACT OF UPPER LIMB RESPONSES TO THE PERCEIVED SELF-MOTION REALIZED DURING A LOCOMTIVE CONTINUOUS POINTING TASK

4.1 – ABSTRACT

In some forms of locomotion, CNS distance perception shows a dependence on coordinated activity performed in the upper limbs (Harrison et al., 2013). The continuous pointing task introduced in Studies 1 and 2 involves target-directed upper limb activity that is distinctly coordinated with locomotive activity. This coordination pattern involves upper limb trajectory deviations that are most frequently linked to the late left-to-early right foot swing phase of the step-cycle. The purpose of Study 3 was to examine whether this upper limb coordination pattern contributed to the CNS self-motion perception. This was examined by attempting to recalibrate the relationship between arm pointing and forward walking during sensory adaptation. Therefore, in Study 3, continuous pointing was performed before and after different sensory adaptation periods where performers either walked or stood stationary on a treadmill while receiving high and low visual or arm gains. Visual gains were achieved by altering the rate of optic flow presented in a head-mounted display, while arm gains were achieved by introducing a representation of the fingertip in virtual space and altering the relationship between actual and represented fingertip position. In the latter conditions, performers were required to point at targets during adaptation. Overall, the results showed that the vision and arm gain adaptation periods had minimal impacts on post-adaptation spatial updating performance. Furthermore, regardless of adaptation condition, measured deviations in the pointing responses were similarly linked to the late left-to-early right foot swing phases of the walking step-cycle. The results were interpreted as showing partial recalibration effects that were overridden by task specific changes to CNS multisensory integration. This

included the task specific development of a reliable and robust prior task expectation, and/or the altering of vision and arm proprioceptive weights.

4.2 – INTRODUCTION

In perceiving self-motion, the CNS optimally integrates the information from a variety of sensory cues to provide a unitary and reliable estimate of perceived distance traveled (Ernst & Bülthoff, 2004). In forward linear walking without vision, proprioceptive cues originating from the lower limb during the step-cycle play a dominant role in informing this perception (e.g., Campos et al., 2012, 2014). Traditionally, these cues were thought to involve the sensory information arising from extrinsic kinematic parameters measured from individual steps, such as stride length and step frequency (Durgin et al., 2009; Lee et al., 1982). However, more recent considerations of spatial updating show it as being fundamentally based on the intrinsic kinematic coupling between the lower limbs (Chrastil & Warren, 2014; Turvey et al., 2009). For example, Turvey et al. (2009) demonstrate that performers misestimate distances traveled on return-to-start walking paths that contain different lower limb temporal couplings than those contained on outbound walking paths. The walking modes used in their study included typical walking and hesitation-walking, the latter of which was characterized with brief pauses between successive steps.

In some locomotive tasks, coordinated activity between the upper and lower limbs has also been shown to impact distance perception. This specifically involves tasks where the arms assist the legs in propelling the body through space. Harrison et al. (2013) demonstrated this in a study where typical and Nordic (i.e., walking with hiking poles) walking movements were performed with different patterns of arm-leg coordination on outbound and return walking paths. In their study, high locomotive coordination involved

the anti-phase arm-leg coordination pattern characteristic to forward locomotion, while low locomotive coordination involved the anti-phase coordination pattern supplemented with tucking the swinging arm into the chest mid-swing. Their results showed differences in distance estimation between outbound and return paths only for the Nordic walking movements, which was the locomotive task where upper limb movements contributed to propelling the body through space. Locomotive movements that require simultaneous and goal-directed upper limb activity have also been shown to involve flexible and integrated CNS control strategies (Chiovetto & Giese, 2013; Marteniuk & Bertram, 2001). This mutual dependence between the upper and lower limbs means that changes in task constraints for the upper limb system can impact the spatial-temporal kinematics demonstrated in the lower limb system, and vice versa. For example, changes in walking stability (Rinaldi & Moraes, 2015) and reaching trajectories (Marteniuk et al., 2000) have been demonstrated in tasks that involve simultaneous upper and lower limb activity compared to instances where the respective movements are performed in isolation. This provides further credence for the notion that the addition of a goal-directed upper limb task during locomotion contributes to the limb coordination patterns necessary for making judgements about perceived distance.

According to this logic, the continuous pointing task used in Studies 1 and 2 represented a unique form of locomotion through space. This was because it involved goal-directed upper limb activity that was distinctly coordinated with lower limb activity. In this coordination pattern, the upper limb pointing responses used to fixate on the side target contained trajectory deviations that were most frequently timed to the late left-to-

early right foot swing phases of the step-cycle (see Studies 1 and 2). This coordination pattern was considered to reflect an iterative spatial updating process that was not a by-product of locomotive arm-swing kinematics (see Study 1 Discussion), and presented a situation where upper limb joint rotations could have possibly contributed to the CNS perception of self-motion. This was because upper limb activity in the continuous pointing task provided a direct indication of target relative spatial location (Campos et al., 2009), despite not actively contributing to physical locomotion through space (c.f., Harrison et al., 2013).

In most daily locomotive tasks, the sensory cues that inform the CNS perception of self-motion provide congruent estimates of distance traveled. However, situations sometimes arise where discrepant estimates of distance traveled are provided by two or more sensory cues (e.g., Rieser et al., 1995). In instances of such cue conflict, the CNS must still generate a unitary and reliable estimation of self-motion through space. In doing so, the conflicting sensory cues that do not align with the CNS perception of self-motion become recalibrated to match (Durgin et al., 2005). This was demonstrated in Study 2, where performers experienced prolonged exposures to sensory cue conflict created by standard rates of treadmill walking paired with low and high rates of optic flow. The results showed that performers over-perceived self-motion following exposure to high visual gain adaptation and under-perceived self-motion following exposure to low visual gain adaptation, despite demonstrating no post-adaptation changes in step-cycle kinematics (e.g., Mohler et al., 2007; Durgin et al., 2005; Rieser et al., 1995). Thus, in

Study 2, the perceptual information arising from unaltered step-cycle kinematics was recalibrated to match the visual contributions to the CNS perception of self-motion.

In the current study, the impact of coordinated upper and lower limb activity to the CNS perception of self-motion was examined by adapting performers to cue conflicts applied to the pointing responses. If upper limb locomotive coordination contributed to the CNS perception of self-motion during continuous pointing task, conflicting upper limb responses should be recalibrated to match the visually specified rates of perceived self-motion. To achieve this, no-vision continuous pointing movements were performed before and after adaptation conditions where arm control was manipulated with respect to different rates of treadmill walking and virtual optic flow. To manipulate arm control, a fingertip representation was introduced into the virtual environment and performers were required to walk and/or continuously point at virtual targets during adaptation. Applied to this fingertip representation were low and high arm gains that required relatively faster and slower arm movements, respectively, to maintain alignment with the virtual targets. In four different conditions, performers were required to: a) walk standard on a treadmill with a congruent visual gain and point at wall targets with high and low arm gains, b) stand stationary on a treadmill with standard visual information (i.e., equivalent to the aforementioned congruent visual gain) and point at wall targets with high and low arm gains, c) walk standard on a treadmill with low and high visual gains (i.e., a replication of Study 2), and d) walk standard on a treadmill with low and high visual gains and point at wall targets with a congruent arm gain.

Therefore, in this study, cue conflicts were created by altering visual gain with respect to standard walking and/or pointing, or altering arm gain with respect to standard vision and/or walking. Of specific interest was whether prolonged adaptations to these cue conflicts resulted in upper limb activities that became recalibrated to match the perceptions of self-motion established by vision. In keeping with this expectation, the hypotheses were that:

I. Exposure to low arm gains would show over-perceptions of distances traveled. This means that the upper limb pointing responses indicate the performers as being further down the walking path than their actual locations. This was expected because aiming with the low arm gains during adaptation, to a target moving at a standard visual rate, requires greater-than-usual upper limb activity (i.e., joint rotations) in keeping the finger fixated on the target. This greater upper limb activity should be recalibrated to match the veridical perception self-motion provided by vision.

II. Exposure to high arm gains would show under-perceptions of distances traveled. This means that the upper limb pointing responses indicate the performers as being not as far down the walking path as their actual location. This was expected because aiming with the high arm gains, to a target moving at a standard visual rate, requires lesser-than-usual upper limb activity in keeping the finger fixated on the target. This reduced upper limb activity should be recalibrated to match the veridical perception of self-motion provided by vision.

III. Exposure to the low and high visual gains should replicate the results of Study 2 by showing under-perceptions of distances traveled following low visual gain adaptations and over-perceptions of distances traveled following high visual gain adaptations. However, the effects should be more extreme when walking with pointing during adaptation compared to only walking. This is because upper limb activity in the former should be recalibrated to match the visually specified self-motion.

IV. In all conditions, step-cycle kinematics should not change following the adaptation periods.

V. If the upper limb responses operate independent of lower limb activity in estimating perceived self-motion during continuous pointing, none of these aforementioned effects should appear. In this situation, the arm should show veridical perceptions of self-motion following both high and low arm gain adaptation conditions. There should also be no difference between the walk only and the walk-point conditions when recalibrating to the low and high visual gains.

4.3 – METHODS

4.3.1 – *Participants*

Twelve individuals (6 male, 6 female) with a mean age of 21.8 years (sd = 1.60 years) participated in this study. Participants were self-reported right hand dominant and had normal or corrected-to-normal vision. Participants were naïve to the purposes of the study and provided written informed consent prior to starting the experiment in

accordance with the McMaster Research Ethics Board and the 1964 Declaration of Helsinki. Participants took part in two experimental sessions over two separate days, with the experimental session on each day taking approximately 2.5 hours to complete. Participants were remunerated $40 for their time. The data from one male participant was removed because of a large number of trials with missing marker data for one of the experimental sessions. Three participants, in addition to the 12 that completed the experiment, withdrew from the study because of simulator sickness experienced in the virtual reality set-up. Their data were not included for analysis.

4.3.2 – *Apparatus*

All participants completed the experiment in athletic shoes and comfortable athletic pants or shorts. Male participants performed the experiment shirtless and female participants performed the experiment in a sports bra. This attire enabled 21 25 mm retro-reflective markers to be attached directly to the skin with double-sided electrode tape and medical tape to the same anatomical locations as in Study 2. These retro-reflective markers were captured by 10 Vicon Nexus MX-T40 cameras (Vicon, Oxford, UK) at a rate of 100 Hz using Vicon Nexus 2.3 software. Participants were also attached with custom splints that consisted of wooden chopsticks wrapped in medical tape. One splint was taped to the dorsal aspect of the hand from the tip of the right index finger proximally to the wrist. This was intended to limit movement of the interphalangeal and metacarpal-interphalangeal joints of the right index finger during continuous pointing. Another splint was taped to the forearm lengthwise along the ulna from the base of the thumb proximally toward the elbow. This was intended to limit ulnar deviation of the wrist during the

continuous pointing movements. Participants were equipped with a remote-controlled vibrating device (I-phone; Apple Inc., Cupertino, California model) to hold in their left hand. The vibrating device used the WhatsApp (WhatsApp Inc., Mountain View, California) application to deliver a vibratory stimulus triggered by an experimenter. Vibratory stimuli were used to cue the starting and stopping of walking on every trial (see below). White noise was provided throughout the duration of the experiment to mask the sound of footsteps and other ambient noises originating from the environment. This was delivered at a comfortable volume using an I-pod Shuffle (Apple Inc., Cupertino, California) and standard headphones (Sennheiser, Wedemark, Germany). Participants were outfitted with a baseball cap to prevent lights on the lab ceiling from providing spatial cues about distance traveled along the walking path.

All walking movements were performed in one direction along the same walking path used in Study 2 (see Figure 3.01). The home position consisted of a black paper "T" taped to the floor, with the long axis indicating the direction of travel. All distances along and beside the walking path were measured with respect to the short and long axes of the home position, respectively. Six side targets were marked on the ground 2 m to the right of the walking path and 1.44 (target 1), 1.95 (target 2), 2.40 (target 3), 3.20 (target 4), 3.90 (target 5) and 4.8 m (target 6) along the walking path. These target locations were indicated with small square pieces of black tape on the lab floor that were visible to the participants at the starting location. The side target location used on each trial was indicated by a black paper circle 20 cm in diameter and placed on the ground directly overtop of one of the indicated positions. Attached to the middle of the target was a 25

mm retro-reflective marker that provided the exact position of side target used on each trial. Another 25 mm retro-reflective marker was placed beside the walking path and used to indicate the distance of home position. As will be elaborated on in the following section, this study consisted of a series of continuous pointing trials performed before and after a sensory adaptation period performed on a nearby treadmill.

A treadmill (Horizon T.93, Johnson, Health, Tech., Taiwan) located approximately 1 m beside and 4 m along the walking path (with respect to the start location) was used during the adaptation periods (see below) to specify the kinematic speed of walking. An Oculus Rift DK (Oculus VR, Irvine, California) head mounted display (HMD) was used during the adaptation periods to present a virtual hallway that specified various rates of optic flow. The Oculus Rift was controlled by an Ogre interface on a Dell Precision T5400 computer (Dell Technologies, Texas, USA) outfitted with a Linux operating system. The resolution of the Oculus rift was 1280 x 800 and was refreshed at a rate of 60 Hz. The virtual hallway was presented stereoscopically and consisted of white crosshatched lines superimposed on a black background (see Figure 3.02). The dimensions of the virtual hallway were similar to those of an actual hallway located immediately outside the laboratory. The vantage point within the virtual hallway was manually scaled to the eye height of each participant. Rotational head movements were measured by the HMD and updated in the visual display. Presented at various distances along the right wall of the virtual hallway were maroon rectangular squares. They were spaced so that only six targets passed beside the participants in each sensory adaptation period. In some of the adaptation conditions, these signs served as targets that

the participants were required to continuously point at as they passed. In these conditions, a virtual red sphere measuring 25 mm in diameter was superimposed in the VE to represent the location of the right index finger. This location was always accurate (i.e., 1:1) when pointed straight down the virtual hallway directly in front of the participant, but travelled rightward with the rotating arm according to different gains depending on the experimental condition (see below). Generating this finger representation required motion capture of the markers located on the right acromioclavicular joint, left acromioclavicular joint, tip of index finger and 2 markers on the Oculus Rift that approximated the locations of the eyes.

Prior to each experimental session, participants completed dynamic and static calibration trials. For the dynamic calibration trial, participants were outfitted with the Oculus Rift and, from the anatomical position, performed two forward and backward shoulder circumduction movements followed by a forward lunge. These movements were captured by the Vicon cameras and immediately labelled, processed and saved using Vicon Nexus 2.3 software. This process used the “calibrate labelling skeleton static” pipeline followed by the “calibrate labelling skeletion ROM” pipeline. This dynamic calibration trial served as a model of the participant marker arrangements so that the Ogre software program could render the fingertip representation in the VE. For the static calibration trial, participants removed the HMD and stood in the anatomical position at the start location. The markers captured from this static pose were used for joint angle calculations performed in Visual 3D.

4.3.3 – *Procedure*

Experimental Task

This section describes the experimental task of continuous pointing. Blocks of continuous pointing trials were performed with and without vision at specific instances throughout the experimental session (see section below). However, the experimental task description in the following subsection is consistent for both vision and no-vision trials, except where indicated.

All performance trials started with participants standing at the start location in the anatomical position. Once the participant was ready and in this position, one of the experimenters started the motion capture and the other experimenter subsequently activated the vibrating device. The vibratory stimulus cued participants to straighten their right arm (i.e., full elbow extension), fully pronate their wrist and point their right index finger toward the side target. This required participants to look directly at the side-target. After returning to a forward gaze, participants attempted to walk along the straight-line path with their eyes open (i.e., vision trial) or closed (i.e., no-vision trial) while keeping their right index finger fixated on the side-target location. While walking and pointing, participants were asked to keep their arm as straight as possible and their palm facing down. Participants were also instructed to walk at a comfortable, but constant velocity, until cued to stop upon receiving a second vibratory stimulus 3-6 m down the walking path. This required participants to finish the step in progress and come to an abrupt stop by aligning their feet side-by-side. Once stopped, the participants immediately closed their eyes, for both vision and no-vision trials, and relaxed their arm while the

experimenter stopped the Vicon system from recording. In order to mask feedback about performance, participants were led back to the start location with their eyes still closed along a random and twisting pathway. Upon returning to the starting location, the experimenter tapped participants on the shoulder to indicate that they could open their eyes and return to the anatomical position. Once in this position, participants were required to not move their feet while awaiting the next trial.

Vision trials were performed to endpoint distances of 3 and 5 m along the walking path and no-vision trials were performed to endpoint distances of 4 and 6 m along the walking path. Different walking distances were used for the vision and no-vision trials to prevent participants from strategically performing the no-vision trials using feedback (e.g., arm rotation, step number/length) acquired from the outcomes of the vision movements. Side targets for each walking distance were in one of three locations: targets 1-3 for 3 m, targets 2-4 for 4 m, targets 3-5 for 5 m, and targets 4-6 for 6 m (see Figure 3.01). Thus, for each walking distance, side target locations represented near, middle and far distances that approximated 50, 65 and 80 percent of the total walking distances, respectively. Three side target locations were used for each walking distance to prevent participants from using a memorized motor experience (e.g., arm trajectory) in performing the task. Additionally, some side target locations served multiple walking distances (see Figure 3.01) to prevent participants from being informed, prior to the start of a trial, about the distance being walked on the upcoming trial. By using several forward walking distances and several side target locations, motor performance was intended to reflect spatial updating and not anticipatory task awareness.

Practice Session

The following subsections describe the order of events and conditions involved in each experimental session. The experiment was performed across two days, referred to as Day 1 and Day 2. On each day, participants were outfitted with the retro-reflective markers, baseball cap and vibrating device. Participants also completed the calibration trials and were measured in height. On Day 1, participants took part in a practice session before performing 4 experimental blocks. On Day 2, participants performed only the 4 experimental blocks. The practice and experimental blocks are discussed in further detail in the following subsections.

Participants first performed 6 practice trials of the continuous pointing task to a side target located 2 m beside and 2.8 m along the walking path. This side target location was not included in the experimental session. Three vision trials were practiced before three no-vision trials. After the practice trials, participants experienced a 5 min familiarization period in the HMD/treadmill set-up. For the first half of the familiarization period, participants walked on the treadmill at a rate of 1.1 m/s and experienced visual flow in the virtual environment that was 1.0 x walking speed (i.e., congruent). During this time, participants lightly grasped the two side handrails. For the last half of the familiarization period, participants were instructed to continue walking on the treadmill and point at targets as they passed along the right wall of the VE. When pointing, participants were instructed to keep their left hand on the handrail and use their right arm to continuously align the red dot (i.e., fingertip representation) with the target upon seeing it appear in the distant virtual hallway. This was completed with the elbow fully extended

and wrist fully pronated. Pointing continued until the target passed out of range behind the participants. At this time, participants returned their right hand to the handrail and resumed looking forward. In the practice session, the red dot always represented a 1:1 mapping of the fingertip position in virtual space with respect to actual space. White noise was not provided during the practice session so that verbal communication could be maintained with the participants.

Experimental Session

Days 1 and 2 of the experiment each involved four blocks of experimental trials. These blocks were organized using the same format as Study 2. Specifically, each block consisted of 18 walking trials that unfolded in this sequential manner: 6 vision continuous pointing trials that served as controls, 6 no-vision pre-adaptation continuous pointing trials, a 10 minute sensory adaptation period performed using the treadmill/HMD set-up, and 6 no-vision post-adaptation continuous pointing trials. Each of these sets of 6 trials consisted of one trial performed to all combinations of 2 walking distances by 3 side target locations. The only stipulation with the trial orders was that no more than 2 consecutive trials could be performed to the same side target. Within each block, the same order of distance by side target was used in the no-vision pre- and post-adaptation trials. The purpose of the vision control trials was to calibrate participants to their typical association between vision and proprioception at the start of each experimental block. Due to the within-subjects design of this study, this was necessary to washout immediate carry-over effects between the different experimental blocks. The purpose of the no-vision pre-adaptation trials was to provide a baseline measure of spatial updating and the

purpose of the no-vision post-adaptation trials was to provide a measure of spatial updating after the sensory adaptation periods.

For the adaptation periods, the baseball cap and vibrating device were removed from the participants. The headphones and I-pod remained with the participant because white noise was provided throughout the adaptation periods. To ensure that participants remained centred on the treadmill while wearing the HMD, participants were instructed to maintain a light grasp on the treadmill handrails with both hands. When required by the experimental condition (see below), participants pointed at the right wall targets in the same way as performed in the practice session. When not engaged in the pointing task, participants were instructed to "look around" the virtual environment and focus on the visual information specified by the walls, ceiling and floor as it passed through the virtual environment. An auditory beep emitted by the treadmill signified the end of the adaptation period after 10 minutes, at which time the treadmill was manually turned-off by an experimenter and the participant was instructed to close their eyes. At this time, the white noise was turned off, the HMD was removed and the participant was led from the treadmill to the start location along an unpredictable and random pathway with their eyes closed. At the start location, participants were verbally instructed to open their eyes after being outfitted with the baseball cap and vibrating device. Once the participants assumed the anatomical position, the white noise was turned on and the no-vision post-adaptation trials began.

The purpose of the adaptation periods was to adapt participants to different sensory cue conflicts. Thus, the 8 experimental blocks differed in the sensory gains

provided during the adaptation periods (see Table 4.01). For the adaptation periods, participants always received visual information and either walked on a treadmill at 1.1 m/s, pointed at the targets as they passed by, or both. Depending on the condition, gains were either applied to the rate of optic flow or the rate of represented arm movement (i.e., red dot) in virtual space. Gains for the optic flow speeds were selected on the basis of their effective use in previous studies (Mohler et al., 2007; Ziemer et al., 2013; see also Study 2), while the gains for the represented arm movement were selected based on pilot testing. The 8 adaptation conditions (4 categories each with 2 manipulations) are described in more detail below.

Vision gain manipulation with walking, no pointing (V_{WALK}): in the adaptation periods of the V_{WALK} conditions, participants walked on the treadmill and received optic flow at a rate either 2.0 x (high visual gain; HVG_W) or 0.5 x (low visual gain; LVG_W) the rate of walking. To ensure that only six targets passed the participants in each condition, the targets were spaced 193 m and 48.25 m apart in virtual space, respectively. These conditions were intended to replicate the HVG and LVG conditions of Study 2, respectively.

Vision gain manipulation with walking and pointing ($V_{WALK\text{-}POINT}$): in the adaptation periods of the $V_{WALK\text{-}POINT}$ conditions, participants walked on the treadmill, received optic flow at a rate either 2.0 x (HVG_{WP}) or 0.5 x (LVG_{WP}) the rate of walking and pointed at the targets with a gain of 1.0 x applied to the motion of the finger representation (i.e., red dot). To ensure that six targets passed the participants in each of these conditions, the targets were spaced 193 m and 48.25 m apart in virtual space,

respectively. Since the potential for fatigue was greater when pointing in the LVG_{WP} versus the HVG_{WP} condition (as determined in pilot testing), of the 6 targets presented in the LVG_{WP} condition only the first, second, fourth and sixth targets were pointed at. This permitted participants to rest their arm during the passage of the third and fifth targets.

Arm gain manipulation with pointing, no walking (A_{POINT}): in the adaptation periods of the A_{POINT} conditions, participants stood stationary on the treadmill, received optic flow at a rate congruent with 1.1 m/s of forward motion (i.e., optic flow similar to the CVG condition in Study 2) and pointed at the targets with a gain of either 1.2 x (high arm gain; HAG_P) or 0.8 x (low arm gain; LAG_P) applied to the motion of the finger representation (i.e., red dot). This arm gain manipulation resulted in a virtual finger position ahead of the actual fingertip position in the HAG_P condition and behind the actual fingertip position in the LAG_P condition. Thus, in these manipulations, participants were required to slow down and speed up the movements of their arm (with respect to the rates of optic flow), respectively, to keep the finger positioned on the targets as they passed. To ensure that six targets passed the participants in each of these conditions, the targets were spaced 96.5 m apart in virtual space in both conditions.

Arm gain manipulation with walking and pointing ($A_{WALK\text{-}POINT}$): in the adaptation periods of the $A_{WALK\text{-}POINT}$ conditions, participants walked on the treadmill, received optic flow at a rate 1.0 x the rate of walking and pointed at the targets with either a gain of 1.2 x (HAG_{WP}) or 0.8 x (LAG_{WP}) applied to the motion of the finger representation (i.e., red dot). This arm gain manipulation resulted in the virtual fingertip position being ahead of the actual fingertip position in the HAG_{WP} condition and behind

the actual fingertip position in the LAG_{WP} condition. Once again, to keep the finger positioned on the target, participants were required to slow the movement of their arm in the HAG_{WP} condition and speed up the movement of their arm in the LAG_{WP} condition. To ensure that six targets passed the participants in each of these conditions, the targets were spaced 96.5 m apart in virtual space in both conditions.

The V_{WALK} and $A_{WALK\text{-}POINT}$ conditions were always performed on the same day, and the A_{POINT} and $V_{WALK\text{-}POINT}$ conditions were always performed on the other day. This organization ensured that one arm gain manipulation and one visual gain manipulation occurred on each day. The day in which these sessions were performed was counterbalanced across participants. On each day, the two visual gain and two arm gain manipulations were always performed in succession. The ordering of all gain manipulations on each day was counterbalanced across participants. Considering the within subjects design of this study, all participants performed a total of 144 continuous pointing trials (48 vision trials, 96 no-vision trials) and experienced a total of 80 minutes in sensory adaptation across the two days of experimental sessions.

4.3.4 – *Data and Statistical Analysis*

Data analysis was carried out in a similar manner as Study 2. The data from all trials were reconstructed using Vicon Nexus 2.3 software (Vicon, Oxford, UK). For each trial, the anatomical markers were labeled at every frame, missing data segments 25 frames or shorter were filled, and the data was saved in the C3D format for further processing in Visual 3D (version 4, C-motion Research Biomechanics, Kingston, Ontario).

In Visual 3D, a custom model was constructed using the static calibration trial and this model was attached to the 3D marker data for all trials. The model created virtual markers representing the wrist joint centre, elbow joint centre, shoulder anterior-posterior joint centre, shoulder joint centre, shoulder girdle joint centre and throax joint centre (see Table 2.2 for the landmarks used to compute each virtual marker). The anatomical and virtual markers were then used to create body segments representing the pelvis, thorax, right upper arm and right forearm (see Table 2.3 for the landmarks used to define each segment). Using these body segments, relative joint angles were calculated for the trunk, shoulder and elbow joints in a manner consistent with the International Society of Biomechanics standards (e.g., Wu et al., 2005). Specifically, trunk angle represented rotation of the thorax segment with respect to the pelvis segment using an X-Y-Z Cardan sequence; shoulder angle represented rotation of the upper arm segment with respect to the thorax segment using a Z-Y-Z Cardan sequence; and elbow angle represented rotation of the forearm segment with respect to the upper arm segment using an X-Y-Z Cardan sequence.

Dependent measures were calculated for each trial using custom Matlab R2014a software (Mathworks, Natick, Massachusetts). All joint angle and marker data were first filtered using a second-order, dual-pass Butterworth filter with a low-pass frequency of 6 Hz. The start and end of each walking trial were then determined using the velocity profiles of the foot responsible for taking the first and last steps, respectively. These velocity profiles were calculated as the derivatives of the displacement profiles for the left foot and right foot markers using a three-point finite difference algorithm. The start of

walking was defined as the first instance where the velocity of the foot that took the first step reached the value of 0.02 m/s and remained above this mark for at least 25 frames (i.e., 250 ms). The end of walking was defined as the first instance where the velocity of the foot that took the last step reached the value of 0.02 m/s and remained below this mark for at least 25 frames. In the odd circumstance where data from the left foot or right foot markers were lost at the end of a walking movement, the end of walking was calculated as the earliest missing data frame amongst the remaining anatomical markers. This had no impact on the results since the walking movements were only analyzed up to 2.5, 3.5, 4.5 and 5.5 m for the 3, 4, 5 and 6 m walking trials, respectively. All dependent variables were calculated between the defined start and end for each walking trial. Outlined in the remainder of this section are the calculations and statistical analyses used for determining and examining all dependent measures. Unless otherwise indicated in the descriptions that follow, data were collapsed across target, examined separately at each distance and examined separately for the vision (i.e., LVG_W, HVG_W, LVG_{WP} and HVG_{WP}) and arm (i.e., HAG_P, LAG_P, HAG_{WP} and LAG_{WP}) gain manipulation conditions. Since the purpose of this study is to examine no-vision spatial updating before and after prolonged exposures to sensory adaptation periods involving low and high vision and arm gains, the results will focus on the no-vision pre- and post-adaptation trials unless otherwise noted.

Perceived/actual distance traveled and velocity

Actual distance traveled was measured as the position of the xyphoid marker with respect to the start location. Actual walking velocity was taken as the derivative of the

actual distance traveled trajectory calculated using a three-point finite difference algorithm. Actual velocity was examined using the sliding ANOVA technique introduced in Study 1. The purpose of this technique is to avoid congesting a single ANOVA with an independent variable whose results carry relatively little significance to the overall research question and whose levels can more or less be arbitrarily defined. This analysis was performed using 2 Adaptation (Walk, Walk-Point) by 2 Visual Gain (low visual gain, high visual gain) by 2 Test (no-vision pre-adaptation, no-vision post-adaptation) repeated measures ANOVAs for the vision gain conditions, and 2 Adaptation (Point, Walk-Point) by 2 Arm Gain (high arm gain, low arm gain) by 2 Test (no-vision pre-adaptation, no-vision post-adaptation) repeated measures ANOVAs for the arm gain conditions. These ANOVAs were performed separately at 0.5 m distance iterations for the 4 m (1.0-3.0 m) and 6 m (1.0-5.0 m) walking trials. Prior to analysis, the within participant averages for actual walking velocity were smoothed using a non-recursive 7-point moving average centred on the point of interest (e.g., 3 points ± 1.0 m/s). This was done to remove fluctuations in the data that remained even after averaging across trials.

Perceived distance traveled was determined using the Reconstructed method of azimuth angle calculation introduced in Study 1. This involves: (a) submitting the shoulder plane of elevation and trunk axial rotation trajectories to Fast Fourier Transforms to determine the frequency contents of the two signals (see Figure 2.03), (b) reconstructing both signals using their respective signal frequency contents less than 0.5 Hz, and (c) summing the two reconstructed signals together. Subsequently, equations 1 and 2 were used to calculate perceived distance traveled at every frame of data collection

(see Figure 1.1), and a perceived distance traveled trajectory for each trial was calculated by accumulating these values across all frames. For the vision control trials, the sliding ANOVA technique was first used to examine perceived distance traveled using 8 Gain (LVG_W, HVG_W, LVG_{WP}, HVG_{WP}, HAG_P, LAG_P, HAG_{WP}, LAG_{WP}) repeated measures ANOVAs run separately at 0.5 m distance iterations for the 3 m (0.5-2.5 m) and 5 m (0.5-4.5 m) walking trials. Considering the within subjects design of this study, this was done to examine whether the vision control trials were systematically impacted by the previously experienced sensory adaptation periods. Another sliding ANOVA was used to compare perceived distance traveled between the vision control and no-vision pre-adaptation trials. For this analysis the 4 m and 6 m pre-adaptation trials were cut down to 2.5 m and 4.5 m, respectively. This analysis was performed using 8 Gain (LVG_W, HVG_W, LVG_{WP}, HVG_{WP}, HAG_P, LAG_P, HAG_{WP}, LAG_{WP}) by 2 Vision (vision control, no-vision pre-adaptation) repeated measures ANOVAs run separately at 0.5 m distance iterations for the 3 m (0.5-2.5 m) and 5 m (0.5-4.5 m) walking trials. This analysis served to examine whether the no-vision blocks of pre-adaptation continuous pointing reflected typical spatial updating (i.e., was similar to the baseline visual control trials).

The sliding ANOVA technique was also used to examine perceived distance traveled in the no-vision pre-and post-adaptation trials. This was performed using 2 Adaptation (Walk, Walk-Point) by 2 Visual Gain (low visual gain, high visual gain) by 2 Test (no-vision pre-adaptation, no-vision post-adaptation) repeated measures ANOVAs for the vision gain conditions, and 2 Adaptation (Point, Walk-Point) by 2 Arm Gain (high arm gain, low arm gain) by 2 Test (no-vision pre-adaptation, no-vision post-adaptation)

repeated measures ANOVAs for the arm gain conditions. These ANOVAs were run separately at 0.5 m distance iterations for the 4 m (0.5-3.5 m) and 6 m (0.5-5.5 m) walking trials.

Azimuth measures

Peak azimuth velocity and azimuth angle at peak azimuth velocity were used to examine how the azimuth pointing responses unfolded during the course of the walking movements. For these analyses, azimuth velocity was calculated by differentiating the azimuth trajectory using a three-point finite difference algorithm. If performing the continuous pointing task as instructed, peak azimuth velocity should occur at 0° azimuth (i.e., arm pointed straight out to side; Campos et al., 2009). These variables were examined separately for the 4 and 6 m walking distances using 2 Adaptation (Walk, Walk-Point) by 2 Visual Gain (low visual gain, high visual gain) by 2 Test (no-vision pre-adaptation, no-vision post-adaptation) repeated measures ANOVAs for the vision gain conditions, and 2 Adaptation (Point, Walk-Point) by 2 Arm Gain (high arm gain, low arm gain) by 2 Test (no-vision pre-adaptation, no-vision post-adaptation) repeated measures ANOVAs for the arm gain conditions. These measures should not be systematically impacted by the sensory adaptation conditions, since they are used to assess whether performers are properly coordinating their azimuth movements with perceived target passage. That is, the sensory adaptation conditions are expected to impact the actual locations of perceived target passage, but not the performers inherent ability to perceive it.

Constant error (i.e., signed error along the walking path) was measured as distance between the location of the participant and the location of the target when the participant achieved 20°, 15°, 10°, 5°, 0°, -5° and -10° azimuth. Negative values indicate positions before actual target passage and positive values indicate positions after actual target passage. This provides a measure of how spatial updating unfolds in what is considered the most sensitive range for measuring changes in azimuth angle. Constant error was examined using the sliding ANOVA technique separately for the 4 and 6 m walking distances. Specifically, 2 Adaptation (Walk, Walk-Point) by 2 Visual Gain (low visual gain, high visual gain) by 2 Test (no-vision pre-adaptation, no-vision post-adaptation) repeated measures ANOVAs were used for the vision gain conditions, and 2 Adaptation (Point, Walk-Point) by 2 Arm Gain (high arm gain, low arm gain) by 2 Test (no-vision pre-adaptation, no-vision post-adaptation) repeated measures ANOVAs were used for the arm gain conditions. These ANOVAs were run separately in 5° azimuth angle increments (i.e., 20° to -10°).

Step characteristics

Step characteristics were calculated using the same criteria as outlined in Studies 1 and 2 (see Figure 2.07; e.g., Multon & Olivier, 2013). Included for analyses were the number of steps, step length, and left and right stride lengths. Since multiple steps and strides occurred on each trial, step length and left and right stride lengths were reduced to average values for each trial. All step characteristics were examined separately for the 4 and 6 m walking distances using 2 Adaptation (Walk, Walk-Point) by 2 Visual Gain (low visual gain, high visual gain) by 2 Test (no-vision pre-adaptation, no-vision post-

adaptation) repeated measures ANOVAs for the vision gain conditions, and 2 Adaptation (Point, Walk-Point) by 2 Arm Gain (high arm gain, low arm gain) by 2 Test (no-vision pre-adaptation, no-vision post-adaptation) repeated measures ANOVAs for the arm gain conditions.

Significant arm deviations

Significant arm deviations were calculated using the kinematic criteria and Shoulder azimuth method outlined in Study 1 (see Figures 2.08, 2.09 and 2.10). The number of significant arm deviations per trial was examined separately for the 4 and 6 m walking distances using 2 Adaptation (Walk, Walk-Point) by 2 Visual Gain (low visual gain, high visual gain) by 2 Test (no-vision pre-adaptation, no-vision post-adaptation) repeated measures ANOVAs for the vision gain conditions, and 2 Adaptation (Point, Walk-Point) by 2 Arm Gain (high arm gain, low arm gain) by 2 Test (no-vision pre-adaptation, no-vision post-adaptation) repeated measures ANOVAs for the arm gain conditions. The actual (i.e., the extent covered on the actual distance traveled trajectory) and perceived (i.e., the extent covered on the perceived distance traveled trajectory) distances traveled were also calculated for each significant deviation. These were examined using 2 Adaptation (Walk, Walk-Point) by 2 Visual Gain (low visual gain, high visual gain) by 2 Test (no-vision pre-adaptation, no-vision post-adaptation) by 4 (or 5) Deviation Number repeated measures ANOVAs for the vision gain conditions, and 2 Adaptation (Point, Walk-Point) by 2 Arm Gain (high arm gain, low arm gain) by 2 Test (no-vision pre-adaptation, no-vision post-adaptation) by 4 (or 5) Deviation Number repeated measures ANOVAs for the arm gain conditions. The Deviation Number level

was selected based on the grand mean of the analysis of the number of significant arm deviations per trial. This number represented 4 for the 4 m trials and 5 for the 6 m trials. Since these were average values, this resulted in situations where some performers did not meet these numbers of deviations. Thus, 9 missing ANOVA cells were replaced in each of these analyses using series means.

Locations of the significant arm deviation starts and ends in the step-cycle were examined using the same criteria outlined in Studies 1 and 2. Specifically, frequency counts for the different test (no-vision pre-adaptation, no-vision post-adaptation) and gain (LVG_W, HVG_W, LVG_{WP}, HVG_{WP}, HAG_P, LAG_P, HAG_{WP}, LAG_{WP}) trials were accumulated across all participants. For statistical analysis, these frequency count data were reduced into the same four categories as Studies 1 and 2: early left foot, late left foot, early right foot and late right foot. To examine the locations of significant arm deviation starts and ends in the step-cycle, three sets of Chi Square analyses were performed separately on the significant arm deviation starts and ends (e.g., Rinaldi & Moraes, 2015). In the first analysis, comparisons were made between the frequency counts of the test conditions in each of the gain conditions. The expected values for each category were based on the percentage of the total number of deviations in each step-phase category multiplied by the number of deviations in each test condition (e.g., Vincent, 2005). In the second analysis, data were pooled across test conditions and frequency counts were examined between the phases of the step-cycle in each gain condition. The expected values for this analysis equalled ¼ of the total number of deviations for each analysis, which represented the null hypothesis of no between

category differences in the total number of deviations. Lastly, the frequency counts between the different gain conditions were compared. This analysis was performed separately for the visual (i.e., LVG_W, HVG_W, LVG_{WP}, HVG_{WP}) and arm (i.e., HAG_P, LAG_P, HAG_{WP}, LAG_{WP}) gain conditions. The expected values for each category were based on the percentage of the total number of deviations in each step-phase category multiplied by the total number of deviations in each gain condition.

All analyses were performed using SPSS software (IBM, Armonk, New York), with the exception of the Chi Square analyses that were performed manually in Microsoft Excel (Microsoft, Redmond, Washington). Alpha was set at $p < 0.05$ for all analyses. Violations of sphericity were accounted for using the Greenhouse-Geisser correction, although the reported degrees of freedom were the sphericity assumed values. All significant ANOVA effects involving more than two means were decomposed using Tukey's Honestly Significant Difference. Post-hoc tests for the Chi Square analyses were performed using SPSS software. Bonferroni adjusted binomial pairwise comparisons were used for the single category analyses, while adjusted standardized residuals that were converted to p-values and Bonferroni adjusted were used for the two category analyses.

4.4 – RESULTS

4.4.1 – *Omnibus Analyses*

Presented first are the results of initial omnibus tests used to determine whether perceived distance traveled increased as a function of actual distance traveled. These analyses were necessary because the sliding ANOVA technique examined between

condition differences at specific distance intervals, without comparing differences between intervals. Gain and test conditions were pooled at all 0.5 m distance intervals for each of the following analyses, which were performed separately for each walking distance. For the 3 m trials, this analysis was performed using a 5 Distance (0.5-2.5 m) repeated measures ANOVA. The results showed significant differences between all distances (0.5 m = 0.19 m; 1.0 m = 0.89 m; 1.5 m = 1.42 m; 2.0 m = 1.92 m; 2.5 m = 2.43 m). For the 4 m trials, this analysis was performed using a 7 Distance (0.5-3.5 m) repeated measures ANOVA. The results showed significant differences between all distances (0.5 m = 0.89 m; 1.0 m = 0.88 m; 1.5 m = 1.36 m; 2.0 m = 1.82 m; 2.5 m = 2.36 m; 3.0 m = 2.90 m; 3.5 m = 3.36 m). For the 5 m trials, this analysis was performed using a 9 Distance (0.5-4.5 m) repeated measures ANOVA. The results showed significant differences between all distances except between 1.0 and 1.5 m, 1.5 and 2.0 m, 2.0 and 2.5 m, 3.5 and 4.0 m, and 4.0 and 4.5 m (0.5 m = -0.02 m; 1.0 m = 0.93 m; 1.5 m = 1.42 m; 2.0 m = 1.79 m; 2.5 m = 2.27 m; 3.0 m = 2.83 m; 3.5 m = 3.40 m; 4.0 m = 3.91 m; 4.5 m = 4.33 m). For the 6 m trials, this analysis was performed using an 11 Distance (0.5-4.5 m) repeated measures ANOVA. The results showed significant differences between all distances except between 1.0 and 1.5-2.0 m, 1.5 and 2.0-2.5 m, 2.0 and 2.5 m, 2.5 and 3.0 m, 3.0 and 3.5 m, 3.5 and 4.0 m, 4.0 and 4.5 m, 4.5 and 5.0 m, and 5.0 and 5.5 m (0.5 m = -0.06 m; 1.0 m = 0.95 m; 1.5 m = 1.36 m; 2.0 m = 1.67 m; 2.5 m = 2.13 m; 3.0 m = 2.63 m; 3.5 m = 3.09 m; 4.0 m = 3.54 m; 4.5 m = 4.01 m; 5.0 m = 4.48 m; 5.5 m = 4.90 m). These analyses showed that perceived distance traveled increased as a function of actual distance traveled.

Presented next are the results for the sliding ANOVAs involving perceived distance traveled in the vision control trials. This is because these were also omnibus analyses performed using all experimental conditions. Analysis of perceived distance traveled in the vision control trials demonstrated no significant effects ($p > 0.20$; see Table 4.02 for F-values of this analysis). Analysis of perceived distance traveled comparing the vision control and no-vision pre-adaptation trials showed no significant effects in the 3 m trials ($p > 0.126$). In the 5 m trials, Vision main effects at 3.5-4.5 m showed greater perceived distances traveled in the vision control versus the no-vision pre-adaptation trials (see Table 4.03 for the F-values of these analyses). Due to the lack of gain related effects in these analyses, the results showed that the blocks of vision trials and no-vision pre-adaptation trials were not systematically biased by the experimental order of gain adaptation conditions. This means that the vision control trials served their intended purpose of washing out immediate carry-over effects in the pointing responses between successive experimental blocks. Thus, any no-vision post-adaptation effects reported below can be assumed as resulting from the sensory conditions experienced in the adaptation periods. The results for the remainder of this section are reported separately for the vision (i.e., LVG_W, HVG_W, LVG_{WP} and HVG_{WP}) and arm (i.e., HAG_P, LAG_P, HAG_{WP}, LAG_{WP}) gain conditions, unless otherwise indicated (i.e., analyses at the end of this section involving locations of significant arm deviations in the step-cycle).

4.4.2 – *Vision Gain manipulations*

Actual velocity was used to examine whether participants adhered to the instruction to walk at a constant velocity during the continuous pointing movements, and

also whether the visual gain manipulations during the adaptation periods had an impact on the participant's actual motions through space. Figures 4.01 and 4.02 present the condition by walking distance graphs for actual walking velocity (unsmoothed data are presented in these figures). F-values for the sliding ANOVAs performed on the 4 and 6 m trials are presented in Tables 4.04 and 4.05, respectively. In the 4 m walking trials, Test main effects at all distance iterations showed greater actual walking velocity in the no-vision post-adaptation trials compared to the no-vision pre-adaptation trials (see Table 4.04). A Gain main effect at 2.5 m showed greater actual walking velocity in the low visual gain conditions (1.11 m/s) compared to the high visual gain conditions (1.10 m/s). For the 6 m walking trials, Test main effects at all distance iterations showed greater actual walking velocities in no-vision post-adaptation compared to no-vision pre-adaptation (see Table 4.05). Gain main effects at 1.5, 2.0, 2.5 and 5.0 m showed greater actual walking velocities in the low visual gain conditions compared to the high visual gain conditions (see Table 4.05).

The step-cycle characteristics (i.e., number of steps, step length, and left and right stride lengths) were used to examine whether the kinematics of walking changed as a function of the visual gain manipulations presented during the adaptation periods. For the analysis of number of steps, no significant effects were demonstrated for the 4 m walking trials ($p > 0.086$; grand mean = 8.28). For the 6 m walking trials however, a Gain main effect, $F(1,10) = 16.80$, $p < 0.01$, showed more steps taken in the high visual gain (11.5) versus low visual gain (11.2) conditions.

Analysis of step length in the 4 m walking trials demonstrated a Gain by Test interaction, $F(1,10) = 12.48$, $p < 0.01$. This showed a more extreme increase in step length in no-vision pre-adaptation compared to no-vision post-adaptation in the high visual gain condition (no-vision pre-adaptation = 0.57 m; no-vision post-adaptation = 0.59 m) versus the low visual gain condition (no-vision pre-adaptation = 0.58 m; no-vision post-adaptation = 0.59 m). A Test main effect, $F(1,10) = 11.18$, $p < 0.01$, showed an increase in step length from no-vision pre-adaptation (.577 m) to no-vision post-adaptation (.592 m). For the 6 m walking trials, a Gain main effect, $F(1,10) = 12.05$, $p < 0.01$, showed a greater step length in the low visual gain (.600 m) versus high visual gain (.587 m) conditions. In addition, a Test main effect $F(1,10) = 67.95$, $p < 0.001$, showed a greater step length in no-vision post-adaptation (.605 m) compared to no-vision pre-adaptation (.582 m).

In the analysis of left stride length, a Test main effect, $F(1,10) = 9.63$, $p < 0.05$, in the 4 m walking trials showed an increase in left stride length from no-vision pre-adaptation (1.17 m) to no-vision post-adaptation (1.20 m). For the 6 m walking trials, a Gain main effect, $F(1,10) = 8.08$, $p < 0.05$, showed a greater left stride length in the low visual gain (1.21 m) compared to the high visual gain conditions (1.19 m). A Test main effect, $F(1,10) = 59.12$, $p < 0.001$, showed a greater left stride length in no-vision post-adaptation (1.22 m) versus no-vision pre-adaptation (1.17 m).

Analysis of right stride length for the 4 m walking trials demonstrated a Test main effect, $F(1,10) = 16.66$, $p < 0.01$. This showed a greater right stride length in no-vision post-adaptation (1.20 m) compared to no-vision pre-adaptation (1.17 m). For the 6 m

walking trials, a Gain main effect, $F(1,10) = 13.07$, $p < 0.01$, showed a greater right stride length in the low visual gain (1.21 m) compared to the high visual gain (1.19 m) conditions. Also, a Test main effect, $F(1,10) = 35.56$, $p < 0.001$, showed a greater right stride length at no-vision post-adaptation (1.22 m) compared to no-vision pre-adaptation (1.17 m).

Therefore, the greater velocities demonstrated in no-vision post-adaptation compared to no-vision pre-adaptation in the 4 and 6 m trials were accompanied by increases in step length, and left and right stride lengths. Increases in these variables also contributed to an increased velocity in the 6 m low visual gain trials.

Perceived distance traveled was used to examine the participant's perceived spatial locations during the course of the continuous pointing movements, with particular interest as to whether these changed as a function of the visual gain manipulations presented during the adaptation periods. The condition by distance graphs for perceived distances traveled are presented in Figures 4.03 and 4.04. F-values for the sliding ANOVAs performed on the 4 and 6 m trials are presented in Tables 4.06 and 4.07, respectively. In the 4 m walking trials, a Test main effect at 1.0 m showed a greater perceived distance traveled in no-vision pre-adaptation (.926 m) compared to no-vision post-adaptation (.829). At 3.5 m, an Adaptation by Test interaction showed a greater perceived distance traveled in the Walk-Point condition for no-vision pre-adaptation (Walk = 3.33 m; Walk-Point = 3.45 m) compared to no-vision post-adaptation (Walk = 3.38 m; Walk-Point = 3.30 m). For the 6 m walking trials, Test main effects at 1.0-5.5 m showed greater perceived distances traveled in no-vision pre-adaptation compared to no-

vision post-adaptation (see Table 4.07). At 3.5 m, a Gain by Test interaction showed a decrease in perceived distance traveled in the low visual gain conditions from no-vision pre-adaptation (low visual gain = 3.19 m; high visual gain = 3.15 m) to no-vision post-adaptation (low visual gain = 2.98 m; high visual gain = 3.13 m). A significant Adaptation by Test interaction at 4.0 m showed a greater perceived distance traveled for the Walk-Point condition in no-vision pre-adaptation (Walk = 3.60 m; Walk-Point = 3.66 m) compared to no-vision post-adaptation (Walk = 3.55 m; Walk-Point = 3.45 m).

Constant error was used to examine the participant's positions along the walking path, with respect to the side-target, at the instances of 20° to -10° azimuth, in 5° increments. This is the most sensitive range for assessing pointing performance, for which changes as a function of the visual gain manipulations presented during the adaptation periods were of particular interest. For the analysis of constant error, relatively greater (i.e., more positive) constant error at the azimuth iterations indicates locations further down the walking path. F-values for the sliding ANOVAs performed on the 4 and 6 m trials are presented in Tables 4.08 and 4.09, respectively. No significant effects were shown for the 4 m walking trials ($p > 0.056$; see Table 4.08). However, for the 6 m walking trials (see Table 4.09), Gain by Test interactions at 15, 10, 5, 0 and -10° showed an increase in constant error from no-vision pre-adaptation to no-vision post-adaptation in the low visual gain conditions (see Figure 4.05). In addition, Test main effects at all distance iterations showed greater constant error in no-vision post-adaptation compared to no-vision pre-adaptation. Overall, these showed partial gain related differences in no-

vision post-adaptation spatial updating performance (see Discussion section for a more elaborate interpretation).

Azimuth angle at peak azimuth was used to examine the azimuth angle at which pointing responses reached maximum velocity during the continuous pointing trials. Effective continuous pointing demonstrates values close to 0° in this measure, which is used as an assessment of perceived target passage. Analysis of azimuth angle at peak azimuth velocity for the 4 m walking trials demonstrated a significant Adaptation by Gain by Test interaction, $F(1,10) = 12.34$, $p < 0.01$. This showed decreasing azimuth angle at peak azimuth velocity from no-vision pre-adaptation to no-vision post-adaptation for the high visual gains of the Walk condition (i.e., HVG_W; see Table 4.10). In the 6 m walking trials, a significant Adaptation by Gain by Test interaction, $F(1,10) = 4.99$, $p < 0.05$, showed increasing azimuth angle at peak azimuth velocity from no-vision pre-adaptation to no-vision post-adaptation for the high visual gains in the Walk-Point condition (i.e., HVG_{WP}; see Table 4.10). For the analysis of peak azimuth velocity, no effects were demonstrated for the 4 m walking trials ($p > 0.076$; grand mean = 40.52 °/s). For the 6 m walking trials, a Gain by Test interaction, $F(1,10) = 6.28$, $p < 0.05$, showed a greater peak azimuth velocity in the high arm gain conditions at no-vision post-adaptation (low visual gain = 36.11 °/s; high visual gain = 39.11 °/s) compared to no-vision pre-adaptation (low visual gain = 37.15 °/s; high visual gain = 36.37 °/s).

The significant arm deviations were trajectory fluctuations calculated using the aforementioned trajectory parsing procedure. They were examined according to number per trial, and actual and perceived distances traveled between the start and end of each

deviation. Analysis of the number of significant arm deviations per trial demonstrated no significant effects for the 4 m ($p > 0.205$; grand mean = 4.48) or 6 m ($p > 0.055$; grand mean = 5.84) walking trials. The analysis of actual distance traveled per significant arm deviation in the 4 m trials demonstrated an Adaptation main effect, $F(1,10) = 7.05$, $p < 0.05$. This showed a greater actual distance traveled per significant arm deviation in the Walk condition (.896 m) versus the Walk-Point condition (.867 m). A Deviation Number main effect, $F(3,30) = 12.29$, $p < 0.001$, showed a greater actual distance traveled in deviation 1 compared to deviations 2-4 (1 = 1.18 m, 2 = 0.890 m, 3 = 0.795 m, 4 = 0.656 m). Analysis of the 6 m walking trials demonstrated a significant Adaptation by Deviation Number interaction, $F(4,40) = 3.43$, $p < 0.05$. This showed a greater actual distance traveled in deviation 1 for the Walk condition (Deviation number: 1 = 1.72 m; 2 = 0.97 m; 3 = 0.81 m; 4 = 0.82 m; 5 = 0.64 m) versus the Walk-Point condition (Deviation number: 1 = 1.57 m; 2 = 0.99 m; 3 = 0.92 m; 4 = 0.79 m; 5 = 0.80 m), and a greater actual distance traveled in deviation 5 for the Walk-Point condition versus the Walk condition. A main effect of Deviation Number, $F(4,40) = 22.60$, $p < 0.001$, showed a greater actual distance traveled in deviation 1 compared to deviations 2-5 (1 = 1.65 m, 2 = 0.980 m, 3 = 0.866 m, 4 = 0.806 m, 5 = 0.718 m).

For the analysis of perceived distance traveled per significant arm deviation, Deviation Number main effects were demonstrated for both the 4 m, $F(3, 30) = 25.91$, $p < 0.001$, and 6 m, $F(4, 40) = 23.00$, $p < 0.001$, trials. In the 4 m trials, perceived distance traveled was greater in deviation 1 compared to deviations 3-4, as well as in deviation 2 compared to deviation 4 (1 = 1.29 m, 2 = 0.906 m, 3 = 0.714 m, 4 = 0.586 m). In the 6 m

trials, perceived distance traveled was greater in deviation 1 compared to deviations 2-5 (1 = 1.38 m, 2 = 0.911 m, 3 = 0.792 m, 4 = 0.718 m, 5 = 0.582 m).

4.4.3 – *Arm Gain manipulations*

Actual velocity was used to examine whether participants adhered to the instruction to walk at a constant velocity during the continuous pointing movements, and also whether the arm pointing conditions during the adaptation periods had an impact on the participant's actual motions through space. F-values for the sliding ANOVAs performed for actual walking velocity are presented in Tables 4.11 and 4.12 for the 4 and 6 m trials, respectively. In the 4 m trials, Adaptation by Test interactions at 1.0-2.5 m showed greater actual walking velocity in no-vision post-adaptation versus no-vision pre-adaptation for the Walk-Point condition (see Table 4.13). For the 6 m trials, Adaptation by Test interactions were demonstrated from 2.0-5.0 m. At 2.0 m, actual walking velocity was greater in the Walk-Point condition compared to the Point condition in the no-vision post-adaptation trials (see Table 4.14). At 2.5-5.0 m, actual walking velocities were greater in no-vision post-adaptation compared to no-vision pre-adaptation for the Walk-Point condition. A Test main effect at 4.0 m showed greater actual walking velocity in no-vision post-adaptation (1.13 m/s) compared to no-vision pre-adaptation (1.11 m/s).

The step-cycle characteristics (i.e., number of steps, step length, and left and right stride lengths) were used to examine whether the kinematics of walking changed as a function of arm pointing conditions presented during the adaptation periods. Analysis of the number of steps demonstrated no significant effects for the 4 m ($p > 0.124$; grand mean = 8.35) or 6 m ($p > 0.157$; grand mean = 11.43) walking trials. Analysis of step

length also demonstrated no significant effects for the 4 m ($p > 0.079$; grand mean = 0.577 m) or 6 m ($p > 0.056$; grand mean = 0.586 m) walking trials.

In the analysis of left stride length, no significant effects were demonstrated for the 4 m walking trials ($p > 0.206$; grand mean = 1.17 m). For the 6 m walking trials, a significant Adaptation by Test interaction, $F(1,10) = 8.70$, $p < 0.05$, showed a greater left stride length for the Walk-Point condition in no-vision post-adaptation (Point = 1.17 m; Walk-Point = 1.20 m) versus no-vision pre-adaptation (Point = 1.17 m; Walk-Point = 1.17 m). A Test main effect, $F(1,10) = 6.82$, $p < 0.05$, showed a greater left stride length in no-vision post-adaptation (1.19 m) versus no-vision pre-adaptation (1.17 m).

Analysis of right stride length for the 4 m walking trials demonstrated a significant Adaptation by Test interaction, $F(1,10) = 15.37$, $p < 0.01$. This showed a greater right stride length for the Walk-Point condition in no-vision post-adaptation (Point = 1.16 m; Walk-Point = 1.19 m) compared to no-vision pre-adaptation (Point = 1.16 m; Walk-Point = 1.15 m). A Test main effect, $F(1,10) = 6.02$, $p < 0.05$, showed a greater right stride length in no-vision post-adaptation (1.18 m) compared to no-vision pre-adaptation (1.16 m). No significant effects were demonstrated in the 6 m walking trials ($p > 0.074$; grand mean = 1.18 m).

Therefore, the greater actual walking velocities demonstrated in no-vision post-adaptation can be attributed to increases in right stride length for the 4 m trials, while those in the 6 m trials can be attributed to increases in left stride length.

Perceived distance traveled was used to examine the participant's perceived spatial locations during the course of the continuous pointing movements, with particular

interest as to whether these changed as a function of the arm pointing conditions presented during the adaptation periods. For the sliding ANOVAs performed on perceived distance traveled, F-values for the 4 and 6 m trials are presented in Tables 4.15 and 4.16, respectively. In the 4 m walking trials, significant Gain by Test interactions were demonstrated at 1.0 and 3.0 m. At 1.0 m, the interaction showed a greater perceived distance traveled in no-vision pre-adaptation for the high arm gain condition (no-vision pre-adaptation = 0.94 m; no-vision post-adaptation = 0.87 m) versus the low arm gain condition (no-vision pre-adaptation = 0.85 m; no-vision post-adaptation = 0.89 m). At 3.0 m, the interaction showed a greater perceived distance traveled in the low arm gain condition for no-vision post-adaptation (high arm gain = 2.87 m; low arm gain = 2.94 m) compared to no-vision pre-adaptation (high arm gain = 2.92 m; low arm gain = 2.85 m). For the 6 m walking trials, an Adaptation by Test interaction at 1.0 m showed a decrease in perceived distance traveled from no-vision pre-adaptation (Point = 1.06 m; Walk-Point = 0.93 m) to no-vision post-adaptation (Point = 1.01 m; Walk-Point = 0.72 m) in the Walk-Point conditions. A Test main effect at 1.0 m showed a greater perceived distance traveled in no-vision pre-adaptation (.994 m) compared to no-vision post-adaptation (.862 m). A Gain main effect at 5.5 m showed a greater perceived distance traveled in the low arm gain conditions (4.94 m) compared to the high arm gain conditions (4.80 m).

Constant error was used to examine the participant's positions along the walking path, with respect to the side-target, at the instances of 20° to -10° azimuth, in 5° increments. This is the most sensitive range for assessing pointing performance, for which changes as a function of the arm pointing conditions presented during the adaptation

periods were of particular interest. F-values for the sliding ANOVAs performed on constant error are presented in Tables 4.17 and 4.18 for the 4 and 6 m trials, respectively. In this analysis, relatively greater (i.e., more positive) constant error at the azimuth iterations indicates locations further down the walking path. In the 4 m walking trials (see Table 4.17), significant Gain by Test interactions were demonstrated at the azimuth angles ranging from 10° to -10°. At 10° and 5°, the high arm gain conditions demonstrated more positive constant error at no-vision post-adaptation compared to no-vision pre-adaptation (see Figure 4.06). However, at 0°, -5° and -10°, the interactions showed significant increases in constant error from no-vision pre-adaptation to no-vision post-adaptation in the high arm gain conditions, while also showing significant decreases in constant error from no-vision pre-adaptation to no-vision post-adaptation in the low arm gain conditions. No significant effects were demonstrated in the 6 m walking trials ($p > 0.057$; see Table 4.18). Similar to the analyses of the visual gain conditions, these results showed partial gain related differences in no-vision post-adaptation (see Discussion section for a more elaborate explanation).

Azimuth angle at peak azimuth was used to examine the azimuth angle at which pointing responses reached maximum velocity during the continuous pointing trials. Effective continuous pointing demonstrates values close to 0° in this measure, which is used as an assessment of perceived target passage. Analysis of azimuth angle at peak azimuth velocity for the 4 m walking trials demonstrated a significant Adaptation main effect, $F(1,10) = 5.43$, $p < 0.05$. This showed a greater azimuth angle at peak azimuth velocity for the Walk-Point (10.74°) versus Point condition (5.06°). No significant effects

were demonstrated for the 6 m walking trials ($p > 0.09$; grand mean = 9.09°). For the analysis of peak azimuth velocity, no significant effects were demonstrated for the 4 m ($p > 0.15$; grand mean = 39.28°/s) or 6 m ($p > 0.063$; grand mean = 36.78°/s) trials.

The significant arm deviations were trajectory fluctuations calculated using the aforementioned trajectory parsing procedure. They were examined according to number per trial, and actual and perceived distances traveled between the start and end of each deviation. Analysis of the number of significant arm deviations per trial demonstrated no significant effects for the 4 m walking trials ($p > 0.169$; grand mean = 4.43). In the 6 m walking trials, a Gain main effect, $F(1,10) = 17.67$, $p < 0.01$, showed a greater number of significant arm deviations in the high arm gain conditions (6.14) compared to the low arm gain conditions (5.68). The analysis of actual distance traveled per significant arm deviation in the 4 m trials revealed a Deviation Number main effect, $F(3,30) = 10.91$, $p < 0.001$. This showed a greater actual distance traveled in deviation 1 compared to deviations 2-4 (1 = 1.21, 2 = 0.869, 3 = 0.786, 4 = 0.643). For the 6 m trials, a Deviation Number main effect, $F(4,40) = 22.95$, $p < 0.001$, demonstrated a greater actual distance traveled in deviation 1 compared to deviations 2-5 (1 = 1.64, 2 = 0.934, 3 = 0.775, 4 = 0.822, 5 = 0.746).

For the analysis of perceived distance traveled per significant arm deviation, Deviation Number main effects were demonstrated for both the 4 m, $F(3, 30) = 33.08$, $p < 0.001$, and 6 m, $F(4, 40) = 27.84$, $p < 0.001$, trials. In the 4 m trials, perceived distance traveled was greater in deviation 1 compared to deviations 2-4, as well as in deviation 2 compared to deviation 4 (1 = 1.32 m, 2 = 0.874 m, 3 = 0.710 m, 4 = 0.539 m). In the 6 m

trials, perceived distance traveled was greater in deviation 1 compared to deviations 2-5 (1 = 1.41 m, 2 = 0.906 m, 3 = 0.758 m, 4 = 0.748 m, 5 = 0.567 m).

4.4.4 – *Significant Arm Deviations in the Step-cycle*

For the analyses involving location of significant arm deviation starts and ends in the step-cycle, the results involving all experimental conditions are reported together. For significant arm deviation starts, there were no significant differences between test conditions in any of the gain conditions (LVG_W: $\chi^2(6) = 4.95$, $p > 0.10$; HVG_W: $\chi^2(6) = 5.35$, $p > 0.10$; LVG_{WP}: $\chi^2(6) = 7.71$, $p > 0.10$; HVG_{WP}: $\chi^2(6) = 4.67$, $p > 0.10$; LAG_P: $\chi^2(6) = 3.10$, $p > 0.10$; HAG_P: $\chi^2(6) = 7.92$, $p > .10$; LAG_{WP}: $\chi^2(6) = 6.40$; $p > 0.10$; HAG_{WP}: $\chi^2(6) = 1.71$). However, when pooled across test condition, the analysis in each gain condition showed significant differences between phases of the step-cycle (LVG_W: $\chi^2(3) = 354.77$, $p < 0.01$; HVG_W: $\chi^2(3) = 260.74$, $p < 0.01$; LVG_{WP}: $\chi^2(3) = 364.61$, $p > 0.01$; HVG_{WP}: $\chi^2(3) = 263.45$, $p < 0.01$; LAG_P: $\chi^2(3) = 382.49$, $p < 0.01$; HAG_P: $\chi^2(3) = 282.25$, $p < 0.01$; LAG_{WP}: $\chi^2(3) = 273.40$, $p < 0.01$; HAG_{WP}: $\chi^2(3) = 330.42$, $p < 0.01$). Accordingly, in all gain conditions, a greater number of significant arm deviation starts appeared in the early right and late left phases compared to the early left and late right phases (see Figures 4.07 and 4.08). The difference between the early right and late left categories was significant in all cases. There were also no significant effects amongst the constituent conditions of the vision, $\chi^2(9) = 10.34$, $p > 0.10$, and arm, $\chi^2(9) = 9.12$, $p > 0.10$, gain manipulations. In consideration of this latter finding, an additional Chi Square analysis was used to compare the frequencies of the vision and arm gain manipulations. For this analysis, frequency counts were pooled amongst the constituent test and gain

conditions of the vision and arm manipulations. The expected values for each category were based on the percentage of the total number of deviations in each step-phase category multiplied by the total number of deviations in each gain manipulation condition. This analysis was non-significant, $\chi^2(3) = 1.60$, $p > 0.10$.

The results for the significant arm deviation ends were quite similar. There were no significant differences between test conditions in any of the gain conditions (LVG_W: $\chi^2(6) = 5.94$, $p > 0.10$; HVG_W: $\chi^2(6) = 10.25$, $p > 0.10$; LVG_{WP}: $\chi^2(6) = 2.75$, $p > 0.10$; HVG_{WP}: $\chi^2(6) = 8.34$, $p > 0.10$; LAG_P: $\chi^2(6) = 3.25$, $p > 0.10$; HAG_P: $\chi^2(6) = 5.84$, $p > 0.10$; LAG_{WP}: $\chi^2(6) = 4.50$, $p > 0.10$; HAG_{WP}: $\chi^2(6) = 5.65$, $p > 0.10$). However, when pooled across test conditions and examined within each gain condition, all analyses showed significant differences between the step-cycle phases (LVG_W: $\chi^2(3) = 330.38$, $p < 0.01$; HVG_W: $\chi^2(3) = 257.07$, $p < 0.01$; LVG_{WP}: $\chi^2(3) = 435.70$, $p < 0.01$, HVG_{WP}: $\chi^2(3) = 338.33$, p K< 0.01; LAG_P: $\chi^2(3) = 420.22$, $p < 0.01$; HAG_P: $\chi^2(3) = 346.33$, $p < 0.01$; LAG_{WP}: $\chi^2(3) = 257.55$, $p < 0.01$; HAG_{WP}: $\chi^2(3) = 359.02$, $p < 0.01$). These analyses demonstrated greater frequencies in the early right and early left phases compared to the late left and late right phases in all of the gain conditions (see Figures 4.09 and 4.10). The difference between the early right and early left categories was different in all cases; and the late left category showed greater frequencies than the late right category for LVG_{WP}, LAG_P, HAG_P, and LAG_{WP}. There were also no significant effects involving the vision, $\chi^2(9) = 11.69$, $p > 0.10$, and arm, $\chi^2(9) = 13.06$, $p > 0.10$, gain manipulations. Once again, in light of this latter finding, an additional analysis was performed comparing the pooled frequencies of the test and gain conditions of the vision and arm gain manipulations. The

expected values for each category were based on the percentage of the total number of deviations in each step-phase category multiplied by the total number of deviations in each gain manipulation condition. This analysis was non-significant, $\chi^2(3) = 1.56$, $p > 0.10$.

Considering there were no test or gain related findings for both significant arm deviation starts and ends, a final Chi Square analysis was performed by pooling frequency counts across all gain and test conditions and examining the difference in frequency counts between significant arm deviation starts and ends. Expected values were based on the percentage of the total number of deviations in each step-phase category multiplied by the total number of deviations in each of the significant arm deviation start and end categories. This analysis was significant, $\chi^2(3) = 666.73$, $p < 0.01$, showing greater significant arm deviation end frequencies in the early left and early right phases, and greater significant arm deviation start frequencies in the late left and late right phases (see Figure 4.11). However, in both significant arm deviation starts and ends, the highest frequency counts were shown in the early right phase.

4.5 – DISCUSSION

The goal of Study 3 was to examine whether the upper limb coordination involved in the continuous pointing task was involved in perceiving self-motion (Harrison et al., 2013). This was examined by introducing cue conflicts to the upper limb aiming responses, performed during a sensory adaptation period, and examining whether they became recalibrated to match the associated visual contributions to perceived self-motion. Overall, Study 3 showed that it was somewhat possible to recalibrate upper limb pointing

responses using cue conflicts created by low and high arm gains. However, the partial recalibration effects demonstrated in this study were likely overridden by task specific changes to CNS multisensory integration.

Evidence for this partial recalibration was demonstrated in the target-relative constant errors at the azimuth angles ranging 20° to -10°. Specifically, in the 4 m walking trials, constant error increased from pre- to post-adaptation in the high arm gain conditions (i.e., HAG_P, HAG_{WP}) at 10° and 5° azimuth. At 0°, -5° and -10° azimuth, constant error increased from pre- to post-adaptation in the high arm gain conditions and decreased in the low arm gain conditions (i.e., LAG_W, LAG_{WP}). Collectively, these results supported the hypotheses by demonstrating pointing responses indicative of over-perceptions of distance traveled following low arm gain adaptations and under-perceptions of distances traveled following high arm gain adaptations.

The constant error results also showed partial replication of Study 2. This was specifically demonstrated in the 6 m walking trials, where constant error increased from pre- to post-adaptation in the low visual gain conditions (i.e., LVG_W, LVG_{WP}) at 15° to -10° azimuth. This supported the hypothesis of an under-perception of distance traveled following the low visual gain manipulations. The high visual gain conditions did not impact constant error. Additionally, no such results were demonstrated in the 4 m trials, and the neither of the visual gain adaptation conditions differentially impacted walking and pointing (with congruent arm gains) compared to only walking.

Therefore, apart from these partially supportive constant error findings, the results of Study 3 demonstrated very few arm or vision gain-related effects in the perceptual

measures of self-motion. This suggested that the adaptation conditions of Study 3 were generally ineffective in inducing sensory recalibration. An initial possibility for explaining these results could be that the hypothesized post-adaptation perceptual effects were in some way muted by reciprocal modifications made to the post-adaptation walking kinematics (Chiovetto & Giese, 2013; Marteniuk & Bertram, 2001). However, of the few walking kinematic findings demonstrated in this study, many were not specifically impacted by the gains applied to the pointing responses. The possibility also remains that the upper and lower limb coordination involved in the continuous pointing task had no impact on perceived self-motion (c.f., Harrison et al., 2013). However, considering that the current study failed to replicate the results demonstrated in Study 2, a more likely explanation for the lack of recalibration effects was that the volume of performance trials and repeated experience with experimental conditions altered the form of CNS multisensory integration used during adaptation. This change in multisensory integration would be impervious to the gain manipulations and result in a typical (i.e., congruent) perception of self-motion being gleaned by the CNS during adaptation. As a result, the incongruence between the CNS perception of self-motion and the individual sensory cues required for sensory recalibration was not created (Durgin et al., 2005; Mohler et al., 2007).

One basis for this explanation could be that the progressive acquisition of salient task knowledge enabled the development of a robust prior expectation about task relevant stimuli. That is, human walking performance involves the optimal integration of sensory information gleaned from ongoing task performance with a prior expectation that is

continually developed across performance trials (i.e., a Bayesian prior; e.g., Ernst & Bülthoff, 2004; see Petzschner, Glasauer, & Stephan, 2015 for a review). This prior expectation represents a central tendency of the already experienced task stimuli (Petzschner & Glasauer, 2011) and when integrated by the CNS, is weighted along with the sensory cues according to their reliabilities (i.e., between trial variability). Importantly, when the sensory cues are highly variable across a series of trials, the prior expectation makes a more prominent contribution to the behavioural response. The range effect common to walking distance estimation is one of many behavioural tasks explained by this type of integration (e.g., Petzschner et al., 2015). The range effect occurs when the walking distance estimations made on individual performance trials regress towards the mean of the already performed walking extents. This results in, for example, the same walking extent (e.g., 10 m) being over-estimated when tested among a distance range of relatively large magnitudes (e.g., 5-20 m) and under-estimated when tested among a distance range of relatively small magnitudes (e.g., 1-16 m). Importantly, without the influence of prior task knowledge, estimated walking extents would primarily be based on sensory information and would presumably remain independent of the distances already tested.

In a similar vein, multisensory integration in the CNS also involves an automatic and dynamic cue reweighting capability that emphasizes the most stable sensory cues within or across a series of trials (Fetsch et al., 2009; Triesch, Ballard, & Jacobs, 2002). That is, accumulated task experience about recent inter-cue relations changes how the CNS weighs the individual sensory cues in the estimate of perceived self-motion

(Campos et al., 2014; Ernst & Bülthoff, 2004). Campos et al. (2014) demonstrated this in a distance estimation task, where the size of the invariably higher proprioceptive weight, compared to vision, depended on the experimental manipulation used to create a visual-proprioceptive cue conflict. Specifically, proprioceptive weights were relatively higher when visual gains were manipulated across trials (and proprioception remained stable) compared to when proprioceptive gains were manipulated across trials (and vision remained stable).

Furthermore, regardless of test or adaptation condition, the relationship between the continuous pointing responses and step-cycle remained consistent throughout the experiment. That is, high frequencies of significant arm deviation starts and ends occurred early in the right swing phase, while high frequencies were also shown for starts in the late left phase and ends in the early left phase (see Figure 4.11). This pattern was consistent with those in Studies 1 and 2 (see Figure 2.19 in Study 1 and Figure 3.12 in Study 2), and also aligned with other findings suggesting that the low between trial variability of step-cycle information makes it a reliable source for estimating distance traveled (Durgin et al., 2009; Chrastil & Warren, 2014). Additionally, the perceptual information gleaned from stable step-cycle information in the Study 3 adaptation periods could have provided a stable reference in which to judge the relative reliabilities of the vision and arm gains (e.g., Atkins, Fiser, & Jacobs, 2001; Ernst, Banks, & Bulthoff, 2000), as well as construct a reliable and congruent prior expectation about task relevant stimuli.

The within subjects design of the current study required participants to perform 144 continuous pointing trials across 8 gain conditions in 2 experimental days. This involved 80 minutes of sensory adaptation that included the repeated use of visual and arm gain manipulations that were either congruent with treadmill walking or equal factors higher and lower with respect to congruency. Because the sensory conditions in the adaptation periods were constantly altered using different combinations of repeated gain manipulations, it is possible that as the experiment progressed the perceived self-motions experienced during adaptation: a) were based on a robust prior expectation representative of a congruent central tendency that was more reliable than the variable individual sensory cues, b) involved lower weights applied to vision and arm proprioception because of their high variability, c) or both. In either circumstance, the self-motion perceptions during the adaptation periods were impervious to the gain manipulations and sensory recalibration was not likely required. Unfortunately however, not enough participants experienced the same counterbalancing of experimental conditions and thus, an in-depth examination of the aforementioned possibilities using trial order effects was not permitted. Further studies designed to specifically examine the multisensory integration involved in sensory recalibration are warranted.

Since Study 2 also employed a within subjects design, it is of specific interest why it was effective in demonstrating sensory recalibration to low and high visual gains (e.g., Mohler et al., 2007; Rieser et al., 1995) compared to the current study. One reason could be that Study 2 involved only three visual adaptation conditions (i.e., congruent, low gain and high gain) and half of the continuous pointing trials used in the current study.

Therefore, there was much less opportunity to develop a robust and reliable prior expectation. Additionally, the critical gain manipulations in Study 2 (i.e., low and high visual gains) were only presented once in the sole experimental session, so participants never experienced repeated exposure to the full range of task-relevant stimuli as they did in the current study. Finally, the low and high visual gain conditions of Study 2 were always preceded with a congruent visual gain condition, so there was less opportunity to make immediate comparisons between the low and high gain applications. A similar fully congruent condition (i.e., treadmill walking with congruent optic flow and congruent pointing) was never experimentally tested in Study 3. In future work, the effects of the different sensory cue conflicts introduced in this study would likely be more apparent by using fewer experimental conditions examined across fewer performance trials.

The limited after-effects demonstrated in this study can be considered in regards to the cue conflict adaptation mechanisms outlined by Redding and Wallace (2005). These mechanisms include strategic calibration and spatial alignment. Specifically, strategic calibration involves changes to motor control processes that adjust for immediate changes in task and workspace constraints, while spatial alignment involves changes to the mappings that exist between the sensory-motor systems involved in task performance. In Study 2, the difference in recalibration effects between the high and low visual gain adaptation conditions was attributed to spatial alignment, since there were no concomitant changes in post-adaptation step-cycle kinematics. However, distinguishing between these two processes was not possible in the current study. This was because the same task was performed in the adaptation period as well as in the pre- and post-

adaptation periods. Thus, the partial post-adaptation effects could have resulted from the transfer of a habituated response created by strategic motor control adjustments, or a change in the aligned mapping between the arm sensory-motor system and the CNS perception of self-motion (Redding & Wallace, 2001). In spite of this, it must remain clear that the goal of this study was not to parse apart the effects of habituation versus recalibration. The primary concern of this study was to demonstrate the arm pointing responses as potential contributors to distance estimations used in the CNS perception of self-motion. Therefore, regardless of whether habituation or sensory recalibration was responsible for the partial post-adaptation effects demonstrated in this study, the arm gain manipulations still had a small but observable impact on post-adaptation performance.

Finally, two methodological considerations arose in this study that were worthy of discussion. First, removing the laser pointer from the current methodological set-up also removed the start-point dependency it created in Study 2. Thus, absolute pointing accuracy with respect to a side-target was not required to effectively capture perceived self-motion during forward linear walking.

Second, this study demonstrated post-adaptation changes in walking velocity that were directly related to treadmill walking during adaptation. Specifically, for all of the visual gain adaptation conditions, walking velocities were greater in the no-vision post-adaptation versus no-vision pre-adaptation continuous pointing movements (see Test main effects in Tables 4.04 and 4.05; similar results were also demonstrated in Study 2, where treadmill walking was always presented during adaptation; see Table 3.1). For the arm adaptation conditions, post-adaptation walking velocities were only greater for the

Walk-Point conditions (see Adaptation by Target interactions in Tables 4.11 and 4.12). This means that across both the vision and arm gain adaptation conditions, the only conditions that did not involve an increase in post-adaptation walking velocity were the ones that did not involve treadmill walking during the adaptation periods (i.e., HAG_P, LAG_P).

These patterns of results can be attributed to a well demonstrated finding that, when set to equivalent rates, perceived self-velocity is greater in treadmill walking compared to over-ground walking (e.g., Kong, Candelaria, & Tomaka, 2009; Kong, Koh, Tan, & Wang, 2012). Since the treadmill rate in the current study was set to the average over-ground walking speeds of the participants in Study 1 (which are comparable to the pre-adaptation speeds in the current study), the perceived self-velocity of treadmill walking was likely greater than the perceived self-velocity of over-ground walking. Therefore, the post-adaptation increases in walking velocity likely reflected a matching of the perceived self-motion most recently experienced during treadmill walking. These increases in velocity were not considered to result from sensory recalibration because they were associated with post-adaptation increases in step and stride lengths, with minimal concomitant changes (i.e., Test main effects) to the perceptual measures of self-motion (see also Study 2; c.f. Test main effects in perceived distance traveled and constant error at azimuth angles for the 6 m walking trials in the vision gain conditions). Further, the sensory recalibration involved with forward walking is considered to be driven by incongruences between the CNS perception of self-motion and the individual sensory cues (e.g., Durgin et al., 2005; Mohler et al., 2007). Therefore, despite adaptation

involving a faster rate of perceived self-motion, recalibration would not occur without this incongruence.

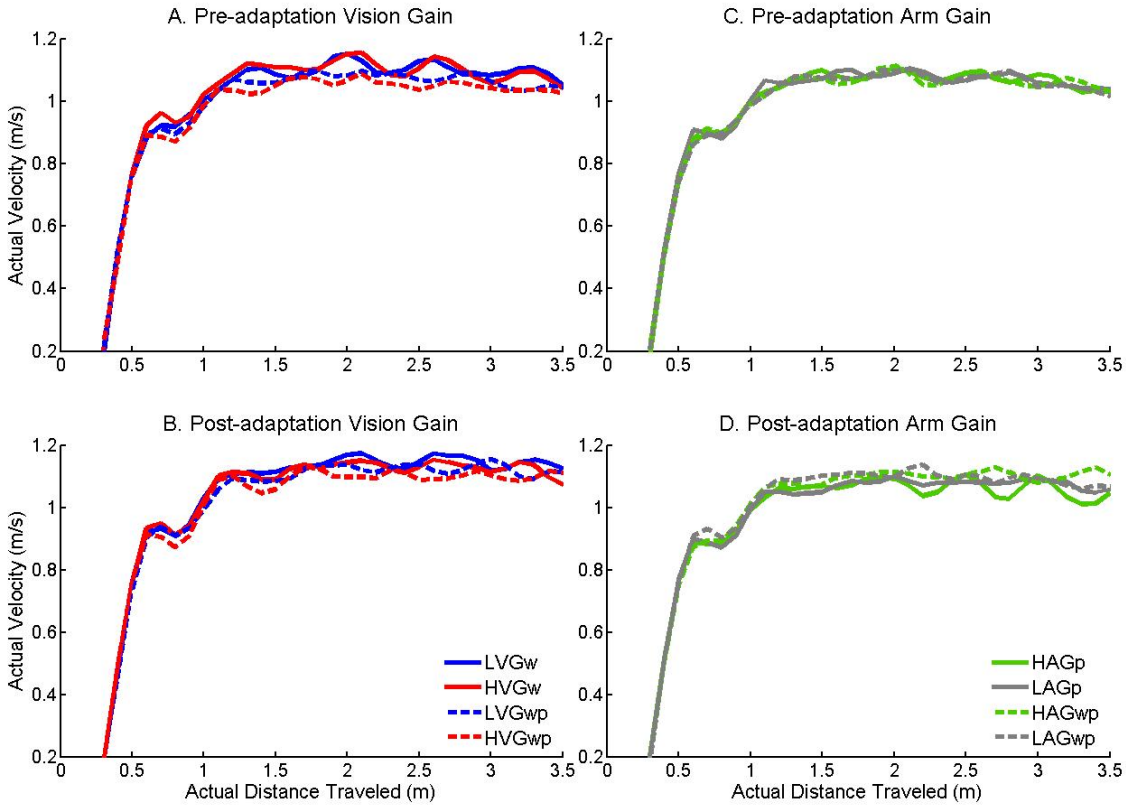

Figure 4.01. Study 3: Actual velocity trajectories in the 4 m no-vision continuous pointing trials for the pre-adaptation vision gain manipulations (top left), post-adaptation vision gain manipulations (bottom left), pre-adaptation arm gain manipulations (top right) and post-adaptation arm gain manipulations (bottom right). LVG_W = low visual gain in the V_{WALK} condition (solid blue); HVG_W = high visual gain in the V_{WALK} condition (solid red); LVG_{WP} = low visual gain in the $V_{WALK\text{-}POINT}$ condition (dashed blue); HVG_{WP} = high visual gain in the $V_{WALK\text{-}POINT}$ condition (dashed red); HAG_P = high arm gain in the A_{POINT} condition (solid green); LAG_P = low arm gain in the A_{POINT} condition (solid grey); HAG_{WP} = high arm gain in the $A_{WALK\text{-}POINT}$ condition (dashed green); LAG_{WP} = low arm gain in the $A_{WALK\text{-}POINT}$ condition (dashed grey).

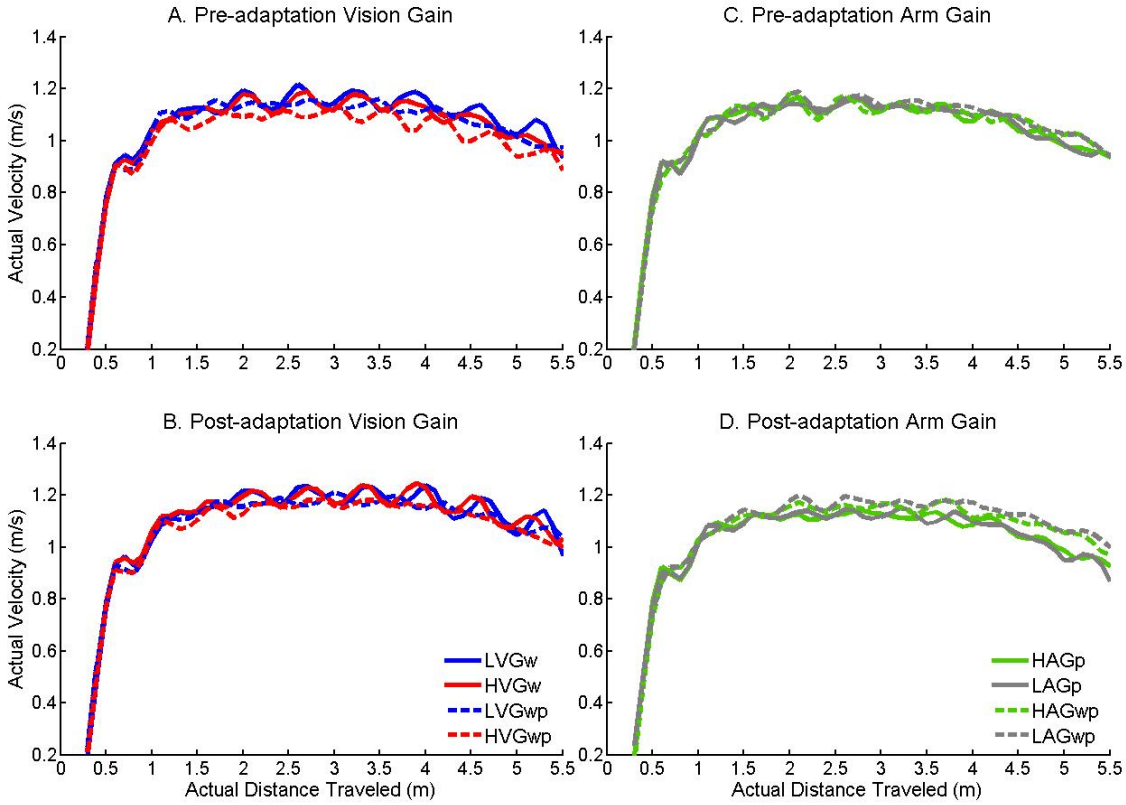

Figure 4.02. Study 3: Actual velocity trajectories in the 6 m no-vision continuous pointing trials for the pre-adaptation vision gain manipulations (top left), post-adaptation vision gain manipulations (bottom left), pre-adaptation arm gain manipulations (top right) and post-adaptation arm gain manipulations (bottom right). LVG_W = low visual gain in the V_{WALK} condition (solid blue); HVG_W = high visual gain in the V_{WALK} condition (solid red); LVG_{WP} = low visual gain in the $V_{WALK\text{-}POINT}$ condition (dashed blue); HVG_{WP} = high visual gain in the $V_{WALK\text{-}POINT}$ condition (dashed red); HAG_P = high arm gain in the A_{POINT} condition (solid green); LAG_P = low arm gain in the A_{POINT} condition (solid grey); HAG_{WP} = high arm gain in the $A_{WALK\text{-}POINT}$ condition (dashed green); LAG_{WP} = low arm gain in the $A_{WALK\text{-}POINT}$ condition (dashed grey).

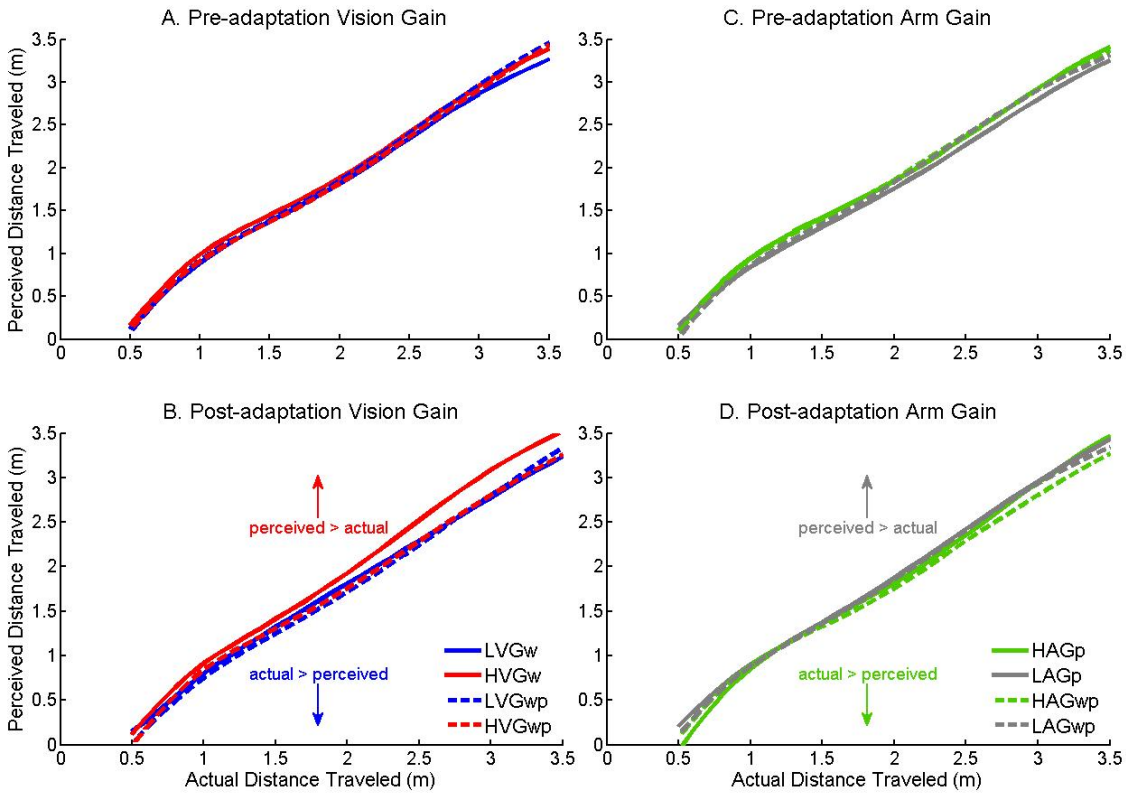

Figure 4.03. Study 3: Perceived distance traveled in the 4 m no-vision continuous pointing trials for the pre-adaptation vision gain manipulations (top left), post-adaptation vision gain manipulations (bottom left), pre-adaptation arm gain manipulations (top right) and post-adaptation arm gain manipulations (bottom right). LVG_W = low visual gain in the V_{WALK} condition (solid blue); HVG_W = high visual gain in the V_{WALK} condition (solid red); LVG_{WP} = low visual gain in the $V_{WALK\text{-}POINT}$ condition (dashed blue); HVG_{WP} = high visual gain in the $V_{WALK\text{-}POINT}$ condition (dashed red); HAG_P = high arm gain in the A_{POINT} condition (solid green); LAG_P = low arm gain in the A_{POINT} condition (solid grey); HAG_{WP} = high arm gain in the $A_{WALK\text{-}POINT}$ condition (dashed green); LAG_{WP} = low arm gain in the $A_{WALK\text{-}POINT}$ condition (dashed grey). The words and arrows in the bottom figures show the hypothesized predictions of the post-adaptation gain related differences.

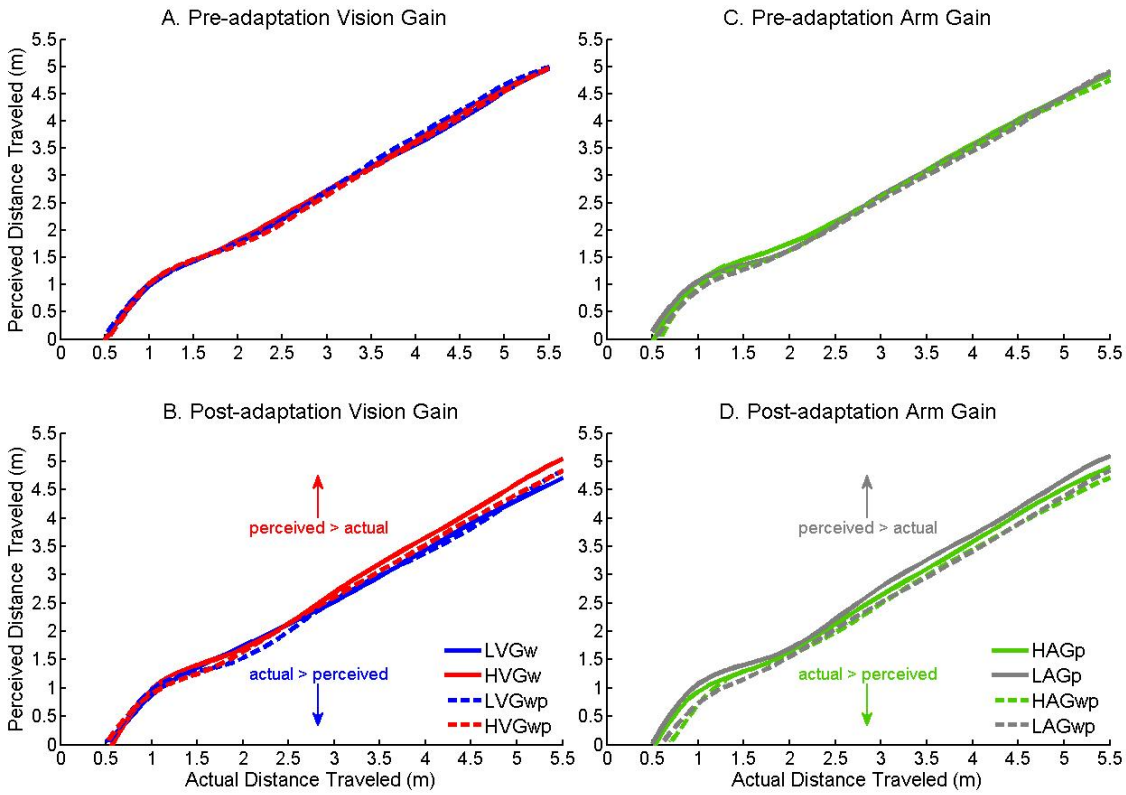

Figure 4.04. Study 3: Perceived distance traveled in the 6 m no-vision continuous pointing trials for the pre-adaptation vision gain manipulations (top left), post-adaptation vision gain manipulations (bottom left), pre-adaptation arm gain manipulations (top right) and post-adaptation arm gain manipulations (bottom right). LVG_W = low visual gain in the V_{WALK} condition (solid blue); HVG_W = high visual gain in the V_{WALK} condition (solid red); LVG_{WP} = low visual gain in the $V_{WALK\text{-}POINT}$ condition (dashed blue); HVG_{WP} = high visual gain in the $V_{WALK\text{-}POINT}$ condition (dashed red); HAG_P = high arm gain in the A_{POINT} condition (solid green); LAG_P = low arm gain in the A_{POINT} condition (solid grey); HAG_{WP} = high arm gain in the $A_{WALK\text{-}POINT}$ condition (dashed green); LAG_{WP} = low arm gain in the $A_{WALK\text{-}POINT}$ condition (dashed grey). The words and arrows in the bottom figures show the hypothesized predictions of the post-adaptation gain related differences.

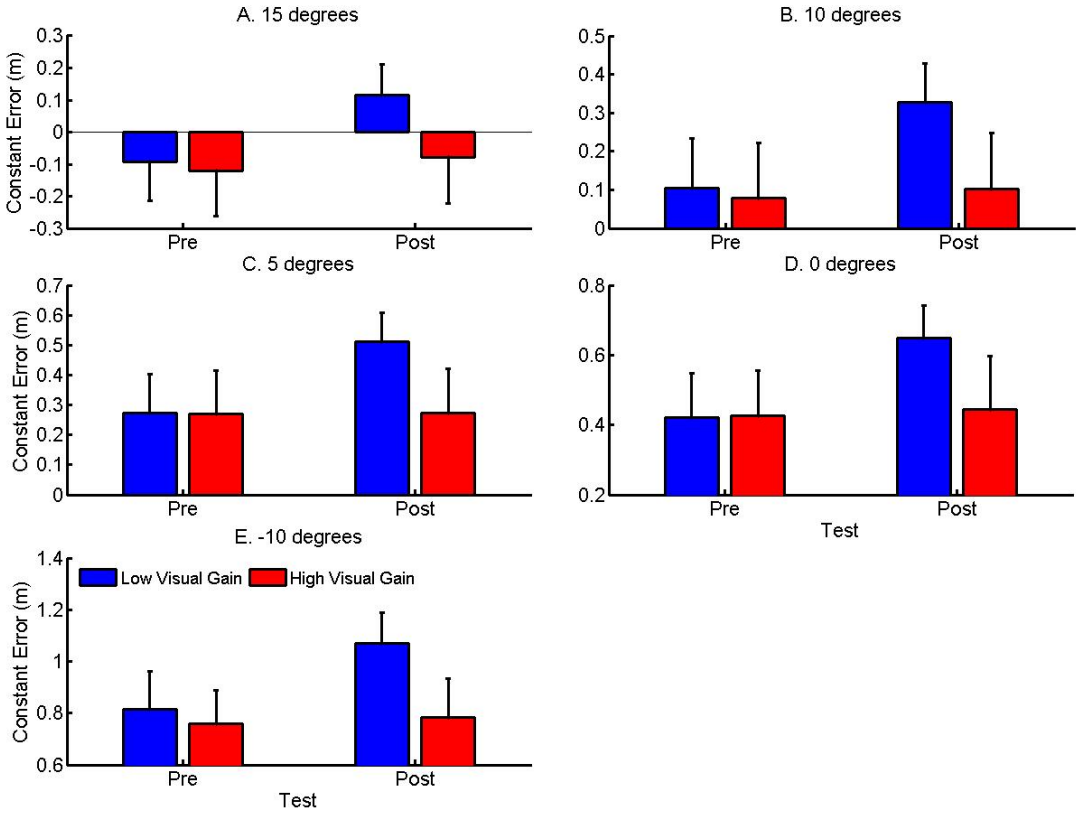

Figure 4.05. Study 3: Gain by Test interactions for the analysis of constant error with respect to the side-target in the 6 m no-vision continuous pointing trials of the vision gain manipulations at 15° (top left), 10° (top right), 5° (middle left), 0° (middle right) and -10° (bottom left) azimuth angle. Blue bars represent low visual gain conditions; red bars indicate high visual gain conditions. Error bars represent one standard error.

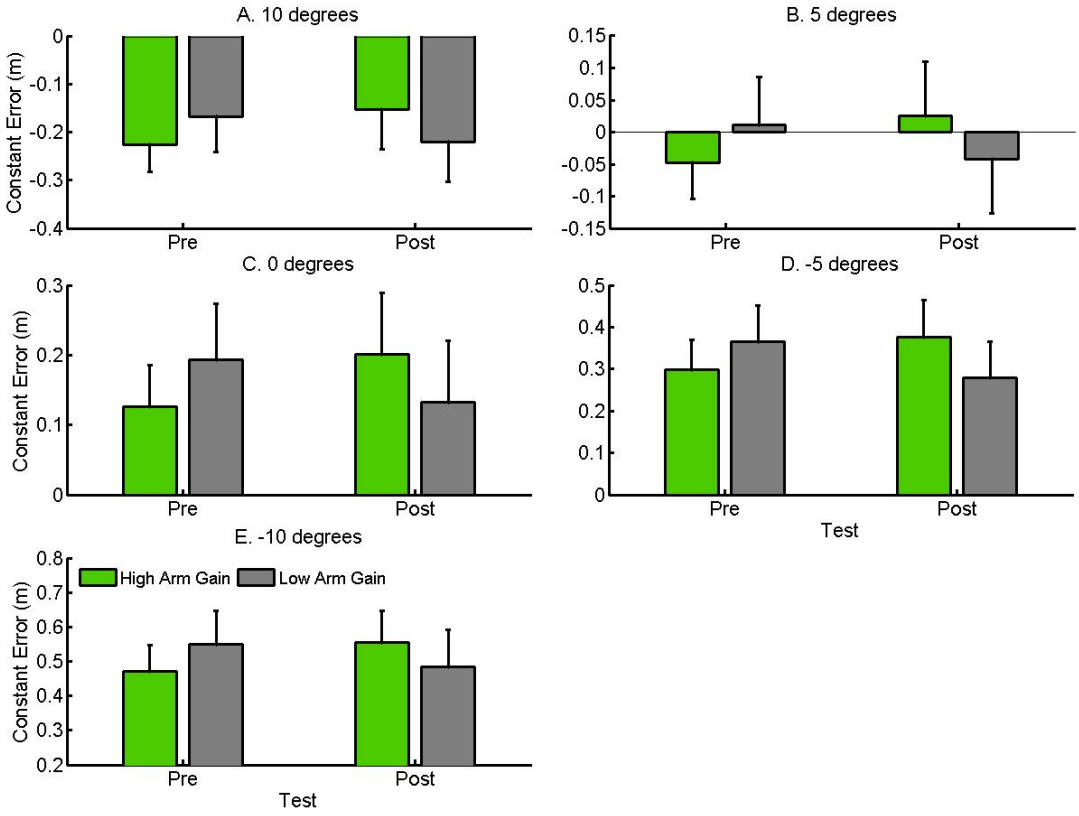

Figure 4.06. Study 3: Gain by Test interactions for the analysis of constant error with respect to the side-target in the 4 m no-vision continuous pointing trials of the arm gain manipulations at 10° (top left), 5° (top right), 0° (middle left), -5° (middle right) and -10° (bottom left) azimuth angle. Green bars represent high arm gain conditions; grey bars indicate low arm gain conditions. Error bars represent one standard error.

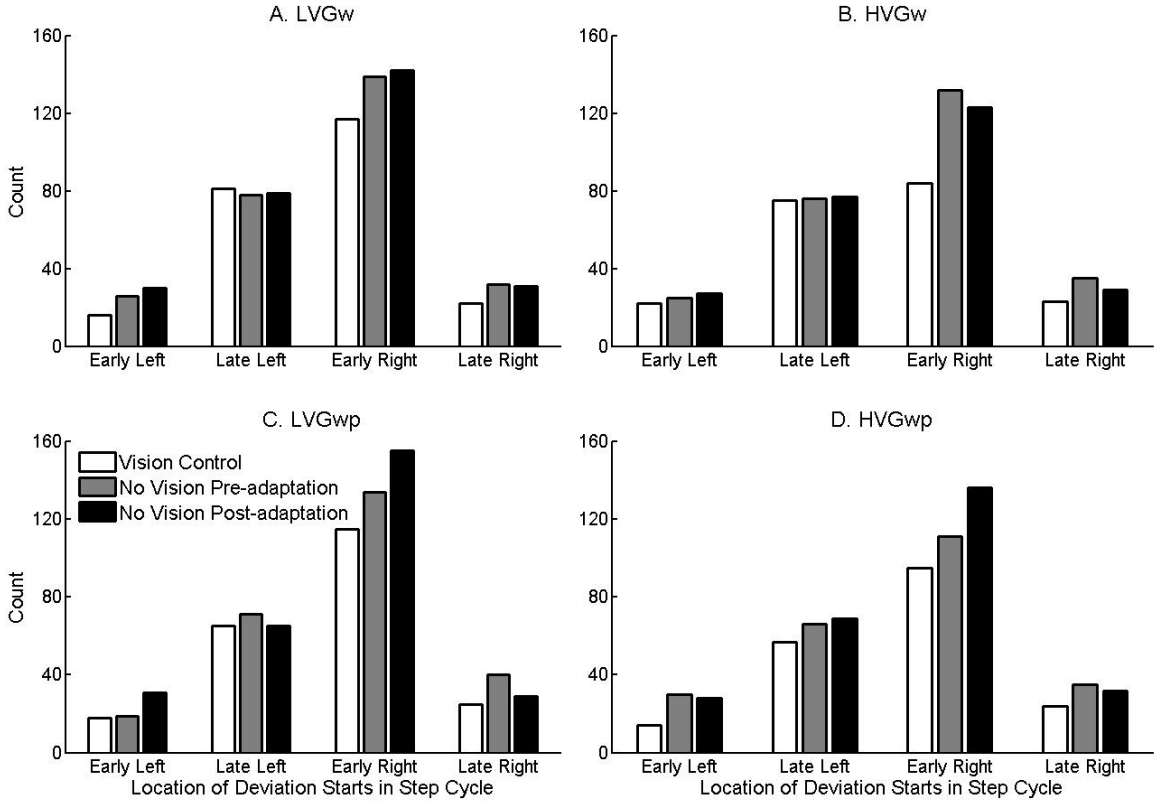

Figure 4.07. Study 3: Frequency counts for the significant arm deviation starts in the four classified phases of the step-cycle for LVG_W (top left), HVG_W (top right), LVG_{WP} (bottom left), HVG_{WP} (bottom right). LVG_W = low visual gain in the V_{WALK} condition; HVG_W = high visual gain in the V_{WALK} condition; LVG_{WP} = low visual gain in the $V_{WALK\text{-}POINT}$ condition; HVG_{WP} = high visual gain in the $V_{WALK\text{-}POINT}$ condition. Open bars represent vision control continuous pointing trials; filled grey bars represent no-vision pre-adaptation continuous pointing trials; filled black bars represent no-vision post-adaptation continuous pointing trials.

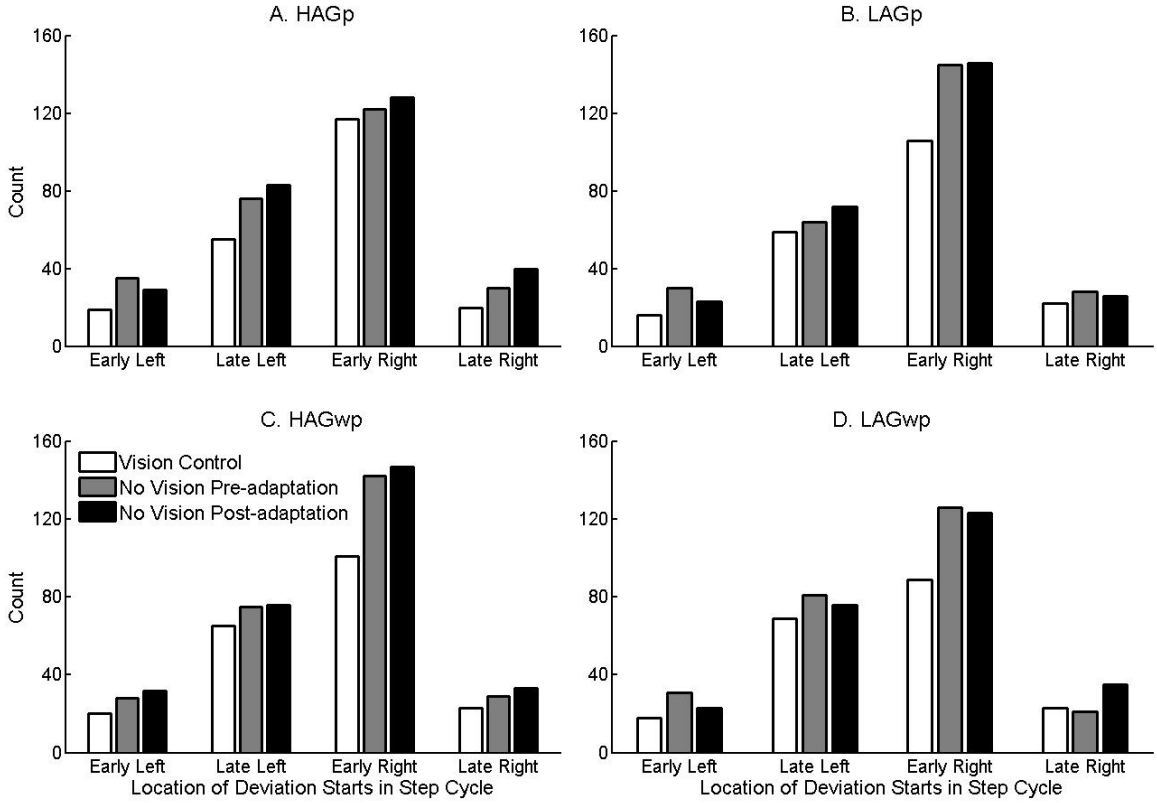

Figure 4.08. Study 3: Frequency counts for the significant arm deviation starts in the four classified phases of the step-cycle for HAG_P (top left), LAG_P (top right), HAG_{WP} (bottom left), LAG_{WP} (bottom right). HAG_P = high arm gain in the A_{POINT} condition; LAG_P = low arm gain in the A_{POINT} condition; HAG_{WP} = high arm gain in the $A_{WALK\text{-}POINT}$ condition; LAG_{WP} = low arm gain in the $A_{WALK\text{-}POINT}$ condition. Open bars represent vision control continuous pointing trials; filled grey bars represent no-vision pre-adaptation continuous pointing trials; filled black bars represent no-vision post-adaptation continuous pointing trials.

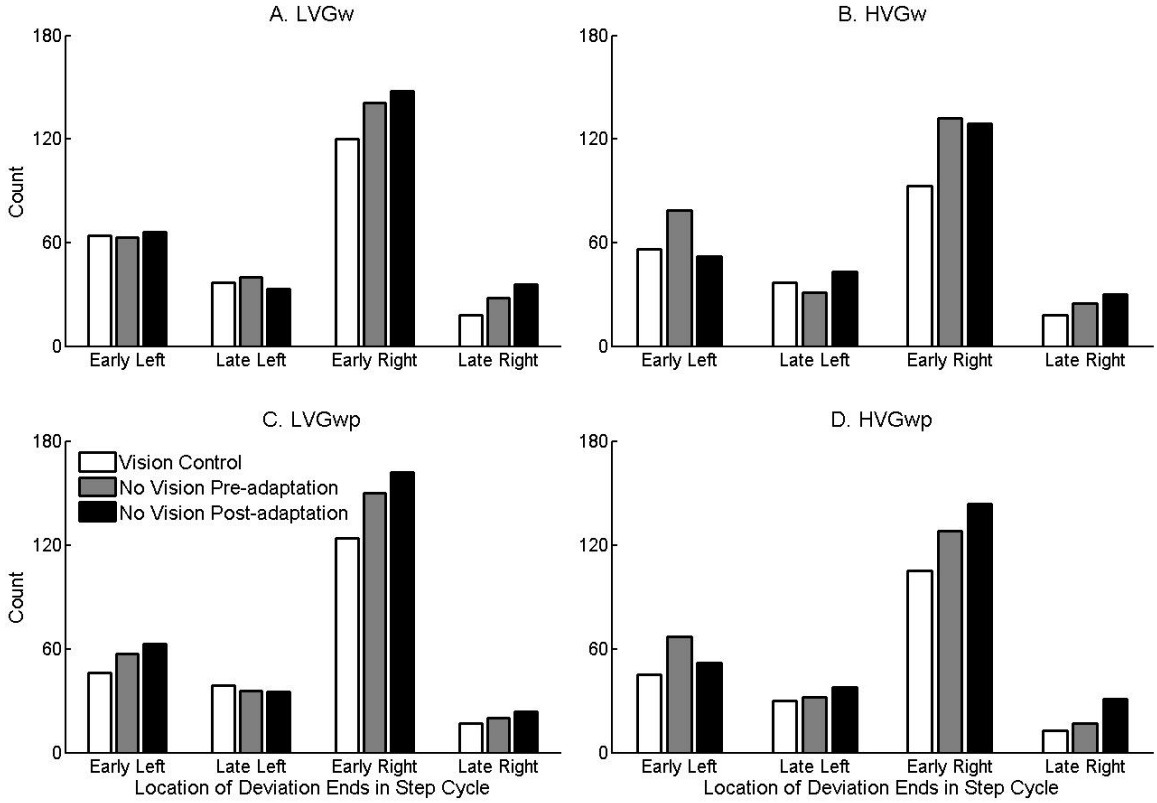

Figure 4.09. Study 3: Frequency counts for the significant arm deviation ends in the four classified phases of the step-cycle for LVG_W (top left), HVG_W (top right), LVG_{WP} (bottom left), HVG_{WP} (bottom right). LVG_W = low visual gain in the V_{WALK} condition; HVG_W = high visual gain in the V_{WALK} condition; LVG_{WP} = low visual gain in the $V_{WALK\text{-}POINT}$ condition; HVG_{WP} = high visual gain in the $V_{WALK\text{-}POINT}$ condition. Open bars represent vision control continuous pointing trials; filled grey bars represent no-vision pre-adaptation continuous pointing trials; filled black bars represent no-vision post-adaptation continuous pointing trials.

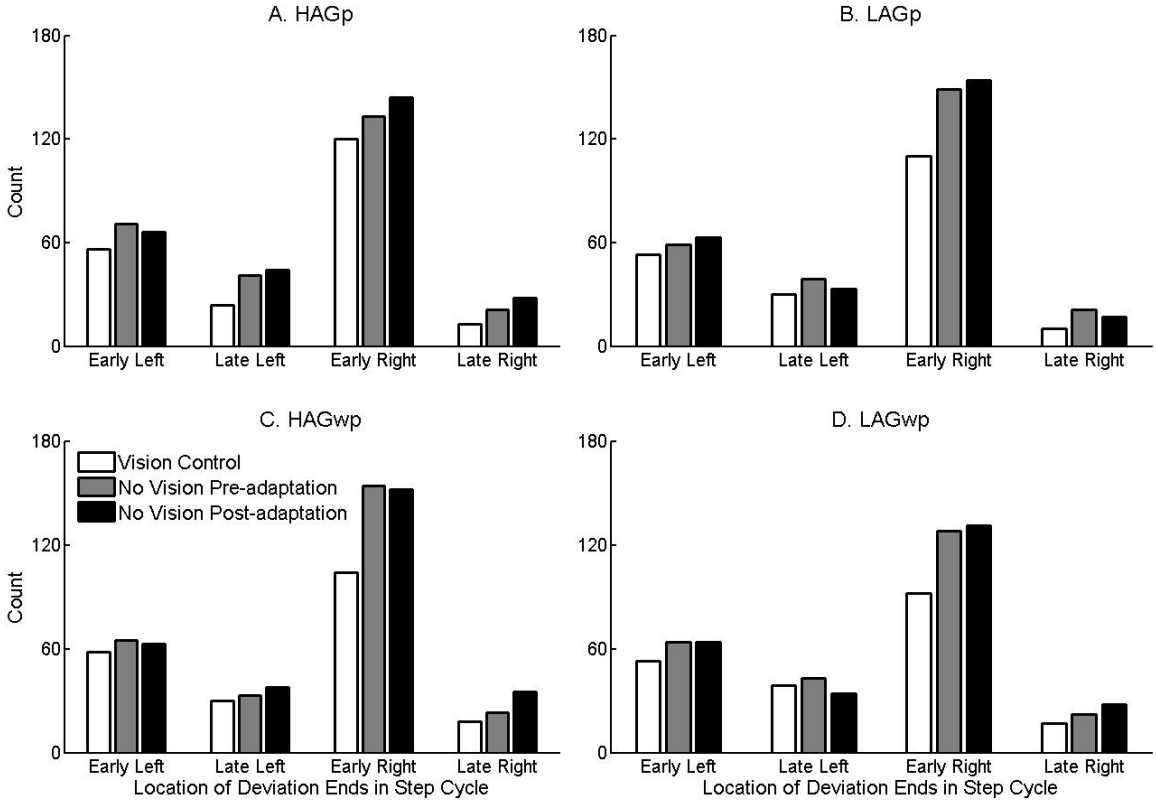

Figure 4.10. Study 3: Frequency counts for the significant arm deviation ends in the four classified phases of the step-cycle for HAG_P (top left), LAG_P (top right), HAG_{WP} (bottom left), LAG_{WP} (bottom right). HAG_P = high arm gain in the A_{POINT} condition; LAG_P = low arm gain in the A_{POINT} condition; HAG_{WP} = high arm gain in the $A_{WALK\text{-}POINT}$ condition; LAG_{WP} = low arm gain in the $A_{WALK\text{-}POINT}$ condition. Open bars represent vision control continuous pointing trials; filled grey bars represent no-vision pre-adaptation continuous pointing trials; filled black bars represent no-vision post-adaptation continuous pointing trials.

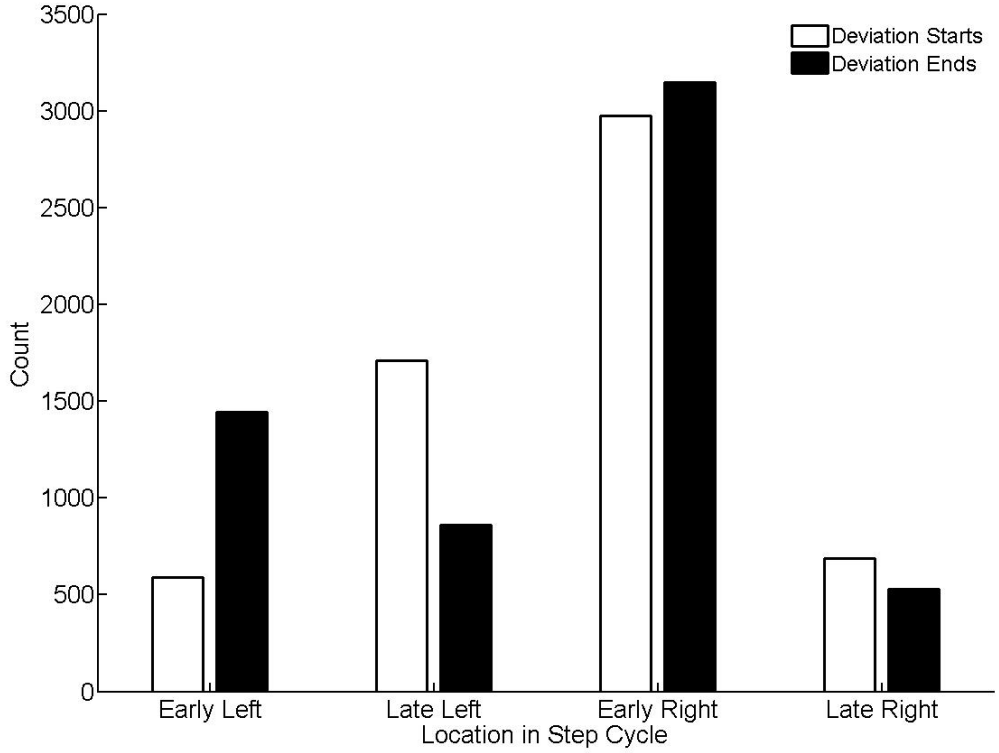

Figure 4.11. Study 3: Frequency counts for the significant arm deviation starts (open bars) and ends (filled bars) in the four classified phases of the step-cycle. Data in this figure are pooled across gain and test conditions.

Table 4.01. Sensory gain manipulations used in the Study 3 sensory adaptation periods.

Manipulation	Gain	Descriptor	Walk Rate	Visual Rate	Arm Rate
V_{WALK}	High	HVG_W	1.1 m/s	2.0 x walk	None
	Low	LVG_W	1.1 m/s	0.5 x walk	None
A_{POINT}	High	HAG_P	N/A	1.1 m/s	1.2 x arm
	Low	LAG_P	N/A	1.1 m/s	0.8 x arm
$V_{WALK-POINT}$	High	HVG_{WP}	1.1 m/s	2.0 x walk	1.0 x arm
	Low	LVG_{WP}	1.1 m/s	0.5 x walk	1.0 x arm
$A_{WALK-POINT}$	High	HAG_{WP}	1.1 m/s	1.0 x walk	1.2 x arm
	Low	LAG_{WP}	1.1 m/s	1.0 x walk	0.8 x arm

Table 4.02. Study 3: Sliding ANOVA results for the analysis of perceived distance traveled in the vision control trials.

	3 m		5 m	
Iteration (m)	F	Grand Mean (m)	F	Grand Mean (m)
0.5	0.289	0.187	0.971	-0.018
1.0	1.27	0.889	0.500	0.925
1.5	0.808	1.42	0.479	1.41
2.0	0.420	1.92	0.513	1.79
2.5	0.635	2.43	0.634	2.26
3.0	-	-	0.944	2.83
3.5	-	-	0.603	3.40
4.0	-	-	0.689	3.91
4.5	-	-	1.45	4.33

Note. *p < 0.05. **p < 0.01. ***p < 0.001. Degrees of freedom: Gain (7,70).

Table 4.03. Study 3: Sliding ANOVA results for the analysis of perceived distance traveled in the vision control and no-vision pre-adaptation trials.

	3 m					5 m				
	F-values			Means (m)		F-values			Means (m)	
Distance (m)	G	V	GV	VC	NVPRE	G	V	GV	VC	NVPRE
0.5	0.201	1.23	0.670	0.187	0.103	0.685	0.012	0.984	-0.018	-0.034
1.0	0.640	0.270	1.10	0.889	0.911	0.163	0.850	0.588	0.925	0.998
1.5	0.504	0.729	1.19	1.42	1.38	0.527	0.034	0.529	1.41	1.40
2.0	0.225	2.79	1.14	1.92	1.83	0.828	0.766	0.823	1.79	1.71
2.5	0.376	1.10	0.967	2.43	2.37	0.915	1.92	0.309	2.26	2.16
3.0	-	-	-	-	-	1.00	4.75	0.248	2.83	2.65
3.5	-	-	-	-	-	0.939	**8.01***	0.413	3.40	3.12
4.0	-	-	-	-	-	1.33	**10.22****	0.348	3.91	3.57
4.5	-	-	-	-	-	1.77	**7.66***	0.245	4.33	4.04

Note. *p < 0.05. **p < 0.01. ***p < 0.001. G = Gain (7,70), V = Vision (1,10), GV = Gain by Vision (7,70). Degrees of freedom in brackets. VC = vision control trials, NVPRE = no-vision pre-adaptation trials.

Table 4.04. Study 3: Sliding ANOVA results for the analysis of actual walking velocity in the 4 m no-vision pre- and post-adaptation trials for the visual gain conditions.

	F-values							Means (m/s)	
Distance (m)	A	G	T	AG	AT	GT	AGT	NVPRE	NVPOST
1.0	0.989	0.050	**5.91***	0.801	0.628	0.025	1.61	0.992	1.01
1.5	1.06	0.355	**10.68****	0.772	0.651	0.189	2.38	1.08	1.11
2.0	1.05	1.91	**12.96****	0.487	0.566	0.137	0.833	1.10	1.13
2.5	1.58	**6.12***	**15.32****	0.512	0.292	0.198	0.846	1.09	1.13
3.0	1.37	3.46	**26.26*****	0.151	0.276	0.176	0.001	1.07	1.12

Note. *p < 0.05. **p < 0.01. ***p < 0.001. A = Adaptation, G = Gain, T = Test, AG = Adaptation by Gain, AT = Adaptation by Test, GT = Gain by Test, AGT = Adaptation by Gain by Test. Degrees of freedom: (1,10) for all effects. NVPRE = no-vision pre-adaptation trials, NVPOST = no-vision post-adaptation trials.

Table 4.05. Study 3: Sliding ANOVA results for the analysis of actual walking velocity in the 6 m no-vision pre- and post-adaptation trials for the visual gain conditions.

	F-values							Means (m/s)			
Distance (m)	A	G	T	AG	AT	GT	AGT	NVPRE	NVPOST	LVG	HVG
1.0	0.568	1.37	**7.38***	0.702	0.085	2.63	0.040	1.01	1.02	1.02	1.01
1.5	0.372	**7.34***	**17.37****	2.69	0.105	1.80	0.035	1.10	1.13	1.13	1.11
2.0	0.774	**10.10****	**35.12*****	1.31	0.181	1.09	0.686	1.13	1.17	1.16	1.14
2.5	1.02	**5.89***	**27.59*****	0.462	0.007	2.91	1.69	1.14	1.18	1.17	1.15
3.0	1.12	3.19	**30.93*****	0.778	0.741	1.71	0.106	1.14	1.19	1.17	1.16
3.5	1.19	2.25	**34.27*****	1.25	0.954	2.32	0.532	1.13	1.19	1.17	1.15
4.0	0.972	2.99	**50.03*****	0.522	0.475	4.76	0.096	1.11	1.17	1.15	1.13
4.5	0.630	4.33	**83.33*****	0.306	1.12	2.29	0.003	1.07	1.14	1.11	1.09
5.0	0.901	**7.63***	**63.38*****	0.030	0.406	3.04	0.033	1.02	1.09	1.07	1.04

Note. *p < 0.05. **p < 0.01. ***p < 0.001. A = Adaptation, G = Gain, T = Test, AG = Adaptation by Gain, AT = Adaptation by Test, GT = Gain by Test, AGT = Adaptation by Gain by Test. Degrees of freedom: (1,10) for all effects. NVPRE = no-vision pre-adaptation trials, NVPOST = no-vision post-adaptation trials, LVG = low visual gain, HVG = high visual gain.

Table 4.06. Study 3: Sliding ANOVA results for the analysis of perceived distance traveled in the 4 m no-vision pre- and post-adaptation trials for the visual gain conditions.

Distance (m)	F-values							Grand Mean (m)
	A	G	T	AG	AT	GT	AGT	
0.5	1.25	0.008	1.48	0.984	0.427	0.819	0.002	0.093
1.0	0.175	2.97	**7.60***	0.704	0.336	1.39	0.972	0.877
1.5	0.558	1.33	3.36	0.590	1.22	0.496	0.489	1.36
2.0	1.79	1.31	1.04	0.635	2.99	0.668	0.097	1.82
2.5	1.56	2.67	1.82	1.35	1.99	2.74	0.628	2.36
3.0	0.370	2.19	2.29	1.86	2.76	3.22	1.95	2.90
3.5	0.046	1.11	1.15	1.45	**6.41***	0.476	3.16	3.36

Note. *p < 0.05. **p < 0.01. ***p < 0.001. A = Adaptation, G = Gain, T = Test, AG = Adaptation by Gain, AT = Adaptation by Test, GT = Gain by Test, AGT = Adaptation by Gain by Test. Degrees of freedom: (1,10) for all effects.

Table 4.07. Study 3: Sliding ANOVA results for the analysis of perceived distance traveled in the 6 m no-vision pre- and post-adaptation trials for the visual gain conditions.

	F-values							Means (m)	
Distance (m)	A	G	T	AG	AT	GT	AGT	NVPRE	NVPOST
0.5	0.060	1.25	0.075	0.133	0.208	0.001	1.55	-0.013	-0.033
1.0	0.004	0.111	**5.29***	0.527	0.001	0.004	.265	1.00	0.931
1.5	0.343	0.052	**8.37***	0.082	1.13	0.159	0.197	1.44	1.33
2.0	0.963	0.075	**8.14***	0.153	1.35	0.460	2.39	1.77	1.65
2.5	0.667	0.289	**6.21***	0.005	0.068	1.63	3.78	2.20	2.10
3.0	0.173	0.508	**8.45***	0.986	0.078	2.73	0.106	2.70	2.59
3.5	0.032	0.623	**9.42***	2.71	1.13	**6.23***	0.128	3.17	3.05
4.0	0.030	1.02	**9.62***	1.70	**5.49***	4.91	1.10	3.63	3.50
4.5	0.085	1.18	**16.7****	1.32	3.70	3.00	2.31	4.11	3.96
5.0	0.039	0.724	**16.4****	2.89	1.25	3.37	0.089	4.58	4.42
5.5	0.005	1.18	**12.7****	2.27	0.256	2.90	2.51	4.98	4.86

Note. *p < 0.05. **p < 0.01. ***p < 0.001. A = Adaptation, G = Gain, T = Test, AG = Adaptation by Gain, AT = Adaptation by Test, GT = Gain by Test, AGT = Adaptation by Gain by Test. Degrees of freedom: (1,10) for all effects. NVPRE = no-vision pre-adaptation trials, NVPOST = no-vision post-adaptation trials.

Table 4.08. Study 3: Sliding ANOVA results for the analysis of constant error at azimuth angle in the 4 m no-vision pre- and post-adaptation trials for the vision gain conditions.

Azimuth angle (°)	F-values							Grand Mean (m)
	A	G	T	AG	AT	GT	AGT	
20	0.535	1.72	0.117	1.19	2.62	0.076	0.392	-0.551
15	0.292	1.36	0.294	0.655	3.40	0.221	0.063	-0.352
10	0.114	1.74	0.227	0.267	2.12	0.161	0.190	-0.157
5	0.128	1.62	0.082	0.412	2.53	1.39	0.125	0.019
0	0.518	1.96	0.255	0.527	4.66	0.828	0.133	0.186
-5	0.740	1.66	0.055	0.590	3.97	0.089	0.003	0.355
-10	0.597	2.51	0.280	0.726	2.18	0.202	0.155	0.524

Note. *p < 0.05. **p < 0.01. ***p < 0.001. A = Adaptation, G = Gain, T = Test, AG = Adaptation by Gain, AT = Adaptation by Test, GT = Gain by Test, AGT = Adaptation by Gain by Test. Degrees of freedom: (1,10) for all effects.

Table 4.09. Study 3: Sliding ANOVA results for the analysis of constant error at azimuth angle in the 6 m no-vision pre- and post-adaptation trials for the vision gain conditions.

	F-values							Means (m)	
Azimuth angle (°)	A	G	T	AG	AT	GT	AGT	NVPRE	NVPOST
20	0.049	1.41	**10.93****	2.11	1.31	3.83	0.084	-0.314	-0.193
15	0.002	2.18	**11.23****	2.57	2.07	**5.52***	0.388	-0.107	0.018
10	0.028	2.62	**11.59****	2.73	2.01	**7.34***	0.761	0.092	0.216
5	0.007	2.07	**13.77****	1.01	1.87	**8.93***	0.855	0.272	0.393
0	0.005	1.67	**10.36****	0.696	0.244	**5.99***	0.002	0.424	0.546
-5	0.035	2.38	**16.25****	0.669	0.189	3.01	0.068	0.598	0.729
-10	0.005	3.28	**5.02***	1.69	0.140	**5.19***	0.160	0.787	0.927

Note. *p < 0.05. **p < 0.01. ***p < 0.001. A = Adaptation, G = Gain, T = Test, AG = Adaptation by Gain, AT = Adaptation by Test, GT = Gain by Test, AGT = Adaptation by Gain by Test. Degrees of freedom: (1,10) for all effects. NVPRE = no-vision pre-adaptation trials, NVPOST = no-vision post-adaptation trials.

Table 4.10. Study 3: Adaptation by Gain by Test interaction means for the analysis of azimuth angle at peak azimuth velocity (°) in the no-vision pre- and post-adaptation trials for the vision gain conditions.

		V_{WALK}		$V_{WALK\text{-}POINT}$	
		Low Visual Gain	High Visual Gain	Low Visual Gain	High Visual Gain
4 m	Pre-adaptation	5.81	10.24	7.82	3.17
	Post-adaptation	10.25	2.93	6.67	8.94
6 m	Pre-adaptation	6.62	15.17	11.64	2.46
	Post-adaptation	7.39	10.50	9.20	13.16

Table 4.11. Study 3: Sliding ANOVA results for the analysis of actual walking velocity in the 4 m no-vision pre- and post-adaptation trials for the arm gain conditions.

Distance (m)	F-values							Grand Mean (m/s)
	A	G	T	AG	AT	GT	AGT	
1.0	0.223	0.009	0.279	0.035	**19.30****	0.007	0.412	0.984
1.5	0.174	0.176	0.462	0.609	**11.89****	0.004	0.460	1.08
2.0	0.195	0.329	1.61	0.013	**9.32***	0.025	0.012	1.09
2.5	0.375	0.136	3.15	0.227	**7.84***	0.016	0.838	1.08
3.0	0.237	0.062	4.27	0.828	4.70	0.081	2.93	1.07

Note. *p < 0.05. **p < 0.01. ***p < 0.001. A = Adaptation, G = Gain, T = Test, AG = Adaptation by Gain, AT = Adaptation by Test, GT = Gain by Test, AGT = Adaptation by Gain by Test. Degrees of freedom: (1,10) for all effects.

Table 4.12. Study 3: Sliding ANOVA results for the analysis of actual walking velocity in the 6 m no-vision pre- and post-adaptation trials for the arm gain conditions.

Distance (m)	F-values							Grand Mean (m/s)
	A	G	T	AG	AT	GT	AGT	
1.0	0.034	0.044	0.055	0.034	0.853	0.091	0.003	0.999
1.5	0.007	0.096	0.010	0.366	1.54	0.246	0.001	1.10
2.0	0.223	1.51	0.136	0.118	**5.93***	0.013	0.334	1.13
2.5	0.322	1.66	0.781	0.381	**9.33***	0.030	0.002	1.14
3.0	0.524	2.12	1.19	0.438	**6.89***	0.017	0.001	1.14
3.5	0.929	0.689	3.45	0.198	**5.65***	0.135	0.019	1.14
4.0	0.944	2.31	**7.08***	0.610	**8.47***	0.041	0.124	1.12
4.5	1.44	0.282	4.28	0.624	**7.00***	0.117	0.672	1.08
5.0	2.89	0.003	3.37	0.824	**6.95***	0.066	0.088	1.02

Note. *p < 0.05. **p < 0.01. ***p < 0.001. A = Adaptation, G = Gain, T = Test, AG = Adaptation by Gain, AT = Adaptation by Test, GT = Gain by Test, AGT = Adaptation by Gain by Test. Degrees of freedom: (1,10) for all effects.

Table 4.13. Study 3: Adaptation by Test interaction means for the analysis of actual walking velocity (m/s) in the 4 m no-vision pre- and post-adaptation trials for the arm gain conditions.

	A_{POINT}		$A_{WALK-POINT}$	
	Pre-adaptation	Post-adaptation	Pre-adaptation	Post-adaptation
1.0 m	0.98	0.97	0.98	1.00
1.5 m	1.07	1.06	1.07	1.090
2.0 m	1.09	1.08	1.08	1.11
2.5 m	1.08	1.07	1.08	1.10

Table 4.14. Study 3: Adaptation by Test interaction means for the analysis of actual walking velocity (m/s) in the 6 m no-vision pre- and post-adaptation trials for the arm gain conditions.

	A_{POINT}		$A_{WALK-POINT}$	
	Pre-adaptation	Post-adaptation	Pre-adaptation	Post-adaptation
2.0 m	1.13	1.12	1.13	1.15
2.5 m	1.14	1.13	1.14	1.16
3.0 m	1.14	1.13	1.14	1.16
3.5 m	1.12	1.12	1.14	1.16
4.0 m	1.10	1.10	1.11	1.15
4.5 m	1.10	1.10	1.07	1.11
5.0 m	0.99	0.99	1.03	1.07

Table 4.15. Study 3: Sliding ANOVA results for the analysis of perceived distance traveled in the 4 m no-vision pre- and post-adaptation trials for the arm gain conditions.

Distance (m)	F-values							Grand Mean (m)
	A	G	T	AG	AT	GT	AGT	
0.5	0.080	3.32	0.015	2.29	2.64	3.02	0.405	0.086
1.0	0.005	2.81	0.226	0.047	0.006	**5.44***	0.482	0.888
1.5	0.013	1.08	0.082	0.403	0.324	2.46	0.180	1.36
2.0	0.002	0.162	0.001	0.553	1.11	4.15	0.019	1.83
2.5	0.037	0.382	0.102	0.573	1.51	3.67	0.213	2.36
3.0	0.041	0.010	0.182	0.869	1.87	**7.17***	0.066	2.90
3.5	0.497	1.83	0.462	0.579	2.64	4.84	0.001	3.36

Note. *p < 0.05. **p < 0.01. ***p < 0.001. A = Adaptation, G = Gain, T = Test, AG = Adaptation by Gain, AT = Adaptation by Test, GT = Gain by Test, AGT = Adaptation by Gain by Test. Degrees of freedom: (1,10) for all effects.

Table 4.16. Study 3: Sliding ANOVA results for the analysis of perceived distance traveled in the 6 m no-vision pre- and post-adaptation trials for the arm gain conditions.

Distance (m)	F-values							Grand Mean (m)
	A	G	T	AG	AT	GT	AGT	
0.5	0.975	3.28	1.52	0.001	0.002	0.147	0.002	-0.098
1.0	1.05	0.801	**5.69***	0.313	**5.36***	0.681	0.224	0.928
1.5	0.946	1.19	1.76	0.791	0.023	0.533	4.31	1.32
2.0	0.709	0.665	0.503	0.034	0.090	0.711	1.62	1.64
2.5	1.09	0.242	0.208	0.001	1.42	1.81	0.108	2.10
3.0	2.41	1.18	0.002	0.673	4.15	2.28	0.378	2.61
3.5	2.47	0.160	0.075	1.70	4.53	1.49	1.60	3.07
4.0	2.44	0.045	0.100	1.24	1.74	1.09	0.874	3.53
4.5	2.71	0.115	0.352	0.368	1.35	0.848	0.456	3.99
5.0	2.24	2.84	0.566	0.001	2.21	0.674	1.74	4.45
5.5	1.35	**5.99***	0.201	0.040	1.73	0.413	1.40	4.87

Note. *p < 0.05. **p < 0.01. ***p < 0.001. A = Adaptation, G = Gain, T = Test, AG = Adaptation by Gain, AT = Adaptation by Test, GT = Gain by Test, AGT = Adaptation by Gain by Test. Degrees of freedom: (1,10) for all effects.

Table 4.17. Study 3: Sliding ANOVA results for the analysis of constant error at azimuth angle in the 4 m no-vision pre- and post-adaptation trials for the arm gain conditions.

Azimuth angle (°)	F-values							Grand Mean (m)
	A	G	T	AG	AT	GT	AGT	
20	0.132	0.112	0.061	0.010	0.348	2.51	2.11	-0.557
15	0.133	0.203	0.001	0.008	1.40	2.60	3.63	-0.369
10	0.134	0.030	0.082	0.029	0.315	**8.44***	2.58	-0.192
5	0.131	0.036	0.074	0.079	3.13	**8.96***	2.15	-0.013
0	0.123	0.001	0.038	0.317	2.34	**10.28****	0.512	0.163
-5	0.148	0.283	0.015	1.03	2.08	**12.51****	0.233	0.330
-10	0.371	0.016	0.029	0.441	2.81	**11.67****	0.151	0.515

Note. *p < 0.05. **p < 0.01. ***p < 0.001. A = Adaptation, G = Gain, T = Test, AG = Adaptation by Gain, AT = Adaptation by Test, GT = Gain by Test, AGT = Adaptation by Gain by Test. Degrees of freedom: (1,10) for all effects.

Table 4.18. Study 3: Sliding ANOVA results for the analysis of constant error at azimuth angle in the 6 m no-vision pre- and post-adaptation trials for the arm gain conditions.

Azimuth angle (°)	F-values							Grand Mean (m)
	A	G	T	AG	AT	GT	AGT	
20	2.14	0.008	0.088	0.959	1.16	0.305	3.14	-0.207
15	1.98	0.039	0.141	0.758	1.96	0.977	0.874	-0.017
10	2.31	0.048	0.068	0.242	3.19	0.919	0.184	0.166
5	2.45	0.766	0.001	0.246	4.15	0.895	0.620	0.338
0	2.67	1.01	0.003	0.153	2.70	1.35	1.07	0.514
-5	3.64	3.05	0.001	1.25	1.32	1.59	0.771	0.675
-10	4.60	4.46	0.046	0.526	1.72	2.45	0.161	0.861

Note. *p < 0.05. **p < 0.01. ***p < 0.001. A = Adaptation, G = Gain, T = Test, AG = Adaptation by Gain, AT = Adaptation by Test, GT = Gain by Test, AGT = Adaptation by Gain by Test. Degrees of freedom: (1,10) for all effects.

CHAPTER 5:

GENERAL DISCUSSION

In three studies, the continuous pointing task was used to examine the online regulation of no-vision walking in typically calibrated (Study 1) and recalibrated (Studies 2 and 3) perceptual motor states. In this General Discussion, four points are highlighted: a) the significant arm deviations measured in the shoulder plane of elevation trajectory reflect iterative CNS spatial updating units, b) the proposed mechanism for CNS spatial updating is the temporal integration of estimated distance traveled across each iteration, followed by the addition of this iterative estimate to an ongoing cumulative sum, c) speculation about the perceptual basis of sensory recalibration and how it transfers between different locomotive tasks, and d) implications for multisensory integration. Following the discussion of these points, current experimental limitations, future directions and study applications will be presented.

5.1 – SIGNIFICANT ARM DEVIATIONS AND SPATIAL UPDATING

This thesis employed the continuous pointing task because it is an effective means of measuring the online regulation of spatial updating (Campos et al., 2009). By measuring shoulder and trunk joint angles during task performance, the overall performance of CNS spatial updating and the kinematic responses reflective its online regulation were both captured. The former was best achieved by creating an azimuth angle measure that combined the shoulder plane of elevation and trunk axial rotation joint angle trajectories, as well as reconstructing these signals using the lower frequency components (i.e., < 0.5 Hz) that were void of artefacts created by gait oscillations (see Figures 2.05 and 2.06). The latter was achieved using a trajectory parsing process, which is a common practice in the goal-directed aiming literature to examine the CNS online

regulation of discrete upper limb reaching and/or grasping movements (e.g., Burkitt et al., 2017; Burkitt et al., 2015; Chua & Elliott, 1993; Khan et al., 2006). The trajectory modifications measured using this process were informative about the organizational criteria used by the CNS to guide human movement (e.g., Bernstein, 1967; Elliott et al., 2010).

Therefore, one purpose of this thesis was to uncover the iterative nature of spatial updating by using a similar parsing procedure on the shoulder plane of elevation trajectory [6]. Although previous models conceptualized spatial updating as an iterative process (e.g., Lappe et al., 2007), little is understood about the exact nature of these iterations. For example, the leaky integrator model suggested that a task-specific state variable was incrementally updated according to a gain rate (i.e., estimation error) applied to each task increment (Lappe & Frenz, 2009; Lappe et al., 2011). However, leaky integration only went as far as estimating these gain rates using the model fitted to behavioural data, without any specific interpretation as to what constituted an incremental task unit. The step-cycle could be an ideal candidate for representing these iterations during walking, since step length and step frequency represent the least variable walking characteristics (Durgin et al., 2009), can be effectively regulated in the approach and homing phases of target directed walking tasks (Laurent & Thomson, 1988; Lee et al., 1982), and receive relatively high sensory weighting in distance estimation tasks (Campos

[6] Trunk axial rotation angles were not used for this analysis because the non-reconstructed trajectories contained step-cycle oscillations that were not reflective of pointing behaviour. Therefore, this analysis only used targets where the azimuth angle calculated with the shoulder plane of elevation trajectory (i.e., SH method in Study 1) approximated perceived distance traveled across the entire walking movement.

et al., 2012, 2014). However, these findings might misrepresent walking steps as CNS updating units because they were directly observable and readily measurable units of performance. This potential conflict was avoided by measuring upper limb aiming responses in the continuous pointing task and by quantifying how they were associated with the step-cycle.

By considering CNS spatial updating to be an iterative process and the azimuth angle trajectory of a continuous pointing movement to be an effective measure of spatial updating, the idea put forth in this thesis was that the discrete modifications in the shoulder plane of elevation trajectory provided the spatial-temporal parameters of the updating iterations. Discrete modifications (i.e., significant arm deviations) were determined as trajectory fluctuations that exceeded the limits of ± 1 standard deviations of the average detrended shoulder plane of elevation angular velocity (see Figure 2.10). Importantly, the shoulder plane of elevation trajectories of the continuous pointing movements did not contain the same ~1 Hz frequency components as those in the typical forward walking movements (see Study 1 Discussion; see Figure 2.20). Thus, the significant arm deviations reflected purposeful and discrete CNS modifications and were not artefacts created by the oscillatory arm swing trajectories typical to forward walking. Further, the perceptual differences associated with no-vision walking in Study 1 and sensory recalibration in Study 2 were at least somewhat reflected in the significant arm deviations. Specifically, perceived distances were underestimated at the updating iterations in the no-vision walking movements of Study 1. In Study 2, perceived distances trended toward being under- and overestimated in the updating iterations for the no-vision

walking movements following adaptations to low and high visual gains, respectively. Collectively, these iterative differences accumulated into more significant perceptual differences toward the ends of the walking movements.

The results from all three studies also showed that the starts and ends of the CNS updating iterations predominantly aligned with the early right foot swing phase. This was not to suggest however, that each instance of an early right foot swing event was associated with an updating iteration [7]. Rather, when the iterations did occur, they were coincident with this step-cycle phase. This means that in performing this spatial updating task, the action units demonstrated in motor performance did not map directly with the perceptual units demonstrated in CNS processing. This indirect mapping of action units with perception units is in support of other work showing that the CNS uses patterns of inter-limb coordination, as opposed to measurements gathered from individual steps, to estimate perceived distance traveled (Chrastil & Warren, 2014; Harrison et al., 2013; Turvey et al., 2009).

Our contention is that linking the significant arm deviation starts and ends to the early right foot swing phase represented a CNS timing mechanism that anchored spatial updating to a consistent part of the step-cycle. Similar timing mechanisms have been demonstrated in other tasks that involve the simultaneous performance of walking and pointing/reaching (e.g., Chiovetto & Giese, 2013; Nashner & Forssberg, 1986; Rinaldi & Moraes, 2015), although the results of this thesis appear to be the first that associate this

[7] In Study 1, for example, the total amounts of right leg steps and significant arm deviation starts that aligned with the early right foot swing phase were 3358 and 1591, respectively.

timing with a spatial updating process. The current proposal is that this anchoring strategy aids in the temporal integration of distance traveled across an updating iteration (i.e., integration of spatial information across a temporal interval), after which it is added to an ongoing cumulative sum (see Study 1). This hypothesis is consistent with research examining other perceptual-motor tasks, which shows that effective CNS performance relies on the temporal integration of task-relevant sensory information. For example, in a target-directed upper-limb reaching task, Brière and Proteau (2017) suggested that the CNS continuously monitored and accumulated visually perceived limb position so that target end point accuracy was optimized amidst online movement perturbations. In their study, aiming movements were performed on a visual display that represented end effector position (i.e., hand) as a 'dot' cursor. On a small proportion of trials, the cursor received two successive perturbations en route to the target. The first perturbation occurred soon after movement initiation and resulted in a 15 mm lateral displacement perpendicular to the direction of travel. The second perturbation occurred successively after 100 ms and involved a lateral displacement that brought the cursor back to its original trajectory (i.e., 15 mm in the direction opposite to the first perturbation). After the second perturbation, vision remained available for 16, 40 or 64 milliseconds. Results showed that the correction initiated for the first cursor jump was progressively more subdued as the duration of visual availability increased after the second cursor jump. This suggested that the CNS accumulated visual information over time when defining end effector position, as opposed to guiding performance with the most recently sampled instantaneous visual estimate (which would have resulted in the duration of visual

availability after the second perturbation having no impact). Their results further predicted that the correction for the first cursor perturbation would have been altogether aborted if a 70 ms visual sample were available after the second perturbation.

In another study, Whitaker, Levi, and Kennedy (2008) had performers detect the direction (i.e., up or down) of path deviations involving horizontal object motion profiles on a visual display. Their results showed that the critical factor in establishing the detection thresholds was the temporal duration of the motion profile prior to the trajectory deviation. Interestingly, the detection thresholds continued to improve as the duration of object motion profiles reached up to 700 ms. Accordingly, Whitaker et al. suggested that directional trajectory information was integrated across this temporal window and enabled optimal deviation judgments. That is, longer duration object motion profiles enabled more accurate estimates of path direction, which lowered the threshold for detecting a future path deviation.

By inferring that this type of temporal integration strategy is a general feature of CNS information processing (e.g., White, 2015), this thesis proposes that temporal integration is used for estimating distance traveled (i.e., performing spatial updating) across the task-specific updating iterations (i.e., significant arm deviations). Subsequently, the resulting estimate is added to an ongoing cumulative sum and the temporal integrator is reset for the next iteration. This type of updating strategy is generally consistent with leaky integration (e.g., Lappe & Frenz, 2009), which attributes updating errors to the gain rate applied to task increments (i.e., updating iterations) and the leak rate applied to the CNS integrator (i.e., ongoing cumulative sum). Furthermore,

the discrete form of temporal integration introduced here differs from the continuous form posited by Brière and Proteau (2017) in their upper-limb aiming task. This makes sense, considering that walking involves different information processing requirements than those involved in upper-limb reaching. This includes the travel of greater spatial extents, experience of longer temporal durations and the estimation of a different task-relevant parameter (distance traveled versus visually perceived target-relative limb position).

The temporal integration strategy demonstrated here would require the involvement of the CNS substrate(s) that comprises the internal metric for distance traveled. One candidate brain region for this metric could involve the hippocampal grid cells, which are particularly responsive to translational path integration (e.g., Etienne & Jeffery, 2004; Evans, Bicanski, Bush, & Burgess, 2016; Philbeck, Behrmann, Levy, Potolicchio, & Caputy, 2004; Yamamoto et al., 2014). By integrating the firing patterns in these cells across the temporal window of an updating iteration, for example, the CNS could potentially estimate the linear extent traveled during a forward walking movement. Unfortunately, further speculation on a causal link between arm trajectory deviations and neural response patterns is well beyond the scope of this thesis. However, discussions between biomechanical, behavioural and neural researchers should consider distinctions between the iterative units that guide overt behaviour, the iterative units that guide perception, and the neural structures that underlie both.

5.2 – SENSORY RECALIBRATION

Another goal of this thesis was to use the continuous pointing task to examine the online regulation of spatial updating following sensory recalibration. Study 2 replicated

previous accounts of sensory recalibration by showing changes in perceived self-motion following prolonged adaptations to low and high visual gains (e.g., Mohler et al., 2007). Specifically, Study 2 showed post-adaptation under-perceptions of distances traveled following adaptations to low visual gains and over-perceptions of distances traveled following adaptations to high visual gains. These effects resulted in post-adaptation distance traveled estimations that were less than and greater than, respectively, the performers actual distances traveled. Importantly, these changes in perceived self-motion occurred without any concomitant changes to the step-cycle kinematics (Durgin et al., 2005; Lackner & DiZio, 1988; Rieser et al., 1995). Study 3 did not replicate these results and demonstrated only partial recalibration effects involving adaptations to high and low arm gains. However, the Study 3 design was more favourable toward developing robust task priors (e.g., Petzschner et al., 2015) and/or unreliable sensory information (i.e., visual and arm proprioception; e.g., Campos et al., 2014) that could have impeded the cue incongruence (with the perception of self-motion) necessary to induce sensory recalibration (Mohler et al., 2007). Altogether, Studies 2 and 3 highlighted sensory recalibration as a multisensory process (Durgin et al., 2005; c.f., Rieser et al., 1995) that depended on incongruences between the CNS perception of self-motion and reliable sensory cues.

Redding and Wallace (1992, 1993, 2001, 2002, 2005) described two independent CNS mechanisms responsible for the types of sensory recalibration effects demonstrated in Studies 2 and 3. These include strategic calibration and spatial alignment. Strategic calibration referred to adjustments in movement planning and online control processes

that served to reduce the sensory discrepancies created by cue conflicts. Spatial alignment referred to adjustments in the sensory-motor mappings between the component elements of a perception-action system in response to prolonged cue conflict. In Study 2, the distance under-perceptions following low visual gain adaptations and over-perceptions following high visual gain adaptations can be reconciled as adaptive changes in spatial alignment. In particular, this was considered to involve a realigned mapping between leg sensory-motor systems and the CNS perception of self-motion. This was based on the aforementioned post-adaptation changes in perceived self-motion being associated with no post-adaptation changes in lower limb step-cycle kinematics. Changes in the latter would have indicated strategic motor control changes in response to the cue conflict. Presumably, in Study 2, the proprioceptive contributions to CNS self-motion perception were realigned to match the visual contributions because the adaptation task was guided by visual optic flow (Redding & Wallace, 1987, 1996).

The partial recalibration results demonstrated in Study 3 were more difficult to interpret in the context of these mechanisms. This was because the task used to present the cue conflicts during adaptation was also used to assess recalibration in the post-adaptation periods. Therefore, the partial recalibration effects demonstrated in Study 3 could have resulted from either a habituated motor response carried over from the adaptation period (i.e., strategic calibration), or represented a change in the aligned mapping between the arm sensory-motor system and the CNS perception of self-motion (i.e., spatial alignment). Irrespective of this, most important to Study 3 was that upper

limb activity during continuous pointing was demonstrated as a potential contributor to the CNS perception of self-motion.

The results of Studies 2 and 3 also made important contributions to the spatial updating model summarized in the previous subsection. That is, perceptual differences in estimates of distance traveled at individual CNS updating iterations led to larger performance differences that accumulated toward the end of the no-vision post-adaptation continuous pointing movements. These differences systematically depended on the low and high visual gain adaptation conditions. Overall, these findings support the contention that the CNS integrates perceived distance traveled across the temporal duration of an updating iteration, after which it is added to an ongoing cumulative sum. Furthermore, despite demonstrating this sensory recalibration, the significant arm deviations in Study 2 remained linked to the late left-to-early right foot swing phases of the step-cycle. This was similar to the pattern demonstrated in Study 1 and highlights the importance of step-cycle information for estimating forward displacement, even in sensory conditions where the self-motion perception associated with the step-cycle was changed from what is typically experienced. In Study 3, a similar linkage between the significant arm deviations and step-cycle showed the latter as being a stable metric that can be used to assess the reliability of constantly changing sensory cues (Atkins, Fiser, & Jacobs, 2001; Ernst, Banks, & Bulthoff, 2000), while also remaining a reliable source for measuring perceived distance traveled (Chrastil & Warren, 2014).

Measuring the joint kinematics involved with continuous pointing performance enabled this novel insight into the online regulation of sensory recalibration. This type of

insight was not available in many previous accounts of sensory recalibration, since these studies could only infer about its online control using locomotive tasks that employed end point measures (e.g., Durgin et al., 2005; Philbeck et al., 2008; Rieser et al., 1995; Ziemer et al., 2013). This includes, for example, measuring a performer's physical location with respect to an intended stationary target at the end of a walking path. In many studies, insight into the perceptual basis of sensory recalibration was gathered by examining whether the recalibration effects demonstrated in one task (e.g., forward walking) transferred or failed to transfer to other tasks (e.g., side-stepping). The idea here was that kinematic similarities between tasks that showed strong recalibration transfer were considered the perceptual bases for spatial updating and sensory recalibration. Important to the current thesis is how these previous accounts of sensory recalibration transfer are reconciled within the presented spatial updating model.

In their seminal work, Rieser et al. 1995 put forth a functional account of sensory recalibration by suggesting that transfer occurred between tasks that shared CNS functional goals. These functional goals referred to comprehensive and intended task purposes. This account was supported when the recalibration of walking transferred to sidestepping, but not to turning in place or ball throwing (e.g., Bruggeman & Warren, 2010; Pick et al., 1999). In this perspective, transfer occurred because walking and sidestepping shared the functional goal of target-directed spatial translation, while functional goals were distinct between turning in place or ball throwing. Kunz et al. (2013) advanced this perspective by suggesting that transfer occurred only when tasks involving the same effector system shared CNS functional goals. This was based on their

work showing that the recalibration of walking and wheelchair locomotion that was demonstrated within each task, weakly transferred between tasks. This was attributed to forward translation being performed by different effector systems in walking and wheeling (i.e., legs versus arms), thus prohibiting the effective task transfer.

In another perspective, Durgin et al. (2005) suggested that sufficient overlap in task kinematic action units, used by the CNS to glean estimates of perceived self-motion, formed the basis of recalibration transfer. The adaptation periods in their study used no-vision forward treadmill walking, for which the primary kinematic action unit was the step-cycle. This account was supported when recalibration transferred to no-vision over-ground walking and running in place, but was much less effective in transferring to sidestepping. This was despite running in place involving a different functional goal than the adaptation task (i.e., remaining stationary versus forward progression) and sidestepping involving a similar functional goal as the adaptation task (i.e., forward progression) [8]. However, the assumption made by Durgin et al. was that the kinematic action units of a spatial updating task were direct reflections of CNS perceptual updating units. This was not supported in the current thesis, where an indirect mapping appeared between the action (i.e. step-cycle) and perceptual (i.e., significant arm deviations) updating units during continuous pointing. Therefore, the spatial updating model presented in the current thesis advances the Durgin et al. perspective by speculating that

[8] Durgin et al. (2005) attributed the more complete transfer of walking to sidestepping in the Rieser et al. (1995) study to their treadmill-tractor set-up (see General Introduction), which required large corrections to lateral drift during treadmill walking because of turns made by the tractor. These corrections were considered to have transferred to the lateral (i.e., primary) kinematic component of sidestepping.

recalibration transfer occurs when there is sufficient between-task overlap in the perceptual units used by the CNS to glean estimates of self-motion. More specifically, the spatial updating model discussed in the current thesis suggests that sensory recalibration optimally transfers between tasks when: a) the tasks use similar sensory cues in estimating self-motion, and when b) the tasks involve similar forms of locomotive coordination to which the CNS perceptual updating units can be applied. The latter point reflects the notion that locomotive tasks can involve similar sensory inputs, but different locomotive coordination patterns. Considering that this perspective is currently speculative, the discussion in the remainder of this subsection makes conceptual links with previous literature.

The first point suggests that for recalibration transfer to be optimal, the recalibrated sensory cue must be present in the transfer task. This point was confounded in the Kunz et al. (2013) account of functional sensory recalibration, which was posited to be effector specific since the recalibration of walking did not transfer to wheelchair locomotion and vice versa (see also Gordon, Fletcher, Melvill Jones, & Block, 1995). Confounding this functional interpretation is that walking and wheelchair locomotion use different sensory contributions in forming their respective CNS representations of self-motion. In typical forward walking, perceived self-motion receives a prominent and stable contribution from proprioceptive information involved with the step-cycle. In wheeling however, arm proprioception makes this contribution. Beyond the notion that different effector systems were used to complete different functional goals, a plausible explanation for Kunz et al.'s lack of between-task recalibration transfer is that the

recalibrated sensory cues were not actually used in post-adaptation transfer task performance (e.g., Durgin et al., 2005). Thus, with the recalibrated sensory cue removed, the CNS gleaned estimates of distance traveled from an effector system that likely remained in a typically calibrated state. This interpretation is corroborated by Durgin et al. (2003), who demonstrated limb-specific recalibration in the legs and attributed this to the unique sensory contributions to CNS self-motion provided by each leg (i.e., hopping versus no hopping).

The second point suggests that recalibration transfer should occur when two tasks integrate estimates of distance traveled across perceptual iterations linked to similar forms of locomotive kinematics. For example, the strong transfer between walking and running in place (Durgin et al., 2005) can potentially be explained as both tasks involving perceptual updating units that are linked to continuous step-cycle activity. This linkage would likely be reflected in the timing of the updating iterations to early kinematic activity in the right leg. This supports the work of Turvey et al. (2009), which showed differences in distance estimation between locomotive gaits that involved different action modes. The action modes used by Turvey et al. included walking and hesitation walking. Therein, walking involved a continuous cycle of left foot and right foot forward translation and hesitation walking involved a similar cycle that was interrupted with intermittent pauses that briefly aligned the feet between forward translations. Turvey et al. (2009) interpreted their results to suggest that CNS distance estimation was intrinsically scaled to the idiothetic information involved with the inter-limb coordination patterns of specific action modes (Chrastil & Warren, 2014). The current thesis speculates that the

coordination patterns within different action modes are iteratively linked to specific leg kinematic events, and that interrupting these coordination patterns (e.g., with intermittent pauses between steps) disrupts the temporal integration strategy used to iteratively estimate distance traveled. On this basis, sensory recalibration experienced in forward walking should not transfer to hesitation walking.

This interpretation aligns with other models of sensory recalibration that conceptualize recalibration as involving the task-specific use of a more general CNS perceptual metric. For example, Redding and Wallace (2005) suggest that internally represented mappings between perceptual-motor systems (i.e., spatial alignment) provide the foundation on which motor control adjustments can be made in a task-specific manner (i.e., strategic calibration). Bingham, Pan, and Mon-Williams (2014) suggest that calibration involves a mapping between embodied units of perception and embodied units of action. That is, a change in perceptual units (i.e., a change in perceived distance by altering inter-pupillary distance) transfers to all tasks that use this metric for perceiving the performance space, while altering the task-specific application of this metric (i.e., with response produced feedback) applies only to the tasks that use this perception-action calibration (Pan, Coats, & Bingham, 2014). In the instance of perceiving self-motion by integrating multiple sensory cues, this thesis suggests that the sensory cues available for perceiving self-motion and the task-specific expression of these cues in locomotive coordination are critical elements for optimal recalibration transfer.

5.3 –IMPLICATIONS FOR MULTISENSORY INTREGRATION

This thesis makes some casual contributions to ideas about the CNS multisensory integration process used to estimate the self-motion experienced during forward linear walking. It draws upon the widely accepted account that the multisensory integration involved with perceiving self-motion involves the merging of individual sensory cues into a unitary perceptual estimate using a maximum likelihood estimate weighted linear sum (Ernst & Bülthoff, 2004). Accordingly, cues are integrated in a statistically optimal manner, where the contributions made by individual cues are determined by relative cue weighting. Specifically, cue weights are determined by individual cue variances, with higher weights being provided to cues that are less variable (i.e., more reliable). Therefore, by combining cues in this statistically optimal manner, one cue does not consistently dominate the perceptual response. Instead, cue dominance is tied to cue reliability, which can change across sensory contexts (Sun et al., 2004).

As previously mentioned, Study 3 was informative about possible changes to multisensory integration created by the trial-to-trial variations in the self-motion estimates provided by visual and arm proprioceptive cues. In addition, Study 3 fostered the potential use of a robust task prior that served to integrate acquired knowledge about the sensory environment into the weighted linear estimate (Cheng, Shettleworth, Huttenlocher, & Rieser, 2007; Petzschner et al., 2015). Therefore, Study 3 showed behavioural patterns consistent with a CNS multisensory integration process that applied high weights to stable step-cycle information and a robust task prior, and low weights to vision and arm proprioceptive information. In addition, the trial-to-trial stability of the

step-cycle likely served as a standard to which the trial-to-trial variability of the vision and arm proprioceptive cues could be assessed (Atkins et al., 2001; Campos et al., 2014; Ernst et al., 2000)

Furthermore, the focus of the current thesis was on the step-cycle kinematics (i.e., step and stride lengths) used during forward walking performance. These were considered in respect to the role of leg proprioceptive information in the estimation of forward linear self-motion, as well as in respect to the coordinative linkage between the upper and lower limbs during the forward walking performance. However, considering that vestibular information plays a role in the multisensory integration used for perceiving self-motion in many spatial tasks (Lackner & DiZio, 2005), it is also important to point out its role in the continuous pointing movements performed in this thesis.

Vestibular information pertains to the linear and rotational accelerations of the head detected by the otolith organs and semicircular canals, respectively (Angelaki & Cullen, 2008). The reliability of these cues in perceiving self-motion has traditionally been examined in updating tasks where the body is passively translated or rotated through space. Depending on the sensory context, these cues can be relatively useful in isolation for estimating forward linear (Harris et al., 2000) or curvilinear (Frissen et al., 2011) translation. Furthermore, in estimating distance traveled during forward linear walking, vestibular information has also demonstrated a predominant role in the CNS estimation of self-motion acquired through multisensory integration (Campos et al., 2012). That is, when integrated with visual and proprioceptive estimates of self-motion, vestibular cues can often receive a relatively high weighting. However, it must also be recognized that

the vestibular system is not a necessary requirement for perceiving linear self-motion, since bilateral labyrinthine-defective participants (i.e., a population with compromised vestibular function) can adequately perform linear goal-directed locomotive movements, albeit with less consistency (Glasauer, Amorim, Viaud-Delmon, & Berthoz, 2002; Glasauer, Amorim, Vitte, & Berthoz, 1994). Additionally, situations sometimes arise in other locomotive tasks where vestibular information is subsidiary to the other sensory cues (Campos et al., 2012; Sun et al., 2004). This speaks to the multisensory nature of CNS self-motion perception, as well as the conditional nature of cue dominance.

Therefore, in the continuous pointing task performed in all three thesis studies, vestibular information would have contributed to the perceptions of self-motion experienced during the over ground walking movements. However, in the treadmill walking experienced during the adaptation periods of Studies 2 and 3, vestibular information likely provided a sense of no self-motion through space. This is because performers remained stationary on the treadmill and only experienced minimal forward accelerations through space. While this scenario likely created a cue conflict with respect to the forward senses of self-motion provided by vision and leg proprioception (Campos & Bulthoff, 2012), the fact that it was present in all sensory conditions (e.g., CVG, LVG, and HVG) suggests that it can be factored out in when comparing the role of altered leg proprioceptive information between the examined sensory conditions.

5.4 – CURRENT LIMITATIONS AND FUTURE DIRECTIONS

The current thesis employed the continuous pointing task (Campos et al., 2009; Siegle et al., 2009) to measure perceived self-motion during forward linear walking in a

variety of different sensory contexts. However, in carrying out this purpose, one limitation of the current thesis was that the experimental protocols did not provide redundant measures of perceived self-motion that remained independent of the locomotive responses. Specifically, perceived self-motion was measured using upper limb pointing responses that, by the nature of the task, were also involved in locomotive coordination (Chiovetto & Giese, 2013; Harrison et al., 2013; Marteniuk & Bertram, 2001; Marteniuk et al., 2000; Rinaldi & Moraes, 2015). In many previous studies that examined spatial updating, self-motion was inferred from end point error measures collected from walking to an intended target location (e.g., Loomis & Philbeck, 2012; Rieser et al., 1995). While these latter measures were not informative about online control, they avoided potential confounds with locomotive performance. Avoiding this confound in the current thesis, while also providing measures of online control, would require that performers approximate end point target locations in addition to continuous pointing toward the side-target locations. This was not permitted however, because constraints posed by the lab space and the range of motion capture limited walking paths to lengths of 3-6 m. Pilot testing revealed that walking paths of these lengths enabled step counting as a potential performance strategy, which effectively limited the performer's actual need to perform spatial updating. This limitation, while not considered critical, was particularly evident in Study 3. In Study 3, cue conflicts were applied to upper limb pointing responses performed during the sensory adaptation periods. By virtue of using this manipulation however, the post-adaptation continuous pointing responses were tainted in their abilities to indicate how performers actually perceived their self-motions

through space. Even though Study 3 was adequately designed to assess the arm as a potential contributor to self-motion, future work will need to examine how performers actually perceive self-motion after experiencing adaptation to gained upper limb pointing responses. This can be addressed by having participants continuously point to side-targets while approximating specific end of path locations in a more accommodating lab space.

Introducing target-directed walking to the continuous pointing task also enables a more precise examination of the leaky integrator model forwarded by Lappe and Frenz (2009). According to this model, performers over-perceive distances traveled when walking to a previously viewed target and under-perceive distances traveled when reproducing a previously walked extent. Lappe and Frenz (2009) attribute these task-dependent perceptual differences to a CNS state variable that is under-perceived due to estimation error across task specific updating iterations, and due to the continuous decay of its CNS representation. These results were determined by fitting functions to patterns of end point distance estimations collected across various walking extents. However, using this type of protocol limited the capacity of their model to be most informative about how CNS distance estimation decayed as a function of walking distance. By examining distance reproduction and target-directed walking using continuous pointing responses, the model can be more informative about how the perceptual differences accumulate across the CNS updating iterations involved in forward walking. This can be specifically achieved using the measure of significant arm deviations introduced in this thesis.

Furthermore, Lee et al. (1982) suggested that target-directed locomotion was composed of two distinct online processes. There was an initial pre-planned process that was characterized by low between trial stride length variability and an accumulation of target relative error. This was followed by a homing phase characterized by high between trial stride length variability that served to reduce the target-relative error accumulated in the previous phase. Since performers were not explicitly required to achieve an end point target location in the current thesis studies, the walking responses most likely resembled only the initial phase. Therefore, it is of specific interest how the CNS estimates distance traveled across updating iterations (i.e., significant arm deviations) in the homing phase of target directed movements. More specifically, would the robust linking of the significant arm deviations to the late left-to-early right foot swing phase of the step-cycle change as the performer approaches the target. One possibility that can be examined is whether distance estimation during target-directed walking transitions from being an intrinsically based (Chrastil & Warren, 2014; Turvey et al., 2009) to an extrinsically based (Durgin et al., 2009; Lee et al., 1982) CNS process.

5.5 – APPLICATION

The findings presented in the current thesis have a broader application to general society. One such example is related to the emerging use of virtual reality as a training interface for skill learning in a variety of tasks and professions (e.g., Campos & Bulthoff, 2012). In these situations, training in virtual reality enables repeated and erred performance for real-life scenarios that are either too infrequent or too high risk for the novice learner to gain sufficient practice. However, in using virtual reality to mimic real-

life locomotive scenarios, a consistent experimental finding is the drastic under-estimation of walked virtual extents (e.g., Kelly, Hammel, Sjolund, & Siegel, 2015; Loomis & Knapp, 2003). This is a well-documented finding for which potential remedies have received attention (Kelly, Hammer, Siegel, & Sjolund, 2014; Kunz, Wouters, Smith, Thompson, & Creem-Regehr, 2009; Mohler, Creem-Regehr, Thompson, & Bulthoff, 2010; Richardson & Waller, 2005, 2007). However, one implication brought about by this thesis is for virtual reality users to consider coordinated upper limb control when designing virtual reality training scenarios. This has a potentially meaningful impact for virtual reality training environments that involve locomotion paired with goal-directed upper limb-activity (e.g., Chiovetto & Giese, 2013). This is because the coordination of upper limb activity during locomotion, in some contexts, can impact distance perception (Harrison et al., 2013). For example, Study 3 showed partial recalibration effects involving gained upper limb pointing responses that highlighted a potential role for the upper limb in the CNS perception of self-motion. The overall point to gather from this discussion is that if CNS locomotive distance estimation depends on coordinated activity in the upper limb, not properly including this information into the virtual scenario could have major implications for transfer to the real-world task.

5.6 – SUMMARY

This thesis employed the continuous pointing task to examine the online regulation of the spatial updating process that guides forward linear no-vision walking. Our main theoretical contribution was identifying the online iterations of this spatial updating process, which is an important consideration since these online iterations have

either been implied, or readily linked to observable step-cycle parameters (e.g., step length). These online iterations also reflect perceptual differences created by sensory recalibration. Furthermore, this thesis was novel in demonstrating a robust linkage of these spatial updating iterations to the late-left to early right foot swing phase of the step-cycle.

5.7 – REFERENCES

Abbs, J., & Cole, K. (1987). Neural mechanisms of motor equivalence and goal achievement. In S. Wise (Ed.), *Higher brain functions: recent explorations of the brain's emergent properties*. New York: John Wiley and Sons, Inc.

Alais, D., Newell, F., & Mamassian, P. (2010). Multisensory processing in review: from physiology to behaviour. *Seeing and Perceiving*, *23*, 3–38.

Angelaki, D., & Cullen, K. (2008). Vestibular system: the many facets of a multimodal sense. *Annual Review of Neuroscience*, *31*, 125–150.

Angelaki, D. E., Gu, Y., & DeAngelis, G. C. (2009). Multisensory integration: psychophysics, neurophysiology, and computation. *Current Opinion in Neurobiology*, *19*(4), 452–458.

Atkins, J. E., Fiser, J., & Jacobs, R. A. (2001). Experience-dependent visual cue integration based on consistencies between visual and haptic percepts. *Vision Research*, *41*, 449–461.

Bernstein, N. (1967). *The coordination and regulation of movements*. London: Pergamon Press.

Bingham, G., Pan, J., & Mon-Williams, M. (2014). Calibration is both functional and anatomical. *Journal of Experimental Psychology: Human Perception and Performance*, *40*(1), 61–70.

Brière, J., & Proteau, L. (2017). Visual monitoring of goal-directed aiming movements. *The Quarterly Journal of Experimental Psychology*, *70*(4), 736–749.

Bruggeman, H., & Warren, W. H. (2010). The direction of walking - but not throwing or kicking - is adapted by optic flow. *Psychological Science*, *21*(7), 1006–1013.

Burkitt, J. J., Bongers, R. M., Elliott, D., Hansen, S., & Lyons, J. L. (2017). Extending Energy Optimization in Goal-Directed Aiming from Movement Kinematics to Joint Angles. *Journal of Motor Behavior, 49*, 129-140.

Burkitt, J. J., Staite, V., Yeung, A., Elliott, D., & Lyons, J. L. (2015). Effector mass and trajectory optimization in the online regulation of goal-directed movement. *Experimental Brain Research*, *233*(4), 1097–1107.

Butler, J. S., Campos, J. L., & Bülthoff, H. H. (2015). Optimal visual-vestibular integration under conditions of conflicting intersensory motion profiles. *Experimental Brain Research*, *233*(2), 587–597.

Campos, J. L., & Bulthoff, H. H. (2012). Multimodal integration during self-motion in virtual reality. In M. MM & Wallace MT (Eds.), *The Neural Bases of Multisensory Processes* (pp. 603–628). Boca Raton.

Campos, J. L., Butler, J. S., & Bülthoff, H. H. (2012). Multisensory integration in the estimation of walked distances. *Experimental Brain Research, 218*, 551–565.

Campos, J. L., Butler, J. S., & Bülthoff, H. H. (2014). Contributions of visual and proprioceptive information to travelled distance estimation during changing sensory congruencies. *Experimental Brain Research, 232*, 3277–3289.

Campos, J. L., Byrne, P., & Sun, H.-J. (2010). The brain weights body-based cues higher than vision when estimating walked distances. *European Journal of Neuroscience, 31*, 1889–1898.

Campos, J. L., Siegle, J. H., Mohler, B. J., Bülthoff, H. H., & Loomis, J. M. (2009). Imagined self-motion differs from perceived self-motion: Evidence from a novel continuous pointing method. *PLoS ONE*, *4*(11).

Carnahan, H., McFadyen, B. J., Cockell, D. L., & Halverson, A. H. (1996). The combined control of locomotion and prehension. *Neuroscience Research Communications, 19*(2), 91–100.

Cheng, K., Shettleworth, S., Huttenlocher, J., & Rieser, J. (2007). Bayesian integration of spatial information. *Psychological Bulletin, 4*, 625–637.

Chiovetto, E., & Giese, M. A. (2013). Kinematics of the coordination of pointing during locomotion. *PLoS ONE, 8*(11).

Chrastil, E. R., & Warren, W. H. (2014). Does the human odometer use an extrinsic or intrinsic metric? *Attention, Perception & Psychophysics, 76*, 230–46.

Chua, R., & Elliott, D. (1993). Visual regulation of manual aiming. *Human Movement Science, 12*, 365–401.

Durgin, F. H., Akagi, M., Gallistel, C. R., & Haiken, W. (2009). The precision of locomotor odometry in humans. *Experimental Brain Research, 193*, 429–436.

Durgin, F. H., Fox, L. F., & Kim, D. H. (2003). Not Letting the Left Leg Know What the Right Leg is Doing: Limb-Specific Locomotor Adaptation to Sensory-Cue Conflict. *Psychological Science, 14*(6), 567–572.

Durgin, F. H., & Pelah, A. (1999). Visuomotor adaptation without vision? *Experimental Brain Research, 127*, 12–18.

Durgin, F. H., Pelah, A., Fox, L. F., Lewis, J., Kane, R., & Walley, K. A. (2005). Self-motion perception during locomotor recalibration: more than meets the eye. *Journal of Experimental Psychology. Human Perception and Performance, 31*(3), 398–419.

Elliott, D. (1986). Continuous visual information may be important after all: a failure to replicate Thomson (1983). *Journal of Experimental Psychology: Human Perception and Performance*, *12*(3), 388–391.

Elliott, D. (1987). The influence of walking speed and prior practice on locomotor distance estimation. *Journal Of Motor Behavior*, *19*(4), 476–485.

Elliott, D., Hansen, S., Grierson, L. E. M., Lyons, J., Bennett, S. J., & Hayes, S. J. (2010). Goal-directed aiming: two components but multiple processes. *Psychological Bulletin*, *136*, 1023–1044.

Elliott, D., Helsen, W., & Chua, R. (2001). A century later: Woodworth's (1899) two-component model of goal-directed aiming. *Psychological Bulletin*, *127*, 342–357.

Elliott, D., Lyons, J., Hayes, S. J., Burkitt, J. J., Roberts, J. W., Grierson, L. E. M., … Bennett, S. J. (2017). The multiple process model of goal-directed reaching revisited. *Neuroscience and Biobehavioral Reviews*, *72*, 95–110.

Ernst, M. O., & Banks, M. S. (2002). Humans integrate visual and haptic information in a statistically optimal fashion. *Nature*, *415*, 429–433.

Ernst, M. O., Banks, M. S., & Bulthoff, H. H. (2000). Touch can change visual slant perception. *Nature Neuroscience*, *3*(1), 69–73.

Ernst, M. O., & Bülthoff, H. H. (2004). Merging the senses into a robust percept. *Trends in Cognitive Sciences*, *8*(4), 162–169.

Etienne, A. S., & Jeffery, K. J. (2004). Path integration in mammals. *Hippocampus*, *14*, 180–192.

Evans, T., Bicanski, A., Bush, D., & Burgess, N. (2016). How environment and self-motion combine in neural representations of space. *The Journal of Physiology*, *594*(22), 6535–6546.

Farrell, M. J., & Thomson, J. A. (1999). On-Line Updating of Spatial Information During Locomotion Without Vision. *Journal of Motor Behavior*, *31*(1), 39–53.

Fetsch, C. R., Turner, A. H., DeAngelis, G. C., & Angelaki, D. E. (2009). Dynamic reweighting of visual and vestibular cues during self-motion perception. *The Journal of Neuroscience*, *29*(49), 15601–15612.

Fitts, P. M. (1954). The information capacity of the human motor system in controlling the amplitude of movement. *Journal of Experimental Psychology*, *47*(6), 381–391.

Frissen, I., Campos, J. L., Souman, J. L., & Ernst, M. O. (2011). Integration of vestibular and proprioceptive signals for spatial updating. *Experimental Brain Research*, *212*, 163–176.

Fukusima, S. S., Loomis, J. M., & Da Silva, J. A. (1997). Visual perception of egocentric distance as assessed by triangulation. *Journal of Experimental Psychology: Human Perception and Performance*, *23*(1), 86–100.

Georgopoulos, A. P., & Grillner, S. (1989). Visuomotor Coordination in Reaching and Locomotion. *Science, 245*(4923), 1209–1210.

Glasauer, S., Amorim, M., Viaud-Delmon, I., & Berthoz, A. (2002). Differential effects of labyrinthine dysfunction on distance and direction during blindfolded walking of a triangular path. *Experimental Brain Research, 145*, 489–497.

Glasauer, S., Amorim, M., Vitte, E., & Berthoz, A. (1994). Goal-directed linear locomotion in normal and labyrinthine-defective subjects. *Experimental Brain Research, 98*, 323–335.

Gordon, C., Fletcher, W., Melvill Jones, G., & Block, E. (1995). Adaptive plasticity in the control of locomotor trajectory. *Experimental Brain Research, 102*, 540–545.

Harris, L. R., Jenkin, M., & Zikovitz, D. C. (2000). Visual and non-visual cues in the perception of linear self motion. *Experimental Brain Research, 135*(1), 12–21.

Harrison, S. J., Kuznetsov, N., & Breheim, S. (2013). Flexible kinesthetic distance perception: When do your arms tell you how far you have walked? *Journal of Motor Behavior, 45*(3), 239–247.

Kallie, C., Schrater, P., & Legge, G. (2007). Variability in stepping direction explains the veering behavior of blind walkers. *Journal of Experimental Psychology: Human Perception and Performance, 33*(1), 183–200.

Kelly, J., Hammel, W., Sjolund, L., & Siegel, Z. (2015). Frontal extents in virtual environments are not immune to underperception. *Attention, Perception & Psychophysics*, *77*, 1848–1853.

Kelly, J., Hammer, W., Siegle, Z., & Sjolund, L. (2014). Recalibration of perceived distance in virtual environments occurs rapidly and transfers asymmetrically across scale. *IEEE Transactions on Visualization and Computer Graphics, 20*(4), 588–595.

Khan, M. A., Franks, I. M., Elliott, D., Lawrence, G. P., Chua, R., Bernier, P. M., … Weeks, D. J. (2006). Inferring online and offline processing of visual feedback in target directed movements from kinematic data. *Neuroscience and Biobehavioral Reviews, 30*, 1106–1121.

Kong, P. W., Candelaria, N. G., & Tomaka, J. (2009). Perception of self-selected running speed is influenced by the treadmill but not footwear. *Sports Biomechanics*, *8*(1), 52–59.

Kong, P. W., Koh, T. M. C., Tan, W. C. R., & Wang, Y. S. (2012). Unmatched perception of speed when running overground and on a treadmill. *Gait and Posture*, *36*, 46–48.

Kunz, B. R., Creem-Regehr, S. H., & Thompson, W. B. (2009). Evidence for motor simulation in imagined locomotion. *Journal of Experimental Psychology: Human Perception and Performance, 35*(5), 1458–1471.

Kunz, B. R., Creem-Regehr, S. H., & Thompson, W. B. (2013). Does Perceptual-Motor Calibration Generalize across Two Different Forms of Locomotion? Investigations of Walking and Wheelchairs. *PLoS ONE, 8*(2).

Kunz, B. R., Wouters, L., Smith, D., Thompson, W., & Creem-Regehr, S. H. (2009). Revisiting the effect of quality of graphics on distance judgements in virtual environments: A comparison of verbal reports and blind walking. *Attention, Perception & Psychophysics, 71*(6), 1284–1293.

Lackner, J., & DiZio, P. (1988). Visual stimulation affects the perception of voluntary leg movements during walking. *Perception, 17*, 71–80.

Lackner, J., & DiZio, P. (2005). Vestibular, proprioceptive, and haptic contributions to spatial orientation. *Annual Review of Psychology, 56*, 115–147.

Lappe, M., & Frenz, H. (2009). Visual estimation of travel distance during walking. *Experimental Brain Research, 199*, 369–375.

Lappe, M., Jenkin, M., & Harris, L. R. (2007). Travel distance estimation from visual motion by leaky path integration. *Experimental Brain Research, 180*, 35–48.

Lappe, M., Stiels, M., Frenz, H., & Loomis, J. M. (2011). Keeping track of the distance from home by leaky integration along veering paths. *Experimental Brain Research, 212*, 81–89.

Laurent, M., & Thomson, J. A. (1988). The role of visual information in control of a constrained locomotor task. *Journal Of Motor Behavior, 20*(1), 17–37.

Lee, D., Lishman, J., & Thomson, J. (1982). Regulation of gait in long jumping. *Journal of Experimental Psychology: Human Perception and Performance, 8*(3), 448–459.

Loomis, J., Klatzky, R. L., & Giudice, N. (2013). Representing 3D space in working memory: spatial images from vision, hearing, touch and language. In S. Lacey & R. Lawson (Eds.), *Multisensory Imagery* (pp. 131–155). New York: Springer.

Loomis, J., & Knapp, J. (2003). Visual perception of egocentric distance in real and virtual environments. In L. Hettinger & M. Hass (Eds.), *Virtual and Adaptive Environments* (pp. 21–46). Mahwah NJ: Erlbaum.

Loomis, J. M., Da Silva, J. A., Fujita, N., & Fukusima, S. S. (1992). Visual space perception and visually directed action. *Journal of Experimental Psychology: Human Perception and Performance, 18*, 906–921.

Loomis, J., & Philbeck, J. W. (2012). Measuring spatial perception with spatial updating and action. In R. L. Klatzky, B. MacWhinney, & M. Behrmann (Eds.), *Embodiment, Ego-Space, and Action* (pp. 1–43). Hoboken: Taylor & Francis.

Lyons, J., Hansen, S., Hurding, S., & Elliott, D. (2006). Optimizing rapid aiming behaviour: movement kinematics depend on the cost of corrective modifications. *Experimental Brain Research*, *174*, 95–100.

Marteniuk, R., & Bertram, C. (2001). Contributions of gait and trunk movements to prehension: perspectives from world- and body-centered coordinates. *Motor Control*, *2*, 151–165.

Marteniuk, R. G., Ivens, C. J., & Bertram, C. P. (2000). Evidence of motor equivalence in a pointing task involving locomotion. *Motor Control*, *4*, 165–184.

Mauerberg, E., & Adrian, M. (1995). Temporal coupling between external auditory information and the phases of walking. *Perceptual and Motor Skills*, *80*, 851–861.

Mittelstaedt, M. L., & Mittelstaedt, H. (2001). Idiothetic navigation in humans: estimation of path length. *Experimental Brain Research*, *139*, 318–332.

Mohler, B. J., Creem-Regehr, S. H., Thompson, W. B., & Bulthoff, H. H. (2010). The effect of viewing a self-avatar on distance judgements in an HMD-based virtual environment. *Presence*, *19*(3), 230–242.

Mohler, B. J., Thompson, W. B., Creem-Regehr, S. H., Willemsen, P., Pick, Jr., H. L., & Rieser, J. J. (2007). Calibration of locomotion resulting from visual motion in a treadmill-based virtual environment. *ACM Transactions on Applied Perception*, *4*(1).

Multon, F., & Olivier, A.-H. (2013). Biomechanics of walking in real world: naturalness we wish to reach in virtual reality. In F. Steinicke, Y. Visell, J. Campos, & A. Lecuyer (Eds.), *Human Walking in Virtual Environments* (pp. 55–77). New York: Springer.

Muzii, R. A., Lamm Warburg, C., & Gentile, A. M. (1984). Coordination of the upper and lower extremities. *Human Movement Science*, *3*, 337–354.

Nashner, L. M., & Forssberg, H. (1986). Phase-dependent organization of postural adjustments associated with arm movements while walking. *Journal of Neurophysiology*, *55*(6), 1382–1394.

Pan, J., Coats, R., & Bingham, G. (2014). Calibration is action specific but perturbation of perceptual units is not. *Journal of Experimental Psychology: Human Perception and Performance*, *40*(1), 404–415.

Petzschner, F. H., & Glasauer, S. (2011). Iterative Bayesian estimation as an explanation for range and regression effects: a study on human path integration. *The Journal of Neuroscience*, *31*(47), 17220–17229.

Petzschner, F. H., Glasauer, S., & Stephan, K. E. (2015). A Bayesian perspective on magnitude estimation. *Trends in Cognitive Sciences*, *19*(5), 285–293.

Philbeck, J. W., Behrmann, M., Levy, L., Potolicchio, S. J., & Caputy, A. (2004). Path integration deficits during linear locomotion after human medial temporal lobectomy, *16*, 510–520.

Philbeck, J. W., & Loomis, J. M. (1997). Comparison of two indicators of perceived egocentric distance under full-cue and reduced-cue conditions. *Journal of Experimental Psychology: Human Perception and Performance,* 72-85.

Philbeck, J. W., Loomis, J. M., & Beall, A. C. (1997). Visually perceived location is an invariant in the control of action. *Perception & Psychophysics*, *59*(4), 601–612.

Philbeck, J., Woods, A., Arthur, J., & Todd, J. (2008). Progressive locomotor recalibration during blind walking. *Perception and Psychophysics*, *70*(8), 1459–1470.

Pick, Jr., H. L., Rieser, J. J., Wagner, D., & Garing, A. E. (1999). The recalibration of rotational locomotion. *Journal of Experimental Psychology: Human Perception and Performance*, *25*(5), 1179–1188.

Prokop, T., Schubert, M., & Berger, W. (1997). Visual influence on human locomotion. Modulation to changes in optic flow. *Experimental Brain Research*, *114*, 63–70.

Redding, G., & Wallace, B. (1987). Perceptual-motor coordination and prism adaptation during locomotion: A control for head posture contributions. *Perception & Psychophysics*, *42*(3), 269–274.

Redding, G., & Wallace, B. (1992). Effects of pointing rate and availability of visual feedback on visual and proprioceptive components of prism adaptation. *Journal of Motor Behavior*, *24*(3), 226–237.

Redding, G., & Wallace, B. (1993). Adaptive coordination and alignment of eye and hand. *Journal of Motor Behavior*, *25*(2), 75–88.

Redding, G., & Wallace, B. (1996). Adaptive spatial alignment and strategic perceptual-motor control. *Journal of Experimental Psychology: Human Perception and Performance*, *22*(2), 379–394.

Redding, G., & Wallace, B. (2001). Calibration and alignment are separable: Evidence from prism adaptation. *Journal of Motor Behavior*, *33*(4), 401–412.

Redding, G., & Wallace, B. (2002). Strategic calibration and spatial alignment: A model from prism adaptation. *Journal of Motor Behavior*, *34*(2), 126–138.

Redding, G., & Wallace, B. (2005). Applications of prism adaptation: a tutorial in theory and method. *Neuroscience and Biobehavioral Reviews*, *29*, 431–444.

Richardson, A., & Waller, D. (2005). The effect of feedback training on distance estimation in virtual environments. *Applied Cognitive Psychology*, *19*, 1089–1108.

Richardson, A., & Waller, D. (2007). Interaction with an immersive virtual environment corrects users' distance estimates. *Human Factors*, *49*(3), 507-517.

Rieser, J. J., Ashmead, D. H., Talor, C. R., & Youngquist, G. A. (1990). Visual perception and the guidance of locomotion without vision to previously seen targets. *Perception*, *19*, 675–689.

Rieser, J. J., Guth, D. A., & Hill, E. W. (1986). Sensitivity to perspective structure while walking without vision. *Perception*, *15*, 173–188.

Rieser, J. J., Pick Jr, H. L., Ashmead, D. H., & Garing, A. E. (1995). Calibration of human locomotion and models of perceptual-motor organization. *Journal of Experimental Psychology: Human Perception and Performance*, *21*(3), 480–497.

Rinaldi, N. M., & Moraes, R. (2015). Gait and reach-to-grasp movements are mutually modified when performed simultaneously. *Human Movement Science*, *40*, 38–58.

Robertson, G. E. (2013). *Introduction to biomechanics for human motion analysis* (3rd ed.). Waterloo: Waterloo Biomechanics.

Sarlegna, F., Blouin, J., Bresciani, J.-P., Bourdin, C., Vercher, J.-L., & Gauthier, G. M. (2003). Target and hand position information in the online control of goal-directed arm movements. *Experimental Brain Research*, *151*, 524–535.

Scotto Di Cesare, C., Bringoux, L., Bourdin, C., Sarlegna, F. R., & Mestre, D. R. (2011). Spatial localization investigated by continuous pointing during visual and gravitoinertial changes. *Experimental Brain Research*, *215*, 173–182.

Siegle, J. H., Campos, J. L., Mohler, B. J., Loomis, J. M., & Bülthoff, H. H. (2009). Measurement of instantaneous perceived self-motion using continuous pointing. *Experimental Brain Research*, *195*, 429–444.

Steenhuis, R., & Goodale, M. (1988). The effects of time and distance on accuracy of target-directed locomotion: does an accurate short-term memory for spatial location exist? *Journal Of Motor Behavior*, *20*(4), 399–415.

Sun, H.-J., Campos, J. L., & Chan, G. S. (2004). Multisensory integration in the estimation of relative path length. *Experimental Brain Research*, *154*, 246–254.

Triesch, J., Ballard, D. H., & Jacobs, R. A. (2002). Fast temporal dynamics of visual cue integration. *Perception, 31*, 421–434.

Turvey, M. T., Romaniak-Gross, C., Isenhower, R. W., Arzamarski, R., Harrison, S., & Carello, C. (2009). Human odometer is gait-symmetry specific. *Proceedings of the Royal Society B, 276*, 4309–4314.

Van Der Wel, R. P. R. D., & Rosenbaum, D. A. (2007). Coordination of locomotion and prehension. *Experimental Brain Research, 176*, 281–287.

Vincent, W. J. (2005). *Statistics in kinesiology* (3rd ed.). Champaign: Human Kinetics.

Whitaker, D., Levi, D. M., & Kennedy, G. J. (2008). Integration across time determines path deviation discrimination for moving objects. *PLoS ONE*, *3*(4).

White, P. A. (2015). The pre-reflective experience of "I" as a continuously existing being: The role of temporal functional binding. *Consciousness and Cognition, 31*, 98–114.

Withagen, R., & Michaels, C. (2002). The calibration of walking transfers to crawling: are action systems calibrated? *Ecological Psychology*, *14*(4), 223–234.

Wittlinger, M., Wehner, R., & Wolf, H. (2006). The ant odometer: stepping on stilts and stumps. *Science*, *312*, 1965–1967.

Woodworth, R. (1899). The accuracy of voluntary movement. *Psychological Review, 3 (monograph)*, 1–119.

Wu, G., van der Helm, F. C. T., Veeger, H. E. J., Makhsous, M., Van Roy, P., Anglin, C., … Buchholz, B. (2005). ISB recommendation on definitions of joint coordinate systems of various joints for the reporting of human joint motion - Part II: shoulder, elbow, wrist and hand. *Journal of Biomechanics*, *38*(5), 981–992.

Yamamoto, N., Philbeck, J., Woods, A., Gajewski, D., Arthur, J., Potolicchio, S., … Caputy, A. (2014). Medial temporal lobe roles in human path integration. *PLoS ONE*, *9*(5), 1–14.

Ziemer, C. J., Branson, M. J., Chihak, B. J., Kearney, J. K., Cremer, J. F., & Plumert, J. M. (2013). Manipulating perception versus action in recalibration tasks. *Attention, Perception, & Psychophysics*, *75*, 1260–1274.